RADIOLOGY AND ONCOLOGY

vol.57 no.1
march 2023

RADIOLOGY AND ONCOLOGY

Mach 2023
Vol. 57 No. 1
Pages 1-140
ISSN 1318-2099
UDC 616-006
CODEN: RONCEM

Publisher
Association of Radiology and Oncology

Aims and Scope
Radiology and Oncology is a multidisciplinary journal devoted to the publishing original and high-quality scientific papers and review articles, pertinent to oncologic imaging, interventional radiology, nuclear medicine, radiotherapy, clinical and experimental oncology, radiobiology, medical physics, and radiation protection. Papers on more general aspects of interest to the radiologists and oncologists are also published (no case reports).

Editorial office

Radiology and Oncology
Zaloška cesta 2
P. O. Box 2217
SI-1000 Ljubljana
Slovenia
Phone: +386 1 5879 369
Phone/Fax: +386 1 5879 434
E-mail: gsersa@onko-i.si

Reader for English
Vida Kološa

Secretary
Mira Klemenčič, Zvezdana Vukmirović, Vijoleta Kaluža, Uroš Kuhar

Design
Monika Fink-Serša, Samo Rovan, Ivana Ljubanović

Layout
Matjaž Lužar

Printed by
Tiskarna Ozimek, Slovenia

Published quarterly in 400 copies

Beneficiary name: DRUŠTVO RADIOLOGIJE IN ONKOLOGIJE
Zaloška cesta 2
1000 Ljubljana
Slovenia

Beneficiary bank account number: SI56 02010-0090006751
IBAN: SI56 0201 0009 0006 751
Our bank name: Nova Ljubljanska banka, d.d.,
Ljubljana, Trg republike 2,
1520 Ljubljana; Slovenia

SWIFT: LJBASI2X

Subscription fee for institutions EUR 100, individuals EUR 50

The publication of this journal is subsidized by the Slovenian Research Agency.

Indexed and abstracted by:

- *Baidu Scholar*
- *Case*
- *Chemical Abstracts Service (CAS) - CAplus*
- *Chemical Abstracts Service (CAS) - SciFinder*
- *CNKI Scholar (China National Knowledge Infrastructure)*
- *CNPIEC - cnpLINKer*
- *Dimensions*
- *DOAJ (Directory of Open Access Journals)*
- *EBSCO (relevant databases)*
- *EBSCO Discovery Service*
- *Embase*
- *Genamics JournalSeek*
- *Google Scholar*
- *Japan Science and Technology Agency (JST)*
- *J-Gate*
- *Journal Citation Reports/Science Edition*
- *JournalGuide*
- *JournalTOCs*
- *KESLI-NDSL (Korean National Discovery for Science Leaders)*
- *Medline*
- *Meta*
- *Microsoft Academic*
- *Naviga (Softweco)*
- *Primo Central (ExLibris)*
- *ProQuest (relevant databases)*
- *Publons*
- *PubMed*
- *PubMed Central*
- *PubsHub*
- *QOAM (Quality Open Access Market)*
- *ReadCube*
- *Reaxys*
- *SCImago (SJR)*
- *SCOPUS*
- *Sherpa/RoMEO*
- *Summon (Serials Solutions/ProQuest)*
- *TDNet*
- *Ulrich's Periodicals Directory/ulrichsweb*
- *WanFang Data*
- *Web of Science - Current Contents/Clinical Medicine*
- *Web of Science - Science Citation Index Expanded*
- *WorldCat (OCLC)*

This journal is printed on acid- free paper

On the web: ISSN 1581-3207
https://content.sciendo.com/raon
http://www.radioloncol.com

contents

review

radiology

experimental oncology

clinical oncology

review

Oral verrucous carcinoma: a diagnostic and therapeutic challenge

Nejc Kristofelc[1], Nina Zidar[2], Primoz Strojan[3,4]

[1] Department of Otorhinolaryngology, General Hospital Dr. Franc Derganc Nova Gorica, Šempeter pri Gorici, Slovenia
[2] Institute of Pathology, Faculty of Medicine, University of Ljubljana, Ljubljana, Slovenia
[3] Department of Radiation Oncology, Institute of Oncology, Ljubljana, Slovenia
[4] Faculty of Medicine, University of Ljubljana, Ljubljana, Slovenia

Radiol Oncol 2023; 57(1): 1-11.

Received 17 December 2022
Accepted 29 January 2023

Correspondence to: Nejc Krištofelc, M.D., Department of Otorhinolaryngology, General Hospital Dr. Franc Derganc Nova Gorica, Ulica padlih borcev 13 A, SI-5290 Šempeter pri Gorici, Slovenia. E-mail: nejc.kristofelc@bolnisnica-go.si

Disclosure: No potential conflicts of interest were disclosed.

Background. Verrucous carcinoma is a low-grade variant of squamous cell carcinoma with specific morphologic, cytokinetic and clinical features. Despite low mitotic activity and slow growth, it can infiltrate adjacent tissues in advanced stages but does not metastasize. The most frequently affected site is the oral cavity. The following article provides latest updates in the etiology, clinical presentation, diagnostics and treatment options in oral verrucous carcinoma and discusses the existing dilemmas linked to this unique malignancy.

Conclusions. Oral verrucous carcinoma must be differentiated from conventional squamous cell carcinoma due to its less aggressive behaviour with a more favourable prognosis. Close communication between clinician and pathologist is mandatory for making a correct diagnosis. Primary surgery with negative surgical margins seems to be the most successful treatment. However, management recommendations are not uniform since they are mostly based on case reports and small retrospective case series. Prospective and pooled multi-institutional studies are therefore needed.

Key words: verrucous carcinoma; oral verrucous carcinoma; squamous cell carcinoma; diagnostics; differential diagnosis; treatment

Introduction

Head and neck cancer is the world's seventh most common cancer with over 870,000 new cases in 2020. Lip and oral cavity malignancies accounted for almost half of them.[1] More than 90% of oral cavity cancers arises from squamous epithelium.[2] Verrucous carcinoma is a low-grade variant of squamous cell carcinoma (SCC) with specific morphologic, cytokinetic and clinical features.[3] It is a locally aggressive tumour and does not metastasize to regional lymph nodes or to distant sites.[4] In 1941, Friedell and Rosenthal first reported verrucous papillary lesions on the buccal mucosa in eight tobacco chewers.[5] Seven years later, Ackerman described histopathologic and clinical features of this neoplasm. He defined it as a distinct clinicopathologic entity and introduced a term »verrucous carcinoma«.[6]

Verrucous carcinoma most often arises on mucous membranes of the head and neck region with the oral cavity most commonly involved, particularly buccal mucosa, gum and tongue.[3] Oral verrucous carcinoma accounts for 0.57-16.08% of oral squamous cell carcinoma (SCC)[7–9] and is predominantly seen in males with the reported mean age at diagnosis between 49 and 69.5 years.[9–11] In a study by Koch *et al.*, glottic larynx was the most frequently affected nonoral site.[3] Other reported locations in the head and neck region affected by

verrucous carcinoma are nasal cavity, paranasal sinuses, nasopharynx, oesophagus and temporal bone.[12-14] Verrucous carcinoma on the skin and mucosa of the anogenital region and extremities are described in the literature as well.[15,16]

Etiology

The etiopathogenesis of oral verrucous carcinoma is not completely understood. As in conventional oral SCC, there is a strong association with alcohol consumption and inhaled as well as chewing tobacco use. Other irritants to the oral mucosa such as betel nut chewing, poor oral hygiene, a poorly fitting dental prosthesis and earlier mucosal injuries or scars have also been described as risk factors in the development of oral verrucous carcinoma.[9,17–19] There is growing evidence that oral microbiota and its imbalances may play a role in the etiology of oral cancers through activation of smoking and alcohol related carcinogens locally and chronic inflammation systemically.[20] Human papillomaviruses (HPVs) have been considered as a possible etiologic factor in verrucous carcinoma, with the reported prevalence of HPV in verrucous carcinoma ranging from 0% to 100%.[21–23] However, using highly sensitive and specific molecular methods, it has been shown that HPVs are not associated with the etiopathogenesis of verrucous carcinoma of the head and neck. Furthermore, no evidence of transcriptionally active high-risk α-HPV was found in verrucous carcinoma by real-time polymerase chain reaction (RT-PCR) for HPV E6/E7 messenger ribonucleic acid (mRNA). It appears that verrucous carcinoma of the head and neck is not associated with infection with HPV.[4,24,25]

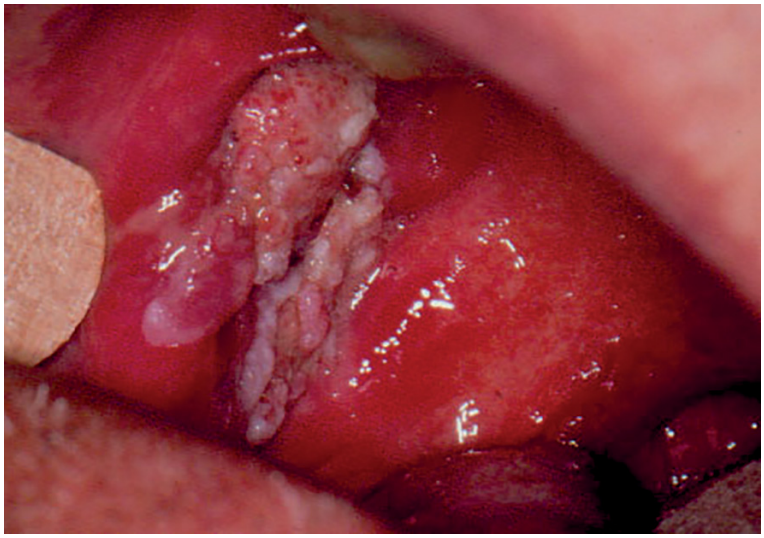

FIGURE 1. Verrucous carcinoma of the right buccal mucosa (clinical stage T2N0M0) in an 81-year-old male patient. He presented with a whitish exophytic tumour mass of the inner side of the right cheek and without suspicious lymph nodes on the neck. The lesion was noticed by the patient a month before initial examination, and it occasionally hurt, but he had no problems feeding. Due to associated diseases, he was treated with radiotherapy (55 Gy, 2.2 Gy/fraction) and concurrent intravenous chemotherapy (vinblastine 2 mg, day 1; methotrexate 50 mg, day 2; bleomycin 15 mg, days 2 and 3). The patient died of injury 5.5 years after completion of treatment for verrucous carcinoma with no evidence of malignant disease in oral cavity.

Clinical presentation

Verrucous carcinoma is characterized by low mitotic activity reflecting in slow growth[7]; hence it can take several years to reach the size that causes symptoms. Patients may report oral discomfort, difficulty chewing or swallowing, and bad breath. Pain usually indicates tumour invasion into the surrounding structures.[26,27]

Oral verrucous carcinoma typically appears as an exophytic broad-based lesion with a cauliflower-like warty surface[28] as presented in Figure 1. Despite its slow growth, it can reach a significant size and infiltrate adjacent tissues such as muscles and bone.[3] However, even when locally advanced, oral verrucous carcinoma has no tendency to metastasize to regional lymph nodes and distant sites.[4] Cervical lymphadenopathy is commonly seen at initial clinical or radiological examination and is mostly considered reactive secondary to inflammation at the tumour-stromal interface.[3]

Initial reports of neck metastasis in verrucous carcinoma were later attributed to incorrect pathologic diagnosis or to a presence of foci of conventional SCC of varying degree of differentiation within a verrucous carcinoma. The so-called hybrid verrucous carcinoma was first described by Batsakis *et al*. in 1982 in three verrucous lesions of the larynx.[29] Medina *et al*. later reported coexistence of verrucous carcinoma and conventional SCC in 20% of 104 patients with oral verrucous carcinoma.[30] In contrast to the classic, histologically uniform verrucous carcinoma, a hybrid verrucous carcinoma is capable of metastasizing and must therefore be managed as a more common and aggressive conventional SCC.[31] However, it is not possible to differentiate these lesions at clinical examination due to similar appearance. Moreover, examination of small tumour samples obtained with biopsy could be misleading as an invasive component is often missed at sampling.[32] Gokavarapu *et al*. reported that 51% of cases preoperatively diagnosed as oral

verrucous carcinoma or its benign precursors were actually hybrid lesions.[33] Although multiple biopsies from different areas of the tumour might be helpful to identify invasive component, surgical excision and histopathological examination of whole resection specimen is needed for definitive diagnosis.[32] If hybrid verrucous carcinoma is recognized, the pathologist should quantitate each component of the tumour, define the degree of differentiation of the conventional SCC component and comment on depth of the tumour invasion, potential presence of lymphatic or perineural invasion and the adequacy of the resection margins. These features help the clinicians to decide about adjuvant treatment options.[31]

Various mucosal abnormalities including verrucous hyperplasia and dysplasia are frequently found adjacent to the oral verrucous carcinoma supporting the view that verrucous carcinoma develops from precursor lesions.[28] Patients with oral verrucous carcinoma are also at high risk of developing metachronous second primary tumours. This can be explained with the concept of »field cancerization« proposed by Slaughter *et al*. who postulated that prolonged exposure of the upper aerodigestive tract to carcinogens leads to genomic instability even beyond the area of clinically and histopathologically evident mucosal changes.[34]

Diagnostics and differential diagnosis

Diagnosis of oral verrucous carcinoma is based on a patient's history, clinical manifestation and histopathologic features of the lesion. However, establishing the correct diagnosis is often difficult due to other oral lesions with often similar verrucous presentation and/or insufficient biopsy specimen as well.[9] Medical history should include information on the duration of the growth of the lesion and potential etiologic factors (smoking, alcohol abuse). Computed tomography (CT) and/or magnetic resonance imaging (MRI) is helpful to determine local extent of the lesion with potential invasion to surrounding structures and to exclude tumour spread to regional lymph nodes.[35]

The clinician's impression of a malignant lesion frequently does not match its benign nature described in the histopathology report. Therefore, biopsies are often repeated, which can significantly delay the start of a treatment.[10,36] Close communication between the clinician and the pathologist is therefore of the utmost importance.[33]

Microscopically, verrucous carcinoma consists of filiform projections lined by thick, well-differentiated keratinized squamous epithelium, composed of one to a few layers of basal cells, and multiplied, voluminous spinous cells lacking cytological atypia. It invades the underlying stroma with a well-defined, pushing margin.[37] When oral verrucous carcinoma is highly suspicious by clinical appearance, it is recommended that the lesion is surgically excised if not too extensive.[38]

Lesions in oral cavity with a verrucous appearance may belong to a broad spectrum, extending from verrucous hyperplasia, proliferative verrucous leukoplakia, oral squamous papilloma, oral verrucous carcinoma, hybrid oral verrucous carcinoma to conventional oral SCC with an exophytic growth pattern (Figure 2). It is difficult to distinguish them clinically from each other; they may also coexist.[39]

Oral verrucous hyperplasia resembles oral verrucous carcinoma both clinically and histopathologically. It presents as a white elevated mucosal plaque or mass with exophytic verrucous surface. In oral verrucous hyperplasia and oral verrucous carcinoma, hyperplastic epithelium is superficial to adjacent normal mucosa, but in oral verrucous carcinoma, broad epithelial processes also extend deeper, exhibiting a pushing-border invasion into the underlying connective tissue but the basement membrane remains intact.[40] Therefore, it was suggested that oral verrucous carcinoma can be best differentiated from oral verrucous hyperplasia with biopsies taken from the deep portion and the margin of the tumour where adjacent normal mucosa is evident to compare.[33] Oral verrucous hyperplasia is an irreversible precancerous lesion that may transform into oral verrucous carcinoma. Wang *et al*. reported a 10% of malignant transformation rate in their series of 60 oral verrucous hyperplasia cases. Thus, once diagnosed, oral verrucous hyperplasia should be treated as oral verrucous carcinoma.[41]

Proliferative verrucous leukoplakia is an aggressive form of nonhomogeneous multifocal oral leukoplakia characterized by a progressive clinical course with changing clinical and histopathologic features. It is more commonly seen among elderly women. Although etiology of proliferative verrucous leukoplakia remains unclear, it seems that consumption of tobacco and alcohol does not play a role.[42] Proliferative verrucous leukoplakia usually begins as a single white mucosal plaque that eventually becomes multifocal with exophytic, verrucous or erythematous appearance. Its de-

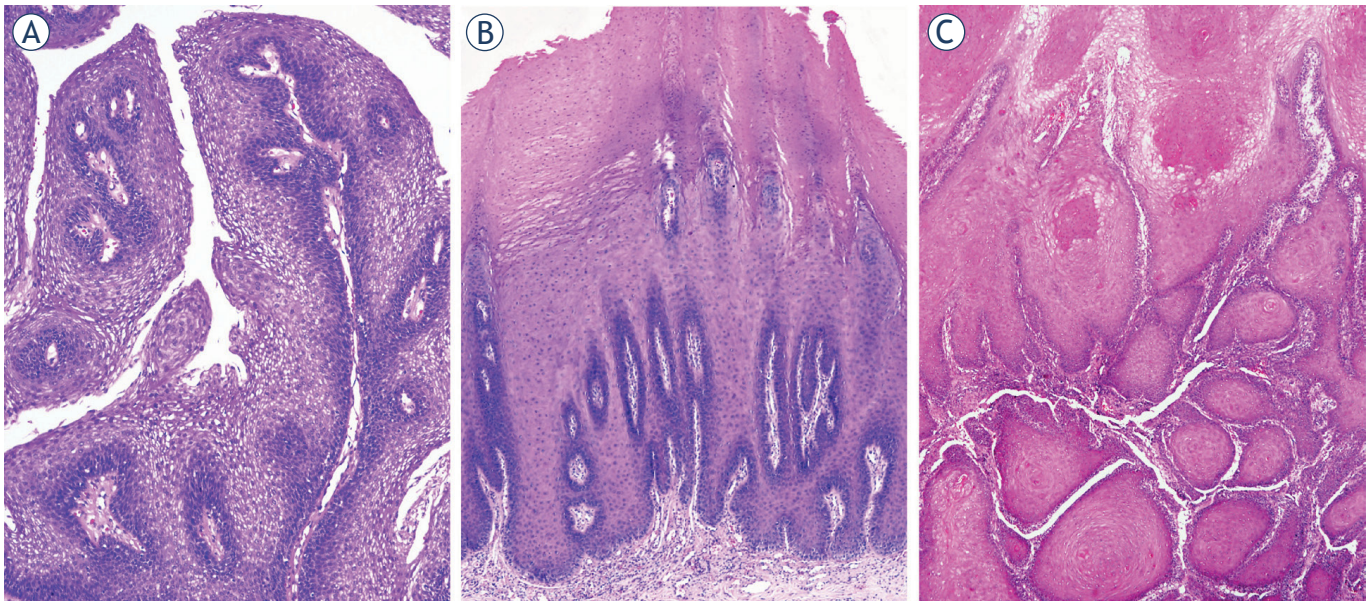

FIGURE 2. Histopathology images of oral verrucous lesions. Squamous cell papilloma **(A)** exophytic lesion, composed of finger-like projections, lined by non-keratinizing stratified squamous epithelium and a central connective tissue core. Verrucous hyperplasia **(B)** exophytic lesion, composed of hyperplastic keratinizing squamous epithelium with no invasion into the underlying stroma. Verrucous carcinoma **(C)** exophytic tumour, resembling verrucous hyperplasia, but with invasive growth, consisting of broad epithelial islands and processes, with no atypia, exhibiting a pushing-border into the underlying stroma.

scription includes a histopathological continuum ranging from benign hyperkeratosis to lesions with increasing degree of dysplasia. Therefore, proliferative verrucous leukoplakia has no specific histological features and microscopic findings depend on the histopathologic stage of proliferative verrucous leukoplakia.[43] According to the World Health Organization, proliferative verrucous leukoplakia is a potentially malignant disorder with the highest rate of malignant transformation either to oral verrucous carcinoma or conventional oral SCC.[42] In addition, several authors proposed different clinical and histopathological criteria for diagnosing proliferative verrucous leukoplakia.[44,45] In the meta-analysis by Palaia *et al*. which included 22 studies with a total of 699 proliferative verrucous leukoplakia patients, a malignant transformation rate of proliferative verrucous leukoplakia was 45.8%.[46] Thus, once proliferative verrucous leukoplakia is confirmed, active therapy should be undertaken, such as surgery, laser ablation, photodynamic therapy or radiotherapy.[47] However, proliferative verrucous leukoplakia responds poorly to various treatment modalities and its recurrence rate is high, even after surgical removal.[48]

Squamous cell papilloma (SCP) in the oral cavity appears as a pink to white mucosal exophytic lesion with a warty or granular surface. It is most commonly caused by HPV type 6 and type 11, tends to progress slowly and has a very low risk of becoming malignant. SCP is possible to differentiate from oral verrucous carcinoma microscopically. In contrast to oral verrucous carcinoma which shows epithelial processes with downgrowth into the underlying connective tissue, SCP presents with long, thin and finger-like projections, extending above the mucosal surface. Each of these projections is lined by stratified squamous epithelium and contains a central connective tissue core.[49]

Conventional oral SCC most commonly presents as an ulcerated mucosal lesion with necrotic central area, surrounded by irregular raised and indurated borders. However, an exophytic growth with a smooth, ulcerated or verrucous surface may also be seen.[50,51] In comparison to oral verrucous carcinoma, conventional oral SCC is histopathologically marked by a greater degree of atypia and mitotic activity of the tumour cells and invasion beyond the basement membrane.[31] It grows more rapidly, frequently metastasizes to the regional and distant sites and has a worse prognosis.[8] Oral verrucous carcinoma with foci of conventional SCC can be found at histopathological examination, which dictates treatment choices and prognosis.[31]

Molecular biomarkers

The development of oral verrucous carcinoma is modulated by genetic predisposition and environmental influences resulting in a wide range of genetic and epigenetic alterations that can be detected by various tumour markers. Molecular mechanisms of oral verrucous carcinoma are therefore increasingly being investigated. Although many different molecules associated with diagnosis, tumour progression and prognosis of oral verrucous carcinoma have been proposed, a reliable and effective biomarker has still not been identified.[35]

Genetic studies have shown that several genes are differently expressed between oral verrucous carcinoma and oral SCC.[52] Most investigated markers in carcinogenesis of oral verrucous carcinoma are p53[53,54], Ki-67[53,55,56], cyclin-B1[56,57] and cyclin-D1.[58] Except for Ki-67, their expression levels were significantly higher in conventional oral SCC than in oral verrucous carcinoma. Tumour suppression markers p21 and p27 may not be of much diagnostic use in distinguishing oral verrucous carcinoma from oral verrucous hyperplasia [59] and oral SCC.[54,60] Components of extracellular matrix and basement membrane play an important role in tumour invasion and metastasis. Oral verrucous carcinoma is associated with lower expression of matrix metalloproteinase 9 (MMP-9)[53] and higher expression of laminin[61] in comparison to oral SCC. Laminin and type IV collagen are good markers for basement membrane integrity and their discontinuity is more evident in severe oral epithelial dysplasia than in verrucous carcinoma.[61] Among cell surface proteins, high level of expression of glucose transporter 1 (GLUT-1) in both oral SCC and oral verrucous carcinoma could differentiate them from oral epithelial dysplasia.[62] Oral SCC could be distinguished from oral verrucous carcinoma based on a higher density of CD68 (marking tumour associated macrophages) and CD31 (marking microvessel density) found in immunohistochemical studies.[63] Regarding cytoskeletal proteins, CK20 is highly expressed in oral verrucous carcinoma and oral SCC but not in benign squamous lesions[64], and CD34 along with α-smooth muscle actin (α-SMA) seem to be helpful in the diagnosis of oral verrucous hyperplasia.[65] Different expression of desmosomal proteins (up-regulation of plakophilin 1, desmoglein 2, desmoglein 3, desmoplakin), microRNA (miRNA) molecules (up-regulation of miRNA-203, down-regulation of miRNA-125a-5p, miRNA-125b) and proteins (down-regulation of p63) in verrucous carcinoma is useful in differentiation from conventional SCC and detecting foci of SCC in hybrid verrucous carcinoma as well.[37,66]

Treatment

Due to the rarity of oral verrucous carcinoma, treatment recommendations found in the literature is mostly based on case reports and small retrospective case series, and are consequently not uniform. The treatment modalities available include surgery, radiotherapy, chemotherapy, or combinations thereof.

Surgery

Wide surgical excision is usually considered the treatment of choice because of the wide spectrum of reconstruction possibilities of the resulting tissue defect in the oral cavity with good functional results, and encouraging locoregional control and survival rates.[17,38,67] However, there is ongoing debate about the optimal width of surgical margins and the need for elective neck dissection (END). Similar to conventional oral SCC, clinical surgical margin of 10–15 mm and histological margin of at least 5 mm are still generally considered sufficient to not increase the risk of local recurrence of oral verrucous carcinoma[68-70], although no worse outcomes were reported in patients with close histological margins (*i.e.* less than 5 mm) who did not receive adjuvant radiotherapy.[10] Since histologically pure oral verrucous carcinoma does not metastasize, END is usually not performed during primary surgery but is indicated in hybrid oral verrucous carcinoma and when microvascular flap is used for reconstruction of tumour defect.[10,67,68] Some authors advocate a selective supraomohyoid neck dissection (neck levels I–III) also in patients with advanced primary tumour stages (cT3–4) and/or clinically overt lymphadenopathy. However, in several studies, no patient with END had histologically proven nodal metastasis.[10,17,38,71]

Radiotherapy

Oral verrucous carcinoma is thought to be less sensitive to radiotherapy than conventional oral SCC.[72,73] Radiotherapy targets DNA in rapidly dividing cells, whereas studies on cytokinetic characteristics of verrucous carcinoma have shown that only low proportion of tumour cells are in S-phase compartment of the cell cycle during which DNA is synthesized, corresponding to a low mitotic ac-

TABLE 1. Primary surgery in the treatment of oral verrucous carcinoma - review of the literature series

Authors and study year	Number of patients	Local control (%)	Survival	Follow-up time
Kraus and Perezmesa, 1966[74]	64	55 (85.9)	N.S.	N.S.
Medina *et al*, 1984[30]	90	74 (82.2)	N.S.	At least 2 years
Jyothirmayi *et al*, 1997[8]	11	N.S.	5-year DFS 68%	Median 56 months (range 7–110)
Koch *et al*, 2001[3]	484	N.S.	5-year RSR 85.7%	N.S.
Kang *et al*, 2003[38]	38	38 (100) at 3 years	3-year OSR 94.7%	Median 37.5 months (range 13–76)
Walvekar *et al*, 2009[17]	101	80 (79.2)	5-year DFS 77.6%	Median 4.61 years (range 0.5–14.3)
Huang *et al*, 2009[67]	39	38 (97.4)	5-year CSS 89.1%	Median 90 months (range, 13–171)
Candau-Alvarez *et al*, 2014[68]	13	12 (92.3)	OSR 92.9% for a mean follow-up of 2 years	Mean 24.8 months (range 6–53)
Franklyn *et al*, 2017[10]	22	21 (95.5) (recurrence in a patient with hybrid OVC)	N.S.	Median 24 months

CSS = cancer specific survival; DFS = disease free survival; N.S. = not specified; OSR = overall survival rate; OVC = oral verrucous carcinoma; RSR = relative survival rate

tivity of this tumour and reduced susceptibility to irradiation.[29] Mohan *et al*. demonstrated that patients with oral verrucous carcinoma who received postoperative radiotherapy trended toward worse disease-specific survival (DSS) than those with oral SCC, suggesting relative radioresistance of oral verrucous carcinoma.[7]

Studies reporting local control rate and survival rate for upfront surgery and primary radiotherapy are summarized in Table 1 and Table 2.

However, a fair comparison between oncological results of surgery and radiotherapy is difficult to make due to obvious lack of well-designed prospective studies or even comparisons. In most series, patients were recruited over a longer time period which resulted in suboptimal treatments in at least part of these patients. Thus, local control and survival rates of irradiated patients must be interpreted with caution and understanding that irradiation techniques and fractionation schemes used in the past changed significantly over time. Nevertheless, radiotherapy is an acceptable alternative to surgery for patients who refuse proposed operation or are medically unfit for major surgery as well as in whom surgery would cause an important functional and/or cosmetic impairment.[77] In cases of radiotherapy failure, surgical salvage remains an option.[78]

In the past, radiotherapy was burdened with the phenomenon of anaplastic transformation which assumed the possibility of conversion of verrucous carcinoma to a less-differentiated SCC after irradiation.[79] In older literature, its incidence has been reported to be as high as 30%.[80] Recently, different authors questioned the concept of this phenomenon and raised the possibility of hybrid lesions containing foci of conventional SCC that had been missed at the initial biopsy and not controlled by irradiation, resulting in tumour recurrence.[3,79,81] This hypothesis is further justified by the reports of anaplastic transformation following primary surgery as well, probably due to the same reason as in the case of radiotherapy, *i.e.* an incorrect histopathologic diagnosis.[73]

Postoperative radiotherapy

The benefit of postoperative radiotherapy (PORT) in oral verrucous carcinoma is controversial. The decision about PORT usually follows recommendations for patients with conventional oral SCC (*i.e.* positive or close surgical margins, pT3–T4 primary tumour, perineural and lymphovascular invasion).[67,82] Analysing the SEER database, however, Mohan *et al.* demonstrated a statistically significant improvement in DSS in patients solely operated compared to those receiving surgery and PORT.[7] In a recent retrospective cohort study of the National Cancer Database (NCDB), Naik *et al*. showed that positive surgical margins were associated with significantly worse overall survival (OS) (hazard ratio [HR] 2.85, P = 0.006).[82] However,

TABLE 2. Primary radiotherapy in the treatment of oral verrucous carcinoma - review of the literature series

Authors and study year	Number of patients	Local control rate with primary radiotherapy (%)	Surgical salvage	Local control rate with primary radiotherapy and salvage surgery (%)	Survival	Follow-up time
Kraus and Perezmesa, 1966[74]	13	0 (0)	8/13	7 (53.8)	N.S.	N.S.
Memula *et al*, 1980[75]	32	19 (59.4)	6/13	25 (78.1)	5-year DFS 31%	N.S.
Medina *et al*, 1984[30]	12	7 (58.3)	3/5	10 (83.3)	N.S.	At least 2 years
Nair *et al*, 1988[76]	50	22 (44) at 3 years	4/28	N.S.	3-year DFS 44%	At least 3 years
Vidysagar *et al*, 1992[36]	107	55 (51.4) (residual disease in 19 patients, recurrence in 33 patients)	20/52	N.S.	5-year DFS 49%	Range 6–60 months
Jyothirmayi *et al*, 1997[8]	42	16 (38.1) (residual disease in 10 patients, recurrence in 16 patients)	9/26	N.S.	5-year DFS 66%	Median 56 months (range 7–110)
Koch *et al*, 2001[3]	33	N.S.	N.S.	N.S.	5-year RSR 41.8%	N.S.

DFS = disease free survival; N.S. = not specified; OVC = oral verrucous carcinoma; RSR = relative survival rate

in those patients the use of PORT showed no OS benefit (HR 3.12, P = 0.072). These findings suggest that the role of PORT is limited in oral verrucous carcinoma, favouring surgical re-resection, when feasible, over adjuvant radiotherapy in patients with adverse pathologic features or clinically overt residual tumour after surgery.[82]

Chemotherapy

Experiences with chemotherapy, alone or in combination with other modalities, in oral verrucous carcinoma are scarce.[83] Chemotherapy can be implemented in a neo-adjuvant setting to reduce tumour size before subsequent surgery, which is expected to be less extensive and mutilating, resulting in better functional and cosmetic outcome.[84] It can also be used as a salvage treatment for patients with recurrent disease and to palliate symptoms in advanced tumours not suitable for aggressive radical treatment.[85,86] Although the data on the use of older chemotherapy drugs are available in the literature, there is no information on the use of modern drugs (targeted agents, check-point inhibitors) in oral verrucous carcinoma.

Encouraging results were reported by Wu *et al*. using intra-arterial methotrexate infusion as a primary therapy in 15 patients with oral verrucous carcinoma. Despite locally advanced T3–4 tumours in eight of these patients, a complete tumour remission was observed in all patients who were without disease recurrence at a mean follow-up of 42 months.[83] Karkazoglou *et al*. reported on 12 oral verrucous carcinoma patients who had also been treated with methotrexate, given by various routes and in different doses, because of either the extent of the tumour or poor general condition of the patient. Only one patient failed to respond. Authors concluded that methotrexate reduced morbidity and improved quality of life with minimal and reversible toxicity.[87] Preliminary observations in two elderly patients with locally advanced oral verrucous carcinoma showed that single cycle of oral fluoropyrimidine capecitabine induced rapid and clinically significant response with near complete resolution of oral lesions within 3 weeks of initiating therapy. A durable partial response was seen at 6 months and 1 year and was associated with significant improvement in life quality with acceptable toxicity profile.[88]

Chemoradiotherapy

In addition, chemotherapy can be given simultaneously with radiotherapy. In a group of 12 patients with previously untreated verrucous carcinoma of different head and neck mucosal sites, concurrent chemoradiotherapy with at least two cycles of intravenous vinblastine, methotrexate and bleomycin and radiotherapy dose of 44–70 Gy (median 65.2 Gy) resulted in local control (median follow-up of 3.4 years) in 11 patients, nine of whom had advanced T3–4 tumours.[85] Authors concluded that concomitant chemotherapy seems to successfully compensate lower effectiveness of radiotherapy in verrucous carcinoma and even allows reduction of

radiation dose bellow the standard 66–70 Gy, and, therefore, alleviates its toxicity and contributes to organ sparing.[84] Promising results of chemoradiotherapy were also reported by Yoshimura *et al*. using 5-fluorouracil and its analogues.[89]

Non-surgical techniques

Non-surgical methods are well established treatment modalities in low risk nonmelanoma skin cancers and to some extent in oral benign and precancerous lesions but there are only a few case reports regarding their use in oral verrucous carcinoma.

Cryotherapy acts by freezing a lesion in situ which leads to disruption of cell membranes, damage of tumour vasculature, activation of cytotoxic immune mechanisms and finally cell necrosis.[90] Yeh *et al*. reported clinically complete response to shave excision and subsequent cryotherapy with liquid nitrogen in 11 of 18 patients with oral verrucous hyperplasia and oral verrucous carcinoma. After a mean follow-up of 23 months, recurrence was found in three cases and all were successfully treated by the same technique.[91]

Photodynamic therapy (PDT) is based on topical or systemic administration of an exogenous photosensitiser which increases tumour tissue sensitiveness to light of a specific wavelength.[92] It mediates tumour destruction by creating oxygen free radicals, damaging tumour vasculature and activating immune response against tumour cells. Chen *et al*. reported a complete clinical regression and no tumour recurrence at 6 months follow-up after 22 cycles of PDT using topical 5-aminolevulinic acid followed by multiple fractionated irradiations with LED red light in a 56-year-old male with oral verrucous carcinoma extending from mouth angle to buccal mucosa.[93] In order to better expose deeper part of the lesion under mucosal surface to cryotherapy or PDT and make a definitive histopathologic diagnosis, its exophytic part may initially be removed with debulking methods such as shave or laser excision.[91]

CO_2 laser destructs a lesion with tissue vaporization and is therefore proposed for treatment of tumours involving cosmetically critical areas such as lips, where wide surgical excision may lead to unacceptable aesthetic and/or functional impairment.[94] Several authors reported good clinical response with complete tumour removal and no recurrence in a follow-up from 15 to 48 months.[94-96]

Described procedures are non-invasive and can be safely carried out in a local anaesthesia in the outpatient clinic. Other reported advantages are short procedure duration, ability to treat multifocal lesions, limited pain and scarring, fast homeostasis and healing process, low risk of secondary infection and little or no side effects.[91,93,95] However, their effect is limited by a depth of agent penetration, which therefore makes them suitable only for a treatment of superficial oral lesions.[92] They also lack working precision since it is difficult to judge the final extent of tissue necrosis during a procedure. Moreover, tumour resolution can only be assessed clinically and not histopathologically.[91] Large-scale clinical studies with longer follow-up are further necessary to evaluate their effectiveness in the management of oral verrucous carcinoma.

Conclusions

Oral verrucous carcinoma is a rare variant of oral SCC that must be differentiated from conventional SCC due to its locally invasive and non-metastasizing behaviour with a more favourable prognosis. For making a correct diagnosis, close communication between clinician and pathologist is mandatory. Primary surgery with negative surgical margins seems to be the optimal treatment for patients with oral verrucous carcinoma; whether to perform the END remains controversial. The concern about anaplastic transformation after irradiation should not affect the decision on treatment with radiotherapy which is usually proposed to patients with extensive tumours or patients in poor general condition. The role of systemic therapy, particularly immunotherapy and targeted therapy, and non-surgical treatment methods are yet to be defined. Due to rarity of the disease, pooled multi-institutional analyses are warranted to properly address opened questions.

Acknowledgments

This review was funded by the Slovenian Research Agency (ARRS), grant number P3-0307.

References

1. Sung H, Ferlay J, Siegel RL, Laversanne M, Soerjomataram I, Jemal A, et al. Global cancer statistics 2020: GLOBOCAN estimates of incidence and mortality worldwide for 36 cancers in 185 countries. *CA Cancer J Clin* 2021; **71:** 209-49. doi: 10.3322/caac.21660

2. Van Dijk BAC, Brands MT, Geurts SME, Merkx MAW, Roodenburg JLN. Trends in oral cavity cancer incidence, mortality, survival and treatment in the Netherlands. *Int J Cancer* 2016; **139:** 574-83. doi: 10.1002/ijc.30107

3. Koch BB, Trask DK, Hoffman HT, Karnell LH, Robinson RA, Zhen W, et al. National survey of head and neck verrucous carcinoma: patterns of presentation, care, and outcome. *Cancer* 2001; **92:** 110-20. doi: 10.1002/1097-0142(20010701)92:1<110::AID-CNCR1298>3.0.CO;2-K

4. Patel KR, Chernock RD, Zhang TR, Wang X, El-Mofty SK, Lewis JSJ. Verrucous carcinomas of the head and neck, including those with associated squamous cell carcinoma, lack transcriptionally active high-risk human papillomavirus. *Hum Pathol* 2013; **44:** 2385-92. doi: 10.1016/j.humpath.2013.07.011

5. Friedell HL, Rosenthal LM. The etiologic role of chewing tobacco in cancer of the mouth: report of eight cases treated with radiation. *J Am Med Assoc* 1941; **116:** 2130-5. doi: 10.1001/jama.1941.02820190006002

6. Ackerman LV. Verrucous carcinoma of the oral cavity. *Surgery* 1948; **23:** 670-8. PMID: 18907508

7. Mohan S, Pai SI, Bhattacharyya N. Adjuvant radiotherapy is not supported in patients with verrucous carcinoma of the oral cavity. *Laryngoscope* 2017; **127:** 1334-8. doi: 10.1002/lary.26443

8. Jyothirmayi R, Sankaranarayanan R, Varghese C, Jacob R, Nair MK. Radiotherapy in the treatment of verrucous carcinoma of the oral cavity. *Oral Oncol* 1997; **33:** 124-8. doi: 10.1016/S0964-1955(96)00059-0

9. Rekha KP, Angadi PV. Verrucous carcinoma of the oral cavity: a clinicopathologic appraisal of 133 cases in Indians. *Oral Maxillofac Surg* 2010; **14:** 211-8. doi: 10.1007/s10006-010-0222-0

10. Franklyn J, Janakiraman R, Tirkey AJ, Thankachan C, Muthusami J. Oral verrucous carcinoma: ten year experience from a tertiary care hospital in India. *Indian J Med Paediatr Oncol* 2017; **38:** 452-5. doi: 10.4103/ijmpo.ijmpo_153_16

11. Alonso JE, Kuan EC, Arshi A, St. John MA. A population-based analysis of verrucous carcinoma of the oral cavity. *Laryngoscope* 2018; **128:** 393-7. doi: 10.1002/lary.26745

12. Alonso JE, Han AY, Kuan EC, Suh JD, John MAS. Epidemiology and survival outcomes of sinonasal verrucous carcinoma in the United States. *Laryngoscope* 2018; **128:** 651-6. doi: 10.1002/lary.26790

13. Sweetser S, Jacobs NL, Wong Kee Song LM. Endoscopic diagnosis and treatment of esophageal verrucous squamous cell cancer. *Dis Esophagus* 2014; **27:** 452-6. doi: 10.1111/j.1442-2050.2012.01434.x

14. Miller ME, Martin N, Juillard GF, Bhuta S, Ishiyama A. Temporal bone verrucous carcinoma: outcomes and treatment controversy. *Eur Arch Oto-Rhino-Laryngology* 2010; **267:** 1927-31. doi: 10.1007/s00405-010-1281-4

15. Prince ADP, Harms PW, Harms KL, Kozlow JH. Verrucous carcinoma of the foot: a retrospective study of 19 cases and analysis of prognostic factors influencing recurrence. *Cutis* 2022; **109:** E21-8. doi: 10.12788/cutis.0499

16. Koch H, Kowatsch E, Hödl S, Smola MG, Radl R, Hofmann T, et al. Verrucous carcinoma of the skin: long-term follow-up results following surgical therapy. *Dermatol Surg* 2004; **30:** 1124-30. doi: 10.1111/j.1524-4725.2004.30338.x

17. Walvekar RR, Chaukar DA, Deshpande MS, Pai PS, Chaturvedi P, Kakade A, et al. Verrucous carcinoma of the oral cavity: a clinical and pathological study of 101 cases. *Oral Oncol* 2009; **45:** 47-51. doi: 10.1016/j.oraloncology.2008.03.014

18. Gokavarapu S, Parvataneni N, Charan CR, Puthamakula S, Kulkarni G, Reddy BS. Multi centricity of oral verrucous carcinoma: a case series of 22 cases. *Indian J Otolaryngol Head Neck Surg* 2015; **67:** 138-42. doi: 10.1007/s12070-015-0835-6

19. Rahali L, Omor Y, Mouden K, Mahdi Y, Elkacemi H, Elmajjaoui S, et al. Oral verrucous carcinoma complicating a repetitive injury by the dental prosthesis: a case report. *Pan Afr Med J* 2015; **20:** 297. doi: 10.11604/pamj.2015.20.297.6135

20. Ahn J, Chen CY, Hayes RB. Oral microbiome and oral and gastrointestinal cancer risk. *Cancer Causes Control* 2012; **23:** 399-404. doi: 10.1007/s10552-011-9892-7

21. Johnson TL, Plieth DA, Crissman JD, Sarkar FH. HPV detection by polymerase chain reaction (PCR) in verrucous lesions of the upper aerodigestive tract. *Mod Pathol* 1991; **4:** 461-5.

22. Fliss DM, Noble-Topham SE, McLachlin M, Freeman JL, Noyek AM, van Nostrand AW, et al. Laryngeal verrucous carcinoma: a clinicopathologic study and detection of human papillomavirus using polymerase chain reaction. *Laryngoscope* 1994; **104:** 146-52. doi: 10.1288/00005537-199402000-00005

23. Mitsuishi T, Ohara K, Kawashima M, Kobayashi S, Kawana S. Prevalence of human papillomavirus DNA sequences in verrucous carcinoma of the lip: genomic and therapeutic approaches. *Cancer Lett* 2005; **222:** 139-43. doi: 10.1016/j.canlet.2004.09.019

24. del Pino M, Bleeker MCG, Quint WG, Snijders PJF, Meijer CJLM, Steenbergen RDM. Comprehensive analysis of human papillomavirus prevalence and the potential role of low-risk types in verrucous carcinoma. *Mod Pathol* 2012; **25:** 1354-63. doi: 10.1038/modpathol.2012.91

25. Odar K, Kocjan BJ, Hošnjak L, Gale N, Poljak M, Zidar N. Verrucous carcinoma of the head and neck - not a human papillomavirus-related tumour? *J Cell Mol Med* 2014; **18:** 635-45. doi: 10.1111/jcmm.12211

26. Terada T. Verrucous carcinoma of the oral cavity: a histopathologic study of 10 Japanese cases. *J Maxillofac Oral Surg* 2011; **10:** 148-51. doi: 10.1007/s12663-011-0197-x

27. Kamath VV, Varma RR, Gadewar DR, Muralidhar M. Oral verrucous carcinoma. An analysis of 37 cases. *J Craniomaxillofac Surg* 1989; **17:** 309-14. doi: 10.1016/s1010-5182(89)80059-9

28. Sonalika W, Anand T. Oral verrucous carcinoma: a retrospective analysis for clinicopathologic features. *J Cancer Res Ther* 2016; **12:** 142-5. doi: 10.4103/0973-1482.172709

29. Batsakis JG, Hybels R, Crissman JD, Rice DH. The pathology of head and neck tumors: verrucous carcinoma, part 15. *Head Neck Surg* 1982; **5:** 29-38. doi: 10.1002/hed.2890050107

30. Medina JE, Dichtel W, Luna MA. Verrucous-squamous carcinomas of the oral cavity: a clinicopathologic study of 104 cases. *Arch Otolaryngol* 1984; **110:** 437-40. doi: 10.1001/archotol.1984.00800330019003

31. Devaney KO, Ferlito A, Rinaldo A, El-Naggar AK, Barnes L. Verrucous carcinoma (carcinoma cuniculatum) of the head and neck: what do we know now that we did not know a decade ago? *Eur Arch Otorhinolaryngol* 2011; 2**68:** 477-80. doi: 10.1007/s00405-011-1495-0

32. Gokavarapu S, Rao.S LMC, Tantravahi US, Gundimeda SD, Rao TS, Murthy S. Oral hybrid verrucous carcinoma: a clinical study. *Indian J Surg Oncol* 2014; **5:** 257-62. doi: 10.1007/s13193-014-0345-0

33. Gokavarapu S, Chandrasekhara Rao LM, Patnaik SC, Parvataneni N, Raju KVVN, Chander R, et al. Reliability of incision biopsy for diagnosis of oral verrucous carcinoma: a multivariate clinicopathological study. *J Maxillofac Oral Surg* 2015; **14:** 599-604. doi: 10.1007/s12663-014-0715-8

34. Slaughter DP, Southwick HW, Smejkal W. Field cancerization in oral stratified squamous epithelium; clinical implications of multicentric origin. *Cancer* 1953; **6:** 963-8. doi: 10.1002/1097-0142(195309)6:5<963::aid-cncr2820060515>3.0.co;2-q

35. Peng Q, Wang Y, Quan H, Li Y, Tang Z. Oral verrucous carcinoma: from multifactorial etiology to diverse treatment regimens (review). *Int J Oncol* 2016; **49:** 59-73. doi: 10.3892/ijo.2016.3501

36. Vidyasagar MS, Fernandes DJ, Kasturi DP, Akhileshwaran R, Rao K, Rao S, et al. Radiotherapy and verrucous carcinoma of the oral cavity: a study of 107 cases. *Acta Oncol* 1992; **31:** 43-7. doi: 10.3109/02841869209088264

37. Odar K, Boštjančič E, Gale N, Glavač D, Zidar N. Differential expression of microRNAs miR-21, miR-31, miR-203, miR-125a-5p and miR-125b and proteins PTEN and p63 in verrucous carcinoma of the head and neck. *Histopathology* 2012; **61:** 257-65. doi: 10.1111/j.1365-2559.2012.04242.x

38. Kang CJ, Chang JTC, Chen TM, Chen IH, Liao CT. Surgical treatment of oral verrucous carcinoma. *Chang Gung Med J* 2003; **26:** 807-12. PMID: 14765750

39. Alkan A, Bulut E, Gunhan O, Ozden B. Oral verrucous carcinoma: a study of 12 cases. *Eur J Dent* 2010; **4:** 202-7. doi: 10.1055/s-0039-1697831

40. Zhu LK, Ding YW, Liu W, Zhou YM, Shi LJ, Zhou ZT. A clinicopathological study on verrucous hyperplasia and verrucous carcinoma of the oral mucosa. *J Oral Pathol Med* 2012; **4:** 131-5. doi: 10.1111/j.1600-0714.2011.01078.x

41. Wang YP, Chen HM, Kuo RC, Yu CH, Sun A, Liu BY, et al. Oral verrucous hyperplasia: histologic classification,prognosis, and clinical implications. *J Oral Pathol Med* 2009; **38:** 651-6. doi: 10.1111/j.1600-0714.2009.00790.x

42. Warnakulasuriya S, Kujan O, Aguirre-Urizar JM, Bagan JV, González-Moles MÁ, Kerr AR, et al. Oral potentially malignant disorders: a consensus report from an international seminar on nomenclature and classification, convened by the WHO collaborating centre for oral cancer. *Oral Dis* 2021; **27:** 1862-80. doi: 10.1111/odi.13704

43. Moussa M, Salem H, ElRefai SM. Oral proliferative verrucous leukoplakia: the unsolved paradox. *Madridge J Dent Oral Surg* 2017; **2:** 55-8. doi: 10.18689/mjdl-1000114

44. Cerero-Lapiedra R, Baladé-Martínez D, Moreno-López LA, Esparza-Gómez G, Bagán J V. Proliferative verrucous leukoplakia: a proposal for diagnostic criteria. *Med Oral Patol Oral Cir Bucal* 2010; **15:** 839-45. PMID: 20173704

45. Carrard VC, Brouns EREA, van der Waal I. Proliferative verrucous leukoplakia: a critical appraisal of the diagnostic criteria. *Med Oral Patol Oral Cir Bucal* 2013; **18:** 411-3. doi: 10.4317/medoral.18912

46. Palaia G, Bellisario A, Pampena R, Pippi R, Romeo U. Oral proliferative verrucous leukoplakia: progression to malignancy and clinical implications. Systematic review and meta-analysis. *Cancers* 2021; **13:** 4058. doi: 10.3390/cancers13164085

47. Capella DL, Gonçalves JM, Abrantes AAA, Grando LJ, Daniel FI. Proliferative verrucous leukoplakia: diagnosis, management and current advances. *Braz J Otorhinolaryngol* 2017; **83:** 585-93. doi: 10.1016/j.bjorl.2016.12.005

48. Proaño-Haro A, Bagan L, Bagan J V. Recurrences following treatment of proliferative verrucous leukoplakia: A systematic review and meta-analysis. *J Oral Pathol Med* 2021; **50:** 820-8. doi: 10.1111/jop.13178

49. Alan H, Agacayak S, Kavak G, Ozcan A. Verrucous carcinoma and squamous cell papilloma of the oral cavity: report of two cases and review of literature. *Eur J Dent* 2015; **9:** 453-6. doi: 10.4103/1305-7456.163224

50. Santosh ABR, Boyd D, Laxminarayana KK. Proposed clinico-pathological classification for oral exophytic lesions. *J Clin Diagnostic Res* 2015; **9:** ZE01-8. doi: 10.7860/JCDR/2015/12662.6468

51. Bouckaert, Munzhelele TI, Feller L, Lemmer J, Rag K. The clinical characteristics of oral squamous cell carcinoma in patients attending the Medunsa Oral Health Centre, South Africa. *Integr Cancer Sci Ther* 2016; **3:** 575-8. doi: 10.15761/ICST.1000207

52. Wang YH, Tian X, Liu OS, Fang XD, Quan HZ, Xie S, et al. Gene profiling analysis for patients with oral verrucous carcinoma and oral squamous cell carcinoma. *Int J Clin Exp Med* 2014; **7:** 1845-52.

53. Mohtasham N, Babakoohi S, Shiva A, Shadman A, Kamyab-Hesari K, Shakeri MT, et al. Immunohistochemical study of p53, Ki-67, MMP-2 and MMP-9 expression at invasive front of squamous cell and verrucous carcinoma in oral cavity. *Pathol Res Pract* 2013; **209:** 110-4. doi: 10.1016/j.prp.2012.11.002

54. Vallonthaiel AG, Singh MK, Dinda AK, Kakkar A, Thakar A, Das SN. Expression of cell cycle-associated proteins p53, pRb, p16, p27, and correlation with survival: A comparative study on oral squamous cell carcinoma and verrucous carcinoma. *Appl Immunohistochem Mol Morphol AIMM* 2016; **24:** 193-200. doi: 10.1097/PAI.0000000000000179

55. Zargaran M, Eshghyar N, Baghaei F, Moghimbeigi A. Assessment of cellular proliferation in oral verrucous carcinoma and well-differentiated oral squamous cell carcinoma using Ki67: a non-reliable factor for differential diagnosis? *Asian Pac J Cancer Prev* 2012; **13:** 5811-5. doi: 10.7314/apjcp.2012.13.11.5811

56. de Spíndula-Filho JV, da Cruz AD, Oton-Leite AF, Batista AC, Leles CR, de Cássia Gonçalves Alencar R, et al. Oral squamous cell carcinoma versus oral verrucous carcinoma: an approach to cellular proliferation and negative relation to human papillomavirus (HPV). *Tumour Biol* 2011; **32:** 409-16. doi: 10.1007/s13277-010-0135-4

57. Patil GB, Hallikeri KS, Balappanavar AY, Hongal SG, Sanjaya PR, Sagari SG. Cyclin B1 overexpression in conventional oral squamous cell carcinoma and verrucous carcinoma - a correlation with clinicopathological features. *Med Oral Patol Oral Cir Bucal* 2013; **18:** e585-90. doi: 10.4317/medoral.18220

58. Menaka TR, Ravikumar SS, Dhivya K, Thilagavathi N, Dinakaran J, Kalaichelvan V. Immunohistochemical expression and evaluation of cyclin D1 and minichromosome maintenance 2 in oral squamous cell carcinoma and verrucous carcinoma. *J Oral Maxillofac Pathol* 2022; **26:** 44-51. doi: 10.4103/jomfp.jomfp_446_21

59. Lin HP, Wang YP, Chiang CP. Expression of p53, MDM2, p21, heat shock protein 70, and HPV 16/18 E6 proteins in oral verrucous carcinoma and oral verrucous hyperplasia. *Head Neck* 2011; **33:** 334-40. doi: 10.1002/hed.21452

60. Adegboyega PA, Boromound N, Freeman DH. Diagnostic utility of cell cycle and apoptosis regulatory proteins in verrucous squamous carcinoma. *Appl Immunohistochem Mol Morphol AIMM* 2005; **13:** 171-7. doi: 10.1097/01.pai.0000132190.39351.9b

61. Arduino PG, Carrozzo M, Pagano M, Broccoletti R, Scully C, Gandolfo S. Immunohistochemical expression of basement membrane proteins of verrucous carcinoma of the oral mucosa. *Clin Oral Investig* 2010; **14:** 297-302. doi: 10.1007/s00784-009-0296-y

62. Angadi VC, Angadi P V. GLUT-1 immunoexpression in oral epithelial dysplasia, oral squamous cell carcinoma, and verrucous carcinoma. *J Oral Sci* 2015; **57:** 115-22. doi: 10.2334/josnusd.57.115

63. El-Rouby DH. Association of macrophages with angiogenesis in oral verrucous and squamous cell carcinomas. *J Oral Pathol Med* 2010; **39:** 559-64. doi: 10.1111/j.1600-0714.2010.00879.x

64. Gao HW, Ho JY, Lee HS, Yu CP. The presence of Merkel cells and CD10- and CD34-positive stromal cells compared in benign and malignant oral tumors. *Oral Dis* 2009; **15:** 259-64. doi: 10.1111/j.1601-0825.2009.01518.x

65. Paral KM, Taxy JB, Lingen MW. CD34 and α smooth muscle actin distinguish verrucous hyperplasia from verrucous carcinoma. *Oral Surg Oral Med Oral Pathol Oral Radiol* 2014; **117:** 477-82. doi: 10.1016/j.oooo.2013.12.401

66. Odar K, Zidar N, Bonin S, Gale N, Cardesa A, Stanta G. Desmosomes in verrucous carcinoma of the head and neck. *Histol Histopathol* 2012; **27:** 467-74. doi: 10.14670/HH-27.467

67. Huang TT, Hsu LP, Hsu YH, Chen PR. Surgical outcome in patients with oral verrucous carcinoma: long-term follow-up in an endemic betel quid chewing area. *ORL* 2009; **71:** 323-8. doi: 10.1159/000267306

68. Candau-Alvarez A, Dean-Ferrer A, Alamillos-Granados FJ, Heredero Jung S, García-García B, Ruiz-Masera JJ, et al. Verrucous carcinoma of the oral mucosa: an epidemiological and follow-up study of patients treated with surgery in 5 last years. *Med Oral Patol Oral Cir Bucal* 2014; **19:** 506-11. doi: 10.4317/medoral.19683

69. Verma DK, Bansal S, Gupta D, Bansal A. Neck dissection in verrucous carcinoma: a surgical dilemma. *IJSS Case Reports Rev* 2015; **1:** 42-5. doi: 10.17354/cr/2015/28

70. Rath S, Gandhi AK, Rastogi M, Agarwal A, Singhal A, Sharma V, et al. Treatment pattern and outcomes in verrucous carcinoma of oral cavity: a single institutional retrospective analysis from a tertiary cancer center and review of literature. *Indian J Otolaryngol Head Neck Surg* 2022; **74(Suppl 2):** 1790-6. doi: 10.1007/s12070-020-01798-w

71. Sadasivan A, Thankappan K, Rajapurkar M, Shetty S, Sreehari S, Iyer S. Verrucous lesions of the oral cavity treated with surgery: analysis of clinicopathologic features and outcome. *Contemp Clin Dent* 2012; **3:** 60-3. doi: 10.4103/0976-237X.94548

72. Lundgren JA, van Nostrand AW, Harwood AR, Cullen RJ, Bryce DP. Verrucous carcinoma (Ackerman's tumor) of the larynx: diagnostic and therapeutic considerations. *Head Neck Surg* 1986; **9:** 19-26. doi: 10.1002/hed.2890090105

73. Ferlito A, Rinaldo A, Mannarà GM. Is primary radiotherapy an appropriate option for the treatment of verrucous carcinoma of the head and neck? *J Laryngol Otol* 1998; **112:** 132-9. doi: 10.1017/s0022215100140137

74. Kraus FT, Perezmesa C. Verrucous carcinoma: clinical and pathologic study of 105 cases involving oral cavity, larynx and genitalia. *Cancer* 1966; **19:** 26-38. doi: 10.1002/1097-0142(196601)19:1<26::aid-cncr2820190103>3.0.co;2-l

75. Memula N, Ridenhour GDL. Radiotherapeutic management of oral verrucous carcinoma. *Oncol Biol Phys* 1980; **6:** 1404.

76. Nair MK, Sankaranarayanan R, Padmanabhan TK, Madhu CS. Oral verrucous carcinoma. Treatment with radiotherapy. *Cancer* 1988; **61:** 458-61. doi: 10.1002/1097-0142(19880201)61:3<458::aid-cncr2820610309>3.0.co;2-t

77. Chang BA, Katz S, Kompelli AR, Nathan CAO. Is primary radiotherapy an acceptable treatment modality for verrucous carcinoma of the larynx? *Laryngoscope* 2019; **129:** 1964-5. doi: 10.1002/lary.27985

78. Huang SH, Lockwood G, Irish J, Ringash J, Cummings B, Waldron J, et al. Truths and myths about radiotherapy for verrucous carcinoma of larynx. *Int J Radiat Oncol Biol Phys* 2009; **73:** 1110-5. doi: 10.1016/j.ijrobp.2008.05.021

79. Tharp ME, Shidnia H. Radiotherapy in the treatment of verrucous carcinoma of the head and neck. *Laryngoscope* 1995; **105:** 391-6. doi: 10.1288/00005537-199504000-00011

80. Demian SD, Bushkin FL, Echevarria RA. Perineural invasion and anaplastic transformation of verrucous carcinoma. *Cancer* 1973; **32:** 395-401. doi: 10.1002/1097-0142(197308)32:2<395::aid-cncr2820320217>3.0.co;2-e

81. Schwade JG, Wara WM, Dedo HH, Phillips TL. Radiotherapy for verrucous carcinoma. *Radiology* 1976; **120:** 677-9. doi: 10.1148/120.3.677

82. Naik AN, Silverman DA, Rygalski CJ, Zhao S, Brock G, Lin C, et al. Postoperative radiation therapy in oral cavity verrucous carcinoma. *Laryngoscope* 2022; **132:** 1953-61. doi: 10.1002/lary.30009

83. Wu CF, Chen CM, Shen YS, Huang IY, Chen CH, Chen CY, et al. Effective eradication of oral verrucous carcinoma with continuous intraarterial infusion chemotherapy. *Head Neck* 2008; **30:** 611-7. doi: 10.1002/hed.20751

84. Strojan P, Ferlito A, Wu CF, Rinaldo A. Intraarterial chemotherapy: a valid option in the treatment of verrucous carcinoma? *Eur Arch Oto-Rhino-Laryngology* 2010; **267:** 835-7. doi: 10.1007/s00405-009-1178-2

85. Strojan P, Šoba E, Budihna M, Auersperg M. Radiochemotherapy with vinblastine, methotrexate, and bleomycin in the treatment of verrucous carcinoma of the head and neck. *J Surg Oncol* 2005; **92:** 278-83. doi: 10.1002/jso.20422

86. De Keukeleire S, De Meulenaere A, Deron P, Huvenne W, Fréderic D, Bouckenooghe O, et al. Verrucous hyperplasia and verrucous carcinoma in head and neck: use and benefit of methotrexate. *Acta Clin Belg* 2021; **76:** 487-91. doi: 10.1080/17843286.2020.1752455

87. Karagozoglu KH, Buter J, Leemans CR, Rietveld DHF, Van Den Vijfeijken S, Van Der Waal I. Subset of patients with verrucous carcinoma of the oral cavity who benefit from treatment with methotrexate. *Br J Oral Maxillofac Surg* 2012; **50:** 513-8. doi: 10.1016/j.bjoms.2011.09.011

88. Salesiotis A, Soong R, Diasio RB, Frost A, Cullen KJ. Capecitabine induces rapid, sustained response in two patients with extensive oral verrucous carcinoma. *Clin Cancer Res* 2003; **9:** 580-5.

89. Yoshimura Y, Mishima K, Obara S, Nariai Y, Yoshimura H, Mikami T. Treatment modalities for oral verrucous carcinomas and their outcomes: contribution of radiotherapy and chemotherapy. *Int J Clin Oncol* 2001; **6:** 192-200. doi: 10.1007/PL00012104

90. Yu CH, Lin HP, Cheng SJ, Sun A, Chen HM. Cryotherapy for oral precancers and cancers. *J Formos Med Assoc* 2014; **113:** 272-7. doi: 10.1016/j.jfma.2014.01.014

91. Yeh CJ. Treatment of verrucous hyperplasia and verrucous carcinoma by shave excision and simple cryosurgery. *Int J Oral Maxillofac Surg* 2003; **32:** 280-3. doi: 10.1054/ijom.2002.0331

92. Chen HM, Yu CH, Lin HP, Cheng SJ, Chiang CP. 5-Aminolevulinic acid-mediated photodynamic therapy for oral cancers and precancers. *J Dent Sci* 2012; **7:** 307-5. doi: 10.1016/j.jds.2012.03.023

93. Chen HM, Chen CT, Yang H, Lee MI, Kuo MYP, Kuo YS, et al. Successful treatment of an extensive verrucous carcinoma with topical 5-aminolevulinic acid-mediated photodynamic therapy. *J Oral Pathol Med* 2005; **34:** 253-6. doi: 10.1111/j.1600-0714.2004.00267.x

94. Hsu CK, Lee JYY, Yu CH, Hsu MML, Wong TW. Lip verrucous carcinoma in a pregnant woman successfully treated with carbon dioxide laser surgery. Vol. 157, The British journal of dermatology. *Br J Dermatol* 2007; **157:** 813-5. doi: 10.1111/j.1365-2133.2007.08078.x

95. Azevedo LH, Galletta VC, de Paula Eduardo C, de Sousa SOM, Migliari DA. Treatment of oral verrucous carcinoma with carbon dioxide laser. *J Oral Maxillofac Surg* 2007; **65:** 2361-6. doi: 10.1016/j.joms.2006.10.024

96. Lee CN, Huang CC, Lin IC, Lee JYY, Ou CY, Wong TW. Recalcitrant lip verrucous carcinoma successfully treated with acitretin after carbon dioxide laser ablation. *JAAD case reports* 2018; **4:** 576-8. doi: 10.1016/j.jdcr.2018.02.002

review

Molecular profiling of rare thymoma using next-generation sequencing: meta-analysis

Jelena Kostic Peric[1], Andja Cirkovic[2], Sanja Srzentic Drazilov[1], Natalija Samardzic[3], Vesna Skodric Trifunovic[3,4], Dragana Jovanovic[5], Sonja Pavlovic[1]

[1] Institute for Molecular Genetics and Genetic Engineering, University of Belgrade, Belgrade, Serbia
[2] Department for Medical Statistics and Informatics, Faculty of Medicine, University of Belgrade, Serbia
[3] University Hospital of Pulmonology, Clinical Centre of Serbia, Belgrade, Serbia
[4] Faculty of Medicine, University of Belgrade, Belgrade, Serbia
[5] Internal Medicine Clinic "Akta Medica", Belgrade, Serbia

Radiol Oncol 2023; 57(1): 12-19.

Received 21 October 2022
Accepted 31 January 2023

Correspondence to: Assist. Prof. Jelena Kostic Peric, Ph.D., Institute for Molecular Genetics and Genetic Engineering, University of Belgrade, Serbia. E-mail: jelena.kostic@imgge.bg.ac.rs

Disclosure: No potential conflicts of interest were disclosed.

Background. Thymomas belong to rare tumors giving rise to thymic epithelial tissue. There is a classification of several forms of thymoma: A, AB, B1, B2, B3, thymic carcinoma (TC) and thymic neuroendocrine thymoma. In this meta-analysis study, we have focused on thymoma using articles based on the disease's next-generation sequencing (NGS) genomic profiling.

Materials and methods. We conducted a systematic review and meta-analysis of the prevalence of studies that discovered the genes and variants occurring in the less aggressive forms of the thymic epithelial tumors. Studies published before 12th December 2022 were identified through PubMed, Web of Science (WoS), and SCOPUS databases. Two reviewers have searched for the bases and selected the articles for the final analysis, based on well-defined exclusion and inclusion criteria.

Results. Finally, 12 publications were included in the qualitative as well as quantitative analysis. The three genes, *GTF2I*, *TP53,* and *HRAS*, emerged as disease-significant in the observed studies. The Odds Ratio for all three extracted genes *GTF2I* (OR = 1.58, CI [1.51, 1.66] $p < 0.00001$), *TP53* (OR = 1.36, CI [1.12, 1.65], $p < 0.002$), and *HRAS* (OR = 1.02, CI [1.00, 1.04], $p < 0.001$).

Conclusions. According to obtained data, we noticed that the *GTF2I* gene exhibits a significant prevalence in the cohort of observed thymoma patients. Moreover, analyzing published articles NGS has suggested *GTF2I, TP53,* and *HRAS* genes as the most frequently mutated genes in thymoma that have pathogenic single nucleotide variants (SNV) and Insertion/Deletion (InDel), which contribute to disease development and progression. These variants could be valuable biomarkers and target points specific to thymoma.

Key words: thymoma; next-generation sequencing (NGS); SNVs/InDels; meta-analysis

Introduction

Thymic epithelial tumors (TETs) are localized in the anterior mediastinum and comprise several forms of thymomas with different malignant potentials, aggressive forms of thymic carcinoma (TC), and thymic neuroendocrine thymoma.[1] Thymomas originate from thymic epithelial tissue. Thymoma and TC are similar and overlapping in many characteristics, but despite these histopathological and cytological features, thymomas could be considered a more benign form of TETs in comparison with TC with aggressive forms. That is the reason why thymomas and TC, exhibit

main differences in therapy approach.[2,3] Here we analyze thymoma including the following subtypes A, AB, B1, B2, and B3.[4] A and AB subtypes belong to *GTF2I*, B1, and B2 are the T-cell signaling group, B2 is as well chromosomal stability group, and B3 (atypical thymoma because is the most aggressive, if we exclude TC) belongs to the chromosomal instability group. Thymomas are classified as rare thoracic tumors with an overall incidence of 0.15 per 100 000 persons per year.[5,6] The majority of thymomas are less aggressive forms and their treatment is based on surgery, while in the case of more aggressive TC treatment approach includes multimodal therapy. This tumor characterizes high heterogeneity which is the reason for precise molecular profiling to choose an adequate precision therapy approach.[7,8] Due to the rarity of the disease, there is still a lack of information about external factors that cause diseases, such as smoke or alcohol. Moreover, epidemiological studies suggest that it is poorly known if various environmental impacts have any specific impact on disease development.[8] The role of mutated genes is one of the crucial factors for thymoma formation and development. Identification of potentially pathogenic variants is obligatory to better explain the molecular milieu of the disease. Our latest study published in January 2020 related to this pathology exhibited variants that play an important role in thymoma.[9]

To that end, advances in high-throughput technology (next-generation sequencing-NGS) have enabled assess of the mutational profiling of various types of diseases including cancer. NGS in genomics includes whole-genome sequencing (WGS), whole-exome sequencing (WES), and targeted sequencing (TS).[10] WGS covers all genomes but provides lower sequencing coverage in comparison to TS. Advances in NGS have contributed to a better understanding of molecular events that lead to disease origin as well as the development of various genetic tests and potential targeted therapy. TS approach targets specific regions of interest and is more cost-effective and often suitable for diagnostic panels which include a specific set of genes characteristic of the disease. Thus, TS provides a patient-specific mutational landscape for effective targeted therapy and better patient management.[11,12] Different approaches are used depending on the need required by the type of study. WGS represents the most comprehensive method for genome analysis and covers the entire DNA of interest. The main limitation of WGS is low sequencing coverage (25 - 30x), high cost per sample (which is lower with the increasing role of methodology), and complex and demanding computation analyzed genome, in comparison to WGS or TS.[13]

This study aimed to identify all relevant articles that evaluate the frequency of SNVs and InDels in thymomas using NGS technology through PubMed, Web of Science, and SCOPUS databases, and to perform a meta-analysis of the prevalence to get better insight into their possible involvement in thymomas. The introduction should summarize the rationale for the study or observation, citing only the essential references and stating the aim of the study.

Materials and methods

This systematic review was performed by the Preferred Reporting Items for Systematic Reviews and Meta-Analyses.[14]

Study selection Systematic review

Publications were screened for inclusion and exclusion in the meta-analysis of prevalence in two phases, and all disagreements were solved by a discussion with the third reviewer. We included studies that analyze the molecular landscape of thymoma using next-generation sequencing (NGS) genomics. Studies were excluded if they: 1) investigated related diseases but not thymoma; 2) evaluated other outcomes (NGS genomics for gene expression); 2) explored populations other than human (animal models, cell lines); 3) were abstracts; 4) were not original articles (reviews, systematic reviews, case reports, etc.).

Database search

Two researchers have conducted a meta-analysis of the prevalence of the genes and variants involved in thymoma disease. The meta-analysis of all published peer-reviewed articles related to the study was performed by searching the PubMed, Web of Science (WoS), and SCOPUS electronic databases, until the 12th of December 2022. Keywords used for article search in all databases were next-generation sequencing (NGS) and thymoma. Only publications written in English were considered. Additionally, reference lists of articles identified through electronic retrieval were manually searched, as well as relevant reviews and editorials. Experts in the field were contacted to identify other potentially relevant articles.

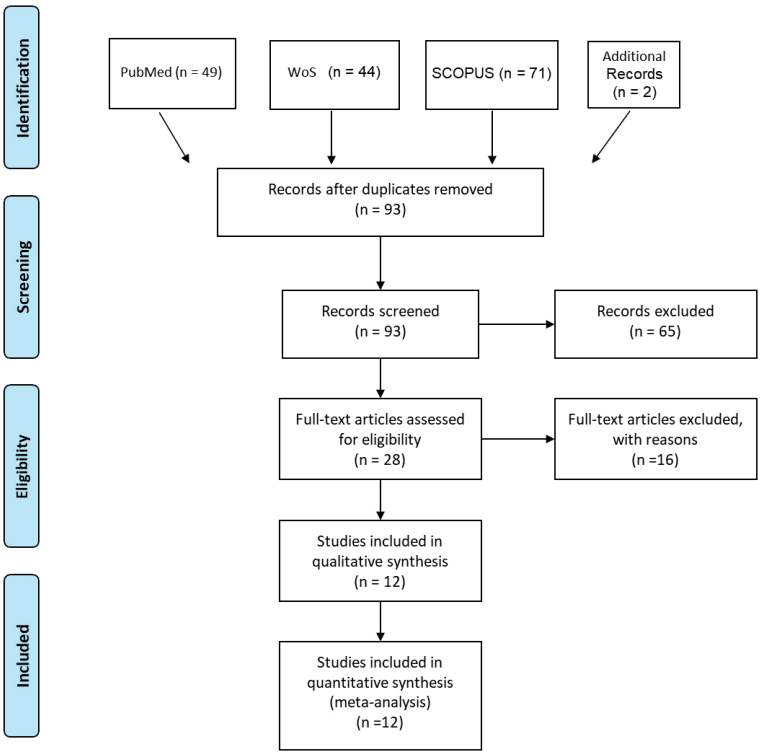

FIGURE 1. Flow chart to illustrate the process by which articles were selected or rejected for inclusion in the study.

Article screening and selection

Two reviewers (JKP, AC) independently evaluated the eligibility of all titles and abstracts. Studies were included in the full-text screening if either reviewer identified the study as being potentially eligible, or if the abstract and title did not include sufficient information. Studies were eligible for full-text screening if they included NGS genomics analysis of thymoma. TETs include thymoma and TC forms, which have been distinguished. The same reviewers independently performed full-text screening to select articles for inclusion according to the criteria listed under the Inclusion and Exclusion Criteria. Disagreements were resolved by consensus (JKP, AC) or arbitration (SP).

Data extraction and quality assessment

Two reviewers independently abstracted the following data: author(s), country of research, year of publication, study design, sample size, study population, type of thymoma, inclusion and exclusion criteria used in the original articles, method of NGS variant detection, genes harboring variants, number of patients having genes with SNVs/InDel variants. Each reviewer independently evaluated the quality of selected manuscripts.

Statistical analysis

The primary outcome was the number of patients harboring SNVs/InDels variants per gene. The odds ratio was evaluated as the ratio between patients with variants in a specific gene per total number of observed patients with thymoma.

Heterogeneity was assessed using the Chi-square Q and I2 statistics. I2 presents the inconsistency between the study results and quantifies the proportion of observed dispersion that is real, i.e., due to between-study differences and not due to random error. The categorization of heterogeneity was based on the Cochrane Handbook and states that I2 < 30%, 30% to 60%, or > 60%, corresponds to low, moderate, and high heterogeneity, respectively.[15] Funnel plots were used to evaluate publication bias. Forest plots were constructed for each analysis showing the Odds Ratio (box), 95% confidence interval (lines), and weight (size of box) for each trial. The overall effect size was represented by a diamond. A p-value < 0.05 was considered to be statistically significant. For graph plots (Forest and Funnel) we used Cohrain's RevMan 5.4 version.[16]

Results

Systematic review

The literature search for original articles was conducted according to the Preferred Reporting Items for Systematic reviews and Meta-Analysis (PRISMA) statement. A total of 166 potentially eligible publications were found in search of PubMed, WoS, and SCOPUS electronic databases PubMed 49 articles, WoS 44 articles, and SCOPUS 71. Moreover, we included 3 additional studies from an additional PubMed search (Additional records). After duplication removal, and exclusion of review articles, case reports, abstracts, investigations on animals, cell lines, and articles with unsuitable outcomes, 65 articles were excluded. After exclusion, according to previously defined criteria, 44 articles were assessed in full text. Totally, 12 full-text articles were considered for final analyses. The flow diagram represents the selection workflow of publications (Figure 1).

Selected studies have been presented with the names of studies' authors, year of published works, NGS approach, type of tumor, and genes that har-

bored any single nucleotide variants (SNVs) or small insertions/deletions (InDels) in Table 1.

The number of patients harboring or not genes with variants, as well as a total number of patients is shown in the same table. Finally, selected studies were published from 2014 to 12th December 2022. The total number of patients analyzed for *GTF2I* was 433 and 193 patients harbored SNVs/InDels variants in this gene. The total number of cases with SNVs/InDels variants was 58 in *TP53* in the group of 309 thymoma patients. The number of analyzed patients for variants in *HRAS* was 187, while 15 among them had SNVs/InDel variants. The maximum sample size per group was 270. Four studies were from China (4), Japan (2), the USA (1), Italy (1), Austria (1), France (1), Poland (1), and Serbia (1). Analyzed studies used different study designs, mostly cross-section, and case-control designs.

Meta-analysis of prevalence

The analyses of the original articles related to the next-generation sequencing genomics of thymoma have suggested the prevalence of three genes, namely, *GTF2I, TP53*, and *HRAS*. The results of analyzed genes have been represented on Forest plots (Figure 2., Figure 3., and Figure 4.) and Funnel plots (Figure 5., Figure 6., and Figure 7.) with corresponding Odds Ratio (box), Confidence Interval (CI, lines), weight (size of box), and overall size effect in diamonds.

The prevalence of the *GTF2I* gene was the highest (58%), a bit lower was for the *TP53* gene (36%) and the lowest was the *HRAS* gene (2%), for the thymoma population. According to obtained data, we pointed out genes *GTF2I* and *TP53* that exhibit the prevalence in the cohort of observed thymoma patients.

Discussion

The aim of this study was to explore genomic background of indolent forms of thymoma using genomic high-throughput approach. Thymoma epithelial tumors (TETs) comprise thymoma, thymic carcinoma (TC), and thymic neuroendocrine thymoma, as we said previously. In this meta-analysis, we take into consideration several forms of thymomas, including A, AB, B1, B2, and B3 subtypes, which have diverse invasive (malignant) potential. Thymoma is a tumor type that belongs to rare types of thoracic tumors, which is the reason for a lower number of studies that we have

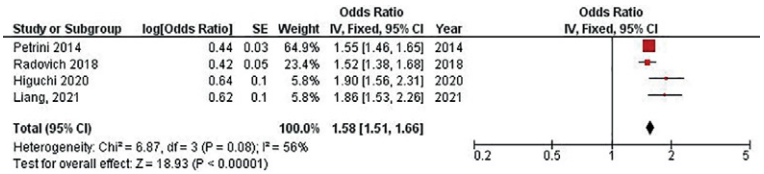

FIGURE 2. Forest plot of *GTH2I* gene in thymoma.

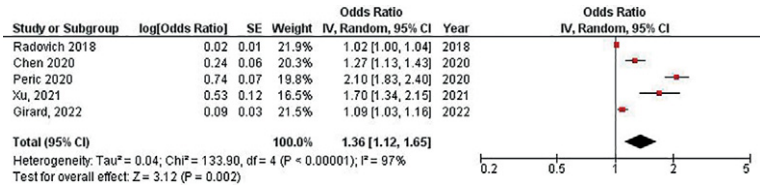

FIGURE 3. Forest plot of *TP53* gene in thymoma.

FIGURE 4. Forest plot of *HRAS* gene in thymoma.

finally selected as eligible for analysis, along with the relatively recently developed method of analysis that we have applied.

As well, keywords used in this research are limited to the NGS genomics approach to analyzing genes included in thymoma. The potential of high-throughput sequencing or NGS enables the detection of the molecular profile, typical for specific tumors or a variety of diseases. All genomic sequencing methods, including WGS, WES, and TS have been applied in the research or in diagnostics. The selection of methodology depends on all advantages or disadvantages suitable for appropriate use. Applying previously explained inclusion/exclusion criteria we were able to select and analyze articles related to this topic, and we were able to find genes associated with thymoma.

Meta-analysis of the prevalence of the gene variants that we performed using selected studies, has indicated that the majority of patients exhibited variants in *GTF2I, TP53*, and *HRAS* genes. The number of analyzed articles was relatively low, due to the rarity of the disease. Moreover, most of the studies have been published from 2014 to 2022.

The molecular background of this pathology is still poorly understood, including all types of A,

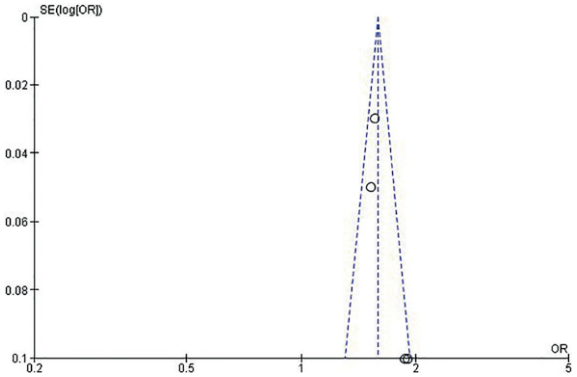

FIGURE 5. Funnel plot of *GTF2I* gene in thymoma.

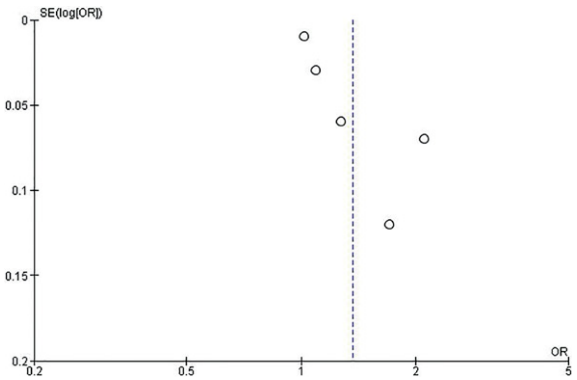

FIGURE 6. Funnel plot of *TP53* gene in thymoma.

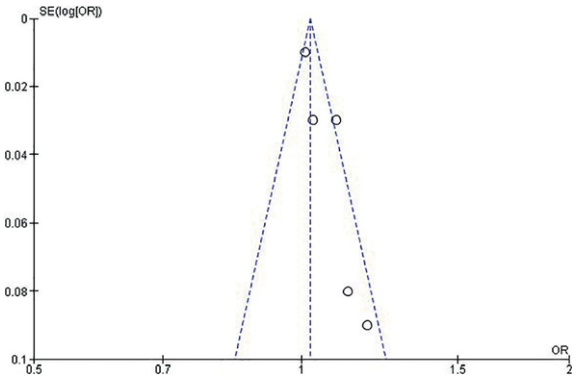

FIGURE 7. Funnel plot of *HRAS* gene in thymoma.

AB, B1, B2, and B3 thymoma. We have analyzed only NGS genomics-based articles. Further in the discussion will also be considered other methodological approaches to better explain obtained results. The newest data that appeared 2022, have indicated that *KIT* gene is an important factor in different processes related to thymoma disease. Unfortunately, we have not had enough data to demonstrate the statistical significance of this gene to put it in a group of prevalent genes for thymoma.[17,18]

GTF2I (General Transcription Factor IIi) encodes a phosphoprotein that binds to the initiator element (Inr) and Inbox element in promoters regulating transcription.[20] *GTF2I* gene is a member of a B cell receptor signaling pathway, the AKT signaling pathway (genecards.org), and is involved in crucial processes particularly, cell proliferation, cell cycle, and development.[19] Finally, the advances in next-generation sequencing characterized *GTF2I* as a master gene in TETs pathology.[20] The frequency of *GTF2I* variants is typical for less aggressive forms of thymoma.[21] *GTF2I* is a gene that embryonic aberration could lead to lethality, which indicates its essential role in embryo development.

The most pathogenic variants in this gene are Chr 7 c.1211T > A and c.1271 (COSM5095139) which could be used in targeted therapy that could lead to successful clinical application.[21,22] Despite *GTF2I* pathogenicity in thymomas, *GTF2I* mutations are very rare (< 1%) in other types of cancer, according to TCGA. Moreover, many types of molecular events lead to thymoma genesis. TCGA's studies of thymoma have shown recurrent mutations in the *GTF2I* gene and suggested this gene as a potential drug target for this disease.[23-25] Our findings confirm the prevalence of the SNVs/InDels variants in *GTF2I* in thymoma. Results have been reported in several articles which have been presented in the Forest and Funnel plots. Petrini and colleagues, using WES have discovered missense mutation Chr 7 c.1211T > A and subsequent protein change p. Leu404His in all types of thymoma A, AB, B1, B2, B3, and TC.[19,26] In the publications that we selected for analysis, *GTF2I* harbored p. Leu404His and p. Leu424His (COSM5095139) pathogenic variants, recognized as a disease-marker gene in thymoma.[22,26-28]

TP53 is a crucial tumor suppressor gene regulating the most important processes in the cell including cell cycle regulation, DNA repair, senescence, and apoptosis.[29] *TP53* has been described as the gene responsible for disease pathogenesis. A recent study has demonstrated common loss-of-function in *TP53* in type B thymomas and TCs.[30] In a study by Peric *et al*., two variants with stop codon have been identified R213* and V91*, as well as four pathogenic missense changes namely, D281N, G244S, R158C, E221K.[22,31,32] One of the newest studies by Xu S *et al*., included in our meta-

TABLE 1. Characteristics of 12 selected studies

Author	Year	Study design	Thymoma	Gene (SNV)	Number of cases	Total number of cases	NGS genomics
Chen K, China	2020	Cross-sectional	Type A, AB, B1, B2, B3	*APC* *TP53* *ATM* *AKT1* *SMAD4* *ALK* *KRAS* *NRAS*	23 12 22 5 12 19 2 2	50	TS
Enkner F, Austria	2017	Cross-sectional	Type A, B	*HRAS* *SMARCB1* *STK11*	3 1 1	19	TS
Higuchi R, Japan	2020	Cross-sectional	Type A, AB, B	*GTF2I*	14	22	TS
Petrini I, Italia	2014	Cross-sectional	Type A, AB	*GTF2I*	119	270	ES
Radovich M, USA	2017	Case-control	Type A, AB	*GTF2I* *HRAS* *TP53*	44 10 2	105	MOPA
Sakane T, Japan	2020	Cross-sectional	Type A, B2, B3, B4, B5	*HRAS* *PIK3CA* *AKT1* *RAS pathway* *EGFR pathway*	1 2 1 1 3	33	SNaPshot Multiplex
Song ZB, China	2016		Type B2, B3	*PIK3CA* *EGFR*	1 1	37	TS IonAmpliSeq
Peric J, Serbia	2020	Case-control	Type A, B1, B2, B3	*SMAD4* *APC* *ATM* *ERBB4* *TP53*	27 27 26 24 26	35	TSACP
Xu S, China	2021	Cross-sectional	Type A, AB B1, B2, B3	*TP53* *HRAS*	9 2	17	ES
Liang N, China	2021	Cross-sectional	Type A, AB, B1, B2, B3	*GTF2I*	15	24	SureSelectXT TS
Szpechcinski A, Poland	2022	Cross-sectional	Type B2B3	KIT ERBB2	1 1	19	TS
Girard N, France	2022	Cross-sectional	Type A, B1, B2, B3	KIT TP53 HRAS Other genes	1 8 1 80	90	WES

MOPA = multi-omics platform analysis; SNaPshot Multiplex = Snapshot multiplex assay for point mutation; TS = targeted enrichment-based sequencing: TSACP = TruSeq amplicon cancer panel; (WES) = whole exome sequencing

analysis, has analyzed the genomic profile of TETs that has indicated *TP53* as the most mutated gene especially in both B3 and C thymoma causing worse prognosis.[33]

HRAS gene belongs to the Ras signaling pathway, commonly mutated in many tumors harboring pathogenic variants, for instance, G13V in thymoma. One study suggests gain-off function mutations in *HRAS*, especially in type A and AB thymomas.[30] A recent study by Jovanovic D *et al.* has identified recurrent mutations in *HRAS*, marked as a thymoma-specific oncogene.[34] TCGA's studies of thymoma observed enrichment in the *HRAS* gene, as well as *NRAS* and *TP53*.[24,25] Our meta-analysis of prevalence has reported the *HRAS* gene to be involved in the pathogenesis of thymoma.[22,33,35,36] Genes that have shown the prevalence in less aggressive forms of thymoma, especially thymoma-specific oncogene *GTF2I* (transcription factor), TP53, and members of Ras family *HRAS* have been involved in crucial processes including cell cycle regulation, cell proliferation, cell differentiation, apoptosis, and cell survival. Therefore, pathogenic variants within these genes could be important

disease markers and potential therapeutic targets for thymoma.

Conclusions

Our meta-analysis of articles that analyze a mutational portrait using NGS of thymoma has pointed out *GTF2I, HRAS,* and *TP53* genes as thymoma-specific oncogenes. These genes harbor variants SNVs/InDels which contribute to disease development. Moreover, this study indicated the highest prevalence of the *GTF2I* gene (58%). Some of the identified variants are driver mutations, for instance, *GTF2I* (Chr7 c.1211T > A, p. Leu404His and c.1271T > A, p. Leu424His), associated with thymoma pathology. In addition, the majority of detected molecular changes are classified as passenger variants, unable to cause disease and further progression, without the presence of other molecular events. However, the thymoma molecular landscape is still insufficiently understood and explored. Therefore, there is a need for additional analysis and information to get a comprehensive genomic picture for better precision treatment of the patients.

Acknowledgments

This work was supported by the Ministry of Education, Science and Technological Development Republic of Serbia, EB: 451-03-68/2022-14/200042.

References

1. Cowen D, Richaud P, Mornex F, Bachelot T, Jung GM, Mirabel X, et al. Thymoma: results of a multicentric retrospective series of 149 non-metastatic irradiated patients and review of the literature. FNCLCC trialists. Federation Nationale des Centres de Lutte Contre le Cancer. *Radiother Oncol* 1995; **34:** 9-16. doi: 10.1016/0167-8140(94)01493-m
2. Levine GD, Rosai J. Thymic hyperplasia and neoplasia: a review of current concepts. *Human Pathology* 1978; **9:** 495-515. doi: 10.1016/s0046-8177(78)80131-2
3. Falkson CB, Bezjak A, Darling G, Gregg R, Malthaner R, Maziak DE, et al. The management of thymoma: a systematic review and practice guideline. *J Thorac Oncol* 2009; **4:** 911-9. doi: 10.1097/jto.0b013e3181a4b8e0
4. Okumura M, Ohta M, Tateyama H, Nakagawa K, Matsumura A, Maeda H, et al. The World Health Organization histologic classification system reflects the oncologic behavior of thymoma: a clinical study of 273 patients. *Cancer* 2002; **94:** 624-32. doi: 10.1002/cncr.10226
5. Engels EA, Pfeiffer RM. Malignant thymoma in the United States: demographic patterns in incidence and associations with subsequent malignancies. *Int J Cancer* 2003; **105:** 546-51. doi: 10.1002/ijc.11099
6. Tomaszek S, Wigle DA, Keshavjee S, Fischer S. Thymomas: review of current clinical practice. *Ann Thorac Surg* 2009; **87:** 1973-80. doi: 10.1016/j.athoracsur.2008.12.095
7. Chau NG, Kim ES, Wistuba I. The multidisciplinary approach to thymoma: combining molecular and clinical approaches. *J Thorac Oncol* 2010; **5:** S313-7. doi: 10.1097/JTO.0b013e3181f20d9a
8. Miyamoto K, Acoba JD. Thymomas and thymic carcinomas: a review on pathology, presentation, staging, treatment, and novel systemic therapies. *EMJ Respir* 2017; **5:** 100-7. doi: 10.33590/emjrespir/10310358
9. Peric J, Samaradzic N, Skodric Trifunovic V, Tosic N, Stojsic J, Pavlovic S, et al. Genomic profiling of thymoma using a targeted high-throughput approach. *Arch Med Sci* 2020. doi: 10.5114/aoms.2020.96537
10. Slatko BE, Gardner AF, Ausubel FM. Overview of next-generation sequencing technologies. *Curr Protoc Mol Biol* 2018; **122:** e59. doi: 10.1002/cpmb.59
11. Duncavage EJ, Abel HJ, Szankasi P, Kelley TW, Pfeifer JD. Targeted next generation sequencing of clinically significant gene mutations and translocations in leukemia. *Mod Pathol* 2012; **25:** 795-804. doi: 10.1038/modpathol.2012.29
12. Xu H, DiCarlo J, Satya RV, Peng Q, Wang Y. Comparison of somatic mutation calling methods in amplicon and whole exome sequence data. *BMC Genomics* 2014; **15:** 244. doi: 10.1186/1471-2164-15-244
13. Chakravarty D, Gao J, Phillips SM, Kundra R, Zhang H, Wang J, et al. OncoKB: A Precision Oncology Knowledge Base. *JCO Precis Oncol* 2017; **2017:** PO.17.00011. doi: 10.1200/PO.17.00011
14. Liberati A, Altman DG, Tetzlaff J, Mulrow C, Gotzsche PC, Ioannidis JP, et al. The PRISMA statement for reporting systematic reviews and meta-analyses of studies that evaluate health care interventions: explanation and elaboration. *J Clin Epidem* 2009; **62:** e1-34. doi: 10.1016/j.jclinepi.2009.06.006
15. Higgins JP, Thomas J, Chandler J, Cumpston M, Li T, Page M J, et al. A Cochrane handbook for systematic reviews of interventions. *Cochrane handbook for systematic reviews of interventions*. 2019. (cited 2022 Dec 19). Available at: https://training.cochrane.org/handbook
16. Cohrain Training. RevMan 5. (accessed 2021 Aug 3). Available at: https://training.cochrane.org/online-learning/core-software-cochrane-reviews/revman/revman-5-download
17. Girard N, Basse C, Schrock A, Ramkissoon S, Killian K, Ross JS. Comprehensive genomic profiling of 274 thymic epithelial tumors unveils oncogenic pathways and predictive biomarkers. *Oncologist* 2022; **27:** 919-29. doi: 10.1093/oncolo/oyac115
18. Szpechcinski A, Szolkowska M, Winiarski S, Lechowicz U, Wisniewski P, Knetki-Wroblewska M. Targeted next-generation sequencing of thymic epithelial tumours revealed pathogenic variants in KIT, ERBB2, KRAS, and TP53 in 30% of thymic carcinomas. *Cancers* 2022; **14:** 3388. doi: 10.3390/cancers14143388
19. GeneCards®: The Human Gene Database. (Updated: 2023 Jan 10). Available at: https://www.genecards.org/
20. Müllauer L. GTF2I gene mutation – a driver of thymoma pathogenesis. *Mediastinum* 2017; **1:** 11. doi: 10.21037/med.2017.11.03
21. Feng Y, Lei Y, Wu X, Huang Y, Rao H, Zhang Y, et al. GTF2I mutation frequently occurs in more indolent thymic epithelial tumors and predicts better prognosis. *Lung Cancer* 2017; **110:** 48-52. doi: 10.1016/j.lungcan.2017.05.02022
22. Radovich M, Pickering CR, Felau I, Ha G, Zhang H, Jo H, et al. The integrated genomic landscape of thymic epithelial tumors. *Cancer Cell* 2018; **33:** 244-58.e10. doi: 10.1016/j.ccell.2018.01.003
23. Liu D, Zhang P, Zhao J, Yang L, Wang W. Identification of molecular characteristics and new prognostic targets for thymoma by multiomics analysis. *BioMed Res Int* 2021; **2021:** Article ID 5587441, 1-15. doi: 10.1155/2021/5587441
24. TCGA's Study of Thymoma. (cited 2022 Dec 5). Available at: https://www.cancer.gov/about-nci/organization/ccg/research/structural-genomics/tcga/studied-cancers/thymoma
25. Venuta F, Rendina EA, Anile M, de Giacomo T, Vitolo D, Coloni GF. Thymoma and thymic carcinoma. *Gen Thorac Cardiovasc Surg* 2012; **60:** 1-12. doi: 10.1007/s11748-011-0814-0
26. Petrini I, Meltzer PS, Kim IK, Lucchi M, Park KS, Fontanini G, et al. A specific missense mutation in GTF2I occurs at high frequency in thymic epithelial tumors. *Nature Genetics* 2014; **46:** 844-9. doi: 10.1038/ng.3016

27. Higuchi R, Goto T, Hirotsu Y, Yokoyama Y, Nakagomi T, Otake S, et al. Primary driver mutations in GTF2I specific to the development of thymomas. *Cancers* 2020; **12:** 1-12. doi: 10.3390/cancers12082032

28. Liang NX, Liu L, Huang C, Liu HS, Guo C, Li J, et al. Transcriptomic and mutational analysis discovering distinct molecular characteristics among chinese thymic epithelial tumor patients. *Front Oncol* 2021; **11:** 647512. doi: 10.3389/fonc.2021.647512

29. Hafner A, Bulyk ML, Jambhekar A, Lahav G. The multiple mechanisms that regulate p53 activity and cell fate. *Nat Rev Mol Cell Biol* 2019; **20:** 199-210. doi: 10.1038/s41580-019-0110-x

30. Marx A, Belharazem D, Lee DH, Popovic ZV, Reissfelder C, Schalke B, et al. Molecular pathology of thymomas: implications for diagnosis and therapy. *Virchows Arch* 2021; **478:** 101-10. doi: 10.1007/s00428-021-03068-8

31. Chen K, Che JM, Zhang XF, Jin RS, Xiang J, Han DP, et al. Next-generation sequencing in thymic epithelial tumors uncovered novel genomic aberration sites and strong correlation between TMB and MSH6 single nucleotide variations. *Cancer Letters* 2020; **476:** 75-86. doi: 10.1016/j.canlet.2020.02.001

32. Xu S, Li XF, Zhang HY, Zu LL, Yang LQ, Shi T, et al. Frequent genetic alterations and their clinical significance in patients with thymic epithelial tumors. *Front Oncol* 2021; **11:** 667148. doi: 10.3389/fonc.2021.667148

33. Jovanovic D, Markovic J, Ceriman V, Peric J, Pavlovic S, Soldatovic I. Correlation of genomic alterations and PD-L1 expression in thymoma. *J Thorac Dis* 2020; **12:** 7561-70. doi: 10.21037/jtd-2019-thym-13

34. Enkner F, Pichlhöfer B, Zaharie AT, Krunic M, Holper TM, Janik S, et al. Molecular profiling of thymoma and thymic carcinoma: genetic differences and potential novel therapeutic targets. *Pathol Oncol Res* 2017; **23:** 551-64. doi: 10.1007/s12253-016-0144-8

35. Rajan A, Girard N, Marx A. State of the art of genetic alterations in thymic epithelial tumors. *J Thorac Oncol* 2014; **9:** S131-S6. doi: 10.1097/JTO.0000000000000298

36. Sakane T, Murase T, Okuda K, Saida K, Masaki A, Yamada T, et al. A mutation analysis of the EGFR pathway genes, RAS, EGFR, PIK3CA, AKT1 and BRAF, and TP53 gene in thymic carcinoma and thymoma type A/B3. *Histopathology* 2019; **75:** 755-66. doi: 10.1111/his.13936

research article

Multimodality CT imaging contributes to improving the diagnostic accuracy of solitary pulmonary nodules: a multi-institutional and prospective study

Gaowu Yan[1], Hongwei Li[2], Xiaoping Fan[1], Jiantao Deng[1], Jing Yan[1], Fei Qiao[3], Gaowen Yan[4], Tao Liu[1], Jiankang Chen[1], Lei Wang[1], Yang Yang[1], Yong Li[1], Linwei Zhao[1], Anup Bhetuwal[5], Morgan A McClure[6], Na Li[7], Chen Peng[8]

[1] Department of Radiology, Suining Central Hospital, Suining, China
[2] Department of Radiology, The Third Hospital of Mianyang and Sichuan Mental Health Center, Mianyang, China
[3] Department of CT and MRI, The First Affiliated Hospital, Shihezi University School of Medicine, Shihezi, China
[4] Department of Radiology, The First People's Hospital of Suining, Suining, China
[5] Sichuan Key Laboratory of Medical Imaging and Department of Radiology, Affiliated Hospital of North Sichuan Medical College, Nanchong, China
[6] Department of Radiology and Imaging; Institute of Rehabilitation and Development of Brain Function, The Second Clinical Medical College of North Sichuan Medical College Nanchong Central Hospital, Nanchong, China
[7] Department of Oncology, Suining Central Hospital, Suining, China
[8] Department of Gastroenterology, The First People's Hospital of Suining, Suining, China

Radiol Oncol 2023; 57(1): 20-34.

Received 15 August 2022
Accepted 5 December 2022

Correspondence to: Yong Li, Department of Radiology, Suining Central Hospital, Suining, China. E-mail: 13890893057@163.com and Na Li, Department of Oncology, Suining Central Hospital, Suining, China. E-mail: lny2008hy@163.com and Gaowu Yan, Department of Radiology, Suining Central Hospital, Suining, China. E-mail: yangaowu1989@163.com

Gaowu Yan, Hongwei Li, Xiaoping Fan, Jiantao Deng, Jing Yan, and Fei Qiao all have contributed equally to this study.

Disclosure: No potential conflicts of interest were disclosed.

Background. Solitary pulmonary nodules (SPNs) are one of the most common chest computed tomography (CT) abnormalities clinically. We aimed to investigate the value of non-contrast enhanced CT (NECT), contrast enhanced CT (CECT), CT perfusion imaging (CTPI), and dual- energy CT (DECT) used for differentiating benign and malignant SPNs with a multi-institutional and prospective study.

Patients and methods. Patients with 285 SPNs were scanned with NECT, CECT, CTPI and DECT. Differences between the benign and malignant SPNs on NECT, CECT, CTPI, and DECT used separately (NECT combined with CECT, DECT, and CTPI were methods of A, B, and C) or in combination (Method A + B, A + C, B + C, and A + B + C) were compared by receiver operating characteristic curve analysis.

Results. Multimodality CT imaging showed higher performances (sensitivities of 92.81% to 97.60%, specificities of 74.58% to 88.14%, and accuracies of 86.32% to 93.68%) than those of single modality CT imaging (sensitivities of 83.23% to 85.63%, specificities of 63.56% to 67.80%, and accuracies of 75.09% to 78.25%, all $p < 0.05$).

Conclusions. SPNs evaluated with multimodality CT imaging contributes to improving the diagnostic accuracy of benign and malignant SPNs. NECT helps to locate and evaluate the morphological characteristics of SPNs. CECT helps to evaluate the vascularity of SPNs. CTPI using parameter of permeability surface and DECT using parameter of normalized iodine concentration at the venous phase both are helpful for improving the diagnostic performance.

Key words: solitary pulmonary nodule; non-enhanced computed tomography; contrast-enhanced computed tomography; computed tomography perfusion imaging; dual-energy computed tomography

Introduction

A solitary pulmonary nodule (SPN) is defined as a focal, round or oval area of increased opacity in the lung with its maximum diameter no larger than 3.0 cm.[1-3] It is also one of the most common chest radiography (CR) or computed tomography (CT) abnormalities that are often identified incidentally in clinical practice with 150,000 SPNs incidentally detected in the United States on CR or CT every year.[1] It is estimated that the prevalence of SPNs in the general population is about 2.0% to 24.0%. Among those with more risk factors of lung malignancies (*e.g.* an older age, male, history of smoking or tumor, *etc.*), the prevalence of a SPN is up to 17.0% to 53.0%.[4] With the generally increased use of CT worldwide, it can be understood that more SPNs will be detected in the coming years.

The etiology of SPNs includes neoplasms (*e.g.*, primary pulmonary carcinoma, solitary metastasis, or chondroma), infection (*e.g.*, infectious granuloma or round pneumonia), inflammation (*e.g.*, rheumatoid arthritis or granulomatosis with polyangiitis), vascular (*e.g.*, arteriovenous malformation, infarct, or hematoma) and congenital abnormities (*e.g.*, sequestration or bronchogenic cyst). As a result, it is important to accurately distinguish between benign and malignant SPNs before invasive managements; especially for solid nodules with sizes of ≥ 15 mm (≥ 1767 mm^3). As the Lung-RADS guidelines have reported that their risk of malignancy is more than 15%.[2] This is because for benign SPNs, conservative treatments such as drugs or observation may suffice. While for lung cancer and other malignant SPNs, we usually need surgical treatments as soon as possible.

Compared with CR, magnetic resonance imaging (MRI), and positron emission tomography (PET), a CT plays an important role in the diagnosis and management of SPNs.[1-3,5,6] For conventional CT (non-contrast enhanced CT, NECT), it is usually used to evaluate the size, margins, contour, and internal characteristics of a SPN. For contrast enhanced CT (CECT), it helps evaluate the vascularity of a SPN. With the development of CT technologies, CT perfusion imaging (CTPI) and dual-energy CT (DECT) are increasingly used in clinical practice.[7-10] For example, in a study by Wen *et al.*[10], quantitative measures (the slope of the spectral Hounsfield Unit (HU) curve (λ_{HU}), normalized iodine concentration (NIC), CT values of 40 keV monochromatic images (CT_{40keV}), and normalized arterial enhancement fraction (NAEF)) from DECT can help to differentiate benign from malignant SPNs.

We hypothesized that multimodality CT imaging may contribute to improving the diagnostic accuracy of SPNs. However, to the authors' knowledge, there are no publications in the literature in which NECT, CECT, CTPI and DECT were comprehensively used to differentiate benign or malignant SPNs. Thus, the aim of this study was to investigate the value of NECT, CECT, CTPI, and DECT in the differentiation of benign or malignant SPNs with a multi-institutional and prospective study.

Patients and methods

Patients

This study was conducted at our three teaching hospitals and approved by the institutional review committee of Suining Central Hospital (Suining, China; approval no. LLSNCH20200004). All patients were included after providing informed consent.

Patients with SPNs were admitted and treated at one of the three hospitals from January 2019 to June 2021 and were consecutively enrolled into our study. The inclusion criteria were: (1) SPNs were detected with NECT in the lung window; (2) each SPN size is 1.5 cm–3.0 cm; (3) benign or malignant SPNs were confirmed by CT-guided percutaneous biopsy or pathology after surgery; (4) CTPI and DECT were performed within one week prior to CT-guided percutaneous biopsy or surgery; (5) SPNs were not treated by any antitumor therapies (*e.g.*, radiotherapy, chemotherapy, or targeted drug therapy); (6) age > 18 years old; and (7) patients had acceptable liver and kidney functions and no history of allergies (for example, allergic to iodine or seafood). The exclusion criteria were: (1) SPNs appearing as pure ground-glass opacity (pGGO) or as subsolid nodules that could not be measured in the mediastinal window; (2) majority components of the SPNs have been calcified or liquefactive necrosis, leading to region of interests (ROIs) cannot be drawn; (3) body mass index (BMI) is greater than 30.0 kg/m^2; (4) poor image quality (*e.g.*, significant anomalies by heart beats or others artifacts); and (5) incomplete clinical data. Three hundred and twenty-three patients were included and 38 of them were excluded because of the exclusion criteria (Figure 1).

CT examination

All patients were scanned with the same DECT system (Revolution CT, GE Healthcare, Milwaukee,

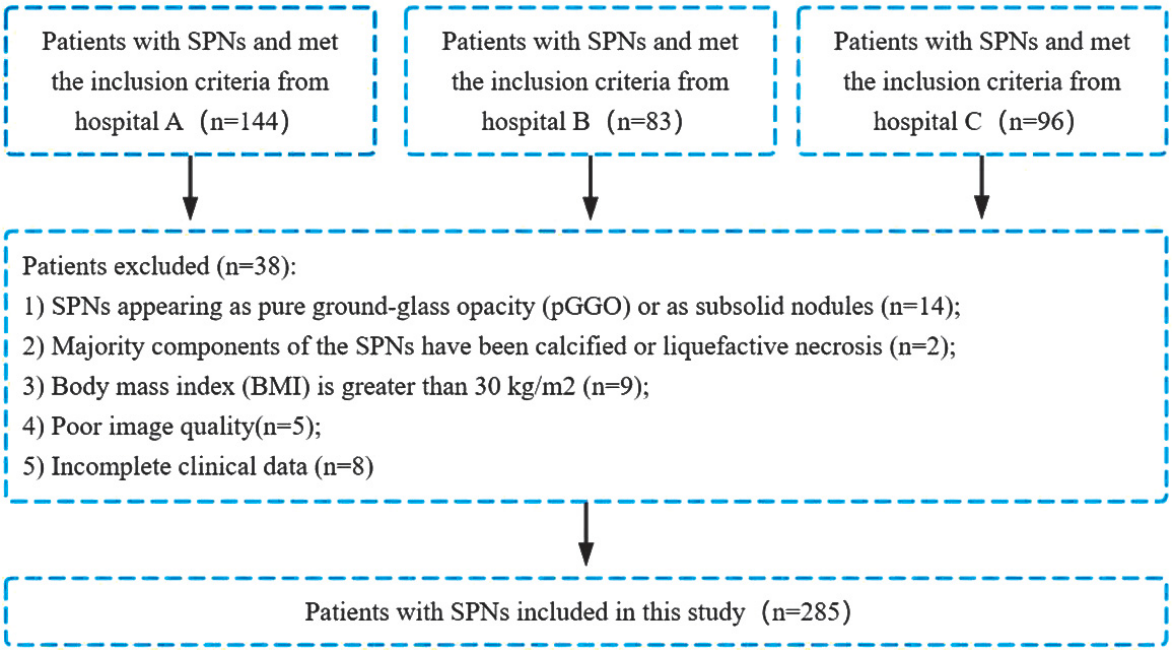

FIGURE 1. Flow chart of patient selection.

SPNs = solitary pulmonary nodules

WI, USA), and all the scanning parameters were set at the same level. The multimodality CT imaging protocol included three steps, *i.e.*, NECT, CTPI, and DECT.

For NECT, the patients were asked to hold their breath at the end of inspiration, and the scanning ranges were taken from the thoracic inlet to the bilateral costophrenic angle. The tube voltage was 100 kVp; the tube current was modulated by a SmartmA technology, which provides reasonable tube current to decrease the radiation dose; and the preset noise index was adjusted for patient circumference.

For CTPI, the patients were asked to take relaxed and slow respiration. After the position of an SPN was determined by the NECT, a GSI Chest Perfusion protocol was used with a scanning range of 3.0 cm above and below the central level of a SPN. A non-ionic iodine contrast agent of 400 mg/ml (Iomeron®, Shanghai Braccosine Pharmaceutical Co., Ltd.) was injected into an antecubital vein with a binocular power injector (Stellant D-CE, MEDRAD, Bayer Healthcare Co., Ltd.), at a flow rate of 5.0 ml/s (40.0 ml). After that, 20.0 ml of normal saline at a speed of 5.0 ml/s was used to flush the tube. The CTPI was performed after injection of the contrast medium with a delay time of 4.0 s. The tube voltage and tube current were 70 kVp and 250 mA respectively. There were 18 scanning phases with an interval of 2.5 s, and the total acquisition time was about 43.0 s.

For DECT, the patients were asked to hold their breath at the end of inspiration, and the scanning ranges were the same as the NECT. Another 50.0 ml contrast agent was injected into the antecubital vein with the binocular power injector, at a flow rate of 2.5 ml/s. After that, 20.0 ml of normal saline at a speed of 2.5 ml/s was used to flush the tube. A ROI was placed in the thoracic aorta at the level of bronchial bifurcation, and the threshold was set to 120 HU. After reaching the threshold, the arterial phase was scanned with a delay time of 7.0 s, and the venous phase delay time was 30.0 s. The tube voltage, tube current, and noise index were the same as the NECT.

The same scanning parameters for NECT, CTPI, and DECT were: detector coverage = 80 mm; pitch = 0.992: 1; coverage speed = 158.75 mm/s; rotation time = 0.5 s; preset adaptive statistical iterative reconstruction-V (ASIR-V) = 50%; postset ASIR-V = 60%; slice thickness = 5.0 mm; slice interval = 5.0 mm; reconstructed slice thickness = 1.25 mm; reconstructed slice interval = 1.25 mm.

Measurement of radiation dose

After the multimodality CT imaging protocol, the volume CT dose index ($CTDI_{vol}$, mGy) and dose-

length product (DLP, mGy.cm) were recorded. The estimated effective dose (ED, mSv) was calculated with the formula: ED = DLP × *k*, where the *k* equals 0.014 mSv/mGy.cm.

Images post-processing

For NECT, the lung window images were further processed with the post-processing workstation AW 4.7 (GE Healthcare, Milwaukee, WI, USA) to obtain multiplanar reconstruction (MPR) coronal and sagittal images (1.25 mm).

For CTPI, the images were transferred to the post-processing workstation AW 4.7 (GE Healthcare, Milwaukee, WI, USA), CTPI parameters of the blood volume (BV, ml/100 g), blood flow (BF, ml/100 g/min), mean transit time (MTT, s), and permeability surface (PS, ml/100 g/min) with their perfusion artificial color maps were automatically generated by the CT perfusion 4D software. The ROI should be placed in the soft tissue area of a SPN at its maximum plane, and the thoracic aorta at the same level plane was selected as the reference vessel for calculating the arterial input function and a time density curve (TDC). When placing a ROI, the calcification, bleeding, liquefaction necrosis area, blood vessels, and anomalies by heart beats or other artifacts should be avoided as much as possible.

For DECT, the arterial and venous phase mediastinal window images were respectively processed with the GSI volume viewer software (AW 4.7, GE Healthcare, Milwaukee, WI, USA), to obtain the arterial and venous phase iodine-based images. The following principles should be followed in outlining the ROI: (1) ROI should be placed in the solid area of a SPN with uniform enhancement, and the outlined area should be as large as possible; (2) the calcification, bleeding, liquefaction necrosis area, blood vessels, and anomalies by heart beats or others artifacts should be avoided as much as possible; (3) the position and size of ROI measurement in each phase should be consistent.

Parameter measurements

The parameter measurements for CTPI, DECT, and the CT enhancement amplitude value were independently measured by two senior radiologists with more than 15 years of experience in chest CT. All indices were measured two times, and the average values were taken as the final results. Disagreements were resolved through consensus. Parameter measurements for CTPI included BV, BF, MTT, and PS. Parameter measurements for DECT included iodine overlay (OL), iodine concentration (IC), and normalized iodine concentration (NIC) at the arterial and venous phases (*i.e.*, aOL, vOL, aIC, vIC, aNIC, and vNIC). The NIC was calculated with the formulae: $NIC = IC_{SPN} / IC_{Thoracic\ aorta}$. The CT values of a SPN at the venous CECT and NECT phases were also measured, and the CT enhancement amplitude value was calculated with the formula: CT enhancement amplitude value = venous CECT value - NECT value.

Multimodality CT imaging for evaluating SPN

First, another two senior radiologists with more than 15 years of experience in chest CT randomly and independently interpreted the conventional NECT images of each SPN. Any disagreements were solved through consensus. The SPNs were then classified into five categories, *i.e.*, I = most likely benign, II = possibly benign, III = uncertain benign or malignant, IV = possibly malignant, and V = most likely malignant. The diagnostic methods were as follows: NECT combined with CECT (Method A), and the diagnostic criteria for CT enhancement were[1]: a CT enhancement amplitude value of 20–60 HU was classified as malignant, and a CT enhancement amplitude value of less than 20 HU or more than 60 HU was classified as benign; NECT combined with DECT (Method B); NECT combined with CTPI (Method C). If methods A, B, or C were consistent when classifying a benign or malignant SPN, the SPN would be judged as benign or malignant. However, if methods A, B, or C were not consistent when classifying a benign or malignant SPN, the following principles would be followed: (1) if a benign or malignant SPN was definitely diagnosed as category I or V by NECT, the diagnostic results of CECT, DECT and CTPI would not be considered, and the SPN would be directly characterized as benign or malignant; (2) if the nature of a benign or malignant SPN could not be confirmed by NECT (*i.e.* a category of II, III or IV SPN), the final diagnosis would be made according to the diagnostic thresholds of CECT, DECT and CTPI, respectively. There were four combined diagnostic methods: method A + B, method A + C, method B + C, and method A + B + C (Figure 2). In combined diagnostic methods, the results of benign or malignant SPNs may be inconsistent according to the diagnostic thresholds of CECT, CTPI or DECT. Our method is that if a SPN is diagnosed as malignant according to one of

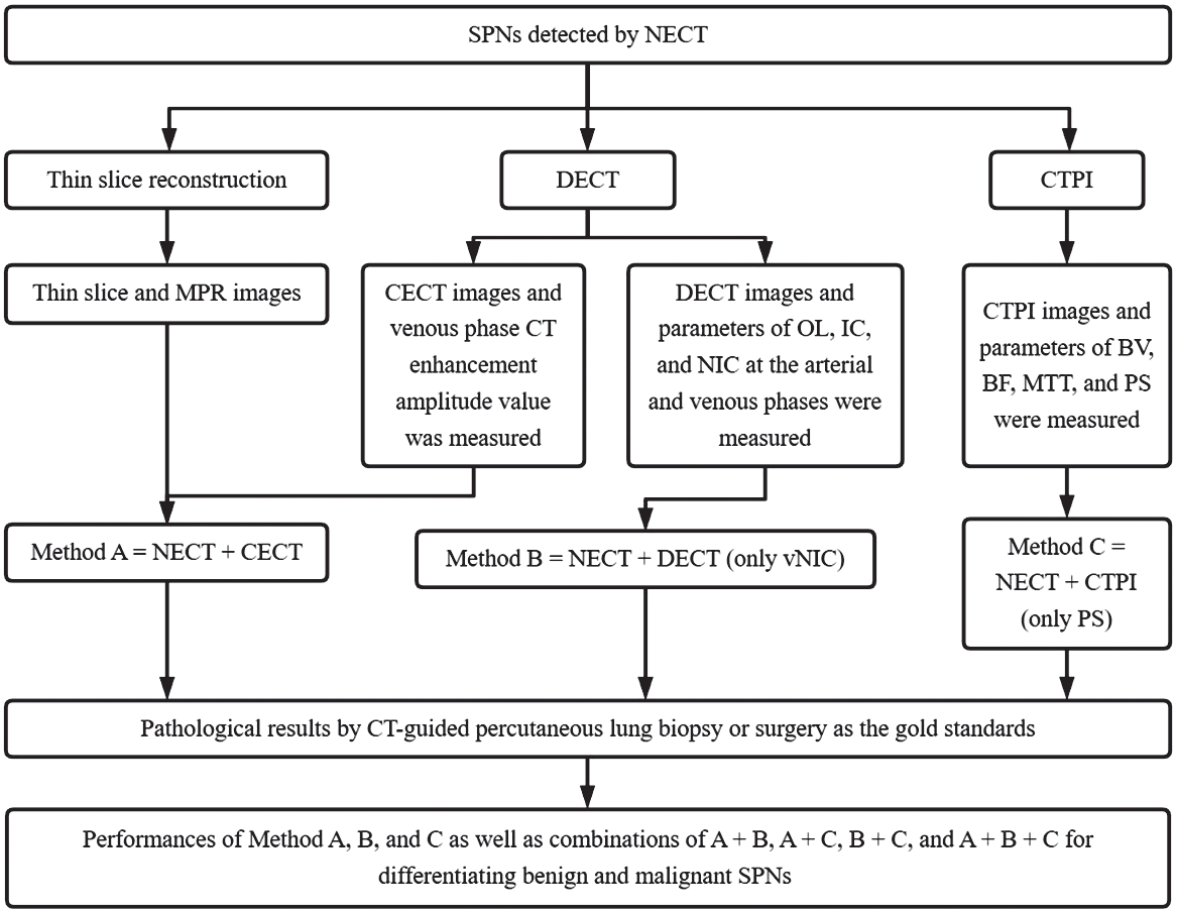

FIGURE 2. Technology roadmap of multimodality computed tomography (CT) imaging for evaluating solitary pulmonary nodules (SPNs).

BF = blood flow; BV = blood volume; CECT = contrast enhanced CT; CTPI = CT perfusion imaging; DECT = dual-energy CT; IC = iodine concentration; MPR = multiplanar reconstruction; NECT = non-contrast enhanced CT; MTT = mean transit time; NIC = normalized iodine concentration; OL = iodine overlay; PS = permeability surface

the thresholds (CECT, CTPI, or DECT), it would be preliminarily categorized as malignant; then, the result would be compared with the pathological result to calculate the sensitivity, specificity and accuracy of the combined diagnostic method.

Statistical analysis

Measurement data were expressed as the mean ± standard deviation or median and interquartile range (P_{25}, P_{75}). The comparisons were performed with the two independent samples *t*-test or Mann Whitney rank sum test, as appropriate. The count data were expressed as the percentage (%) or composition, and the comparisons were performed with the Fisher's exact test. Receiver operating characteristic (ROC) curve analysis was performed on statistically significant CTPI and DECT parameters to obtain the area under the curves (AUC) and diagnostic thresholds, and the Delong-test was performed to compare the differences.[11]

In using the pathological diagnosis as the gold standard, the sensitivities, specificities, accuracies, positive predictive values (PPVs) and negative predictive values (NPVs) of the three diagnostic methods separately used (Method A, B, and C) and in combination (Method A + B, Method A + C, Method B + C, and Method A + B + C) for the diagnosis of benign and malignant SPNs were calculated, and the McNemar's test was used to compare the sensitivity, specificity, and accuracy of the various diagnostic methods.

All statistical analyses were performed by using the software of GraphPad Prism 8.0.0 and MedCalc 19.5.3. Significant differences were set at a p value < 0.05.

Results

Patient characteristics

Ultimately, 285 SPNs were included in this study. Of these, 178 (62.46%, 178/285) SPNs were confirmed by CT-guided percutaneous biopsy, and 107 (37.54%, 107/285) SPNs were confirmed by pathology after surgery. The patients' characteristics are shown in Table 1. There were no significant differences between the malignant and benign SPNs relative to gender, age, smoking status, history of tumors, or tumor biomarkers (all p values > 0.05).

Pathological results

Of the 285 SPNs, 118 were benign SPNs (41.4%, 118/285) and 167 were malignant SPNs (58.6%, 167/285). Of the 118 benign SPNs, 46 were tuberculosis (29.0%, 46/118), 32 were acute and chronic inflammation (27.1%, 32/118), and 14 were inflammatory pseudotumors (11.9%, 14/118). Of the 167 malignant SPNs, 116 (69.5%, 116/167) were primary pulmonary carcinomas (including adenocarcinomas in 52, squamous cell carcinomas in 35, and small cell lung cancer in 17, *etc*.), 23 (13.8%, 23/167) were solitary metastasis (this included five from the liver, five from the breast, etc). Pathological results of the 285 SPNs included in this study are shown in Table 2.

Radiation dose

After the multimodality CT imaging protocol, the $CTDI_{vol}$, DLP, and ED in the SPNs were 66.88 ± 4.36 mGy, 768.29 ± 91.65 mGy.cm, and 10.76 ± 1.28 mSv, respectively.

NECT and CECT in evaluating SPNs

In the malignant SPNs (n = 167), 49 (29.34%, 49/167), 115 (68.86%, 115/167), 108 (78.81%, 108/167), 38 (22.75%, 38/167), 89 (53.29%, 89/167), and 84 (50.30%, 84/167) cases were seen with smooth margins, lobulated sign, spiculated sign, vacuole sign, pleural indentation, and vessel convergence, respectively. In the benign SPNs (n = 118), the same CT findings were seen in 84 (71.19%, 84/118), 29 (24.58%, 29/167), 25 (21.19%, 25/118), 13 (11.02%, 13/118), 25 (21.19%, 25/118), and 33 (27.97%, 33/118) cases (Table 3), respectively. There were significant differences between the malignant and benign SPNs in above mentioned findings on NECT (all p values were < 0.05). However, no significant differences were noted between the malignant and benign SPNs in cavity sign, air bronchogram, calcification, fat (defined as CT attenuation of -40 HU to -120 HU), adjacent bronchial changes, location, or size on NECT (all p values were > 0.05).

TABLE 1. Patient characteristics in 285 patients with solitary pulmonary nodules

Characteristics	Pathology		*P* value
	Benign SPNs (n = 118)	Malignant SPNs (n = 167)	
Gender*			
Male	56 (47.46%)	96 (57.49%)	0.1170
Female	62 (52.54%)	71 (42.51%)	
Age (years)#	50.84 ± 19.60	52.93 ± 20.30	0.3952
Smoking status*			
Yes	52 (44.07%)	81 (48.50%)	0.4721
No	66 (55.93%)	86 (51.50%)	
Tumor history*			
Yes	17 (14.41%)	28 (16.77%)	0.6245
No	101 (85.59%)	139 (83.23%)	
Tumor biomarkers*			
Normal	103 (87.29%)	139 (83.23%)	0.4026
Abnormal	15 (12.71%)	28 (16.77%)	

SPNs = solitary pulmonary nodules; *compared with the Fisher's exact test; #compared with the two independent samples t-test

TABLE 2. Pathological results of the 285 solitary pulmonary nodules (SPNs) included in this study

SPNs	Pathology	Datum (%)
Benign SPNs (n = 118)		
	Tuberculosis	46 (29.0%)
	Acute and chronic inflammation	32 (27.1%)
	Inflammatory pseudotumor	14 (11.9%)
	Hamartoma	9 (7.6%)
	Pulmonary sclerosing hemangioma	6 (5.1%)
	Sequestration	4 (3.4%)
	Bronchogenic cyst	3 (2.5%)
	Rheumatoid arthritis	2 (1.7%)
	Granulomatosis with polyangiitis	2 (1.7%)
Malignant SPNs (n = 167)		
	Primary pulmonary carcinoma	116 (69.5%)
	Solitary metastasis	23 (13.8%)
	Primary lung neuroendocrine tumor	21 (12.6%)
	Primary pulmonary lymphoma	7 (4.2%)

TABLE 3. Solitary pulmonary nodules evaluated with non-contrast enhanced CT

CT findings*	Benign SPNs (n = 118)	Malignant SPNs (n = 167)	*P* Values
Smooth margin			
Yes	84 (71.19%)	49 (29.34%)	< 0.0001
No	34 (28.81%)	118 (70.66%)	
Lobulated sign			
Yes	29 (24.58%)	115 (68.86%)	< 0.0001
No	89 (75.42%)	52 (31.14%)	
Spiculated sign			
Yes	25 (21.19%)	108 (78.81%)	< 0.0001
No	93 (64.67%)	59 (35.33%)	
Vacuole sign			
Yes	13 (11.02%)	38 (22.75%)	0.0120
No	105 (88.98%)	129 (77.25%)	
Cavity sign			
Yes	9 (7.63%)	16 (9.58%)	0.6727
No	109 (92.37%)	151 (90.42%)	
Air bronchogram			
Yes	33 (27.97%)	56 (33.53%)	0.3643
No	85 (72.03%)	111 (66.47%)	
Calcification			
Yes	10 (8.47%)	6 (3.59%)	0.1149
No	108 (91.53%)	161 (96.41%)	
Fat			
Yes	6 (5.08%)	4 (2.40%)	0.3277
No	112 (94.92%)	163 (97.60%)	
Pleural indentation			
Yes	25 (21.19%)	89 (53.29%)	< 0.0001
No	93 (78.81%)	78 (46.71%)	
Vessel convergence			
Yes	33 (27.97%)	84 (50.30%)	0.0002
No	85 (72.03%)	83 (49.70%)	
Adjacent bronchial changes			
Yes	26 (22.03%)	43 (25.75%)	0.4867
No	92 (77.97%)	124 (74.25%)	
Location			
Upper and middle lobes	53 (44.92%)	79 (47.31%)	0.7186
Inferior lobe	65 (55.08%)	88 (52.69%)	
Size (mm)			
15–20	29 (24.58%)	46 (27.54%)	0.5883
20–30	89 (75.42%)	121 (72.46%)	

SPNs = solitary pulmonary nodules; *compared with the Fisher's exact test

For the classification of SPNs (Table 4), among the 118 benign SPNs, there were 39, 9, 48, 22, and 0 SPNs that were classified as the Category I, II, III, IV, and V nodules, respectively. Among the 167 malignant SPNs, there were 0, 5, 54, 19, and 89 SPNs that were classified as the Category I, II, III, IV, and V nodules, respectively.

For CECT, among the 167 malignant SPNs, 118 cases (70.66%, 118/167) were noted with a CT enhancement amplitude value of 20–60 HU; and among the 118 benign SPNs, 75 cases (63.56%, 75/118) were noted with a CT enhancement amplitude value of less than 20 HU or more than 60 HU (Figure 3).

CTPI in evaluating SPNs

The parameters of BF, BV, MTT, and PS of CTPI in malignant SPNs were higher than those of benign SPNs (Figure 4, Table 5). However, there was only significant difference in the PS parameter ($p < 0.05$). A ROC curve analysis was performed on the PS parameter for differentiating benign and malignant SPNs (Figure 5). It showed an AUC of 0.739 (95% confidence interval of 0.684–0.789, $p < 0.0001$) with the sensitivity, specificity, and diagnostic threshold of 85.03 %, 66.10%, and 9.88 ml/100g/min, respectively.

DECT in evaluating SPNs

For DECT in evaluating SPNs (Figure 6), parameters of aOL, vOL, aIC, vIC, aNIC, and vNIC in malignant SPNs were significantly higher than those of benign SPNs (all p values were < 0.05, Table 6). ROC curve analyses were performed on these parameters for differentiating benign and malignant SPNs (Figure 7). The AUCs, sensitivities, and specificities were 0.636 to 0.790, 59.88% to 75.45%, and 61.02% to 80.51%, respectively. The diagnostic thresholds were 13.89 HU, 12.79 HU, 0.65 mg/ml, 0.85 mg/ml, 0.12, and 0.35, respectively (Table 7). Compared with the AUC of aOL, vOL, aIC, vIC, and aNIC by the Delong test, vNIC had the largest AUC (all p values < 0.05, Table 8).

Multimodality CT imaging in evaluating SPNs

For methods A, B, C, A+B, A+C, B+C, and A+B+C, the sensitivities, specificities, accuracies, PPVs, and NPVs were 83.23% to 97.60%, 63.56% to 88.14%, 75.09% to 93.68%, 76.37% to 92.09%, and 72.82% to 96.30%, respectively (Table 9).

There were no significant differences between the methods A, B, and C in sensitivities, specificities, and accuracies, and so did the methods A+B, A+C, B+C, and A+B+C (all p values > 0.05). However, the methods A+B, A+C, B+C, and A+B+C all had higher sensitivities, specificities, and accuracies than the methods A, B, and C for distinguishing benign from malignant SPNs (all p values < 0.05).

Discussion

NECT and CECT in evaluating SPNs

As low-dose CT scanning is more and more widely used in the early screening of lung cancers, to some extent, NECT scanning has become one of the most commonly used examination modalities for SPNs.[12] In addition to confirming the location, NECT is also used to perform a morphologic evaluation of SPNs. Generally speaking, the smaller the SPN, the more likely it is to be a benign lesion. In terms of the margins and contours of an SPN, it can be classified as smooth, lobulated, irregular, or spiculated.[1,5,6] Studies have reported that about 80% of benign SPNs are not larger than 2.0 cm in diameter.[1,5,6,13] However, some studies showed that about 15% of malignant SPNs are not larger than 1.0 cm in diameter, and 42% of malignant SPNs are not larger than 2.0 cm in diameter.[1,14] Most benign SPNs have smooth and well-defined margins. However, about 21% of malignant SPNs have well-defined margins.[15] A lobulated, irregular, or spiculated contour is usually associated with a malignant SPN. However, lobulation also occurs in up to 25% of benign SPNs.[16] Therefore, there are considerable overlaps in the size, margins, and contours of benign and malignant SPNs. Internal characteristics (*e.g.* homogeneous attenuation, cavitation, intranodular fat, presence and pattern of intranodular calcification, *etc.*) and abnormalities surrounding nodules (*e.g.* pleural indentation, vessel convergence, adjacent bronchial changes, *etc.*) are also helpful for distinguishing benign from malignant SPNs.[1] For example, intranodular fat and a popcorn like calcification are typical findings seen in hamartomas. However, intranodular fat or calcification alone cannot be used to differentiate benign from malignant SPNs confidently.

In our study, there were significant differences between the malignant and benign SPNs only in smooth margins (29.34% *vs* 71.19%), lobulated sign (68.86% *vs* 24.58%), spiculated sign (78.81% *vs* 21.19%), vacuole sign (22.75% *vs* 11.02%), pleural indentation (53.29% *vs* 21.19%), and vessel con-

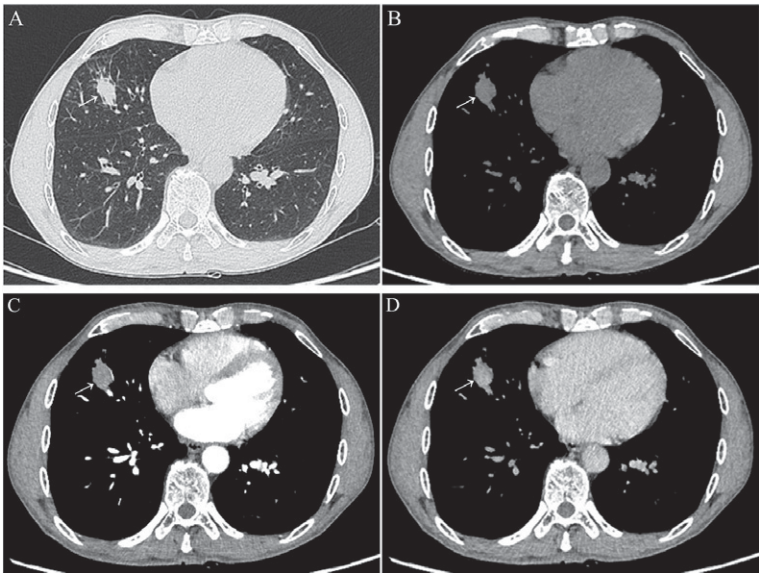

FIGURE 3. A solitary pulmonary nodule (SPN) with the size of 17.0 × 19.0 mm located in the middle lobe of right lung of a 59 years old male. Non-contrast enhanced CT (NECT), both upper **(A)** and **(B)** images, showed that there was sign of smooth margin, but without signs of lobulation, spiculation, vacuole, cavitation, air bronchogram, calcification, fat, pleural indentation, vessel convergence, or adjacent bronchial changes. Contrast enhanced CT (CECT) showed that there were mild and obvious enhancements in the arterial **(C)** and venous **(D)** phases, respectively. The patient was scanned with a CT-guided percutaneous lung biopsy procedure, and the pathological result showed chronic inflammatory disease. This SPN disappeared after a week of antibiotic therapy.

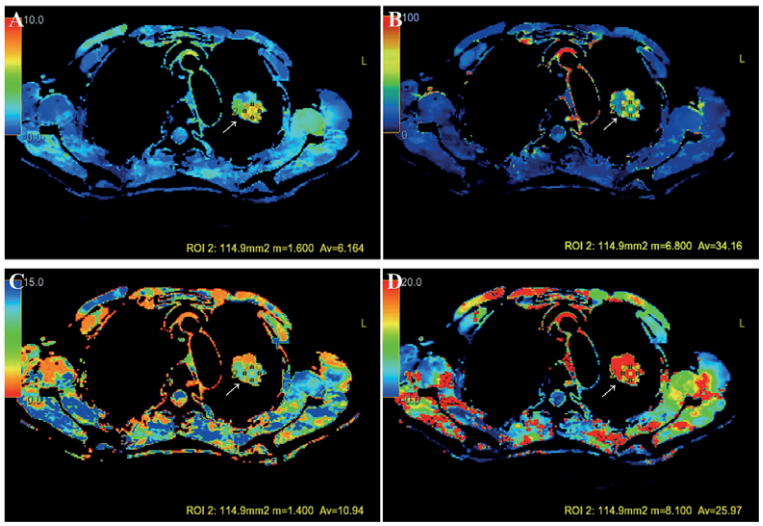

FIGURE 4. A solitary pulmonary nodule (SPN) with the size of 25.0 × 27.0 mm located in the superior lobe of left lung of a 61 years old female evaluated by CT perfusion imaging (CTPI). Blood volume (BV) **(A)**, blood flow (BF) **(B)**, mean transit time (MTT) **(C)**, and permeability surface (PS) **(D)** for the SPN were 6.16 ml/100 g, 34.16 ml/100 g/min, 10.94 s, and 25.97 ml/100 g/min, respectively. Pathology of the SPN after the surgery confirmed the diagnosis of an adenocarcinoma.

TABLE 4. Non-enhanced computed tomography (NECT) in evaluating solitary pulmonary nodules (SPNs) with various categories in 285 patients

Items	Category I	Category II	Category III	Category IV	Category V
Benign SPNs (n = 118)	39	9	48	22	0
Malignant SPNs (n = 167)	0	5	54	19	89

Category I = most likely benign; Category II = possibly benign; Category III = uncertain benign or malignant; Category IV = possibly malignant; Category IV = most likely malignant

TABLE 5. Solitary pulmonary nodules evaluated with CT perfusion imaging

Parameters*	Benign SPNs (n = 118)	Malignant SPNs (n = 167)	*P* values
BF (ml/100 g/min)	49.34 (27.78, 72.81)	58.44 (24.91, 80.47)	0.1022
BV (ml/100 g)	4.79 (2.87, 7.66)	4.84 (2.90, 7.74)	0.1829
MTT (s)	6.71 (3.05, 9.58)	7.66 (3.83, 10.54)	0.2034
PS (ml/100 g/min)	8.89 (4.94, 12.45)	14.37 (11.50, 16.29)	< 0.0001

BF = blood flow; BV = blood volume; CT = computed tomography; MTT = mean transit time; PS = permeability surface; SPNs = solitary pulmonary nodules; *compared with the Mann Whitney rank sum test

TABLE 6. Solitary pulmonary nodules (SPNs) evaluated with dual-energy CT

Parameters*	Benign SPNs (n = 118)	Malignant SPNs (n = 167)	*P* Values
aOL (HU)	13.24 (10.97, 21.58)	19.58 (13.29, 26.07)	< 0.0001
vOL (HU)	11.09 (10.09, 14.86)	14.99 (10.59, 23.98)	< 0.0001
aIC (mg/ml)	0.69 (0.47, 0.985)	1.13 (0.70, 1.56)	< 0.0001
vIC (mg/ml)	0.55 (0.44, 1.00)	0.97 (0.50, 1.46)	< 0.0001
aNIC	0.10 (0.06, 0.13)	0.18 (0.11, 0.25)	< 0.0001
vNIC	0.23 (0.13, 0.32)	0.54 (0.43, 0.65)	< 0.0001

aIC = Iodine concentration at the arterial phase; aNIC = normalized iodine concentration at the arterial phase; aOL = Iodine overlay at the arterial phase; CT = computed tomography; HU = Hounsfield unit; SPNs = solitary pulmonary nodules; vIC = Iodine concentration at the venous phase; vNIC = normalized iodine concentration at the venous phase; vOL = Iodine overlay at the venous phase; *compared with the Mann Whitney rank sum test

vergence (50.30% *vs* 27.97%) on NECT (all p values < 0.05). Our results are consistent with some previous studies.[17-19] Some previous studies also reported that these findings on NECT are risk factors for malignant SPNs. However, we did not identify cavity sign, air bronchogram, calcification, fat, adjacent bronchial changes, location, or size as risk factors for malignant SPNs (all p values > 0.05). This may be explained by the number of patients with SPNs included in our and previous studies which varied largely. Our results and previous studies also showed considerable overlaps in the findings of benign and malignant SPNs on NECT. Therefore, when we performed the classification of the 285 SPNs, there were 157 cases that were classified as the Category II, III, and IV nodules.

For CECT, it is helpful to improve the accuracy of differential diagnosis between benign and malignant SPNs. The degree of enhancement is directly associated with the possibility of malignancy and the vascularity of the SPNs. Swensen *et al.*[20] reported that nodular enhancement of more than 20 HU on CECT highly implies a malignant SPN. Whereas, nodular enhancement of less than 15 HU on CECT typically indicates a benign SPN, with a sensitivity, specificity, accuracy, PPV, and NPV of 98%, 58%, 77%, 68%, and 96%, respectively. In our study, the diagnostic criteria for CT enhancement were: a CT enhancement amplitude value of 20–60 HU was classified as malignant, and a CT enhancement amplitude value of less than 20 HU or more than 60 HU was classified as benign. We also want to highlight that CT postprocessing technology of thin-section and multiplanar reconstruction (MPR) are indeed beneficial when differentiating benign and malignant SPNs. This is because more details would be identified with thin-section CT and MPR. On the other hand, comprehensive morphological features evaluation is far better than a single morphological features assessment because more negative (or positive) morphological features will increase the likelihood of a malignant (or benign) SPN.

CTPI in evaluating SPNs

CTPI allows the derivation of several physiologic parameters, including BV, BF, MTT, and PS. BV is defined as the integral under a corrected attenuation curve for enhancement values from a contrast material bolus. It is a relative measure of the blood volume within small vessels in a region of specific tissue. BV is related to the number and diameter of open vessels, *etc.* MTT is a measure of the time it takes for blood to pass through small vessels. BF refers to the blood flow passing through a section of the blood vessel in unit time which is related

TABLE 7. Solitary pulmonary nodules evaluated with dual-energy CT

Parameters	AUC	Threshold	Sensitivity	Specificity	95% CI	*P* values
aOL (HU)	0.636	13.89	70.66	61.02	0.577–0.692	< 0.001
vOL (HU)	0.638	12.79	59.88	72.03	0.580–0.694	< 0.001
aIC (mg/ml)	0.657	0.65	67.66	69.49	0.599–0.712	< 0.001
vIC (mg/ml)	0.703	0.85	68.86	71.19	0.646–0.755	< 0.001
aNIC	0.728	0.12	67.66	74.58	0.672–0.778	< 0.001
vNIC	0.790	0.35	75.45	80.51	0.738–0.836	0.0001

aIC = Iodine concentration at the arterial phase; aNIC = normalized iodine concentration at the arterial phase; aOL = Iodine overlay at the arterial phase; AUC = area under the curve; CT = computed tomography; HU = Hounsfield unit; vIC = Iodine concentration at the venous phase; vOL = Iodine overlay at the venous phase; vNIC = normalized iodine concentration at the venous phase

95 % CI = 95 % confidence interval

TABLE 8. Pairwise comparison of AUC of dual energy CT parameters in 285 patients with solitary pulmonary nodules

Parameters*	*Z* statistic	*P* value
aOL *vs* vOL	0.0995	0.9207
aOL *vs* aIC	0.813	0.4162
aOL *vs* vIC	2.485	0.0129
aOL *vs* aNIC	3.171	0.0015
aOL *vs* vNIC	5.170	< 0.0001
vOL *vs* aIC	0.702	0.4829
vOL *vs* vIC	2.567	0.0103
vOL *vs* aNIC	3.280	0.0010
vOL *vs* vNIC	5.345	< 0.0001
aIC *vs* vIC	2.034	0.0420
aIC *vs* aNIC	2.755	0.0059
aIC *vs* vNIC	4.728	< 0.0001
vIC *vs* aNIC	1.036	0.3001
vIC *vs* vNIC	3.227	0.0013
aNIC *vs* vNIC	2.708	0.0068

aIC = Iodine concentration at the arterial phase; aOL = Iodine overlay at the arterial phase; aNIC = normalized iodine concentration at the arterial phase; AUC = area under the curve; CT = computed tomography; vIC = Iodine concentration at the venous phase; vNIC = normalized iodine concentration at the venous phase; vOL = Iodine overlay at the venous phase; *compared with the DeLong test

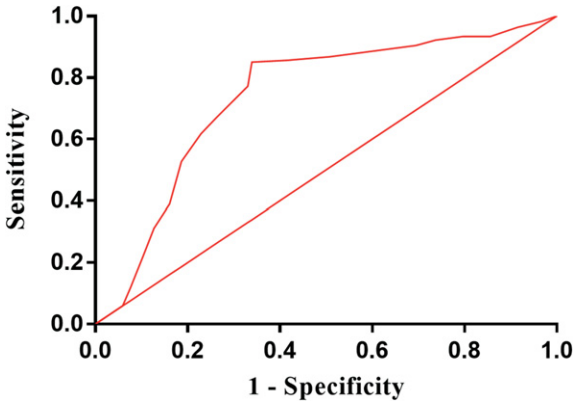

FIGURE 5. Receiver operating characteristic curve for distinguishing benign from malignant nodules using CT perfusion imaging parameter of permeability surface (PS).

to the patency of drainage vein, lymphatic reflux, blood volume level, *etc.* BF is calculated with the equation: BF = BV/MTT, where BV is blood volume and MTT is mean transit time. PS refers to the diffusion coefficient of the unidirectional transmission velocity of the contrast agent through capillary endothelial cells.

CTPI can be used to evaluate the perfusion and vascularity of lesions in the lung and many other organs.[21-28] Wang *et al.*[21] reported that parameters of CTPI (including BF, BV and PS but not MTT) of SPNs were significantly correlated with SPNs' microvessel density (MVD) and luminal vascular parameters such as luminal vascular number (LVN), luminal vascular area (LVA), and luminal vascular perimeter (LVP). Huang *et al.*[22] analyzed the CT perfusion parameters (BF, BV, MTT, and PS) and the microvessel parameters (MVD, LVN, LVA, and LVP) in the non-small cell lung cancer (NSCLC) patients with and without lymph node metastasis.

In our study, only the PS parameter of CTPI was found to be significant difference between the malignant and benign SPNs ($p < 0.05$), and a ROC curve analysis performed on the PS parameter showed that the AUC, sensitivity, specific-

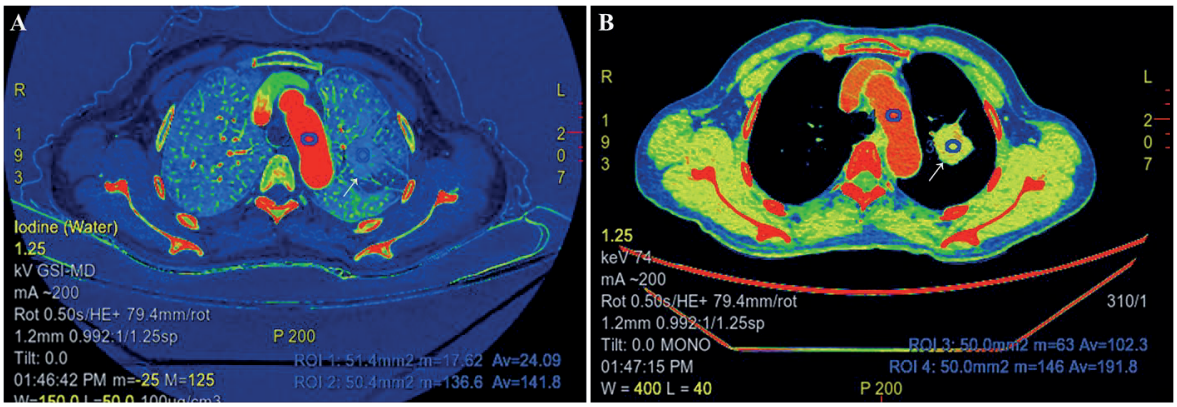

FIGURE 6. A solitary pulmonary nodule (SPN) with the size of 24.0 × 26.0 mm located in the superior lobe of left lung of a 57 years old female evaluated by arterial **(A)** and venous phases **(B)** of dual-energy CT (DECT). Iodine concentration at the arterial phase (aIC), Iodine concentration at the venous phase (vIC), normalized iodine concentration at the arterial phase (aNIC), and normalized iodine concentration at the venous phase (vNIC) were 2.409 mg/mL, 10.23 mg/mL, 0.17 (2.409/14.18), 0.53 (10.23/19.18) respectively. Pathology of the SPN after the surgery confirmed the diagnosis of an adenocarcinoma.

ity, and diagnostic threshold were 0.739, 85.03%, 66.10%, and 9.88 ml/100g/min, respectively. Our results are not completely consistent with previous reports.[7,8,29] For example, in the systematic review and meta-analysis performed by Huang *et al.*[8], lung cancer was found having higher BV, BF, MTT, and PS values than benign lesions; and AUC values of BV and PS were 0.92 (0.90, 0.94) and 0.83 (0.80, 0.86), respectively. The explanations may be as follow. PS mainly reflects the structural integrity of the capillary wall and the osmotic pressure between plasma and tissue fluid. There are a large number of microvessels and rich blood supply in malignant tumors. However, the capillary wall is immature, which is mainly reflected in the incomplete structure of vascular wall, including the basement membrane and epithelial cells. As a result, the vascular permeability will increase, promoting a large number of contrast agents to enter the tissue space. By contrast, the capillary wall of benign nodules is mature with a complete basement membrane and continuous endothelial cells which decreases the contrast agents to enter into the tissue space. On the other hand, although there are abundant microvessels in inflammatory lesions in benign nodules, in addition to the mature development of vascular wall, the edema and congestion of surrounding tissues will lead to the increase of tissue hydrostatic pressure which will also slow down the penetration rate of contrast medium. Therefore, the overall result is that the PS value in malignant SPNs was higher than that of benign SPNs.

TABLE 9. Solitary pulmonary nodules evaluated with multimodality CT imaging

Methods*	Sensitivity (%)	Specificity (%)	Accuracy (%)	PPV (%)	NPV (%)
Method A	83.23	63.56	75.09	76.37	72.82 %
Method B	85.63	67.80	78.25	79.01	76.92 %
Method C	84.43	66.10	76.84	77.90	75.00 %
Method A+B	94.61	74.58	86.32	84.04	90.72 %
Method A+C	92.81	77.97	86.67	85.64	88.46 %
Method B+C	95.81	81.36	89.82	87.91	93.20 %
Method A+B+C	97.60	88.14	93.68	92.09	96.30 %

CT = computed tomography; Method A = non-contrast enhanced CT combined with contrast enhanced CT; Method B = non-contrast enhanced CT combined with dual energy CT; Method C = non-contrast enhanced CT combined with CT perfusion imaging; Method A + B = non-contrast enhanced CT combined with contrast enhanced CT and dual energy CT; Method A + C = non-contrast enhanced CT combined with contrast enhanced CT and CT perfusion imaging; Method B + C = non-contrast enhanced CT combined with dual energy CT and CT perfusion imaging; Method A + B + C = non-contrast enhanced CT combined with contrast enhanced CT, dual-energy CT, and CT perfusion imaging; NPV = Negative predictive value; PPV = Positive predictive value; *compared with the McNemar's test

DECT in evaluating SPNs

There are mainly three techniques commercially available for DECT scanning. These techniques include: (a) fast voltage switching DECT, (b) layer detector DECT, and (c) dual-source DECT.[30] In this study, we used a fast voltage switching DECT system. It has the ability to obtain virtual nonenhanced images, arterial phase and venous phase contrast enhanced images, and iodine maps in one examination.[30]

An iodine map is the decomposition of material components realized by dual DECT according to the different attenuation characteristics of substances under high and low energy. It is the imaging of iodine material density extracted from enhanced iodine components. Iodine maps can effectively inhibit the background CT value and match with artificial color maps which can directly reflect the difference in iodine concentration in the lesion. The iodine concentration in the lesions can be measured quantitatively, and the lesions with slight enhancement can be displayed more sensitively. The CT value of the lesions measured on the iodine maps is the net enhancement value of the lesions. By measuring the enhancement value of lesions in iodine maps, we can evaluate the hemodynamic changes of tumors and the curative effects after tumor treatments.

In our results, parameters of DECT, which included aOL, vOL, aIC, vIC, aNIC, and vNIC, in malignant SPNs, were significantly higher than those of benign SPNs (all p values < 0.05). Compared with the AUC of aOL, vOL, aIC, vIC, and aNIC, the vNIC had the largest AUC (all p values < 0.05). Our results are consistent with many previous publications.[9,10,31-34] For example, Ha *et al.*[31] differentiated pulmonary metastasis from benign lung nodules in thyroid cancer patients by using DECT parameters finding that the DECT parameters (IC, NIC, NIC in using pulmonary artery, λ_{HU}, and Z-effective values) of the metastatic nodules were significantly higher than those of the benign nodules (all p values < 0.05).

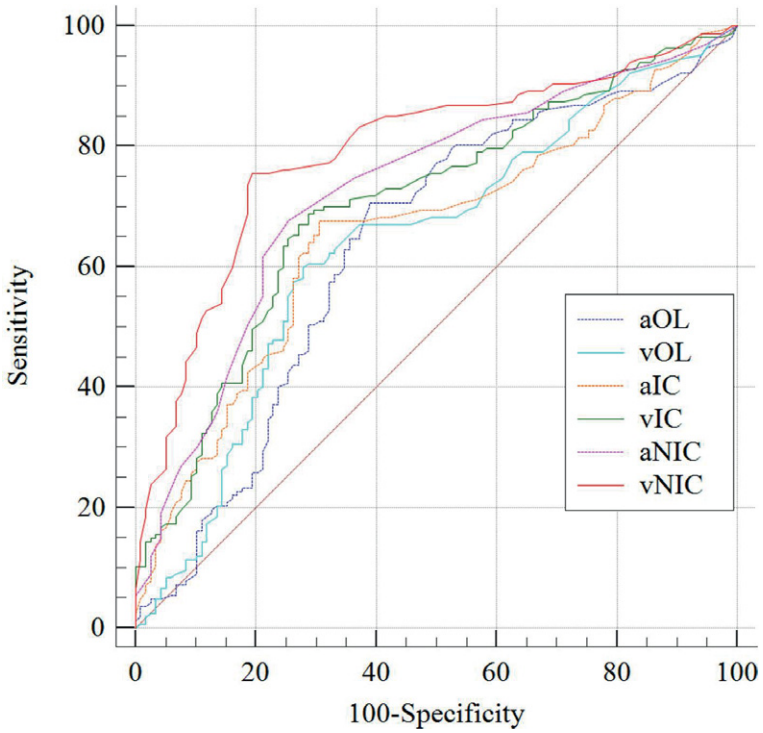

FIGURE 7. Receiver operating characteristic curves for distinguishing benign from malignant nodules using dual-energy CT parameters.

aOL = Iodine overlay at the arterial phase (AUC = 0.636); vOL = Iodine overlay at the venous phase (AUC = 0.638); aIC = Iodine concentration at the arterial phase (AUC = 0.657); vIC = Iodine concentration at the venous phase (area under the curve [AUC] = 0.703); aNIC = normalized iodine concentration at the arterial phase (AUC = 0.728); vNIC = normalized iodine concentration at the venous phase (AUC = 0.790); all p values < 0.05

Multimodality CT imaging in evaluating SPNs

Zhou *et al.*[35] analyzed the relationship between clinical data, tumor markers, chest high-resolution CT (HRCT), and pathology in patients with SPNs finding that a joint evaluation model had better diagnostic efficiency for the diagnosis of SPN with diameter ≤ 2.0 cm. In another study, Zhu *et al.*[9] reported that IC from DECT was significantly correlated with low-dose volume perfusion CT (VPCT) parameters (BF, BV, MTT, flow extraction product (FED), pulmonary nodule enhancement peak (PPnod), and VPCT parameters (BV, FED, and PPnod) had better diagnostic performance for SPN than DECT parameters (IC). Both of the above studies showed that multimodal evaluation is helpful in improving the diagnostic efficiency of SPNs.

In this study, the diagnostic performances of the three diagnostic methods were separately used or in combination for differentiating benign and malignant SPNs were calculated, and the results showed that multimodality CT imaging had higher performances than single modality CT imaging in differentiating between benign and malignant SPNs in sensitivity, specificity, and accuracy (all p values < 0.05). To the best of the authors' knowledge, this is the first study in the literature in which NECT, CECT, CTPI and DECT were comprehensibly used to differentiate benign from malignant SPNs.

TABLE 10. Step-wise approach of multimodality CT imaging for evaluating solitary pulmonary nodules[1,46,47]

Non-contrast enhanced CT	Density	1. Solid
		2. Subsolid
	Shape	3. Round or oval
		4. Triangular or polygonal
	Margins	5. Smooth
		6. Lobulated
		7. Spiculated
	Internal characteristics	8. Fat
		9. Calcification
		10. Cavitation
	Some complex findings	11. Pleural retraction
		12. Air bronchogram
		13. Bubble like lucencies (pseudocavitation)
		14. Cystic airspace
		15. Vascular convergence
Contrast enhanced CT	Parameter (s)	16. Degree of enhancement
CT perfusion imaging	Parameter (s)	17. Permeability surface
Dual-energy CT	Parameter (s)	18. Normalized iodine concentration at the venous phase

Radiation in multimodality CT imaging

Radiation is an important consideration when using a multimodality CT imaging protocol. Previous studies have reported that the radiation dose of CTPI is the key factor hindering its application.[9,36] In our study, the $CTDI_{vol}$, DLP, and ED in the SPNs were 66.88 ± 4.36 mGy, 768.29 ± 91.65 mGy.cm, and 10.76 ± 1.18 mSv, respectively. We have tried to make the radiation dose in our study at an acceptable level by using low tube voltage, SmartmA, and iterative reconstruction.[37-39] Tube voltage and tube current are positively correlated with the radiation dose.[40-42] In addition, it is recommended that postset ASIR-V% (60% in this study) should be higher than or equal to preset ASIR-V% (50% in this study).[43-45] All these radiation reduction techniques have been shown to decrease the radiation dose while maintaining the image quality.[40-45]

Some limitations of this study are: (a) only a fast voltage switching DECT was used in our study, and we did not compare our results with parameters from a layer detector DECT or dual-source DECT; (b) we did not compare our results with parameters from a magnetic resonance imaging (MRI) or positron emission tomography computed tomography (PET/CT); (c) some parameters of CTPI and DECT were not included into our study for evaluating; (d) radiation dose of our multimodality CT imaging protocol is still at a relatively high level; and (e) we did not include some advanced medical image analysis methods, such as artificial intelligence (AI), deep learning, or radiomics in our study. As a result, further investigations are needed to strengthen our findings in the future.

Conclusions

In conclusion, SPNs evaluated with multimodality CT imaging contributes to improving the diagnostic accuracy of benign and malignant SPNs (Table 10). NECT helps to locate and evaluate the morphological characteristics of SPNs. CECT helps to evaluate the vascularity of SPNs. CTPI using parameter of PS and DECT using parameter of vNIC both are helpful for improving the diagnostic performance.

Acknowledgments

The authors would like to thank co-authors AB and MM for their help in editing and proofreading the article. This study was supported by grants

from the Sichuan Provincial Commission of Health (Nos. 18PJ138, 19PJ283, 19PJ284, and 20PJ284), the Sichuan Provincial Department of Science and Technology (No. 2019YFQ0028), the Science and Technology Association of Suining City (Nos. 6 and 10), and the Science and Technology Bureau of Mianyang City (No. 2020YJKY004).

References

1. Erasmus JJ, Connolly JE, McAdams HP, Roggli VL. Solitary pulmonary nodules: Part I. Morphologic evaluation for differentiation of benign and malignant lesions. *Radiographics* 2000; **20:** 43-58. doi: 10.1148/radiographics.20.1.g00ja0343
2. Kastner J, Hossain R, Jeudy J, Dako F, Mehta V, Dalal S, et al. Lung-RADS Version 1.0 versus Lung-RADS Version 1.1: comparison of categories using nodules from the national lung screening trial. *Radiology* 2021; **300:** 199-206. doi: 10.1148/radiol.2021203704
3. Truong MT, Ko JP, Rossi SE, Rossi I, Viswanathan C, Bruzzi JF, et al. Update in the evaluation of the solitary pulmonary nodule. *Radiographics* 2014; **34:** 1658-79. doi: 10.1148/rg.346130092
4. Wyker A, Henderson WW. Solitary Pulmonary Nodule. 2021 Jul 26. In: StatPearls [Internet]. Treasure Island (FL): StatPearls Publishing; 2021. PMID: 32310603
5. MacMahon H, Naidich DP, Goo JM, Lee KS, Leung ANC, Mayo JR, et al. Guidelines for management of incidental pulmonary nodules detected on CT images: from the Fleischner Society 2017. *Radiology* 2017; **284:** 228-43. doi: 10.1148/radiol.2017161659
6. Bueno J, Landeras L, Chung JH. Updated Fleischner Society Guidelines for managing incidental pulmonary nodules: common questions and challenging scenarios. *Radiographics* 2018; **38:** 1337-50. doi: 10.1148/rg.2018180017
7. Sun Y, Yang M, Mao D, Lv F, Yin Y, Li M, et al. Low-dose volume perfusion computed tomography (VPCT) for diagnosis of solitary pulmonary nodules. *Eur J Radiol* 2016; **85:** 1208-18. doi: 10.1016/j.ejrad.2016.03.026
8. Huang C, Liang J, Lei X, Xu X, Xiao Z, Luo L. Diagnostic performance of perfusion computed tomography for differentiating lung cancer from benign lesions: a meta-analysis. *Med Sci Monit* 2019; **25:** 3485-94. doi: 10.12659/MSM.914206
9. Zhu B, Zheng S, Jiang T, Hu B. Evaluation of dual-energy and perfusion CT parameters for diagnosing solitary pulmonary nodules. *Thorac Cancer* 2021; **12:** 2691-7. doi: 10.1111/1759-7714.14105
10. Wen Q, Yue Y, Shang J, Lu X, Gao L, Hou Y. The application of dual-layer spectral detector computed tomography in solitary pulmonary nodule identification. *Quant Imaging Med Surg* 2021; **11:** 521-32. doi: 10.21037/qims-20-2
11. DeLong ER, DeLong DM, Clarke-Pearson DL. Comparing the areas under two or more correlated receiver operating characteristic curves: a nonparametric approach. *Biometrics* 1988; **44:** 837-45. PMID: 3203132
12. Lv E, Liu W, Wen P, Kang X. Classification of benign and malignant lung nodules based on deep convolutional network feature extraction. *J Healthc Eng* 2021; **2021:** 8769652. doi: 10.1155/2021/8769652
13. Borghesi A, Michelini S, Nocivelli G, Silva M, Scrimieri A, Pezzotti S, et al. Solid indeterminate pulmonary nodules less than or equal to 250 mm3: application of the updated Fleischner Society Guidelines in clinical practice. *Radiol Res Pract* 2019; **2019:** 7218258. doi: 10.1155/2019/7218258
14. Yang W, Sun Y, Fang W, Qian F, Ye J, Chen Q, et al. High-resolution computed tomography features distinguishing benign and malignant lesions manifesting as persistent solitary subsolid nodules. *Clin Lung Cancer* 2018; **19:** e75-83. doi: 10.1016/j.cllc.2017.05.023
15. Borghesi A, Michelini S, Scrimieri A, Golemi S, Maroldi R. Solid indeterminate pulmonary nodules of less than 300 mm3: application of different volume doubling time cut-offs in clinical practice. *Diagnostics* 2019; **9:** 62. doi: 10.3390/diagnostics9020062
16. McDonald JS, Koo CW, White D, Hartman TE, Bender CE, Sykes AG. Addition of the Fleischner Society Guidelines to chest CT examination interpretive reports improves adherence to recommended follow-up care for incidental pulmonary nodules. *Acad Radiol* 2017; **24:** 337-44. doi: 10.1016/j.acra.2016.08.026
17. Xu DM, van der Zaag-Loonen HJ, Oudkerk M, Wang Y, Vliegenthart R, Scholten ET, et al. Smooth or attached solid indeterminate nodules detected at baseline CT screening in the NELSON study: cancer risk during 1 year of follow-up. *Radiology* 2009; **250:** 264-72. doi: 10.1148/radiol.2493070847
18. Gould MK, Donington J, Lynch WR, Mazzone PJ, Midthun DE, Naidich DP, et al. Evaluation of individuals with pulmonary nodules: when is it lung cancer? Diagnosis and management of lung cancer, 3rd edition. American College of Chest Physicians evidence-based clinical practice guidelines. *Chest* 2013; **143(5 Suppl):** e93S-120S. doi: 10.1378/chest.12-2351
19. McWilliams A, Tammemagi MC, Mayo JR, Roberts H, Liu G, Soghrati K, et al. Probability of cancer in pulmonary nodules detected on first screening CT. *N Engl J Med* 2013; **369:** 910-9. doi: 10.1056/NEJMoa1214726
20. Swensen SJ, Viggiano RW, Midthun DE, Müller NL, Sherrick A, Yamashita K, et al. Lung nodule enhancement at CT: multicenter study. *Radiology* 2000; **214:** 73-80. doi: 10.1148/radiology.214.1.r00ja1473
21. Wang M, Li B, Sun H, Huang T, Zhang X, Jin K, et al. Correlation study between dual source CT perfusion imaging and the microvascular composition of solitary pulmonary nodules. *Lung Cancer* 2019; **130:** 115-20. doi: 10.1016/j.lungcan.2019.02.013
22. Huang T, Sun H, Luo X, Zhang X, Jin K, Wang F, et al. Correlation study between flash dual source CT perfusion imaging and regional lymph node metastasis of non-small cell lung cancer. *BMC Cancer* 2020; **20:** 547. doi: 10.1186/s12885-020-07032-8
23. Marin A, Murchison JT, Skwarski KM, Tavares AAS, Fletcher A, Wallace WA, et al. Can dynamic imaging, using 18F-FDG PET/CT and CT perfusion differentiate between benign and malignant pulmonary nodules? *Radiol Oncol* 2021; **55:** 259-67. doi: 10.2478/raon-2021-0024
24. Ostman C, Garcia-Esperon C, Lillicrap T, Tomari S, Holliday E, Levi C, et al. Multimodal computed tomography increases the detection of posterior fossa strokes compared to brain non-contrast computed tomography. *Front Neurol* 2020; **11:** 588064. doi: 10.3389/fneur.2020.588064
25. Li Q, Cui D, Feng Y, He Y, Shi Z, Yang R. Correlation between microvessel density (MVD) and multi-spiral CT (MSCT) perfusion parameters of esophageal cancer lesions and the diagnostic value of combined CtBP2 and $P16^{INK4A}$. *J Gastrointest Oncol* 2021; **12:** 981-90. doi: 10.21037/jgo-21-247
26. Zaboriene I, Zviniene K, Lukosevicius S, Ignatavicius P, Barauskas G. Dynamic perfusion computed tomography and apparent diffusion coefficient as potential markers for poorly differentiated pancreatic adenocarcinoma. *Dig Surg* 2021; **38:** 128-35. doi: 10.1159/000511973
27. Woolen S, Virkud A, Hadjiiski L, Cha K, Chan HP, Swiecicki P, et al. Prediction of disease free survival in laryngeal and hypopharyngeal cancers using CT perfusion and radiomic features: a pilot study. *Tomography* 2021; **7:** 10-19. doi: 10.3390/tomography7010002
28. Mathy RM, Fritz F, Mayer P, Klauss M, Grenacher L, Stiller W, et al. Iodine concentration and tissue attenuation in dual-energy contrast-enhanced CT as a potential quantitative parameter in early detection of local pancreatic carcinoma recurrence after surgical resection. *Eur J Radiol* 2021; **143:** 109944. doi: 10.1016/j.ejrad.2021.109944
29. Li Y, Yang ZG, Chen TW, JQ, Sun JY, Chen HJ, et. al. First-pass perfusion imaging of solitary pulmonary nodules with 64-detector row CT: comparison of perfusion parameters of malignant and benign lesions. *Brit J Radiol* 2010; **83:** 785-90. doi: 10.1259/bjr/58020866
30. Marin D, Boll DT, Mileto A, Nelson RC. State of the art: dual-energy CT of the abdomen. *Radiology* 2014; **271:** 327-42. doi: 10.1148/radiol.14131480
31. Ha T, Kim W, Cha J, Lee YH, Seo HS, Park SY, et al. Differentiating pulmonary metastasis from benign lung nodules in thyroid cancer patients using dual-energy CT parameters. *Eur Radiol* 2022; **32:** 1902-11. doi: 10.1007/s00330-021-08278-x
32. Zegadło A, Żabicka M, Kania-Pudło M, Maliborski A, Różyk A, Sośnicki W. Assessment of solitary pulmonary nodules based on virtual monochrome images and iodine-dependent images using a single-source dual-energy CT with fast kVp switching. *J Clin Med* 2020; **9:** 2514. doi: 10.3390/jcm9082514

33. Zhang Y, Cheng J, Hua X, Yu M, Xu C, Zhang F, et al. Can spectral CT imaging improve the differentiation between malignant and benign solitary pulmonary nodules? *PLoS One* 2016; **11:** e0147537. doi: 10.1371/journal.pone.0147537

34. Lin JZ, Zhang L, Zhang CY, Yang L, Lou HN, Wang ZG. Application of gemstone spectral computed tomography imaging in the characterization of solitary pulmonary nodules: preliminary result. *J Comput Assist Tomogr* 2016; **40:** 907-11. doi: 10.1097/RCT.0000000000000469

35. Zhou S, Wang Q, Tang T, Cao M, Tan Y, Bai K, et al. Joint prediction of solitary pulmonary module malignant probability based on logistic regression and malignant tendency comprehensive score. *J BUON* 2021; **26:** 1815-23. PMID: 34761588

36. Chae EJ, Song JW, Krauss B, Song KS, Lee CW, Lee HJ, et al. Dual-energy computed tomography characterization of solitary pulmonary nodules. *J Thorac Imaging* 2010; **25:** 301-10. doi: 10.1097/RTI.0b013e3181e16232

37. U.S. Food and Drug Administration. What are the radiation risks from CT? In: *Medical X-ray imaging*. Available at: https://www.fda.gov/radiation-emitting-products/medical-x-ray-imaging/what-are-radiation-risks-ct

38. McCollough CH, Bushberg JT, Fletcher JG, Eckel LJ. Answers to common questions about the use and safety of CT scans. *Mayo Clin Proc* 2015; **90:** 1380-92. doi: 10.1016/j.mayocp.2015.07.011

39. Yan G, Li H, Bhetuwal A, McClure MA, Li Y, Yang G, et al. Pleural effusion volume in patients with acute pancreatitis: a retrospective study from three acute pancreatitis centers. *Ann Med* 2021; **53:** 2003-18. doi: 10.1080/07853890.2021.1998594

40. Chen CW, Chen PA, Chou CC, Fu JH, Wang PC, Hsu SH, et al. Combination of adaptive statistical iterative reconstruction-V and lower tube voltage during craniocervical computed tomographic angiography yields better image quality with a reduced radiation dose. *Acad Radiol* 2019; **26:** e233-e40. doi: 10.1016/j.acra.2018.07.019

41. Ye K, Chen M, Li J, Zhu Q, Lu Y, Yuan H. Ultra-low-dose CT reconstructed with ASiR-V using SmartmA for pulmonary nodule detection and Lung-RADS classifications compared with low-dose CT. *Clin Radiol* 2021; **76:** 156.e1-156.e8. doi: 10.1016/j.crad.2020.10.014

42. Ren Z, Zhang X, Hu Z, Li D, Liu Z, Wei D, et al. Application of adaptive statistical iterative reconstruction-V with combination of 80 kV for reducing radiation dose and improving image quality in renal computed tomography angiography for slim patients. *Acad Radiol* 2019; **26:** e324-e32. doi: 10.1016/j.acra.2018.12.021

43. Tang H, Yu N, Jia Y, Yu Y, Duan H, Han D, et al. Assessment of noise reduction potential and image quality improvement of a new generation adaptive statistical iterative reconstruction (ASIR-V) in chest CT. *Br J Radiol* 2018; **91:** 20170521. doi: 10.1259/bjr.20170521

44. Afadzi M, Lysvik EK, Andersen HK, Martinsen ACT. Ultra-low dose chest computed tomography: effect of iterative reconstruction levels on image quality. *Eur J Radiol* 2019; **114:** 62-8. doi: 10.1016/j.ejrad.2019.02.021

45. Zhu Z, Zhao Y, Zhao X, Wang X, Yu W, Hu M, et al. Impact of preset and postset adaptive statistical iterative reconstruction-V on image quality in nonenhanced abdominal-pelvic CT on wide-detector revolution CT. *Quant Imaging Med Surg* 2021; **11:** 264-75. doi: 10.21037/qims-19-945

46. Snoeckx A, Reyntiens P, Desbuquoit D, Spinhoven MJ, Van Schil PE, van Meerbeeck JP, et al. Evaluation of the solitary pulmonary nodule: size matters, but do not ignore the power of morphology. *Insights Imaging* 2018; **9:** 73-86. doi: 10.1007/s13244-017-0581-2

47. Hansell DM, Bankier AA, MacMahon H, McLoud TC, Müller NL, Remy J. Fleischner Society: glossary of terms for thoracic imaging. *Radiology* 2008; **246:** 697-722. doi: 10.1148/radiol.2462070712

research article

Ultrasonography of peripheral nerve tumours: a case series

Simon Podnar

Institute of Clinical Neurophysiology, Division of Neurology, University Medical Centre Ljubljana, Ljubljana, Slovenia

Radiol Oncol 2023; 57(1): 35-41.

Received 5 August 2022
Accepted 8 December 2022

Correspondence to: Prof. Simon Podnar, M.D., Ph.D., Institute of Clinical Neurophysiology, Division of Neurology, University Medical Centre Ljubljana, Zaloška cesta 7, SI-1525 Ljubljana, Slovenia. E-mail: simon.podnar@kclj.si

Disclosure: No potential conflicts of interest were disclosed.

Background. Peripheral nerve tumours (PNTs) are rare, but important cause of peripheral nerve dysfunction. The aim of the study was to present a series of consecutive patients with PNTs evaluated in authors' ultrasonography (US) practice.

Patients and methods. The electronic medical records of patients with PNTs examined at our US laboratory from February 2013 to May 2020 were retrospectively reviewed. Data on gender, age, clinical features, PNT location, electrodiagnostic (EDx) features and US findings were collected.

Results. In the analyzed period 2845 patients were examined in our US laboratory. From these 15 patients (0.5%) with PNTs were identified. Four of them (3 with confirmed neurofibromatosis) had multiple PNTs. Half of patients (53%) presented with features of peripheral nerve damage, and others with palpable mass or pain. The most often involved nerve was ulnar (36%). PNT cross sectional areas varied from 24 mm^2 to 1250 mm^2 (median, 61 mm^2). Based in 5 patients on histological and in remaining patients on US features, schwannoma was diagnosed in 40%, neurofibroma in 27%, and perineurioma in 27% of patients.

Conclusions. As in previous reports, PNTs in our series presented with neurological symptoms, palpable mass or pain. In contrast to other focal neuropathies, particularly nerves with schwannomas, in spite of their large thickening, often demonstrated well preserved function. Adding US to our clinical practice, enabled us to diagnose these rare peripheral nerve lesions that we missed before.

Key words: electrodiagnosis; nerve cross-sectional area; peripheral nerves; peripheral nerve tumors; ultrasonography

Introduction

Peripheral nerve tumours (PNTs) are rare, but important cause of peripheral nerve dysfunction. Usually they present with neurological symptoms (muscle atrophy and weakness, paresthesia or sensory loss), palpable mass or pain.[1,2] On examination neurological deficits can be found distally to PNTs in the affected nerve innervation area. Mass movable perpendicular, but not along the peripheral nerve axis, and sensations along the affected nerve elicited on mass percussion (i.e., Tinel's sign) are also pointing to possible PNT.[1,2] Even before PNT diagnosis is known, electrodiagnostic (EDx) testing is often performed to evaluate severity of peripheral nerve damage. However, EDx is not useful for PNT diagnosis[1], but imaging studies are much more relevant. Magnetic resonance (MR) is regarded as the most useful method[1,3], although ultrasonography (US) is also gaining support among clinicians.[3,4] Particularly when diagnosis of PNT is not known, US is most useful, because it is cheap and widely accessible. Imaging delineates the lesion, identifies its relation to peripheral nerve, and helps to differentiate various types of PNTs (Table 1).[5] There are several nice reviews describing US characteristics of PNT.[3,4] However, only few publications written mainly by radiologists

describe actual clinical experiences with US diagnosis of PNTs.[5-7]

In the present study we report a series of consecutive patients referred to our US unit mainly from EDx laboratories in whom we have diagnosed PNTs.

Patients and methods

We retrospectively reviewed the electronic medical records of all patients referred from February 2013 to May 2020 to the US laboratory at the Institute of Clinical Neurophysiology, University Medical Centre Ljubljana, Slovenia. Our unit is the only one dedicated to peripheral nerve US in Slovenia, a country with a population of two million. The National Ethics Committee of Slovenia approved the study (approval code: 63/07/17), and at the time of analysis all patients signed written informed consent. During the whole review process, all patients' personal information was carefully protected.

We were not blinded to the findings of the clinical neurologic examination and EDx testing. Before US examinations we performed a focused neurological examination of patients by ourselves. We used standard US equipment (ProSound Alpha 7, Hitachi Aloka Medical, Ltd., Tokyo, Japan), with a 4–13 MHz linear array transducer. We measured tumor cross sectional areas (CSAs) by a trace method that excluded the hyperechoic rim.[8] During review of US images we observed PNT features typical for neurofibromas and schwannomas (Table 1).[5] In patients without histological diagnosis presumptive PNT diagnoses were based on clinical, EDx and particularly US features. In all included patients, we collected data on gender, age, symptoms (including duration), neurological, EDx features, US findings, and PNT location.

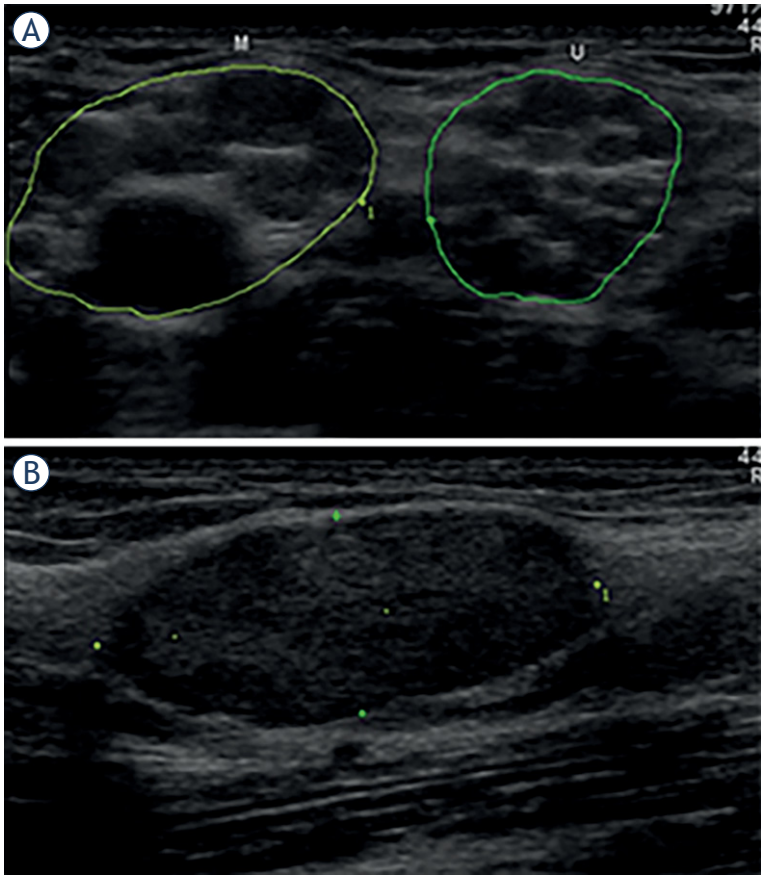

FIGURE 1. (A) Transverse ultrasonographic (US) view of the median (M) and ulnar (U) nerve in the axillary region showing numerous globular hypoechoic peripheral nerve tumours (PNTs) causing largely increased nerve cross sectional areas (CSAs, 148 mm2 and 101 mm^2, respectively). **(B)** Longitudinal view of a single partially encapsulated, slightly lobulated and rather homogenous oval PNT (length 24 mm, thickness 9 mm) with central, but poorly defined nerve-tumour transition.[5] Most probably these numerous PNTs are neurofibromas, although diagnosis in this 52-year-old woman presenting with peripheral neuropathy, primary lymphedema, and history of mitral and aortic valve surgery (patient #13, Tables 2–3), is not known yet.

Results

In the analyzed period, in our US unit we examined 2845 patients, and we found PNTs in 15 (0.5%) of them. Demographic features of individual patients, PNT anatomic, clinical, EDx and US features are shown in Table 2. Our patients' median age was 33 years (range: 16–69 years). Slightly less than half of them were male (47%). Four had multiple PNTs; in 2 neurofibromatosis type 1 (NF1), and in 1 neurofibromatosis type 2 (NF2) were previously diagnosed. In another (patient #13, Tables 2–3) gene sequencing results are pending. Of 11 patients with single PNTs, 7 (64%) had lesions on the right side. Ulnar nerve was involved in 4 (36%), median, sciatic and tibial in 2 (18%) patients each, and fibular in 1 (9%) patient with single PNT. Elbow and forearm were each involved in 3 (27%), thigh and ankle in 2 (18%) patients each, and knee in 1 (9%) patient with single PNT. The most common clinical findings in our patients were weakness and sensory abnormalities, each found in 7 (47%) patients, followed by muscle atrophy in 6 (40%), pain in 3 (20%), sensitivity on mass percussion in 2 (13%) and only palpable mass in 1 patient (7%). At the time of US study, EDx report was available for 12 (80%) patients. Affected nerve compound muscle action potential (CMAP) amplitude was markedly

reduced or absent in 5 (42%) patients, and sensory nerve action potential (SNAP) amplitude in 9 (75%) patients. In our series CSAs of PNT varied from 24 mm^2 to 1250 mm^2 (median, 61 mm^2). Ratio of PNT/unaffected segment of the same nerve CSA varied from 2.9 to 156 (median, 6.0). Morphological features of PNTs are presented in Table 3. Ratio of maximum/minimum PNT diameter varied from 1.5 to > 10 (median, 4.5). Majority (64%) of PNTs were of fusiform shape. PNT contour was smooth in 8 (53%), and lobulated in remaining 7 (47%). PNT encapsulation was complete in 7 (47%), partial in 6 (40%), and absent in 2 (13%). PNTs echotexture was heterogenous in 13 (87%). Nerve entrance into PNT was central in 10 (67%), eccentric in 3 (20%), and not possible to asses in 2 (13%). In our series infiltrative nerve-tumor transition was observed in 7 PNTs (58%), poorly defined in 5 (42%), and could not be observed in 3 (20%). Histological diagnosis was available in 5 patients (Tables 2 and 3) with schwannoma. In another patient with NF1 histology of multiple PNTs could be also established –

TABLE 1. Morphological features useful for differentiation between neurofibromas and schwannomas[5]

Peripheral nerve tumor (PNT) feature	Comment
Maximum to minimum diameter	Ratio > 3 → neurofibroma
Shape: round, oval, fusiform	Fusiform → neurofibroma
Contour: smooth, lobulated	Lobulated → neurofibroma
Encapsulation: absent, partial, complete	Complete → schwannoma
Echogenicity: hypo-, iso-, hyper-	Hypoechoic → PNT
Echo texture: homogenous, heterogenous	Heterogenous → schwannoma
Cystic changes: absent, focal, partial, large	Cystic changes → schwannoma
Calcifications: absent, present	Present → schwannoma
Target sign: absent, present	
Nerve entrance: not identified, identified	
Nerve-tumor position: central, eccentric	Central → neurofibroma
Nerve-tumor transition: clear, poorly defined, infiltrative	Infiltrative → neurofibroma
Vascularity: increased, normal, decreased	Hypovascular → neurofibroma

TABLE 2. Demographic, anatomical, clinical, electrodiagnostic (EDx) and ultrasonographic (US) features of patients with peripheral nerve tumors (PNTs)

#	Gender	Age	Side	Nerve	Location	Symptoms & Signs	CMAP amp. (mV)	SNAP amp. (μV)	Tumor CSA (mm^2)	Tumor diagnosis	Other
1	Male	69	R	Ulnar	Elbow	AWS			43	Neurofibroma	
2	Male	24	L	#Radial	Upper arm	W	0.2	4	24	Schwannoma*	NF2
3	Male	66	R	Median	Forearm	Æ	6.9	5	49	Schwannoma	
4	Male	16	L	#Median	Upper arm	WS			61	Neurofibroma	NF1
5	Female	26	R	Ulnar	Forearm	AWS	0.2	0	30	Perineurioma	
6	Female	18	L	Sciatic	Thigh	AWS	0.4	0	109	Perineurioma	
7	Female	18	R	Fibular	Knee	AWS	0	0	47	Perineurioma	
8	Male	47	L	Ulnar	Elbow	M	7.6	3	348	Schwannoma*	
9	Female	58	R	Median	Forearm	P	7.6	16	45	Neurofibroma	
10	Female	22	R	Sciatic	Thigh	AWS	0	0	97	Perineurioma	
11	Female	34	R	Tibial	Ankle	PAWS	10.6	7	1250	Schwannoma*	
12	Male	63	L	Ulnar	Elbow	L	8.2	5	368	Schwannoma*	
13	Female	52	R	#Ulnar	Forearm		6.2	12	212	Neurofibroma	NF?
14	Male	24	R	#Median	Upper arm	P	6.3	33	26	Neurofibroma*	NF1
15	Female	33	L	Tibial	Ankle	L			92	Schwannoma	

A = muscle atrophy; amp. = amplitude; CMAP = compound muscle action potential; CSA = cross sectional area; L = left; L = local sensitivity; M = palpable mass; NF1 = neurofibromatosis type 1; NF2 = neurofibromatosis type 2; P = pain; R = right; S = sensory loss; SNAP = sensory nerve action potential; W = weakness; # = patients had multiple tumors; * = histological diagnosis of PNT available

TABLE 3. Morphological features of peripheral nerve tumors (PNTs) found on ultrasonographic (US) examination[5] of individual patients

#	Ratio	Shape	Contour	Encapsulation	Echo texture	Nerve position	Nerve transition	Number	Tumor diagnosis
1	5	Fusiform	Lobulated	Partial	Heterogeneous	Central	Infiltrative	Single	Neurofibroma
2	?		Lobulated	Partial	Heterogeneous	?	?	Several	Schwannoma*
3	6	Fusiform	Smooth	Whole	Heterogeneous	Central	Poorly defined	Single	Schwannoma
4	6	Fusiform	Fusiform	None	Heterogeneous	Central	Infiltrative	Several	Neurofibroma
5	8	Fusiform	Lobulated	Partial	Heterogeneous	Central	Infiltrative	Single	Perineurioma
6	> 10	Fusiform	Lobulated	Partial	Heterogeneous	?	?	Single	Perineurioma
7	6	Fusiform	Smooth	None	Homogenous	Central	Infiltrative	Single	Perineurioma
8	3	Oval	Smooth	Whole	Heterogeneous	Central	Poorly defined	Single	Schwannoma*
9	> 10	Fusiform	Lobulated	Partial	Heterogeneous	Eccentric	Infiltrative	Single	Neurofibroma
10	5	Fusiform	Smooth	Whole	Heterogeneous	Central	Infiltrative	Several	Perineurioma
11	1,5	Oval	Smooth	Whole	Homogenous	Eccentric	?	Single	Schwannoma*
12	2,5	Oval	Smooth	Whole	Heterogeneous	Central	Poorly defined	Single	Schwannoma*
13	2,5	Oval	Smooth	Whole	Heterogeneous	Central	Poorly defined	Several	Neurofibroma
14	4	Fusiform	Lobulated	Partial	Heterogeneous	Central	Infiltrative	Several	Neurofibroma*
15	1,7	Oval	Smooth	Whole	Heterogeneous	Eccentric	Poorly defined	Single	Schwannoma

Ratio = Maximum/minimum PNT diameter; * = histological diagnosis of PNT available

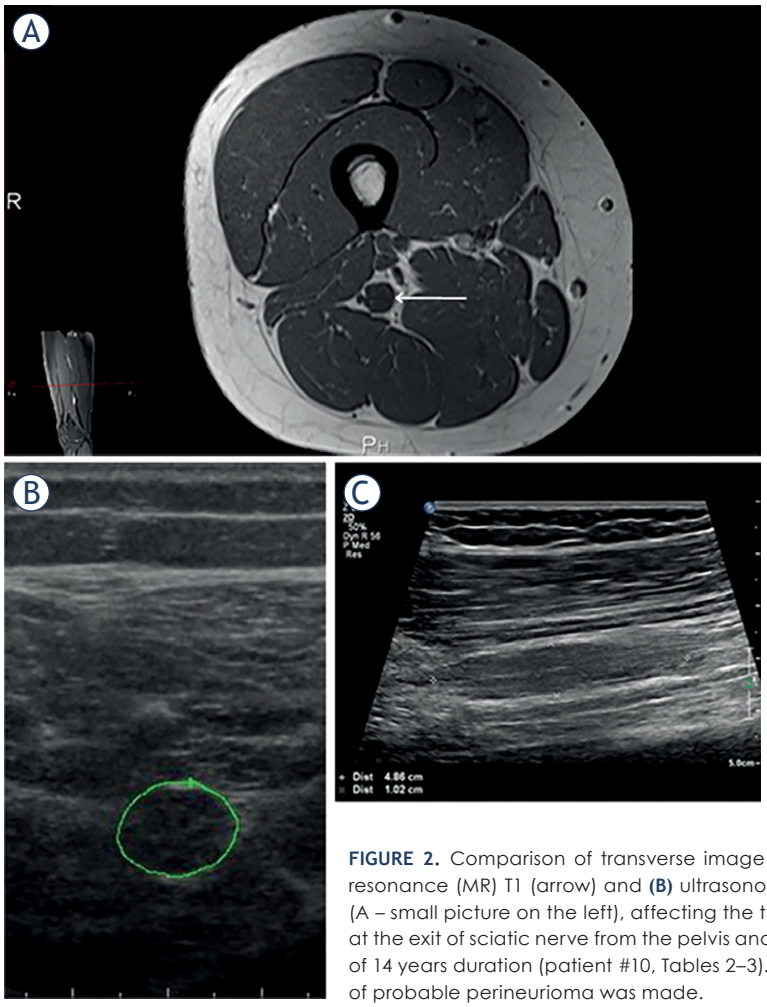

FIGURE 2. Comparison of transverse image of the sciatic peripheral nerve tumour (PNT) on **(A)** magnetic resonance (MR) T1 (arrow) and **(B)** ultrasonography (US). **(C)** Longitudinal US view of PNT in the middle thigh (A – small picture on the left), affecting the tibial portion of sciatic nerve. In this 22-year-old girl MR revealed at the exit of sciatic nerve from the pelvis another PNT affecting its fibular portion, and causing right foot drop of 14 years duration (patient #10, Tables 2–3). Based on clinical and imaging features in this patient diagnosis of probable perineurioma was made.

neurofibroma. Based on histological definite, and based on clinical and US features probable diagnoses of schwannoma were made in 6 (40%), neurofibroma in 5 (27%), and perineurioma in 4 (27%) patients.[5]

Discussion

PNTs are known to be rare, which was also confirmed by our US experience, demonstrating PNTs in only every 200th examined patient. As in our US laboratory we see referrals from a number of Slovenian EDx laboratories, and examine primarily patients with unclear etiology of peripheral nerve lesions, in reality PNTs are probably even rarer. It was reported that PNTs constitute only 5% of adult, and 2% of pediatric upper extremity tumors.[9]

With median age of 33 years our patients were much younger compared to typical oncological patients, which is similar to previously reported series of patients with PNTs reporting mean age of 36 years[10], and 37 years.[7] As reported by others[7,10], we also found equal distribution of PNTs between both genders.

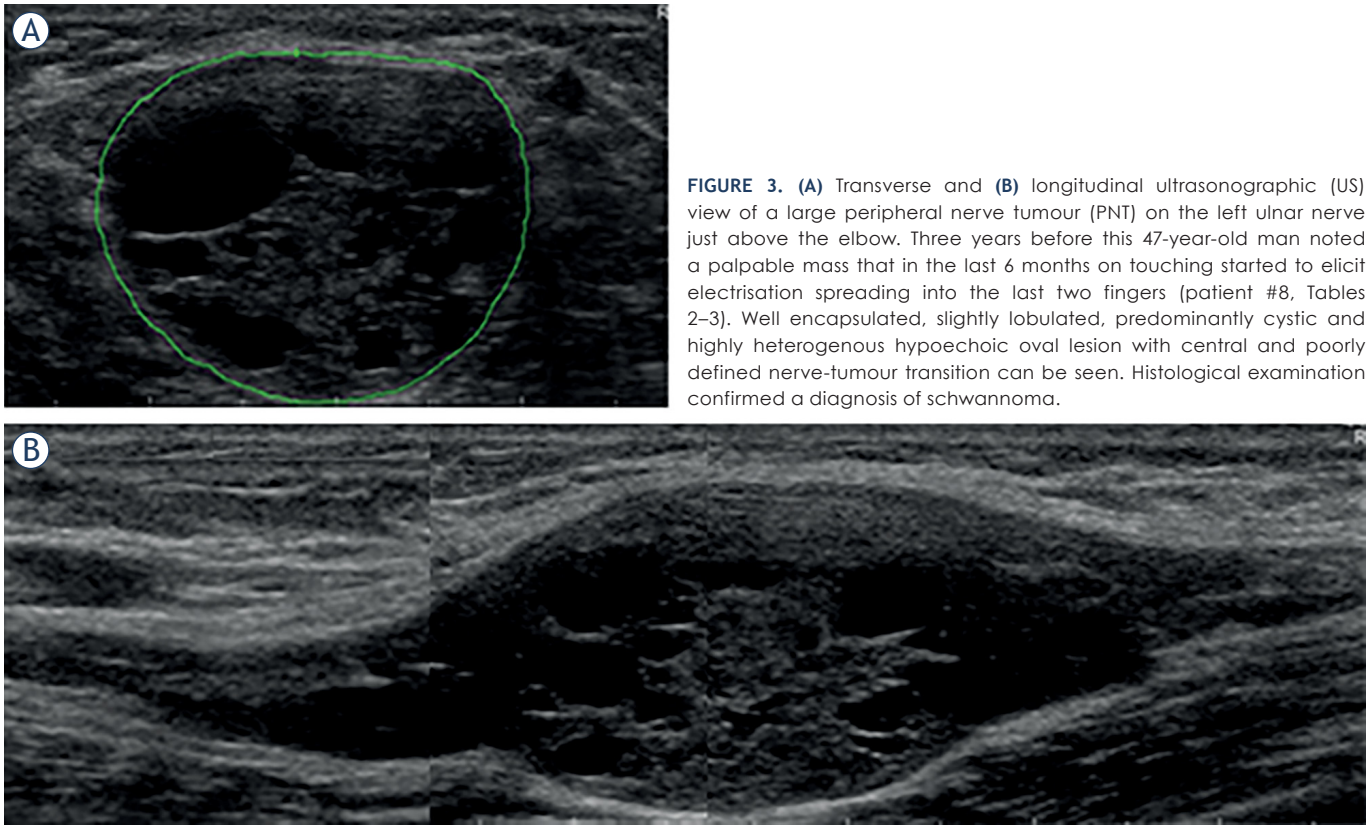

FIGURE 3. (A) Transverse and **(B)** longitudinal ultrasonographic (US) view of a large peripheral nerve tumour (PNT) on the left ulnar nerve just above the elbow. Three years before this 47-year-old man noted a palpable mass that in the last 6 months on touching started to elicit electrisation spreading into the last two fingers (patient #8, Tables 2–3). Well encapsulated, slightly lobulated, predominantly cystic and highly heterogenous hypoechoic oval lesion with central and poorly defined nerve-tumour transition can be seen. Histological examination confirmed a diagnosis of schwannoma.

We could divide our patient cohort into several groups. The first group consisted of 4 patients with numerous PNTs in several peripheral nerves. Two of patients from this group with numerous neurofibromas had known NF1 and a single patient with schwannomas had NF2. Diagnosis in a remaining patient (#13), with numerous neurofibromas in all US examined peripheral nerves (Figure 1), has not been established yet.

The second group consisted of three girls (patients #6, 7, 10) presenting in the first decade of life with unilateral foot drop. Each of them had several lumbo-sacral spine MRs that all proved negative, and their PNTs were not diagnosed until they presented to our US laboratory 8–15 years after symptom onset. At that time their clinical features were unchanged for several years, so none of them decided to have a nerve biopsy to establish a histological PNT diagnosis. Nevertheless, we believe these 3 patients most probably have sciatic nerve perineurioma.[11] One of them (patient #10) had two PNTs, separated by 20–30 cm segment of US relatively normal sciatic nerve. Using US we demonstrated the more distal PNT of the tibial portion of sciatic nerve (Figure 2). Additional more proximal PNT affecting fibular portion of sciatic nerve, and causing foot drop was found on MR.

The third group consisted of four patients with PNTs on the ulnar nerve in the elbow segment (Figure 3). The main challenge in this group of patients is differentiation of PNTs from ulnar neuropathy at the elbow (UNE) due to entrapment under the humeroulnar aponeurosis (i.e., cubital tunnel syndrome). The main distinctive feature of PNTs is their large CSA (43 mm^2, 348 mm^2, 45 mm^2, and 368 mm^2). We found CSA larger than 40 mm^2 in only 1 of 202 (0.5%) UNE patients,[12] and is therefore extremely rare. Another characteristic feature of PNTs is rather well preserved nerve function in spite of large nerve thickening. By contrast, large CSA in UNE is as a rule accompanied by severe nerve dysfunction.[12] What is the reason for such high number of PNTs on ulnar nerve in the elbow area is not clear. One possibility would be exposure of the nerve in this segment to mechanical stress. Alternative explanation would be a sampling artefact, as we see a plenty of patients with suspected UNE. If the latter case that would mean that a large number of PNTs on other nerves and locations are still missed.

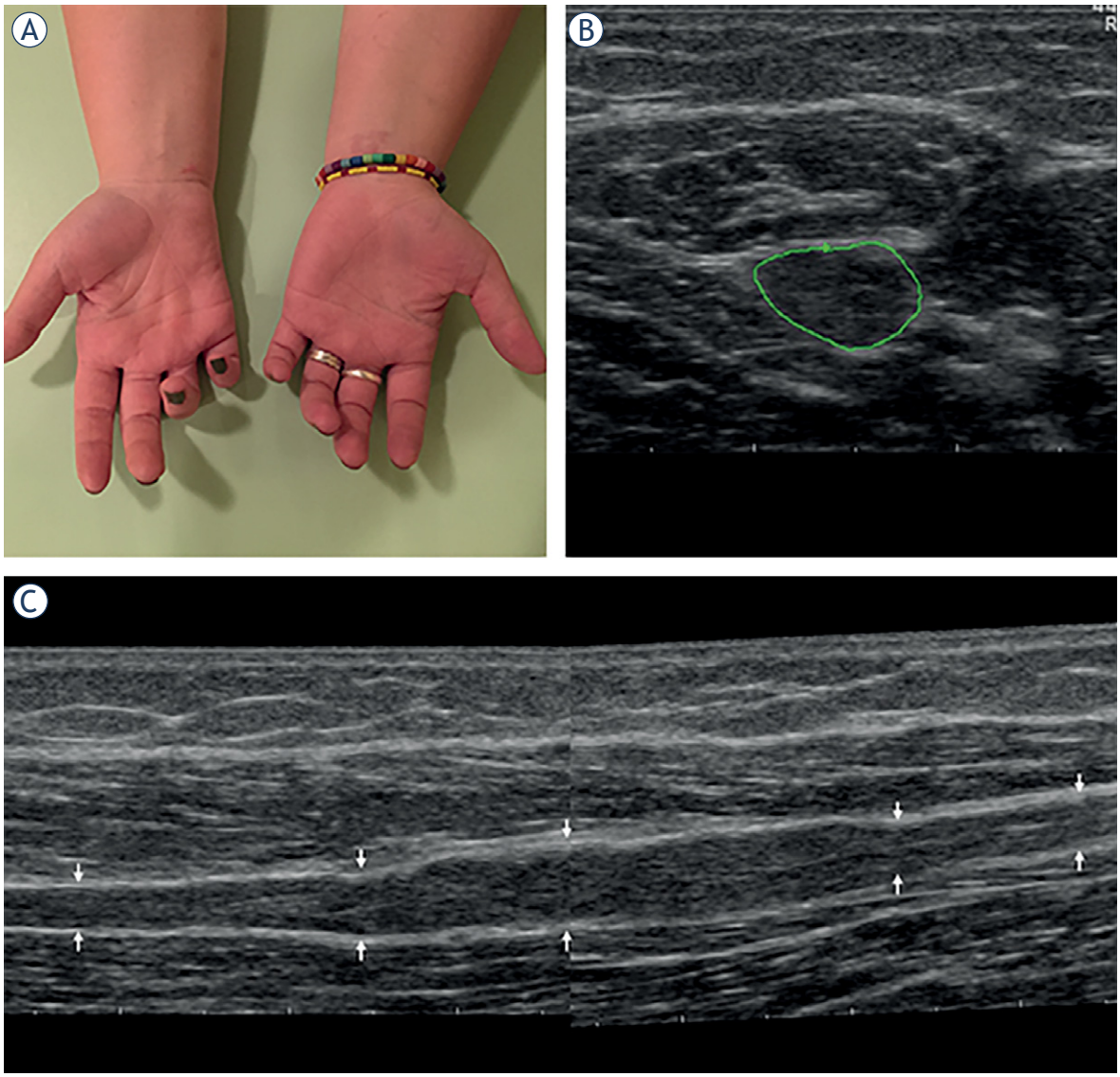

FIGURE 4. (A) Hands of a 26-year-old woman with 4-year history of muscle atrophy, weakness and numbness in the distal ulnar nerve territory (patient #5, Tables 2–3). Note intrinsic right palm muscle atrophy and clawing of the last two fingers. **(B)** On transverse ultrasonographic (US) view ulnar nerve cross sectional area (CSA) increased from 7 mm^2 both proximally and distally to 20 mm^2 in the middle of the lesion. **(C)** On longitudinal view a partially encapsulated, lobulated, fusiform hypoechoic right ulnar peripheral nerve tumour (PNT) of the forearm can be seen. Based on clinical and US features, we made a diagnosis of probable perineurioma.

Of remaining 4 patients, 1 had definite and another probable tibial nerve schwannoma at the ankle, which is again a region of considerable mechanical stress. Another young woman had a fusiform thickening of the ulnar nerve in the forearm (patient #5, Figure 4). She had surgical release of the ulnar nerve exit from the flexor carpi ulnaris muscle, with no apparent benefit. She might also have perineurioma, or less likely neurofibroma. In the fourth man probable median nerve schwannoma in the forearm was a coincidental finding during US evaluation due to Lewis-Sumner syndrome, and caused no additional symptoms.

As described previously[1] according to clinical presentation, our patients could be divided into two groups. Eight (53%) patients presented with features of peripheral nerve lesion (e.g., muscle atrophy, weakness, sensory loss). Remaining 7 patient presented by other clinical features (i.e., pain, local sensitivity, palpable mass), or as coincidental

PNT finding without symptoms. In the first group CMAP and SNAP amplitudes of affected nerves were severely reduced or absent (42% and 75%, respectively), and in the second group they were mainly preserved (58% and 25%, respectively). The first group consisted of all 4 young women with probable perineurioma, and additional 3 patients with probable neurofibroma. By contrast, majority of the second group consisted of 4 patients with probable or definite schwannoma (Table 2).

Before introduction of US into our institution, we diagnosed PNTs only very rarely. This changed after we started to perform US studies. Some PNTs that we finally diagnosed using US, were causing patients' unexplained severe nerve dysfunction for more than a decade. Without US we would probably not be able to diagnose PNTs in majority of patients from this series, and some of them would probably remain without diagnosis to this day.

The main limitation of the present study was that in majority of patients histological diagnosis of PNTs was not available. Therefore, in these patients we based our PNT diagnoses on clinical and particularly imaging features of the lesions. For differentiation between schwannomas and neurofibromas we applied US criteria of Ryu *et al*. that demonstrated high diagnostic accuracy.[5] Unfortunately, no similar criteria are available for US diagnosis of perineurioma. Another limitation of the present study was its retrospective design; at the time of image analysis all projections needed for optimal differentiation between schwannomas and neurofibromas were therefore not available (Table 3).

In conclusion, the present study confirmed that PNTs are rare, but important cause of peripheral nerve dysfunction. We found US critically important for demonstration of PNTs, and published US criteria as useful to differentiate schwannomas from neurofibromas. Unfortunately, no such criteria are available for perineuriomas. PNTs are most likely when their continuity with peripheral nerves is demonstrated, and discrepancy between lesions' large size and well preserved nerve function is found.

Acknowledgments

Author thanks Dr. Gregor Omejec for collaboration in performance of US examinations, and Mr. Boštjan Kastelic for help with preparing of figures. The author is supported by the Republic of Slovenia Research Agency, Grant No. P3-0338.

References

1. July J, Guha A. Peripheral nerve tumors. *Handb Clin Neurol* 2012; **105:** 665-74. doi: 10.1016/b978-0-444-53502-3.00016-1
2. Kubiena H, Entner T, Schmidt M, Frey M. Peripheral neural sheath tumors (PNST) – what a radiologist should know. *Eur J Radiol* 2013; **82:** 51-5. doi: 10.1016/j.ejrad.2011.04.037
3. Abreu E, Aubert S, Wavreille G, Gheno R, Canella C, Cotten A. Peripheral tumor and tumor-like neurogenic lesions. *Eur J Radiol* 2013; **82:** 38-50. doi: 10.1016/j.ejrad.2011.04.036
4. Gruber H, Glodny B, Bendix N, Tzankov A, Peer S. High-resolution ultrasound of peripheral neurogenic tumors. *Eur Radiol* 2007; **17:** 2880-8. doi: 10.1007/s00330-007-0645-7
5. Ryu JA, Lee SH, Cha EY, Kim TY, Kim SM, Shin MJ. Sonographic differentiation between Schwannomas and neurofibromas in the musculoskeletal system. *J Ultrasound Med* 2015; **34:** 2253-60. doi: 10.7863/ultra.15.01067
6. Telleman JA, Stellingwerff MD, Brekelmans GJ, Visser LH. Nerve ultrasound in neurofibromatosis type 1: a follow-up study. *Clin Neurophysiol* 2018; **129:** 354-9. doi: 10.1016/j.clinph.2017.11.014
7. Reynolds DL, Jr., Jacobson JA, Inampudi P, Jamadar DA, Ebrahim FS, Hayes CW. Sonographic characteristics of peripheral nerve sheath tumors. *AJR Am J Roentgenol* 2004; **182:** 741-4. doi: 10.2214/ajr.182.3.1820741
8. Omejec G, Zgur T, Podnar S. Diagnostic accuracy of ultrasonographic and nerve conduction studies in ulnar neuropathy at the elbow. *Clin Neurophysiol* 2015; **126:** 1797-804. doi:
9. Forthman CL, Blazar PE. Nerve tumors of the hand and upper extremity. *Hand Clin* 2004; **20:** 233-42, v. doi: 10.1016/j.hcl.2004.03.003
10. Pedro MT, Antoniadis G, Scheuerle A, Pham M, Wirtz CR, Koenig RW. Intraoperative high-resolution ultrasound and contrast-enhanced ultrasound of peripheral nerve tumors and tumorlike lesions. *Neurosurg Focus* 2015; **39:** E5. doi: 10.3171/2015.6.focus15218
11. Salvalaggio A, Cacciavillani M, Coraci D, et al. Nerve ultrasound and 3D-MR neurography suggestive of intraneural perineurioma. *Neurology* 2016; **86:** 1169-70. doi: 10.1212/wnl.0000000000002488
12. Omejec G, Podnar S. Utility of nerve conduction studies and ultrasonography in ulnar neuropathies at the elbow of different severity. *Clin Neurophysiol* 2020; **131:** 1672-7. doi: 10.1016/j.clinph.2020.02.019

research article

Effects of dynamic contrast enhancement on transition zone prostate cancer in Prostate Imaging Reporting and Data System Version 2.1

Jiahui Zhang[1], Lili Xu[1], Gumuyang Zhang[1], Xiaoxiao Zhang[1], Xin Bai[1], Hao Sun[1,2], Zhengyu Jin[1,2]

[1] Department of Radiology, State Key Laboratory of Complex Severe and Rare Disease, Peking Union Medical College Hospital, Peking Union Medical College, Chinese Academy of Medical Sciences, Beijing, China
[2] National Center for Quality Control of Radiology, Beijing, China

Radiol Oncol 2023; 57(1): 42-50.

Received 9 October 2022
Accepted 18 November 2022

Correspondence to: Hao Sun, Hao Sun, M.D., M.P.H., Department of Radiology, State Key Laboratory of Complex Severe and Rare Disease, Peking Union Medical College Hospital, Peking Union Medical College, Chinese Academy of Medical Sciences, Shuaifuyuan No.1, Wangfujing Street, Dongcheng District, Beijing 100730, China. E-mail: sunhao_robert@126.com; Zhengyu Jin, Department of Radiology, State Key Laboratory of Complex Severe and Rare Disease, Peking Union Medical College Hospital, Peking Union Medical College, Chinese Academy of Medical Sciences, Shuaifuyuan No.1, Wangfujing Street, Dongcheng District, Beijing 100730, China. E-mail: jinzy@pumch.cn

Disclosure: No potential conflicts of interest were disclosed.

Background. The aim of the study was to analyse the effects of dynamic contrast enhanced (DCE)-MRI on transitional-zone prostate cancer (tzPCa) and clinically significant transitional-zone prostate cancer (cs-tzPCa) in Prostate Imaging Reporting and Data System (PI-RADS) Version 2.1.

Patients and methods. The diagnostic efficiencies of T2-weighted imaging (T2WI) + diffusion-weighted imaging (DWI), T2WI + dynamic contrast-enhancement (DCE), and T2WI + DWI + DCE in tzPCa and cs-tzPCa were compared using the score of ≥ 4 as the positive threshold and prostate biopsy as the reference standard.

Results. A total of 425 prostate cases were included in the study: 203 cases in the tzPCa group, and 146 in the cs-tzPCa group. The three sequence combinations had the similar areas under the curves in diagnosing tzPCa and cs-tzPCa (all $P > 0.05$). The sensitivity of T2WI + DCE and T2WI + DWI + DCE (84.7% and 85.7% for tzPCa; 88.4% and 89.7% for cs-tzPCa, respectively) in diagnosing tzPCa and cs-tzPCa was significantly greater than that of T2WI + DWI (79.3% for tzPCa; 82.9% for cs-tzPCa). The specificity of T2WI + DWI (86.5% for tzPCa; 74.9% for cs-tzPCa) were significantly greater than those of T2WI + DCE and T2WI + DWI + DCE (68.0% and 68.5% for tzPCa; 59.1% and 59.5% for cs-tzPCa, respectively) (all $P < 0.05$). The diagnostic efficacies of T2WI + DCE and T2WI + DWI + DCE had no significant differences (all $P > 0.05$).

Conclusions. DCE can improve the sensitivity of diagnosis for tzPCa and cs-tzPCa, and it is useful for small PCa lesion diagnosis.

Key words: prostate cancer; transitional zone; magnetic resonance imaging; dynamic contrast enhancement

Introduction

Prostate cancer (PCa) is a common malignant tumour and has the second highest incidence of all cancers worldwide in males[1]; it is the second deadliest among male cancer patients in the United States.[2] Prostate-specific antigen (PSA) assays and magnetic resonance imaging (MRI) are widespread in the diagnosis and follow-up examination of PCa, and thus the PCa detection rate continues to increase yearly worldwide.[3] MRI is a non-invasive examination and can clearly show the anatomy of the prostate. It is one of the most valuable imaging methods for the diagnosis of PCa.[4,5] PCa is primarily located in the peripheral zone, but approximately 25% of PCa cases are lo-

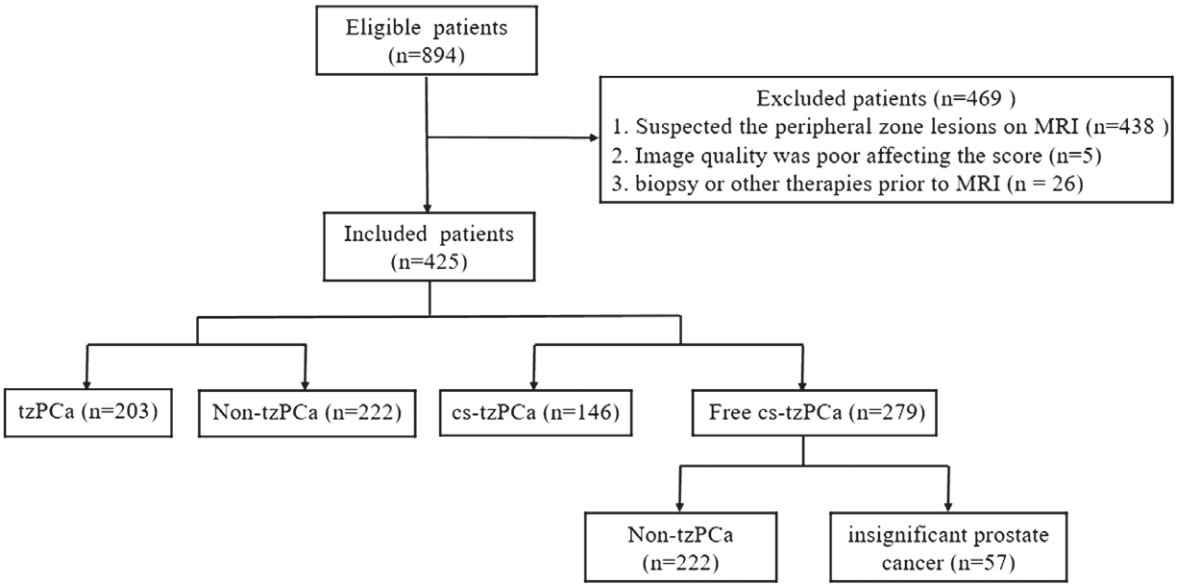

FIGURE 1. Flowchart showing the patient recruitment process.

cated in the transitional zone. The MRI features of PCa in the transitional zone are similar to central glandular benign prostatic hyperplasia (BPH) in signal intensity and morphological characteristics, thus making it difficult to differentiate between BPH and PCa.[6] The early diagnosis and timely intervention of PCa is key to improve the prognosis of PCa patients.[7] Thus, it is of great significance to improve the diagnostic accuracy of transitional-zone prostate cancer (tzPCa).

The Prostate Imaging Reporting and Data System (PI-RADS) is currently recognized as an important guideline for prostate examination and diagnosis via MRI. The first and second editions of PI-RADS guidelines (v1, v2) were proposed in 2012 and 2015, respectively.[8,9] In 2019, PI-RADS Version 2.1 (v2.1) reformulated the research specifications for MRI acquisition technology in prostate scanning and analysed the diagnostic values of multiparametric MRI (mpMRI), which includes T2-weighted imaging (T2WI), diffusion-weighted imaging (DWI), and dynamic contrast-enhanced (DCE)-MRI sequencing.[10] A prostate transitional-zone lesion score criterion of PI-RADS v2.1 only includes T2WI and DWI sequences; DCE-MRI has no effect on the transitional-zone lesion score. The benefits and drawbacks of the DCE-MRI sequence for PCa diagnosis are increasingly being recognized. The advantages of omitting the DCE sequence are that it shortens the scan time and reduces examination costs. However, the DCE sequence with a higher spatial resolution could be less prone to motion artefacts, susceptibility artefacts from metallic implants, or rectal gas. It can be used informally as a "safety-net" or "back-up" sequence to detect lesions that might otherwise be missed on T2WI or DWI, *e.g.*, when the readers have less experience or when there is insufficient image quality.[10-12] Therefore, the value of DCE-MRI as a routine sequence has been debated.[10,13-17]

Prompt intervention is needed for clinically significant prostate cancer (Gleason score ≥ 3 + 4), which usually has poor differentiation, a damaged gland structure, a high degree of malignancy, and strong invasiveness.[9] This study used three sequence combinations (T2WI + DWI, T2WI + DCE, and T2WI + DWI + DCE) to analyse the diagnostic value of DCE-MRI for detecting tzPCa and clinically significant transitional-zone prostate cancer (cs-tzPCa) in PI-RADS Version 2.1, using transperineal ultrasound-guided prostate biopsy as the reference standard.

Patients and methods

Patients

The Institutional Review Board (IRB) of our hospital approved this retrospective study (IRB number JS-2114), and the requirement for informed consent was waived. The clinical and MRI data of 894 patients with prostate diseases admitted to our hospital from January 2015 to December 2019 were continuously collected. The inclusion criteria were

TABLE 1. Sequence parameters for prostate MRI

Parameters	T2WI	DWI	DCE
Sequence	FRFSE	SE-EPI	3D-GRE
TR/TE (ms)	4137/86	4200/90	4.3/1.3
Flip angle	110°	90°	12°
Echo train length	32	1	N/A
FOV (mm × mm)	270 × 270	360 × 360	400 × 400
Matrix size	288 × 192	128 × 96	320 × 192
Slice thickness (mm)	3.0	3.0	3.0
Other		b values = 0, 50, 100, 150, 200, 500, 800, 1000, 1500, 2000 sec/mm^2	Temporal resolution < 10s, total scan time of 5 min

DCE = dynamic contrast-enhancement; DWI = diffusion-weighted imaging; FOV = field of view; FRFSE = fast relaxation fast spin echo; SE-EPI = spin echo echo planar imaging; T2WI = T2-weighted imaging; TE = time echo; TR = repetition time; 3D-GRE = 3D-gradient echo

as follows: (1) a complete MRI examination including T1WI, T2WI, and DWI with the corresponding apparent diffusion coefficient (ADC) map and DCE sequences; (2) diagnosis confirmed by trans-perineal ultrasound-guided prostate biopsy after MRI; and (3) no biopsy, radiation therapy, chemotherapy, hormonal therapy, or other therapies prior to MRI examination. The exclusion criteria were as follows: (1) after MRI examination, the lesion was suspected to be located in the peripheral zone (n = 438); (2) poor MRI image quality affected scoring (n = 5); and (3) biopsy or other therapies prior to MRI (n = 26). Figure 1 shows the flowchart of the patient recruitment process. In total, 425 cases were included. Non-tzPCa indicates transitional-zone lesions other than cancer, such as BPH or normal prostate. Free cs-tzPCa indicates transitional-zone lesions other than clinically significant prostate cancer, including insignificant prostate cancer and non-tzPCa.

MRI protocol

This work used a 3.0-T, eight-channel, surface-phased array coil abdominal MRI scanning system (GE750; GE Health care, Milwaukee, WI, USA). The centre of the coil was placed at the pubic symphysis during positioning and fixed with a band to reduce artefacts from breathing movements. The scan sequence included axial T1WI and T2WI, coronal and sagittal T2WI, DWI, and DCE. When the b-value was 100 and 1000 sec/mm^2, we used the corresponding ADC graph for evaluation. Gadolinium diethylene-triamine penta-acetic acid (Gd-DTPA) offered enhanced contrast at a dose of 0.1 mmol/kg and a flow rate of 3 ml/s. The MRI image-acquisition parameters are shown in Table 1.

Pathological diagnosis

The Gleason grading system for histopathological grading of PCa was adopted.[18] Here, cs-tzPCa was confirmed if the tumour's Gleason score was ≥ 3 + 4 with or without ≥ 0.5-cm^3 tumour volume and/or extraprostatic extension.[9,19] According to the 2014 International Society of Urological Pathology (ISUP) criteria, cs-tzPCa was defined as ISUP grade≥2.[20] Patients biopsied all underwent a 12-core systematic trans-perineal ultrasound-guided prostate biopsy by one urinary specialist. The prostate gland was divided into 11 regions on ultrasound scans. At least one additional targeted biopsy was performed; the cognitive targeted biopsy using cognitive registration was based on zonal anatomy or imaging landmarks such as remarkable nodules. The details of the cognitive targeted biopsy are as follows: first, the urologist reviewed the MRI results; and second, the urologist used the MRI information to perform the targeted biopsy for the most remarkable nodules guided by ultrasound images. A pathologist reported the pathological score of prostate biopsy specimens. The radiologist matched the lesions with the highest PI-RADS v2.1 scores on the MRI images with the pathology report.

Image analysis

Two radiologists with 10 and 5 years of experience in prostate imaging/diagnosis independently

analysed the images under double-blinded conditions. The radiologists scored the images of index lesions in each sequence using PI-RADS v2.1 and then calculated scores for T2WI + DWI, T2WI + DCE, and T2WI + DWI + DCE. When multiple lesions were present, the lesion with the highest PI-RADS score was used for statistical analysis. In the case of disagreement between the two radiologists, the final score was discussed with a third radiologist to reach a consensus. On PI-RADS v2.1, both T2WI and DWI scored 1–5 points whereas the DCE score was binary [negative (–) or positive (+)]. The final total score of T2WI + DCE and T2WI + DWI + DCE was increased by one point when the image showed early and focal enhancement (positive) of DCE; the final total score of T2WI + DCE and T2WI + DWI + DCE remained unchanged when the image was negative regarding DCE. The final score was 5 when the image scored 5 on T2WI regardless of the DWI and DCE scores. Detailed scoring criteria are shown in Table 2. Figure 2 shows a case of cs-tzPCa located in the right lobe of the prostate.

Statistical analysis

SPSS version 22.0 (IBM Corp., Armonk, NY, USA) and MedCalc version 15.0 (MedCalc Software, Ostend, Belgium) were used for statistical analysis. Agreement of readings between the two radiologists was evaluated by a kappa (κ) coefficient with $\kappa < 0.20$ indicating no agreement, $\kappa = 0.21–0.40$ indicating fair agreement, $\kappa = 0.41–0.60$ indicating moderate agreement, $\kappa = 0.61–0.80$ indicating good agreement, and $\kappa = 0.81–1.00$ indicating excellent agreement. Using PI-RADS ≥ 4 as the positive threshold and prostate biopsy as the reference standard, receiver operating characteristic (ROC) curves for T2WI + DWI, T2WI + DCE, and T2WI + DWI + DCE in the diagnosis of tzPCa and cs-tzPCa were separately drawn to calculate areas under the curve (AUCs), sensitivities, specificities, positive predictive values (PPVs), negative predictive values (PNVs), and accuracies to evaluate the corresponding diagnostic efficacies. We also compared differences among the detection rates of tzPCa and cs-tzPCa via three sequence combinations. The DeLong test was used to evaluate differences among AUCs, and McNemar's test was used to compare the sensitivities, specificities, and accuracies of different sequence combinations. The chi-square test was used to compare differences among the detection rates. $P < 0.05$ was considered statistically significant for all statistical tests.

TABLE 2. Scoring criteria of transition zone prostate for three sequence combinations

Scoring Criteria					
T2WI	DWI	DCE	T2WI + DWI	T2WI + DCE	T2WI + DWI + DCE
1	1~5	–	1	1	1
1	1~5	+	1	2	2
2	1~3	–	2	2	2
2	1~3	+	2	3	3
2	4~5	–	3	2	3
2	4~5	+	3	3	4
3	1~4	–	3	3	3
3	1~4	+	3	4	4
3	5	–	4	3	4
3	5	+	4	4	5
4	1~5	–	4	4	4
4	1~5	+	4	5	5
5	1~5	–	5	5	5
5	1~5	+	5	5	5

DCE = dynamic contrast-enhancement; DWI = diffusion-weighted imaging; T2WI = T2-weighted imaging

TABLE 3. Clinicopathological data of patients included in this study

Clinicopathological data	Patients
Age (year), Mean ± SD	66 ± 9.0
T-PSA (ng/ml), Median (Upper and lower quartiles)	9.4 (6.3 + 15.4)
tzPCa, n (%)	203 (48%)
Non-tzPCa, n (%)	222 (52%)
cs-tzPCa, n (%)	146 (34%)
Free cs-tzPCa, n (%)	279 (66%)
Tumor size (mm), Median (Upper and lower quartiles)	12.7 (9.1 + 22.5)
GS, n (%)	
3 + 3	57 (28%)
3 + 4	56 (28%)
4 + 3	24 (12%)
3 + 5	3 (1.5%)
4 + 4	18 (8.9%)
4 + 5	28 (13.8%)
5 + 3	1 (0.5%)
5 + 4	13 (6.4%)
5 + 5	3 (1.5%)

cs-tzPCa = clinically significant transitional-zone prostate cancer; PSA = prostate-specific antigen; SD = standard deviation; tzPCa = transitional-zone prostate cancer

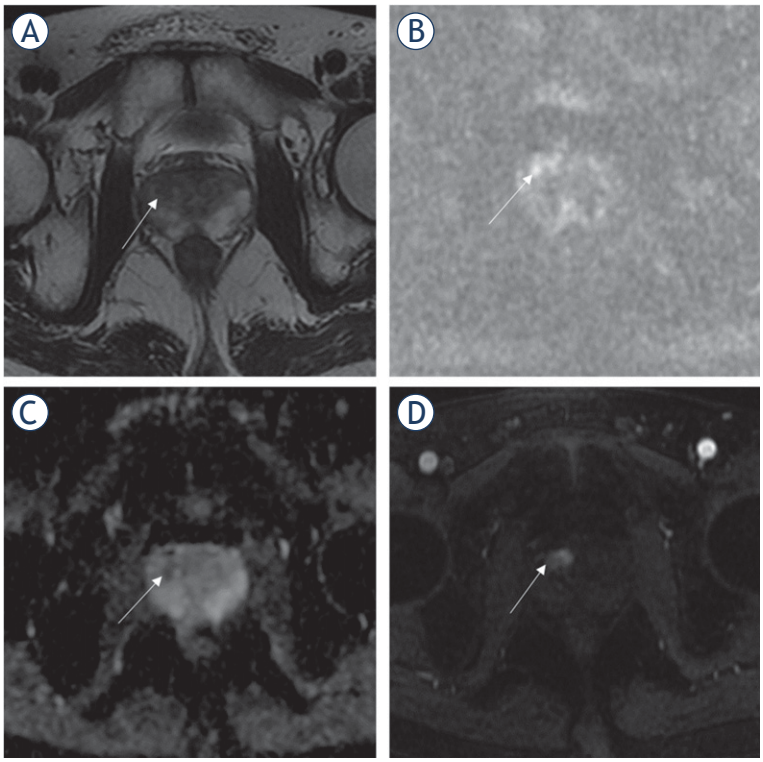

FIGURE 2. Images from a 62-year-old male patient with a total prostate-specific antigen (PSA) of 7.66 ng/mL. **(A)** Axial T2-weighted imaging (T2WI) showed focal hypointensity on the right lobe of the prostate in the transitional zone with a blurred margin and a T2WI score of 3. **(B)** Diffusion-weighted imaging (DWI) showed a slight increase in lesion signal. **(C)** Reduced corresponding apparent diffusion coefficient (ADC) value with a score of 3. **(D)** dynamic contrast-enhancement (DCE) showed obvious enhancement in the early stage of the lesion, thus indicating that the DCE score was positive. Scores were 3, 4, and 4 based on T2WI + DWI, T2WI + DCE, and T2WI + DWI + DCE, respectively. The lesion was confirmed to be clinically significant transitional-zone prostate cancer (cs-tzPCa) based on biopsy (Gleason score of 5 + 4).

Results

Clinicopathological data

This study included 425 prostate cases per the aforementioned inclusion criteria. There were 203 cases in the tzPCa group (48%) and 222 in the non-tzPCa group (52%). There were 146 cases in the cs-tzPCa group (34%) and 279 in the free cs-tzPCa group (66%). The patient age range was 34–86 years (mean age, 66 years), and the median PSA value was 9.4 ng/mL. The main clinical manifestations were elevated PSA, dysuria, frequent urination, and urinary urgency. Abnormalities may be found in the patients during digital rectal examination, including a stiff prostate or palpation of nodules. Table 3 shows the patients' clinicopathological information.

Agreement between the two radiologists

The PI-RADS v2.1 scores provided by the two radiologists were analysed for agreement. The reading agreement between PI-RADS v2.1 scores for T2WI + DWI, T2WI + DCE, and T2WI + DWI + DCE was κ = 0.869, 0.855, and 0.868, respectively.

Comparative analysis of the diagnostic efficacies of three sequence combinations in tzPCa and cs-tzPCa

The diagnostic efficacies of three sequence combinations in tzPCa and cs-tzPCa were shown in Tables 4 and 5. The AUCs were 0.863, 0.868, and 0.863 for tzPCa and 0.840, 0.833, and 0.824 for cs-tzPCa in T2WI + DWI, T2WI + DCE, and T2WI + DWI + DCE, respectively. The AUCs of three sequence combinations in diagnosing tzPCa and cs-tzPCa had no significant differences (all $P > 0.05$). The sensitivity of T2WI + DCE and T2WI + DWI + DCE in diagnosing tzPCa and cs-tzPCa was significantly greater than that of T2WI + DWI (all $P < 0.05$). The specificity and accuracy of T2WI + DWI in diagnosing tzPCa and cs-tzPCa were significantly greater than those of T2WI + DCE and T2WI + DWI + DCE (all $P < 0.05$). The sensitivity, specificity, and accuracy of T2WI + DCE and T2WI + DWI + DCE in diagnosing tzPCa and cs-tzPCa had no significant differences (all $P > 0.05$).

Comparative analysis of the cancer detection rates of three sequence combinations in tzPCa and cs-tzPCa

Figures 3 and 4 show the cancer detection rates of three sequence combinations in tzPCa and cs-tzPCa. When the PI-RADS score was 4, T2WI + DWI had the highest cancer detection rate. The cancer detection rates of T2WI + DWI were significantly greater than those of T2WI + DCE and T2WI + DWI + DCE in tzPCa (69.4%, 29.8%, and 33.7%, respectively, all $P < 0.05$) and cs-tzPCa (43.9%, 19.2%, and 25.0%, respectively, all $P < 0.05$). The cancer detection rates of the three sequence combinations had no significant differences in tzPCa or cs-tzPCa when the PI-RADS score was 1, 2, 3, and 5 (all $P > 0.05$).

Discussion

Some studies questioned whether DCE is a necessary sequence for routine MRI dynamic scanning

TABLE 4. Comparison of diagnostic efficacy of three sequence combinations in tzPCa

		tzPCa (n =203)	Non-tzPCa (n=222)	Sensitivity (%)	Specificity (%)	PPV (%)	NPV(%)	Accuracy (%)	AUC (95% CI)
T2WI + DWI	≥ 4 (n=191)	161	30	79.3	86.5	84.3	82.1	83.1	0.863 (0.827–0.894)
	< 4 (n=234)	42	192						
T2WI + DCE	≥ 4 (n=243)	172	71	84.7	68.0	70.8	83.0	76.0	0.868 (0.832 + 0.899)
	< 4 (n=182)	31	151						
T2WI + DWI + DCE	≥ 4 (n=244)	174	70	85.7	68.5	71.3	84.0	76.7	0.863 (0.827 + 0.895)
	< 4 (n=181)	29	152						
[a]*P*				0.001	< 0.001	NA	NA	0.002	0.424
[b]*P*				< 0.001	< 0.001	NA	NA	< 0.001	0.968
[c]*P*				0.500	1.000	NA	NA	0.250	0.369

AUC = area under curve; CI = confidence interval; DCE = dynamic contrast-enhancement; DWI = diffusion-weighted imaging; NPV = negative predictive value; PPV = positive predictive value; tzPCa = transitional-zone prostate cancer; T2WI = T2-weighted imaging

[a]*P* value between T2WI + DWI and T2WI + DCE; [b]*P* value between T2WI + DWI and T2WI + DWI + DCE; [c]*P* value between T2WI + DCE and T2WI + DWI + DCE

TABLE 5. Comparison of diagnostic efficacy of three sequence combinations in cs-tzPCa

		cs-tzPCa (n=146)	Free cs-tzPCa (n=279)	Sensitivity (%)	Specificity (%)	PPV (%)	NPV (%)	Accuracy (%)	AUC (95%CI)
T2WI + DWI	≥ 4 (n=191)	121	70	82.9	74.9	63.4	89.3	77.6	0.840 (0.802–0.874)
	< 4 (n=234)	25	209						
T2WI + DCE	≥ 4 (n=243)	129	114	88.4	59.1	53.1	90.7	69.2	0.833 (0.795–0.868)
	< 4 (n=182)	17	165						
T2WI + DWI + DCE	≥ 4 (n=244)	131	113	89.7	59.5	53.7	91.7	69.9	0.824 (0.785–0.869)
	< 4 (n=181)	15	166						
[a]*P*				0.008	< 0.001	NA	NA	< 0.001	0.430
[b]*P*				0.002	< 0.001	NA	NA	< 0.001	0.101
[c]*P*				0.500	1.000	NA	NA	0.250	0.193

AUC = area under curve; CI = confidence interval; DCE = dynamic contrast-enhancement; DWI = diffusion-weighted imaging; NPV = negative predictive value; PPV = positive predictive value; tzPCa = transitional-zone prostate cancer; T2WI = T2-weighted imaging

[a]*P* value between T2WI + DWI and T2WI + DCE; [b]*P* value between T2WI + DWI and T2WI + DWI + DCE; [c]*P* value between T2WI + DCE and T2WI + DWI + DCE

of the prostate.[13-17] To the best of our knowledge, no prior studies have yet analysed the value of DCE-MRI in diagnosing tzPCa and cs-tzPCa. To investigate whether DCE-MRI can improve the diagnostic accuracy of tzPCa, this study innovatively compared and analysed the diagnostic efficiencies of T2WI + DWI, T2WI + DCE, and T2WI + DWI + DCE for detecting tzPCa and cs-tzPCa. This study had a large sample size and included 425 prostate cases—the results were reliable. The results of this study showed T2WI + DWI had higher specificity and accuracy, and DCE-MRI had higher sensitivity in diagnosing tzPCa and cs-tzPCa. DCE-MRI could have a potential impact on the detection of tzPCa and cs-tzPCa.

The AUCs of three sequence combinations in diagnosing tzPCa and cs-tzPCa had no significant differences. However, AUC values only reflect the global performance of the test; sensitivity and specificity trade-offs must also be compared between the three sequence combinations. The specificity and accuracy of T2WI + DWI was significantly greater than those of T2WI + DCE and T2WI + DWI + DCE in diagnosing tzPCa and cs-tzPCa. The prostate patients with an elevated PSA value and a positive digital rectal examination were more con-

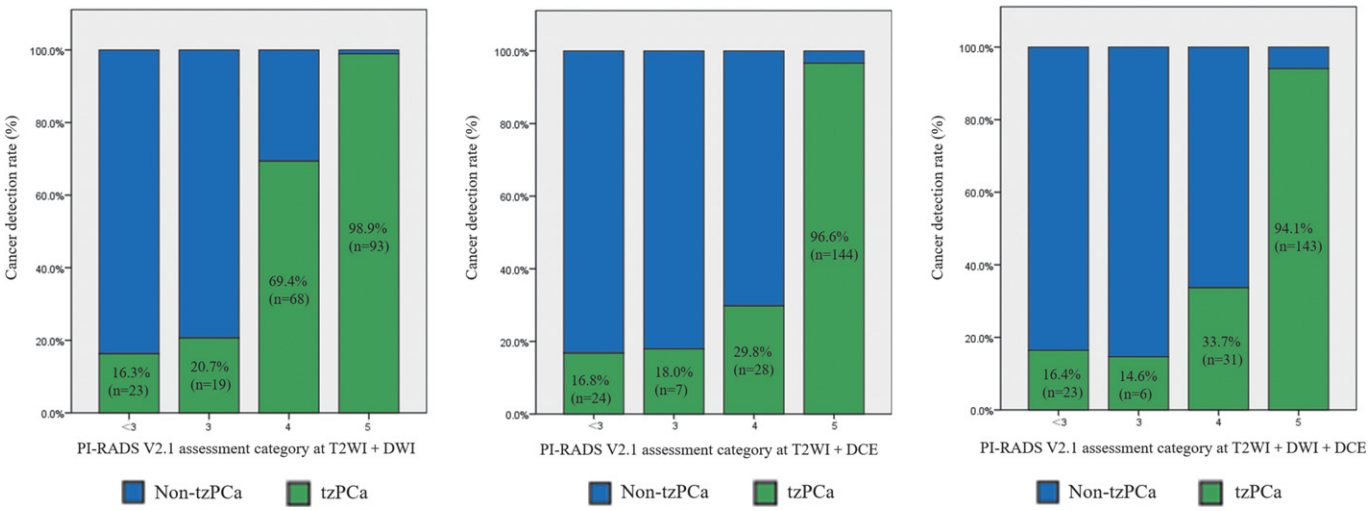

FIGURE 3. Histograms showing cancer detection rates of tzPCa based on the T2-weighted imaging (T2WI) + diffusion-weighted imaging (DWI), T2WI + dynamic contrast-enhancement (DCE), and T2WI + DWI + DCE.

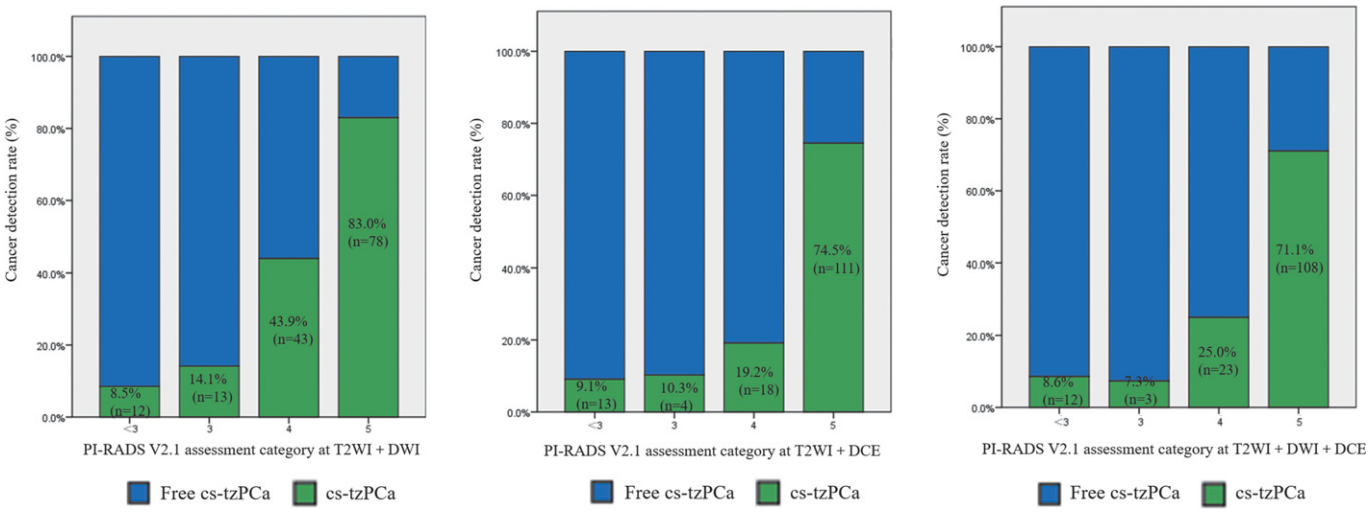

FIGURE 4. Histograms showing cancer detection rates of cs-tzPCa based on the T2-weighted imaging (T2WI) + diffusion-weighted imaging (DWI), T2WI + dynamic contrast-enhancement (DCE), and T2WI + DWI + DCE.

fident in the diagnosis of cancer when DWI results were positive. T2WI + DCE and T2WI + DWI + DCE showed significantly higher sensitivity in both tzPCa and cs-tzPCa. Tamada *et al.*[21] compared and analysed the diagnostic efficiencies of PI-RADS v2.1 scoring between T2WI + DWI + DCE and T2WI + DWI in clinically significant prostate cancer of 165 cases. Their results were similar to ours, but their study did not distinguish between peripheral zone cancers and transitional zone cancers.

Eleven tzPCa cases that were not diagnosed by T2WI + DWI were diagnosed by T2WI + DCE and T2WI + DWI + DCE. The reason is that DCE can clearly show small PCa lesions and improve the sensitivity of diagnosis[22], while the T2WI and DWI sequences are more likely to miss small lesions. A previous study demonstrated that DCE also improves the differential diagnosis of lesions located on the front edge of the peripheral zone with an unclear transition zone from the normal transition zone.[19] T2WI + DCE and T2WI + DWI + DCE had higher diagnostic sensitivity, which could potentially help reduce repeat biopsies when the results were negative. However, active surveillance is still necessary. PCa is characterized by more angiogenic factors and numerous tumour blood vessels

that exhibit increased permeability versus healthy blood vessels. PCa lesions typically enhance earlier and more obviously on DCE than adjacent prostate tissues.[23,24] Vascular permeability also increases in benign diseases such as BPH.[25] These factors might explain the low specificity and high false-positive rate of T2WI + DCE and T2WI + DWI + DCE in the diagnosis of tzPCa and cs-tzPCa.

When the PI-RADS score was 4, the cancer detection rates of T2WI + DWI were significantly greater than those of T2WI + DCE and T2WI + DWI + DCE in tzPCa and cs-tzPCa, which showed T2WI + DWI had lower false-positive rate than T2WI + DCE and T2WI + DWI + DCE. This may be because when BPH lesions strengthened earlier and were more obvious on DCE than adjacent prostate tissues, and when the score of T2WI or T2WI + DWI was 3, the scores of T2WI + DCE and T2WI + DWI + DCE would be increased by one point, thus becoming 4.

This study does have some limitations: (1) This was a single-centre clinical retrospective analysis, which may have selection bias. In future work, we will use a multi-centre, prospective clinical study. (2) This work used prostate biopsy as the reference standard. Prostate biopsy specimens sometimes did not reflect the final pathological findings, which might have yielded false-negative results. (3) In addition to providing qualitative parameters, DCE-MRI can also provide quantitative and semi-quantitative parameters[26], which were not discussed further in this work. It remains unclear whether these parameters are useful in the early diagnosis of tzPCa and cs-tzPCa.

In conclusion, DCE-MRI can improve the sensitivity of diagnosis and has a potential impact on the detection and active surveillance of tzPCa and cs-tzPCa. Meanwhile, DCE-MRI can clearly show small cancers and is useful for small PCa lesion diagnosis.

Acknowledgments

National High Level Hospital Clinical Research Funding (grant no.2022-PUMCH-A-033), the CAMS Innovation Fund for Medical Sciences (grant no.2022-I2M-C&T-B-019), National High Level Hospital Clinical Research Funding (grant no.2022-PUMCH-B-069), National High Level Hospital Clinical Research Funding (grant no.2022-PUMCH-A-035), the Natural Science Foundation of China (grant no.81901742), 2021 Key clinical Specialty Program of Beijing, Beijing Municipal Key Clinical

References

1. Sung H, Ferlay J, Siegel RL, Laversanne M, Soerjomataram I, Jemal A, et al. Global Cancer Statistics 2020: GLOBOCAN estimates of incidence and mortality worldwide for 36 cancers in 185 countries. *CA Cancer J Clin* 2021; **71:** 209-49. doi: 10.3322/caac.21660
2. Siegel RL, Miller KD, Fuchs HE, Jemal A. Cancer Statistics, 2021. *CA Cancer J Clin* 2021; **71:** 7-33. doi: 10.3322/caac.21654
3. Teoh J, Hirai H W, Ho J, Chan F, Tsoi K, Ng C. Global incidence of prostate cancer in developing and developed countries with changing age structures. *PLoS One* 2019; **14:** e221775. doi: 10.1371/journal.pone.0221775
4. Turkbey B, Brown AM, Sankineni S, Wood BJ, Pinto PA, Choyke PL. Multiparametric prostate magnetic resonance imaging in the evaluation of prostate cancer. *CA Cancer J Clin* 2016; **66:** 326-36. doi: 10.3322/caac.21333
5. Ueno Y, Tamada T, Bist V, Reinhold C, Miyake H, Tanaka U, et al. Multiparametric magnetic resonance imaging: current role in prostate cancer management. *Int J Urol* 2016; **23:** 550-7. doi: 10.1111/iju.13119
6. Litjens G, Elliott R, Shih N, Feldman M, Kobus T, Kaa C, et al. Computer-extracted features can distinguish noncancerous confounding disease from prostatic adenocarcinoma at multiparametric MR imaging. *Radiology* 2016; **278:** 135-45. doi: 10.1148/radiol.201514285
7. Remmers S, Roobol M J. Personalized strategies in population screening for prostate cancer. *Int J Cancer* 2020; **147:** 2977-87. doi: 10.1002/ijc.33045
8. Barentsz JO, Richenberg J, Clements R, Choyke P, Verma S, Villeirs G, et al. ESUR prostate MR guidelines 2012. *Eur Radiol* 2012; **22:** 746-57. doi: 10.1007/s00330-011-2377-y. 9
9. Gupta RT, Mehta KA, Turkbey B, Verma S. PI-RADS: past, present, and future. *J Magn Reson Imaging* 2020; **52:** 33-53. doi: 10.1002/jmri.26896
10. Turkbey B, Rosenkrantz AB, Haider MA, Padhani AR, Villeirs G, Macura KJ, et al. Prostate Imaging Reporting and Data System Version 2.1: 2019 Update of Prostate Imaging Reporting and Data System Version 2. *Eur Urol* 2019; **76:** 340-51. doi: 10.1016/j.eururo.2019.02.033
11. Gatti M, Faletti R, Calleris G, Giglio J, Berzovini C, Gentile F, et al. Prostate cancer detection with biparametric magnetic resonance imaging (bpMRI) by readers with different experience: performance and comparison with multiparametric (mpMRI). *Abdom Radiol* 2019; **44:** 1883-93. doi: 10.1007/s00261-019-01934-3
12. Wassberg C, Akin O, Vargas HA, Dave AS, Zhang Jb, Hricak H. The incremental value of contrast-enhanced MRI in the detection of biopsy-proven local recurrence of prostate cancer after radical prostatectomy: effect of reader experience. *AJR Am J Roentgenol* 2012; **199:** 360-6. doi: 10.2214/AJR.11.6923
13. Tamada T, Sone T, Jo Y, Hiratsuka J, Higaki A, Higashi H, et al. Locally recurrent prostate cancer after high- dose-rate brachytherapy: the value of diffusion-weighted imaging, dynamic contrast-enhanced MRI, and T2- weighted imaging in localizing tumors. *AJR Am J Roentgenol* 2011; **197:** 408-14. doi: 10.2214/AJR.10.5772
14. Kuhl CK, Bruhn R, Krämer N, Nebelung S, Heidenreich A, Schrading S. Abbreviated biparametric prostate MR imaging in men with elevated prostate-specific antigen. *Radiology* 2017; **285:** 493-505. doi: 10.1148/radiol.2017170129
15. Junker D, Steinkohl F, Fritz V, Bektic J, Tokas T, Aigner F, et al. Comparison of multiparametric and biparametric MRI of the prostate: are gadolinium-based contrast agents needed for routine examinations? *World J Urol* 2019; **37:** 691-9. doi: 10.1007/s00345-018-2428-y
16. Di Campli E, Delli P A, Seccia B, Cianci R, d'Annibale M, Colasante A, et al. Diagnostic accuracy of biparametric vs multiparametric MRI in clinically significant prostate cancer: comparison between readers with different experience. *Eur J Radiol* 2018; **101:** 17-23. doi: 10.1016/j.ejrad.2018.01.028
17. Huebner NA, Korn S, Resch I, Grubmüller B, Gross T, Gale R, et al. Visibility of significant prostate cancer on multiparametric magnetic resonance imaging (MRI)-do we still need contrast media? *Eur Radiol* 2021; **31:** 3754-64. doi: 10.1007/s00330-020-07494-1
18. Epstein JI, Amin MB, Reuter VE, Humphrey PA. Contemporary Gleason grading of prostatic carcinoma: an update with discussion on practical issues to implement the 2014 International Society of Urological Pathology (ISUP) consensus conference on Gleason Grading of Prostatic Carcinoma. *Am J Surg Pathol* 2017; **41:** e1-7. doi: 10.1097/PAS.0000000000000820

19. Weinreb JC, Barentsz JO, Choyke PL, Cornud F, Haider MA, Macura KJ, et al. PI-RADS Prostate Imaging - Reporting and Data System: 2015, Version 2. *Eur Urol* 2016; **69:** 16-40. doi: 10.1016/j.eururo.2015.08.05

20. Oishi M, Shin T, Ohe C, Nassiri N, Palmer SL, Aron M, et al. Which patients with negative magnetic resonance imaging can safely avoid biopsy for prostate cancer? *J Urol* 2019; **201:** 268-76. doi: 10.1016/j.juro.2018.08.046

21. Tamada T, Kido A, Yamamoto A, Takeuchi M, Miyaji Y, Moriya T, et al. Comparison of biparametric and multiparametric MRI for clinically significant prostate cancer detection with PI-RADS version 2.1. *J Magn Reson Imaging* 2021; **53:** 283-91. doi: 10.1002/jmri.27283

22. Taghipour M, Ziaei A, Alessandrino F, Hassanzadeh E, Harisinghani M, Vangel M, et al. Investigating the role of DCE-MRI, over T2 and DWI, in accurate PI-RADS v2 assessment of clinically significant peripheral zone prostate lesions as defined at radical prostatectomy. *Abdom Radiol* 2019; **44:** 1520-7. doi: 10.1007/s00261-018-1807-6

23. Engelbrecht MR, Huisman HJ, Laheij RJ, Jager GJ, van Leenders GJ, Hulsbergen-Van De Kaa CA, et al. Discrimination of prostate cancer from normal peripheral zone and central gland tissue by using dynamic contrast-enhanced MR imaging. *Radiology* 2003; **229:** 248-54. doi: 10.1148/radiol.2291020200

24. Nicholson B, Theodorescu D. Angiogenesis and prostate cancer tumor growth. *J Cell Biochem* 2004; **91:** 125- 50. doi: 10.1002/jcb.10772

25. Verma S, Turkbey B, Muradyan N, Rajesh A, Cornud F, Haider MA, et al. Overview of dynamic contrast- enhanced MRI in prostate cancer diagnosis and management. *AJR Am J Roentgenol* 2012; **198:** 1277-88. doi: 10.2214/AJR.12.8510

26. Sanz-Requena R, Martí-Bonmatí L, Pérez-Martínez R, García-Martí G. Dynamic contrast-enhanced case- control analysis in 3T MRI of prostate cancer can help to characterize tumor aggressiveness. *Eur J Radiol* 2016; **85:** 2119-26. doi: 10.1016/j.ejrad.2016.09.022

research article

Pancreatic islets implanted in an irreversible electroporation generated extracellular matrix in the liver

Yanfang Zhang[1,2], Yanpeng Lv[2,3], Yunlong Wang[4], Tammy T Chang[5], Boris Rubinsky[2]

[1] Department of Endocrinology, Luoyang Central Hospital Affiliated to Zhengzhou University, Luoyang, China
[2] Department of Mechanical Engineering and Department of Bioengineering, University of California, Berkeley, USA
[3] School of Electrical Engineering, Zhengzhou University, Zhengzhou, China
[4] Henan Bioengineering Research Center, Zhengzhou, China
[5] Department of Surgery, University of California, San Francisco, San Francisco, USA

Radiol Oncol 2023; 57(1): 51-58.

Received 5 November 2022
Accepted 24 November 2022

Correspondence to: Prof. Boris Rubinsky, Department of Mechanical Engineering and Department of Bioengineering, University of California Berkeley, Berkeley CA 94720, USA. E-mail: rubinsky@berkeley.edu

Disclosure: No potential conflicts of interest were disclosed.

Background. Pancreatic islet transplantation via infusion through the portal vein, has become an established clinical treatment for patients with type 1 diabetes. Because the engraftment efficiency is low, new approaches for pancreatic islets implantation are sought. The goal of this study is to explore the possibility that a non-thermal irreversible electroporation (NTIRE) decellularized matrix in the liver could be used as an engraftment site for pancreatic islets.

Materials and methods. Pancreatic islets or saline controls were injected at sites pre-treated with NTIRE in the livers of 7 rats, 16 hours after NTIRE treatment. Seven days after the NTIRE treatment, islet graft function was assessed by detecting insulin and glucagon in the liver with immunohistochemistry.

Results. Pancreatic islets implanted into a NTIRE-treated volume of liver became incorporated into the liver parenchyma and produced insulin and glucagon in 2 of the 7 rat livers. Potential reasons for the failure to observe pancreatic islets in the remaining 5/7 rats may include local inflammatory reaction, graft rejection, low numbers of starting islets, timing of implantation.

Conclusions. This study shows that pancreatic islets can become incorporated and function in an NTIRE-generated extracellular matrix niche, albeit the success rate is low. Advances in the field could be achieved by developing a better understanding of the mechanisms of failure and ways to combat these mechanisms.

Key words: liver cancer; pancreatic islet transplantation; non-thermal irreversible electroporation; tissue engineering; diabetes

Introduction

The experimental work of Ballinger and Lacy was the first to demonstrate the feasibility of using pancreatic islets transplants in the treatment of diabetes.[1] Intraperitoneal and intramuscular injections of pancreatic islets reduced hyperglycemia, polyuria and glycosuria in rats, but consistently normal values were rarely achieved.[1] Kemp *et al.* suggested that since insulin from the pancreatic cells is normally secreted into the portal venous system, the liver may provide a more physiological environment for transplanted islets in intraperitoneal or subcutaneous locations.[2] Indeed, injection of islets into the rat portal vein resulted in normal urine volume, normal glycemia and abolition of glyco-

suria for 2 months after transplantation, suggesting that the liver was an effective site for pancreatic islets transplantation.[2]

Pancreatic islet transplantation via infusion through percutaneous transhepatic access of the portal vein, has since become a clinical treatment for patients with type 1 diabetes or undergoing total pancreatectomy.[3,4,5] Despite major advances in pancreatic islet transplantation via the portal vein, the engraftment efficiency of islets remains low and only about 10–20% of transplanted islets are estimated to survive.[5] Approximately 60% of the transplanted islets are lost in the very early stages of the post-transplantation period.[6] The causes of low islet engraftment and functional durability are multi-factorial. Major contributing factors include early islet death due to failed engraftment and the thrombotic/inflammatory reaction induced within the portal vein.[5] Instant blood-mediated inflammatory reaction triggered by the direct exposure of the islets to blood contributes to the loss of transplanted islets.[7] As the technology to develop stem cell-derived beta-cells and islets mature, demand for islet transplantation is expected to increase and the procedure become more widespread.[8]

Identification of new and improved methods for pancreatic islets implantation has become an important area of research.[9,10] In an attempt to overcome deficiencies related to the injection of pancreatic islets through the portal vein, while retaining the advantages of islet implantation into the liver, Fujita *et al.* reported on a method of direct transplant of pancreatic islets, in the form of an islet-cell-sheet, onto the liver surface.[11] They found that the implanted islet tissue consisted predominantly of insulin-positive beta cells. Glucagon-positive alpha cells were also present, but their numbers were small and they were sparsely distributed within the islet tissue.[11]

Here, we investigate a different approach to transplant pancreatic islets within the liver utilizing the special attributes of non-thermal irreversible electroporation (NTIRE). NTIRE has become a clinically useful modality for cancer treatment in the liver.[12] NTIRE is a minimally-invasive tissue ablation technique in which electric field pulses are delivered across a treatment volume to irreversibly permeabilize the cell membrane. Cell death is induced in the NTIRE-treated volume[13,14] likely through necroptosis and/or pyroptosis pathways.[15,16] The extracellular matrix within the treated volume remains intact and blood vessels remain patent.[14,17] Accordingly, NTIRE has been used to ablate solid tumors near sensitive body structures, such as large blood vessels within the liver[18] and pancreas.[19] Large blood vessels in the NTIRE-treated region remain intact; the blood vessels do not leak and the endothelial layer regenerates.[20] Our earlier research has shown that the extracellular matrix that remains after NTIRE can serve as a scaffold for native cell regeneration in the liver[14], blood vessels[21] intestines.[17] These studies also suggested the use of NTIRE to generate an extracellular matrix for regenerative medicine.[22-24]

This study was motivated by findings from our earlier studies.[25,26] In[25] it was shown that transplanted hepatocytes engraft into host liver parenchyma when directly implanted into an NTIRE pre-treated area. NTIRE improved exogeneous cell engraftment likely by killing host hepatocytes while preserving the extracellular matrix, thereby creating space and a supportive niche for new cell engraftment. Importantly, NTIRE induces a pro-reparative innate immunity milieu, which may further promote integration of transplanted cells.[26] In contrast, an earlier study has shown that in the absence of NTIRE pre-treatment, direct implantation of three-dimensional cell clusters, such as hepatocyte organoids, into the liver, has limited durability and tissue incorporation.[27] In that study, hepatic organoids were directly implanted within a hepatotomy site in the liver of immune competent mice.[27] By day 3 after the implantation, most hepatocytes within organoids were apoptotic or necrotic, and by day 7, chronic inflammatory reactions developed around the implanted organoids.[27]

The goal of this study is to evaluate if a NTIRE decellularized matrix in the liver could serve as a graft site for pancreatic islets directly implanted in the liver and if grafted pancreatic islets could survive and become functional in this type of niche.

Materials and methods

Approvals

Experiments were performed on Sprague Dawley male rats weighing 250–350 g. Seven rats received NTIRE and islet transplants, and 7 rats were used as islet donors. All animals received humane care from properly trained professionals in compliance with both the Principals of Laboratory Animal Care and the Guide for the Care and Use of Laboratory Animals, published by the National Institute of Health (NIH publication no. 85-23, revised 1985), and treated according to an animal protocol approved by the Animal Care and Use Committee of the University of California, Berkeley. The

University of California Berkeley Animal Care and Use Committee approved the animal protocol AUP-2017-12-10605.

NTIRE ablation protocol

After partial mobilization of the liver from adjacent tissue, the liver lobe was gently clamped between two 10-mm-diameter electrodes (Harvard Apparatus, Holliston, MA, USA), as shown in Figure 1. The measured distance between the two electrodes is 3.0 ± 0.2 mm. A sequence of 10 square pulse with an electric field of 1000 V/cm, 100 μs pulse width, separated by 100 ms was applied between the electrodes, across the liver, using an electroporator (ECM 830, Wave Electroporation System (BTX Harvard Apparatus, Holliston, MA, USA). Previous studies with the experimental configuration in this study have shown that this electroporation protocol produces minimal thermal damage, and the tissue is affected primarily by irreversible electroporation.[23] Because the electrodes are flat parallel surfaces, the voltage on the electrodes can be set to achieve a uniform electric field through most of the liver volume bound between the surface electrodes, except at the edges. This voltage was adjusted to yield an electric field of 1000 V/cm in the central area of the parallel electrodes. Two different lobes were electroporated in each animal, one lobe for the injection of pancreatic islets and the second lobe for injection of a control of a phosphate buffered solution (PBS). Seven rats were used as recipients in the pancreatic islet transplant experiment.

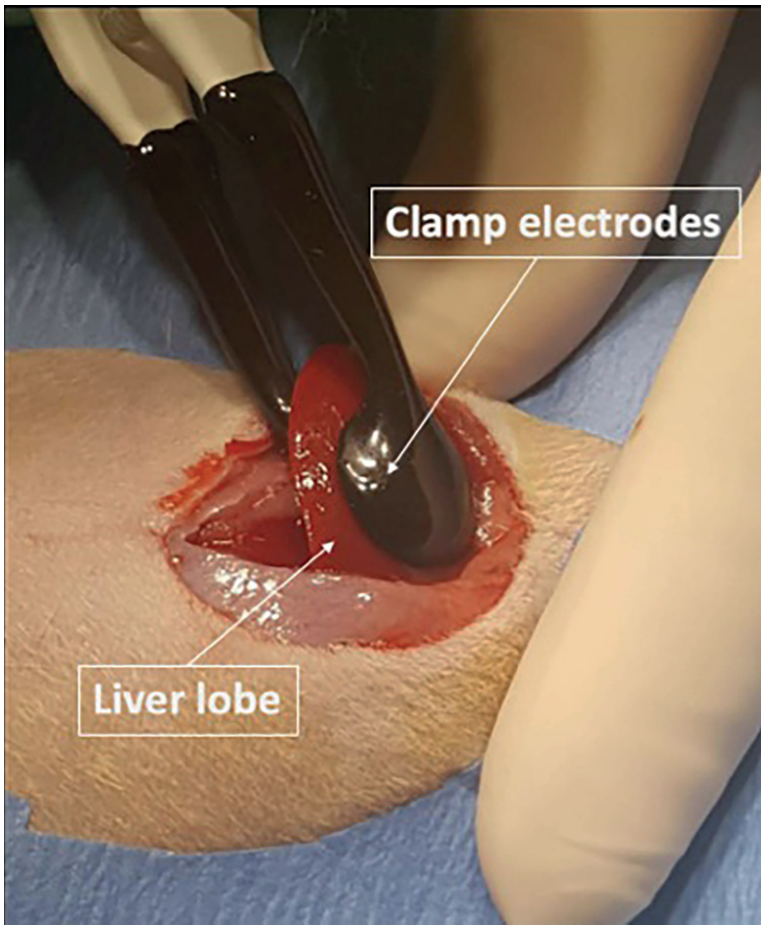

FIGURE 1. Photograph of a clamp electroporation electrode on a liver lobe.

Procurement of pancreatic islets

Pancreatic islets were prepared as described.[28] Rats were initially anesthetized with 3–5% isoflurane by placing them in an induction chamber. No more than 8 mg/kg bupivacaine was injected once subcutaneously prior to skin incision. Once anesthetized, the rat was then transferred to a nose cone respirator connected to a precision vaporizer that delivered 1–3% isoflurane for maintenance. The peritoneal cavity was entered via a midline incision of the abdomen. The common bile duct was cannulated and injected with digestion solution-containing collagenase P (Roche, #11249002001). The pancreas was carefully excised and pulled away from the intestines, stomach, mesentery and spleen, put into a 50 ml centrifuge tube, and immediately incubated in a 37°C water bath for 20 min. The rats were euthanized by a combination of an overdose of vaporized isoflurane and a bilateral chest dissection. Pancreas digestion was then terminated by adding cold washing buffer containing Hanks' Buffered Salt Solution (HBSS, Hyclone SH3058802), 1% Penicillin-Streptomycin (Pen-Strep, Invitrogen, 15070063), 1% 1M N-2-hydroxyethylpiperazine-N-2-ethane sulfonic acid (HEPES, Invitrogen, 15630080), 0.1% Deoxyribonuclease I(DNase I), 1.7 ml 1 M $CaCl_2$/1000 ml and 1.2 ml 1 M $MgCl_2$/1000 ml. After being washed in washing buffer several times and filtered by a strainer, the digested islets were separated on a Histopaque (Sigma-Aldrich, 11191) density gradient. The islets were then hand-picked and the Histopaque was washed out by a washing buffer. The islets were resuspended in 5 ml culture media and poured into a Petri dish for hand-picking. A few sample fresh islets were stained with dithizone (DTZ) to confirm their purity. Stock solution of DTZ (0.5 mg/ml) was prepared in dimethyl sulfoxide (DMSO). The stock solution was diluted five times in Dulbecco's Phosphate

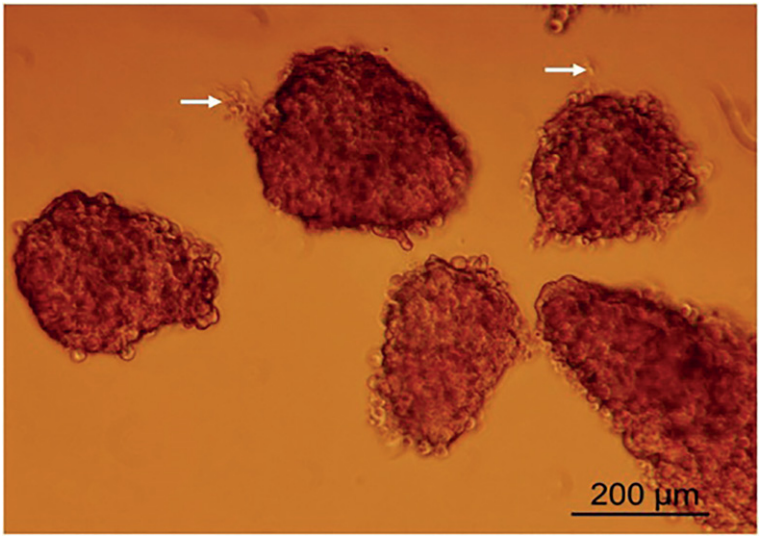

FIGURE 2. Photograph of the pancreatic islets used in this study stained by dithizone (DTZ). Arrows point to the few unstained exocrine cells left after digestion by collagenase.

Buffered Solutions, (DPBS) solution. The morphology of purified islets is shown in Figure 2. The islet cells were scarlet with DTZ staining, while exocrine cells were devoid of staining. Arrows point to the few exocrine cells left after digestion by collagenase. The pancreatic islets were generated in seven rats, with one rat providing the pancreatic islets per transplant recipient.

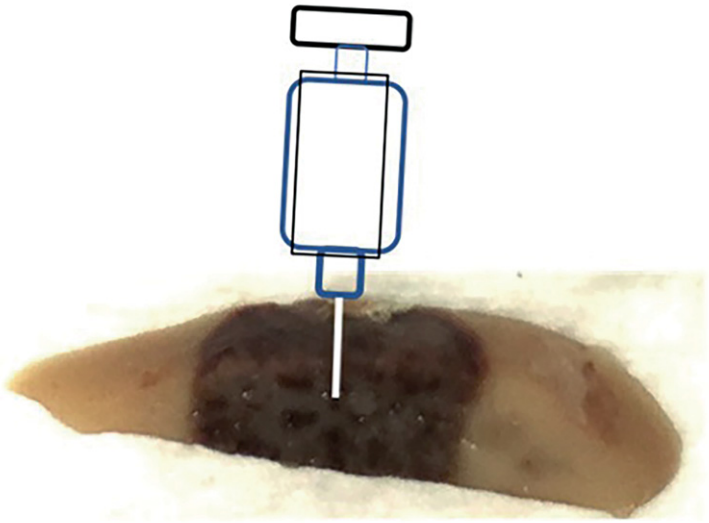

FIGURE 3. An illustration showing the implantation site in the liver. The dark area is the non-thermal irreversible electroporation (NTIRE) treated area.

Implantation of pancreatic islets

Rats pre-treated with NTIRE were anesthetized and the previously made midline incision was re-opened 16 hours later. Approximately 200 pancreatic islets were transplanted into a recipient. Islets were washed and re-suspended in 0.2 ml PBS. Using a 1 ml syringe and 26-gauge needle, islets were injected into the center of one of the IRE-treated liver lobes. The second, control lobe was injected with the same volume of PBS into the IRE- treated region in that lobe. Figure 3 illustrates the site of the injections at the center of the ablated region. At the completion of the pancreatic islet injection procedure, the abdominal wall was closed and sutured. The animals were kept two in a cage, given food and water freely and continuously monitored for well-being by a veterinarian affiliated with the animal care facility. No controls with injection of pancreatic islets in the untreated liver parenchyma was performed. A previous study has shown that in the absence of NTIRE pre-treatment, direct implantation of three-dimensional hepatocytes cell clusters into the liver had limited durability and tissue incorporation.[27] In contrast, transplanted hepatocytes engraft into host liver parenchyma when directly implanted into an NTIRE pre-treated area.[25]

Islet graft analysis

We collected and examined the livers 7 days after the NITRE procedure. Islet graft function was assessed by detecting insulin and glucagon in the liver by immunohistochemistry. The treated liver tissue samples were cut in a plane normal to the liver lobe surface, through the center of the treated lesion. The liver was fixed in formalin, embedded in paraffin, and sectioned 5 µm thick (Histo-Tec Laboratory, Hayward, CA, USA). The samples were sent to UT Health San Antonio STRL Histology/ Immunohistochemistry Laboratory Department of Pathology and Laboratory Medicine where they were stained with guinea pig anti-insulin antibodies and rabbit anti-glucagon antibodies.

Results and discussion

The livers of recipient rats were treated with 1000 V/cm NTIRE in 2 locations. Sixteen hours later, one site was injected with PBS and the other site was injected with approximately 200 donor rat pancreatic islets. We chose to analyze the livers 7 days af-

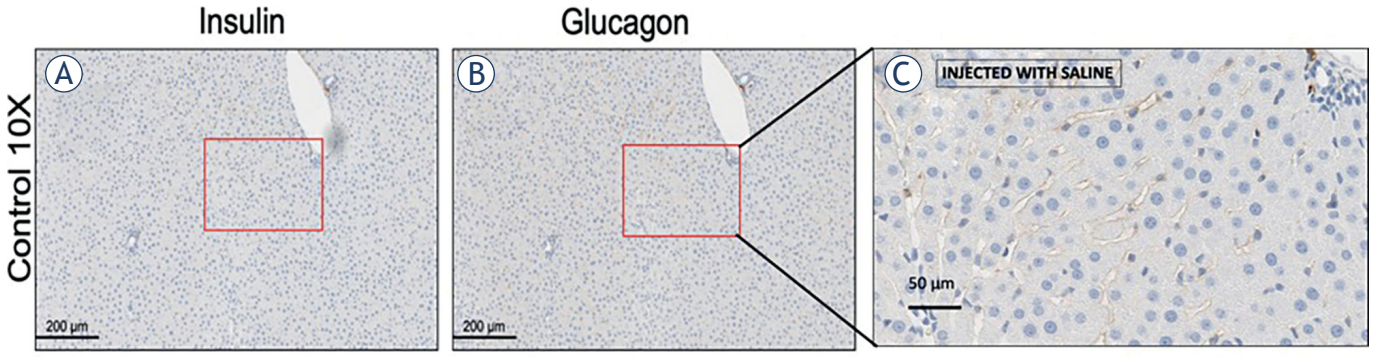

FIGURE 4. Liver tissue treated with non-thermal irreversible electroporation (NTIRE) and injected with PBS served as the control. Seven days after treatment with NTIRE and injection of PBS, immunohistochemical staining was performed on the controls using insulin and glucagon antibodies (University of Texas at Houston, USA). In the control slides, no cells were stained with insulin or glucagon antibodies, shown in **(A)** and **(B)**, respectively. The higher magnification panel 4C shows normal hepatocytes with no evidence of scar tissue.

ter the NTIRE treatment because, in rats, the liver completely regenerates 7 days after injury.[29]

Figure 4 shows the appearance of the NTIRE-treated lobe that was injected with PBS. To show that staining by insulin and glucagon antibodies was specific to the sites injected with pancreatic islets, the sites injected with PBS were stained with insulin or glucagon antibodies, Figure 4 A and B, respectively. The control NTIRE-treated liver regenerated and was not stained by the insulin or glucagon antibodies. Panel 4C is a higher magnification of the previously NTIRE treated region. It shows that 7 days after IRE ablation, the hepatocytes were intact and well-developed. Nuclei were clear, and sinusoids were seen. There was no evidence of scar tissue or fibrosis. This illustrates the regenerative capability of NTIRE-treated livers.

Within the NTIRE-treated liver parenchyma that received islet implantation, we found evidence of engrafted insulin- and glucagon-producing cells in 2 of the 7 animals. Figures 5A and 5B show the presence of engrafted pancreatic islets within the liver as demonstrated by positive insulin and glucagon staining. Insulin-stained cells (beta cells) and glucagon-stained cells (alpha cells) are marked with full arrows in the higher magnification images Fig 5C and 5D, respectively. Fully developed and normal hepatocytes were observed (dotted arrows) around the glucagon- and insulin-positive cells. These findings show that it is possible for pancreatic islets, injected in tissue treated with NTIRE, to become integrated in the liver parenchyma and become functional producing glucagon and insulin.

The fact that 7 days after the implantation the pancreatic islets have become incorporated in the liver parenchyma and generate insulin and glycogen in 2 of the 7 animals, is encouraging. By comparison, in previous experiments with direct injection of hepatocyte organoids in the liver parenchyma, most hepatocytes within implanted organoids were apoptotic or necrotic by day 3 after transplant.[27]

The goal of this study is limited to showing that pancreatic islets can become incorporated in a niche formed by NTIRE treatment of the liver. In that sense, the results are promising. Nevertheless, the incorporation was observed in only 2 of the 7 repeats, which is a low rate of success. It should be emphasized, however, that engraftment efficiency of pancreatic islet transplantation through the portal vein is not optimal, which is why alternative approaches for transplantation are explored.[5] We speculate that there are several reasons for our low rate of success.

An important aspect of the procedure is choosing the optimal time for the exogenous pancreatic islet implantation in the NTIRE treated liver. In view of the limited success in this study, this must be investigated further. In our previous study of implantation of hepatocytes in the liver, the implantation was done 3 days after the NTIRE procedure.[25] In this study, the choice for the time of implantation is based on the results of a previous study on the mechanisms of cell death in the NTIRE-treated liver.[16] That study followed the temporal events in a liver treated with the same NTIRE protocol as in this study. It was observed that the hepatocytes appear morphologically intact one hour after the NTIRE procedure. This suggested that the implantation cannot be done at the same time as the NTIRE ablation, because the hepatocytes still occupied the treated volume. At 6 hours after the procedure, dead hepatocytes are seen

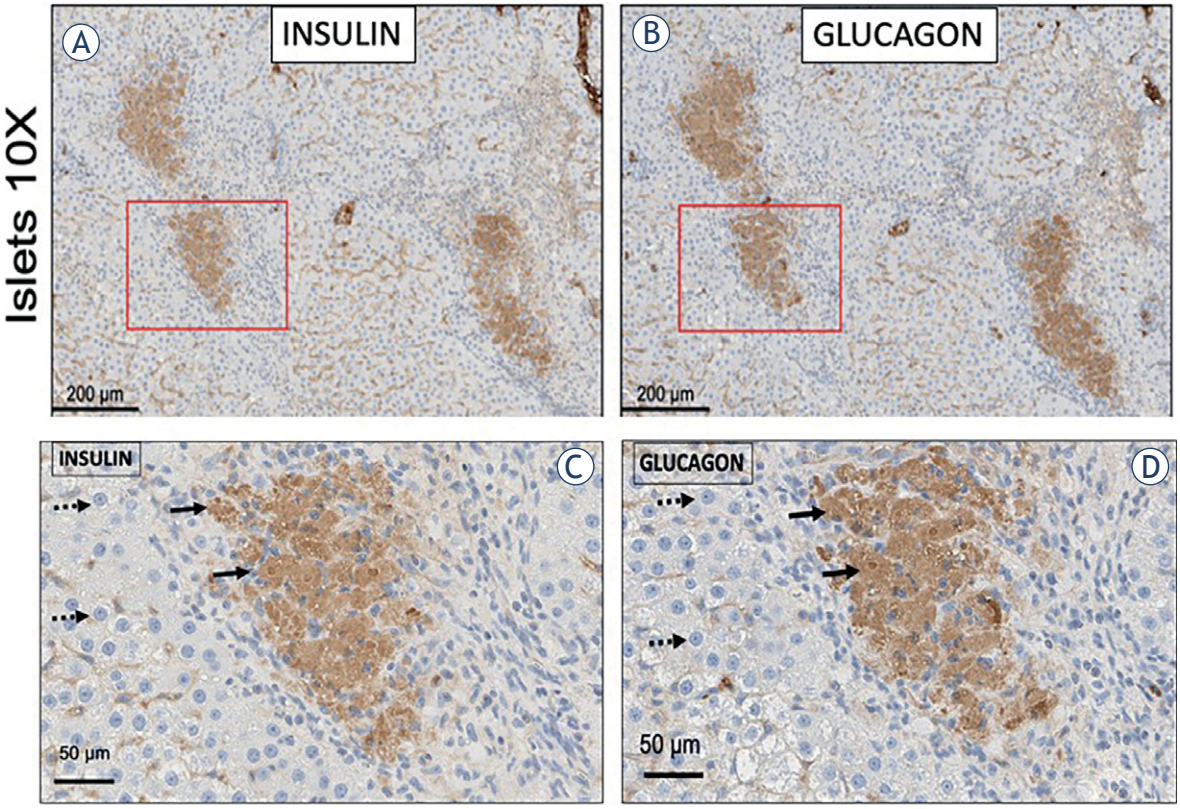

FIGURE 5. Liver tissue treated with non-thermal irreversible electroporation (NTIRE) and injected with 200 rat donor pancreatic islets. Seven days later, immunohistochemical staining was performed with anti-insulin and anti-glucagon antibodies (University of Texas at Houston, USA). In the pancreatic islets injected tissue, insulin-stained cell clusters are shown in **(A)** and **(C)** (full arrows). Normal hepatocytes were observed (dotted arrows) around the insulin-stained cells in the liver lobe. Glucagon-stained cells cluster are shown in **(B)** and **(D)** (full arrows). Normal hepatocytes were observed (dotted arrows) around the glucagon-stained cells in the liver lobe.

throughout the treated volume. By 24 hours after NTIRE, hepatocyte regenerative proliferation may be initiated.[29] On the basis of these considerations, we implanted the pancreatic islets at 16 hours after the NTIRE treatment. Ideally, one would choose a time in which the NTIRE niche is free from dying hepatocytes and from regenerating hepatocytes, so that pancreatic islets have optimized conditions to become incorporated into the extracellular matrix. However, the inflammation and repair responses within of the NTIRE-treated region are also important factors. Our group showed that pro-reparative macrophages start to replace pro-inflammatory macrophages at day 3 after NTIRE treatment and become the dominant macrophage subtype by day 7.[26] Therefore, it is quite possible that 16 hours after the NTIRE treatment is not the optimal time. A later timepoint in which pro-reparative macrophages predominant within the NTIRE-treated volume may be more conducive to islet engraftment. Determining the optimal time for implantation, in context of an immunological response coupled with hepatocyte regeneration, is a critical aspect of this procedure and requires much more research. Finally, islet graft rejection may have had an effect on the limited rate of success. No anti-rejection or immunosuppressive medications were used in this study.

Technical reasons may have also played a role in the results. The rate and mode of injection of the pancreatic islets into the liver parenchyma is important. The injection should be slow, controlled and gradual.[27] In this study, injection with a hand-held syringe may not have been the same in all the repeats. Another technical reason may be the injection of the pancreatic islets along the tract of the 26-gauge needle. As shown in Figure 5, the injection site is relatively narrow, on the order of 200 µm, and therefore, the histology section through the center of the lesion may have missed

the injected islets in some of the repeats. Another technical reason may be the small number of the injected pancreatic islets. In this study, we used 200 pancreatic islets per injection site, and this may have been too low a number.

Obviously, the low rate of success is of concern and should be further investigated.

Conclusions

This study shows that pancreatic islets injected into a niche formed in the liver by NTIRE ablation became incorporated and functional in 2 of 7 experimental animals 7 days after NTIRE treatment. While the rate of success is low, the study demonstrates that pancreatic islets can become incorporated in a tissue niche generated by NTIRE ablation. More research is needed to improve the success rate of this technique before it can have clinical value.

Author contributions

YZ designed and performed the animal experiment and aided in the analysis of the data. YL designed and performed the electroporation. YW advised on the animal experiment and edited the animal experiment section. TC, contributed to the analysis of the results, writing of the paper and with advice. BR supervised the research, designed the experiment, analyzed the data, and wrote the paper.

Acknowledgments

This work was supported by the Department of Mechanical Engineering, University of California, Berkeley, the National Natural Science Foundation of China (No. 81702768), Science and technology project of Henan province (No. 212102310193), Innovative leading talents of science and technology project of Health Commission of Henan Province (No. YXKC2021024), NIH R21-EB024135, and Open Philanthropy Project.

We thank the associate chief pathologist Junhong Li who generously aided in the pathological analysis of slides.

References

1. Ballinger WF, Lacy PE. Transplantation of intact pancreatic islets in rats. *Surgery* 1972; **72:** 175-86. PMID: 4262169
2. Kemp CB, Knight MJ, Scharp DW, Ballinger WF, Lacy PE. Effect of transplantation site on the results of pancreatic islet isografts in diabetic rats. *Diabetologia* 1973; **9:** 486-91. doi: 10.1007/BF00461694
3. Shapiro AJ, Ricordi C, Hering BJ, Auchincloss H, Lindblad R, Robertson RP, et al. International trial of the Edmonton protocol for islet transplantation. *N Engl J Med* 2006; **355:** 1318-30. doi: 10.1056/NEJMoa061267
4. McCall M, Shapiro AJ. Update on islet transplantation. *Cold Spring Harb Perspect Med* 2012; **2:** a007823. doi: 10.1101/cshperspect.a007823
5. Korsgren O, Nilsson B, Berne C, Felldin M, Foss A, Kallen R, et al. Current status of clinical islet transplantation. *Transplantation* 2005; **79:** 1289-93. doi: 10.1097/01.tp.0000157273.60147.7c
6. Biarnés M, Montolio M, Nacher V, Raurell M, Soler J, Montanya E. β-cell death and mass in syngeneically transplanted islets exposed to short-and long-term hyperglycemia. *Diabetes* 2002; **51:** 66-72. doi: 10.2337/diabetes.51.1.66
7. Bennet W, Groth CG, Larsson R, Nilsson B, Korsgren O. Isolated human islets trigger an instant blood mediated inflammatory reaction: implications for intraportal islet transplantation as a treatment for patients with type 1 diabetes. *Upsala J Med Sci* 2000; **105:** 125-33. doi: 10.1517/03009734000000059
8. Silva IB, Kimura CH, Colantoni VP, Sogayar MC. Stem cells differentiation into insulin-producing cells (IPCs): recent advances and current challenges. *Stem Cell Res Ther* 2022; **13:** 1-24. doi: 10.1186/s13287-022-02977-y
9. Cayabyab F, Nih LR, Yoshihara E. Advances in pancreatic islet transplantation sites for the treatment of diabetes. *Front Endocrinol* 2021: **12:** 732431. doi: 10.3389/fendo.2021.732431
10. Rickels MR, Robertson RP. Pancreatic islet transplantation in humans: recent progress and future directions. *Endocr Rev* 2019; **40:** 631-68. doi: 10.1210/er.2018-00154
11. Fujita I, Utoh R, Yamamoto M, Okano T, Yamato M. The liver surface as a favorable site for islet cell sheet transplantation in type 1 diabetes model mice. *Regen Ther* 2018; **8:** 65-72. doi: 10.1016/j.reth.2018.04.002
12. Koethe Y, Wilson N, Narayanan G. Irreversible electroporation for colorectal cancer liver metastasis: a review. *Int J Hyperthermia* 2022; **39:** 682-7. doi: 10.1080/02656736.2021.2008025
13. Davalos RV, Mir LM, Rubinsky B. Tissue ablation with irreversible electroporation. *Ann Biomed Eng.* 2005; **33:** 223-31. doi: 10.1007/s10439-005-8981-8
14. Rubinsky B, Onik G, Mikus P. Irreversible electroporation: a new ablation modality—clinical implications. *Technol Cancer Res Treat* 2007; **6:** 37-48. doi: 10.1177/153303460700600106
15. Al-Sakere B, André F, Bernat C, Connault E, Opolon P, Davalos RV, et al. Tumor ablation with irreversible electroporation. *PloS ONE* 2007; **2:** e1135. doi: 10.1371/journal.pone.0001135
16. Zhang Y, Lyu C, Liu Y, Lv Y, Chang TT, Rubinsky B. Molecular and histological study on the effects of non-thermal irreversible electroporation on the liver. *Biochem Biophys Res Commun* 2018; **500:** 665-70. doi: 10.1016/j.bbrc.2018.04.132
17. Phillips MA, Narayan R, Padath T, Rubinsky B. Irreversible electroporation on the small intestine. *Br J Cancer* 2012; **106:** 490-5. doi: 10.1038/bjc.2011.582
18. Hitpass L, Distelmaier M, Neumann UP, Schöning W, Isfort P, Keil S, et al. Recurrent colorectal liver metastases in the liver remnant after major liver surgery – IRE as a salvage local treatment when resection and thermal ablation are unsuitable. *Cardiovasc Intervent Radiol* 2022; **45:** 182-9. doi: 10.1007/s00270-021-02981-4
19. Lee EW, Shahrouki P, Peterson S, Tafti BA, Ding PX, Kee ST. Safety of irreversible electroporation ablation of the pancreas. *Pancreas* 2021; **50:** 1281-6. doi: 10.1097/MPA.0000000000001916

20. Maor E, Ivorra A, Mitchell JJ, Rubinsky B. Vascular smooth muscle cells ablation with endovascular nonthermal irreversible electroporation. *J Vasc Interv Radiol* 2010; **21:** 1708-15. doi: 10.1016/j.jvir.2010.06.024

21. Maor E, Ivorra A, Leor J, Rubinsky B. Irreversible electroporation attenuates neointimal formation after angioplasty. *IEEE Trans Biomed Eng* 2008; **55:** 2268-74. doi: 10.1109/TBME.2008.923909

22. Phillips M, Maor E, Rubinsky B. Principles of tissue engineering with non-thermal irreversible electroporation. *J Heat Transfer* 2011; **133:** 011004. doi: 10.1115/1.4002301.

23. Phillips M, Maor E, Rubinsky B. Nonthermal irreversible electroporation for tissue decellularization. *J Biomech Eng* 2010; **132:** 091003. doi: 10.1115/1.4001882

24. Phillips M, Maor E, Rubinsky B. Lavee J. Extracellular matrix material created using non-thermal irreversible electroporation. US Patent 08835166, Sep 16 2014.

25. Chang TT, Zhou VX, Rubinsky B. Using non-thermal irreversible electroporation to create an in vivo niche for exogenous cell engraftment. *Biotechniques* 2017; **62:** 229-31. doi: 10.2144/000114547

26. Lopez-Ichikawa M, Vu NK, Nijagal A, Rubinsky B, Chang TT. Neutrophils are important for the development of pro-reparative macrophages after irreversible electroporation of the liver in mice. *Sci Rep* 2021; **11:** 1-3. doi: 10.1038/s41598-021-94016-8

27. Zhou VX, Lolas M, Chang TT. Direct orthotopic implantation of hepatic organoids. *J. Surg. Res* 2017; **211:** 251-60. doi: 10.1016/j.jss.2016.12.028

28. Szot GL, Koudria P, Bluestone JA. Murine pancreatic islet isolation. *J Vis Exp* 2007; **22:** e255. doi: 10.3791/255

29. Michalopoulos GK. Liver regeneration. *J. Cell. Physiol* 2007; **213:** 286-300. doi: 10.1002/jcp.21172

research article

Estimating exposure to extremely low frequency magnetic fields near high-voltage power lines and assessment of possible increased cancer risk among Slovenian children and adolescents

Tina Zagar[1], Blaz Valic[2,3], Tadej Kotnik[3], Sara Korat[1], Sonja Tomsic[1], Vesna Zadnik[1], Peter Gajsek[2,3]

[1] Slovenian Cancer Registry, Institute of Oncology Ljubljana, Ljubljana, Slovenia
[2] INIS - Institute for Non-Ionizing Radiation, Ljubljana, Slovenia
[3] Faculty of Electrical Engineering, University of Ljubljana, Ljubljana, Slovenia

Radiol Oncol 2023; 57(1): 59-69.

Received 25 October 2022
Accepted 10 November 2022

Correspondence to: Peter Gajšek, Ph.D., Department of Dosimetry-Institute of Nonionizing Radiation, Pohorskega bataljona 215, SI-1000 Ljubljana, Slovenia. E-mail: peter.gajsek@inis.si

Disclosure: No potential conflicts of interest were disclosed.

Background. Some previous research showed that average daily exposure to extremely low frequency (ELF) magnetic fields (MF) of more than 0.3 or 0.4 μT could potentially increase risk of childhood leukaemia.

Materials and methods. To allow calculations of ELF MF around high voltage (HV) power lines (PL) for the whole Slovenia, a new three-dimensional method including precision terrain elevation data was developed to calculate the long-term average ELF MF. Data on population of Slovenian children and adolescents and on cancer patients with leukaemia's aged 0–19 years, brain tumours at age 0–29, and cancer in general at age 0–14 for a 12-year period 2005–2016 was obtained from the Slovenian Cancer Registry.

Results. According to the large-scale calculation for the whole country, only 0.5% of children and adolescents under the age of 19 in Slovenia lived in an area near HV PL with ELF MF density greater than 0.1 μT. The risk of cancer for children and adolescents living in areas with higher ELF MF was not significantly different from the risk of their peers.

Conclusions. The new method enables relatively fast calculation of the value of low-frequency magnetic fields for arbitrary loads of the power distribution network, as the value of each source for arbitrary load is calculated by scaling the value for nominal load, which also enables significantly faster adjustment of calculated estimates in the power distribution network.

Key words: exposure assessment; childhood cancer; extremely low frequency magnetic fields; modelling; cancer; high voltage power lines

Introduction

Ionizing radiation is a known risk factor for the development of leukaemia and thyroid cancer, while the carcinogenicity of non-ionizing radiation has so far not been scientifically proven. Non-ionizing radiation includes the extremely low-frequency (ELF) magnetic fields (MF) that originate from electric current flowing through artificial sources, among which the most widely present in the living and working environments are the high-voltage (HV) power lines (PL) and transformer substations.

The exposure to ELF MP is the highest in the immediate vicinity of the source and decreases very rapidly with distance. For sources in the vicinity of residences, the Slovenian legislation prescribes a ten times lower permissible ELF MF values (10 μT) than the European Recommendation (100 μT).

During the last few decades, several pooled analyses have been published that combined all available data with various exposure indices.[1-4] These pooled analyses consistently found statistically significant increased relative risk estimates for childhood leukaemia in the case of prolonged daily high exposure to ELF MF (above 0.3 or 0.4 μT) compared with low exposure (below 0.1 μT).[5-8] In 2001, the International Agency for Research on Cancer (IARC) examined the available body of scientific literature on ELF MF and from the subset of studies concerning childhood leukaemia concluded that ELF MF should be classified in group 2B as possibly carcinogenic to humans based on "limited evidence of carcinogenicity in humans" and "inadequate evidence of carcinogenicity in experimental animals".[9] Associations between other cancers and ELF MF were not observed or were statistically insignificant, while it is emphasized the biological mechanisms on how would ELF MF induce cancer growth remain unknown despite broad research also in this area.[9-14]

The fear of an increased risk of cancer that could occur after long-term exposure to ELF MF is also expressed by general public[15], which additionally drives the research in this area.

ELF MF that originate mainly from the use of electricity have been studied as a risk factor for childhood leukaemia since 1979.[16] The available studies ever since used different approaches on estimating the long-term exposure to ELF MF. The simplest possible way of assessing exposure is to calculate distance to a facility which is likely to be a source of the field.[17] One of the common methods to estimate the ELF MF exposure is socalled wire code which uses the distance to and the configuration of HV PL wiring to estimate the long-term exposure to ELF MF.[16] Wire code method does not require any consent of the participants (compared to measurements at homes) and therefore the selection of the case and control groups is not biased by their willingness to participate.[18-21] However, because of the overlap in field levels between categories, wire code was not a good predictor of ELF MF levels, accounting for less than 21% of the variance in magnetic-field measurements.[22] Another method has used estimated historical fields where the ELF MF exposure was defined by a combination of measurements and calculations at homes.[23] The inclusion criteria for participants was the distance of the dwelling from the HV PL. The calculations took into account all important technical parameters of HV PL.

The aim of the study was to determine the ELF MF due to all HV PL in Slovenia. We developed a new method for more reliable real-life exposure assessment, since previous research revealed this as a major source of bias. Further, we investigated whether children and adolescents exposed to ELF MF due to living near HV PL in Slovenia have a higher risk of leukaemia. Additionally, to address concerns of the Slovenian public, we analysed the possible association of ELF MF exposure and the incidence of brain tumours and of all childhood cancers together.

Materials and methods

High voltage power lines registry in Slovenia

There are about 670 km of 400 kV PL, 330 km of 220 kV PL, 2600 km of 110 kV PL and 25 km of 110 kV underground cables in Slovenia. The technical data necessary to calculate and determine the spatial distribution of the ELF MF in the vicinity of HV PL were obtained from national power grid company ELES and from 5 power distribution companies covering Slovenia. The following data about each PL tower were collected: the coordinates, altitude, height and type. The tower type defines the type of the PL geometry (Barrel, Danube...) as well as the exact geometry of the tower cross arms. To take the sag of each span into account, the data about the exact catenary of each span was also obtained. For most of the HV PL the catenary for each span was available in the form of 3D lines, generated by national power grid company from the results of the measurements with LIDAR system. For a few HV PL where the 3D lines were not available, the values of the sag of each span or cable tension in each span were used to calculate the 3D lines. For 110 kV underground cables their exact course was available in a form of points along the cable course, but detailed information about the geometry and depth of the cables was not available.

Based on these technical data, each PL was further split into sections with identical tower types and identical or very similar geometries (position and length of tower cross arm). If the PL was double circuit (in Slovenia only single or double circuit PL are in use), the load data were checked for

each system of the PL. If the loads were mostly the same, then both systems were deemed as one section, otherwise each system was deemed as separate segment. In total the HV distribution system was split into 17 segments for 400 kV, 13 segments for 220 kV and 411 segments for 110 kV.

The load data provided by national power grid company ELES consisted of the data about the working and reactive energy transferred by each HV PL in 15-minute intervals in the period from 1. 1. 2006 to 31. 12. 2017. From these data the values of electric currents were calculated for every 15 minutes, as well as several geometric mean values: daily, weekly (7 day), monthly (30 day) and total mean value.

There is no unified approach among the studies regarding which mean value to use as the surrogate for long term exposure. Some studies have estimated the variations over time from available data, for example, on electricity consumption.[24,25] Several studies used the yearly mean load value for the year of the diagnosis with some adding also the year of birth.[23,26-29] In this study, the total mean value covers the two-year period from 1. 1. 2006 to 31. 12. 2017.

Calculating ELF MF

The ELF MF level at one location is the result of the contributions of all nearby HV PL. As the ELF MF is a vector quantity, the total value depends not only on the amplitude of each contribution, but also on their direction and the angles between them. Typically, when calculating the ELF MF, a numerical model is created that contains all sources and thus the calculation determines the total ELF MF level for the selected loads of HV PV. With the available programs and computational capacity, such a calculation is not feasible for large areas. In addition, usual approach requires recalculation of the whole model for each load conditions (for example at nominal loads, actual maximum loads, average day or annual loads, conditions in case of one HV PL failure...) or if there are changes in technical characteristics like construction of new or reconstruction of existing HV PL.

To allow largescale ELF MF calculations, a new method was developed and validated, which enables the calculation of the total ELF MF based on the values of the ELF MF of individual sources. The methodology was divided into two steps: the first step was to calculate the ELF MF of one HV PL and the second was to calculate the total ELF MF due to all HV PL for desired loads.

Methodology to calculate the ELF MF of single HV PL

New method to calculate the ELF MF of one HV PL was based on the principle that the distribution of the ELF MF in the vicinity of the PL is not affected by the nearby objects or terrain, and on the fact that as long as the geometry of the PL and its load are the same, the value of the ELF MF in a selected point depends only on the distance between the selected point and the HV PL and on the difference of the altitude of the selected point and the HV PL. Each HV PL was split into sections with identical or quite similar geometries. From the data in the registry, a 3D line was generated for each segment, representing the course of the lowest cable of the HV PL. Additionally, for each HV PL segment the ELF MF distribution in a vertical cross section was calculated with a Narda EFC-400 EP program package at the nominal load. The program package calculated the ELF MF by splitting all conductors into short parts and summing their contributions. The value of the ELF MF of one short part of conductor was calculated by the Biot-Savart law:

$$d\vec{B}(t) = \frac{\mu_o}{4\pi}\frac{d\vec{l}\times\vec{r}}{r^3}I(t)$$

where is magnetic flux density contribution from a short part of the conductor at the point given by positon vector and *I* is electric current in the cable.

The calculation took into account exact geometry of the towers in this segment and extended to the distance where the value of the ELF MF fell below 0.05 μT. The result was stored in a GRID matrix with the step of 1 m and positioned so that the center of the matrix aligned with the 3D line of the segment.

The 3D line representing the course of the PL and the matrix with the values of the ELF MF in a vertical cross section were used as the input to a customdeveloped program that calculated the value of the ELF MF along the whole segment length. The program first split the segment into spans. For each span, the program generated a 1m grid of points that covered the area of the whole length of span in one dimension and the same distance as covered by the matrix of the values of ELF MF in a vertical cross section. At both ends of the span (at location of the HV PL towers), additional points were added by rotating the last line of points as presented by blue and black dots in Figure 1. We can see that blue and black dots do overlap in a certain area around the tower. For each point in the 1m grid, first the height difference was calcu-

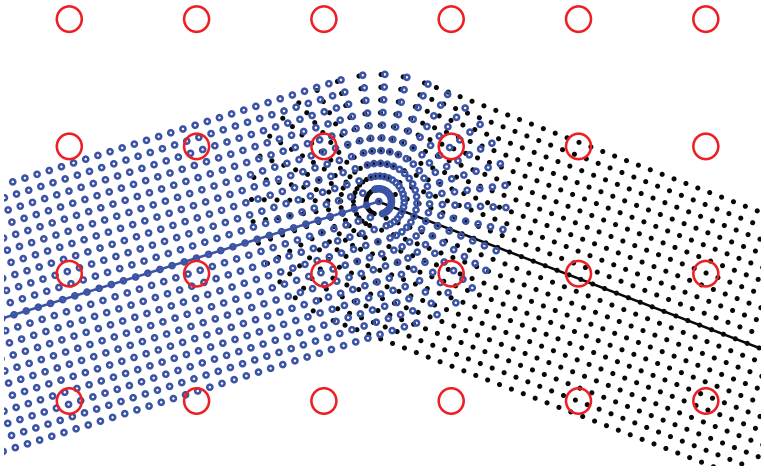

FIGURE 1. Points in 1m grid for two spans of a power line are shown with blue and black dots in which the program determined the values of the extremely low-frequency (ELF) magnetic fields (MF). Red circles represent the final 10 mgrid for which the final results were generated.

lated between the absolute height of the 3D line representing the course of the PL and the point 1 m above the ground. The absolute height of the point 1 m above the ground was determined from the digital elevation model of Slovenia with the resolution of 1 m constructed based on the LIDAR data. Second, the distance of each point in the 1 m grid from the HV PL was calculated. Both values were rounded to the nearest integer and used to pick the corresponding value from the matrix with the calculated values of the ELF MF in a vertical cross section. By this process the proper value of the ELF MF was assigned to each point in the 1 m grid. Finally, a 10 m orthogonal grid was generated (red circles in Figure 1) to which the highest value of nearby points in a 2 m radius was assigned. The output of the program for each segment was a 10m grid of points with the values of the ELF MF.

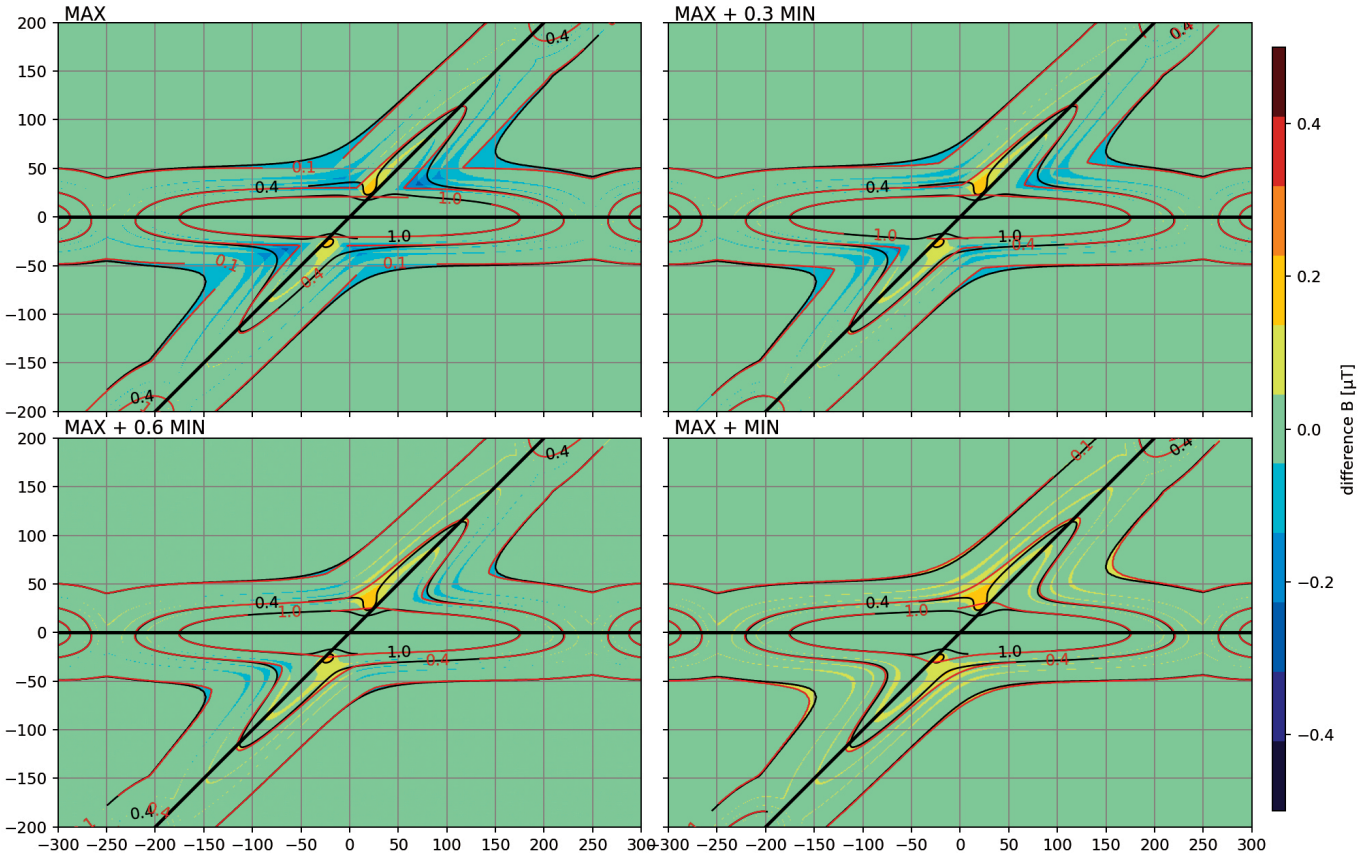

FIGURE 2. Comparison of results obtained by all four algorithms to determine total value of extremely low-frequency (ELF) magnetic fields (MF) for a case of crossing of two 2×110 kV power lines of type barrel under the nominal load of 650 A. The color scale shows the deviation of the estimated value of ELF MF values determined by all four new algorithms from the actual value of ELF MF determined by the usual numerical modeling procedure. The black contours represent the limits of 0.1, 0.4 and 1.0 µT for the actual values, and the red contours for the estimated values.

Finally, if HV PL was split in more than one segment, all 10 m grids of one HV PL were merged together. For those coordinates where values were available in two (or theoretically more) grids, the highest value was used for the final result.

Methodology to calculate the total ELF MF of multiple HV PL

When multiple HV PL either cross or run in parallel, the total value of the ELF MF is a result of the contributions of all nearby HV PL. As ELF MF is a vector quantity, the resulting value is typically significantly lower than a sum of all contributions. Therefore, four different algorithms to determine the total value of the ELF MF in each considered point were analysed and compared:

- the MAX algorithm took the higher value of the two contributions as the total value;
- the MAX + MIN algorithm took the sum of the higher and the lower values as the total value;
- the MAX + 0.3 MIN and MAX + 0.6 MIN calculated the total value by adding to the higher value the lower value multiplied by a specific weight factor of 0.3 and 0.6, respectively.

As, the actual total value of the ELF MF can never exceed the sum of the two values considered, the MAX + MIN algorithm is the most conservative, the MAX algorithm is the least conservative, and the other two are inbetween.

In order to evaluate all four algorithms, various realworld scenarios were analysed where cumulative effects of several HV PL occur, e.g. crossing of two HV PL, or parallel courses of two and three HV PL. Figure 2 presents the analysis of one such case –the intersection of two 110 kV double-circuit HV PL. The colour scale shows the deviation of the estimated ELF MF determined by all four new algorithms from the actual ELF MF determined by usual numerical modelling procedure. Green colour means that there is practically no deviation, red colour marks areas where the algorithm overestimated the values, and blue colour shows areas where the algorithm underestimated the values. Among four proposed algorithms, the MAX algorithm underestimated the values of the ELF MF the most (as the blue areas are the largest) and overestimated them the least (as the red areas are the smallest). The MAX + MIN algorithm never underestimated the values of the ELF MF, and overestimated them the most among the four proposed algorithms. Information regarding the deviation of the estimated value from the actual value is also provided in Figure 2 by black and red contours. The black contours represent the field lines of 0.1, 0.4 and 1.0 μT for the actual value obtained by usual modelling procedure, and the red contours for the estimated value using a novel method. For the MAX + MIN algorithm red contours never lie inside black contours, which means that the MAX + MIN algorithm overestimated the values of the ELF MF. Using the MAX algorithm, red contours often or even predominantly lie within black contours. The analysis showed that the most realistic results for the conditions considered was given by the MAX + 0.6 MIN algorithm, which was thus chosen as the optimal algorithm. Subsequent feasibility analysis showed that calculations could be performed according to all four algorithms, which allowed later sensitivity analysis, i.e. whether the choice of algorithm affects the result of analyses.

A novel program with all four analysed algorithms was developed to determine total value of the ELF MF. The program also featured the functionality to scale the values of each HV PL with a certain factor before calculating the total value of the ELF MF. This functionality enables relatively easy and fast calculation of the total ELF MF not only for the nominal load of HV PL, but for any load conditions or operating conditions of the whole power distribution network. For the later analysis, the total geometric mean value of the load was used that covers the whole period from 1. 1. 2006 to 31. 12. 2017.

Cancer data

We conducted retrospective geographical epidemiological study in population of Slovenian children and adolescents aged 0–19 years diagnosed in a 12-year period 2005–2016.

Address of residence served as a proxy indicator of ELF MF exposure. From Central Population Registry data on permanent address, which was georeferenced to X and Y coordinates, was obtained for all Slovenian children and adolescents in the studied population. Modelled values for ELF MF density near HV PL were used to classify all population of children and adolescents into five categories of ELF MF exposure: $B < 0.1$ μT; 0.1 μT $\leq B < 0.2$ μT; 0.2 μT $\leq B < 0.3$ μT; 0.3 μT $\leq B < 0.4$ μT and 0.4 μT $\leq B$. Georeferenced addresses were allocated to the closest point on the 10m grid by using the k-nearest neighbours (kNN) method on the Quad Tree to avoid calculation of Euclidian distances between each grid point and each address location (building Quad Tree algorithm has running time $O(n \cdot \log(n))$).[30]

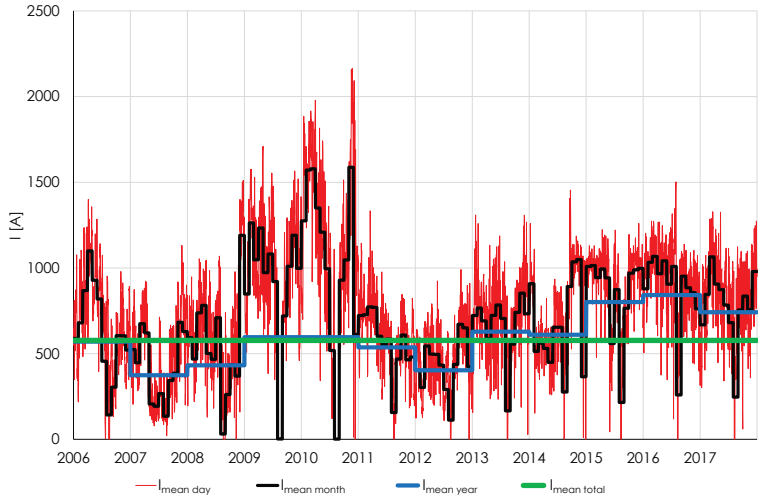

FIGURE 3. The daily, monthly, yearly and total (1. 1. 2006 – 31. 12. 2017) mean values of the load of a 400 kV power line with the highest mean values in Slovenia.

From the Slovenian Cancer Registry incidence (number of all newly diagnosed cancer cases in one calendar year) data on cancer patients were obtained and linked to population data based on Slovenian personal identification number. Patients with leukemias were identified based on codes C91–C95 according to the 10th revision of the International Statistical Classification of Diseases and Related Health Problems (ICD-10). In addition, we analysed all cancer cases occurring in childhood (age at diagnosis 0–14 years) and cases with malignant tumour of the central and autonomic nervous system (or brain tumour in short) with codes C70–C72 diagnosed up to 29 years of age.

Relative risk of cancer was assessed using a standardized incidence ratio (SIR), which is a method for indirect age standardization and is calculated as a ratio between observed and expected incidence for each studied group, i.e. cancer incidence in each of the five categories of ELF MF exposure. Expected incidence is calculated from age distribution in studied group and age-specific incidence rates in the overall population.[31] A SIR value of 1 indicates that observed incidence in the studied group is the same as expected incidence, less than 1 indicates a lower than expected incidence, and over 1 indicates a higher than expected incidence.

Data management and analysis of population and cancer data was performed in R software (version 4.0.2) and R packages dplyr (version 1.0.2) and SearchTrees (version 0.5.2).

Results

ELF MF around HV PL

To measure the ELF MF at the participants homes it is necessary to obtain their consent. This can be potential source of selection bias.[29] It is suggested [32] that although it is an imperfect measure of magnetic field exposure, wire code is the only method applicable to nonparticipating subjects. But if technical data about the HV PL near the residence of participants are available, it is possible to determine the exposure at the desired time interval based on the numerical calculations. Such combined estimation of ELF MF exposure has been used in several studies.[8,27-29] As numerical calculation of ELF MF is very demanding for larger areas, the studies usually limit the area of interest to a pre-selected distance to the HV PL, usually in the range of a few hundreds of meters.

The value of the ELF MF in a selected point near PL depends on the geometry of the PL, the load of the PL, the distance from the HV PL, and the elevation difference between the PL and the selected point. It is not affected by the terrain and nearby objects. This principle was used by Miravet-Garret[33], where the distance and difference of the altitude of the HV PL and of the selected point was determined from the detailed technical data of the HV PL and the ground profile, and then the value of the ELF MF at the selected point was calculated by a simplified analytical formula.

The mean values of the load of HV PL in Slovenia have an increasing tendency, meaning that on average the energy transfer through HV PL is increasing. For 110 kV PL the average value of geometric means of the loads of all PL was 84 A in 2006 and 87 A in 2017, for 220 kV PL it was 185 A in 2006 and 213 A in 2017, and for 400 kV PL it was 282 A in 2006 and 360 A in 2017. The increase is significantly higher for 400 KV PL compared to either 220 or 110 kV PL. However, the mean loads are not high. Among all 400 kV PL, the highest total mean value of the load for one PL for the whole period from 1. 1. 2006 to 31. 12. 2017 was 742 A and it increased to 842 A for the highest yearly mean value (in year 2016). In Figure 3 the daily, monthly and yearly mean values for this HV PL are presented.

Yearly mean loads do not differ significantly from the total mean loads (1. 1. 2006 – 31. 12. 2017). The highest yearly value was achieved in 2016 (842 A), whereas the lowest was achieved in 2007 (374 A). The fluctuations in monthly mean loads are larger, the highest monthly load was achieved in November 2010 (1588 A) and the lowest in August

2010 (1 A). For weekly mean loads, the highest values were achieved at the end of November 2010 (1987 A).

The ELF MF around HV PL was calculated for the entire territory of Slovenia on the 10m grid. On Figure 4 the value of the ELF MF of several HV PL around one transformer stations are presented for nominal load (top) and the total mean geometric load covering the period from 1. 1. 2006 to 31. 12. 2017. The value of the ELF MF was determined by the new algorithm (from chapter Methodology to calculate the total ELF MF of multiple sources). For the total mean geometric load, the value of the ELF MF was higher than 0.1 μT on almost 2 million points. This represents the area of about 191 km^2, which means that on about 1% of the territory of Slovenia the value of the ELF MF is 0.1 μT or higher, while on more than 99% of the territory of Slovenia the value of the ELF MF is below 0.1 μT. For 0.4 μT the areas are significantly smaller, as this value is exceeded only on 0.36% of Slovenian territory.

The results were validated by comparing calculated values of ELF MF with measurements in the vicinity of two 400 kV PL and two 220 kV PL. The same load conditions (nominal load) were used for comparison. For the 400 kV PL with the highest mean load, the comparison is given in Table 2.

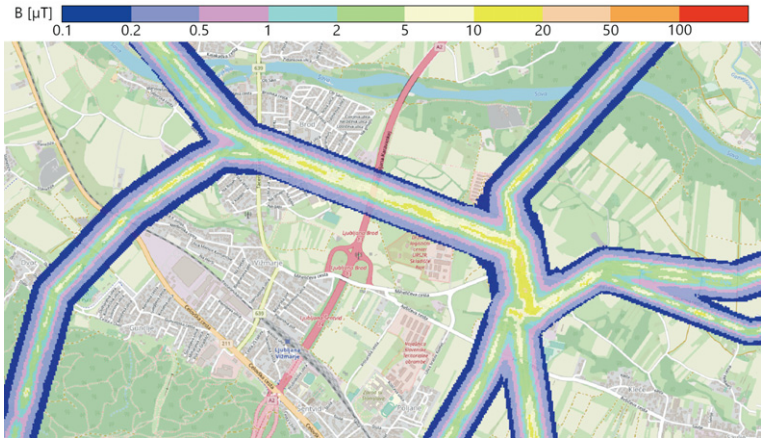

FIGURE 4. Example of the total value of the extremely low-frequency (ELF) magnetic fields (MF) of several high voltage power lines around distribution transformer stations for nominal load in the area of the capital city of Ljubljana (approximately 5 x 2.7 km).

Childhood cancers and ELF MF exposure

Cancer in children and adolescents is a rare disease, as it represents less than 1% of all cancers in Slovenia as well as in Europe.[34,35] In recent years, around 70 cancers are diagnosed annually in Slovenia during childhood and adolescence (from birth to the age of 19), 20% more among boys than among girls.[34] Age-standardized incidence rate has been increasing by an average of slightly more than 1% annually since 1961 in Slovenia and also increased by about 1% per annum in Europe in the past three decades.[34,36] The causes for the increasing incidence are unknown; although it is largely attributed to improved diagnostic and registration procedures, the possibility of increased exposure to different harmful factors, especially intrauterine, cannot be excluded.[36]

The most common groups of malignant cancers in the age group of 0–19 years are leukaemias, lymphomas and tumours of the central nervous system (in short brain tumours). According to the average for the period 1961–2019, leukaemias represented a quarter of all newly diagnosed cancers, followed by brain tumours with around 15%, Hodgkin's lymphoma with 10% and non-Hodgkin's lymphoma with 8%.[34] Apart from exposure to benzene and ionizing radiation, the risk factors for leukaemias are not well known.[37,38] The so-called hygiene hypothesis is also possible, where, due to the improvement of infection prevention in the modern era, leukaemia may develop in geneti-

TABLE 1. The distances from the 400 kV power line with the highest mean load, at which the value of the extremely low frequency magnetic field falls below 0.1, 0.2, 0.3 and 0.4 μT, respectively

Distance	B = 0.1 μT	B = 0.2 μT	B = 0.3 μT	B = 0.4 μT
Nominal load	340 m	238 m	193 m	167 m
Highest daily mean load (2164 A, 23. 11. 2010)	303 m	212 m	172 m	149 m
Highest weekly mean load (1987A, 22. – 28.11.2010)	290 m	203 m	165 m	143 m
Highest monthly mean load (1588 A, 11. 2010)	258 m	181 m	147 m	127 m
Highest yearly mean load (842A, 2016)	187 m	131 m	107 m	92 m
Total mean load (742 A, 1. 1. 2006 – 31. 12. 2017)	175 m	123 m	99 m	87 m

TABLE 2. Comparison of the calculated and measured value of the extremely low frequency magnetic field for 400 kV power line with the highest mean load

Location	1	2	3	4	5
Calculated value [μT]	7.4	3.8	3.0	9.1	3.4
Measured value [μT]	7.3	3.4	4.1	12.3	2.7

cally predisposed individuals due to an incorrect response to infection by the immune system of a child who did not come into contact with non-dangerous infectious agents in early childhood at the right time (early enough).[39] Some (but not all) studies have shown that the risk may be increased (only) for childhood leukaemias with longterm daily exposure to ELF MF densities greater than 0.3 or 0.4 μT, depending on the study.

The key advantage of our study was that with inclusion of the population data from the Slovenian Cancer Registry, we avoided performing a case-control study and, at the same time, selection and participation bias.[8] Research indicates that the fraction of children exposed to higher values of ELF MF (>0.4 μT) is likely to be less than 2% of the population.[40,41] For Slovenia, it was estimated in the past that no more than 1% of children were exposed to long term ELF MF greater than 0.4 μT.[42] In presented study, using an innovative model for evaluating ELF MF on a small spatial network and georeferencing residences and sources of the electricity network in Slovenia, we precisely determined the exposure to ELF MF in children aged up to 14 years in the period 2005–2016 in Slovenia, who live nearby HV PL. We found that as many as 99.5% of all children did not live in the areas with the mean value of ELF MF 0.1 μT or higher. And only 0.09% of all children were exposed for at least one year to the area of potentially carcinogenic ELF MF density, that is greater than 0.4 μT, in the vicinity of HV PL. This population results and results for age groups 0–19 and 0–29 are presented in Table 3 (the results are equal to the first decimal point). These results emphasize the importance of performing exact calculations on real-life population-based data in order to obtain realistic picture of the situation in a specific country.

In Table 3 we also present results according to five categories of ELF MF exposure for observed and expected number of cancer cases, and standardized incidence ratio for all cancers combined, leukaemia and brain tumours. All of the 516 cancer cases in children aged 0–14 years in 2005–2016 were classified in the lowest category of exposure (ELF MF below 0.1 μT) near HV PL. Relative risk cannot be calculated for other categories of ELF MF exposure, since there were no cases.

Among 195 diagnosed cases of leukaemia in children and adolescents aged 0–19 years in 2005–2016 only one adolescent was classified in the category of ELF MF density between 0.1 and 0.2 μT – a person lived in the vicinity of 110 kV PL. This single case of leukaemia represents big variability and thus "shifted" all residents from this group from a relative risk of zero to a relative risk of more than one. Although the value for relative risk in this group appears high (2.4), the confidence interval is far too wide for statistical significance (since it is based on only one case). No leukaemia case was classified in categories with higher ELF MF exposures (i.e., above 0.2 μT).

Among 196 patients aged 0–29 years diagnosed with brain tumour only one adolescent was classified in the category of ELF MF exposure between 0.2 and 0.3 μT, giving standardized incidence ratio 4.4 with wide 95% confidence interval (0.1-24.6). Also, this person lived in the vicinity of 110 kV PL at the time of diagnosis. No brain tumour case was classified in other categories of ELF MF exposure.

We conclude that none of the cases of leukaemia in the studied population can be attributed to exposure to ELF MF – the relative risk of leukaemia in children and adolescents living near HV PL does not differ from the average risk in the general population. Additionally, we could not assess a possible risk trend over exposure categories, because there were also no cases of leukaemias in other categories.

Our findings are in line with other similar studies, but we cannot directly compare the results with other studies due to the different (in our opinion better, more accurate assessment methodology based on actual exposure and availability of exact coordinates for all dwellings on Slovenian population.[41,43] Using place of residence as a surrogate indicator of ELF MF exposure is more reliable in children than in adults, as they spend most of the day in the vicinity of home and the surrounding area. In addition, they migrate less.

Discussion

For the ELF MF exposure assessment, we developed an innovative, accurate model on a fine spatial grid, which is more reliable than exposure approximations used by previous studies (e.g. Euclidean distance from guides, questionnaires,

TABLE 3. The proportion of Slovenian population of children and adolescents in 2005–2016, observed and expected number of cancer cases, and standardized incidence ratio with 95% confidence interval for all cancers combined (age 0–14 years), leukemia (age 0–19 years) and brain tumors (age 0–29 years) are presented according to five categories of ELF MF exposure

	< 0.1 mT	0.1–0.2 mT	0.2–0.3 mT	0.3–0.4 mT	≥ 0.4 mT
Population* (proportion)	99.5 %	0.2 %	0.1 %	0.1 %	0.1 %
All cancers (age 0–14 years)					
Observed number of cases	516	0	0	0	0
Expected number of cases	513.6	1.1	0.6	0.3	0.5
Standardized incidence ratio (95% confidence interval)	1.0 (0.9–1.1)	no cases	no cases	no cases	no cases
Leukemia (age 0–19 years)					
Observed number of cases	194	1	0	0	0
Expected number of cases	194.1	0.4	0.2	0.1	0.2
Standardized incidence ratio (95% confidence interval)	1.0 (0.9–1.2)	2.4 (0.1–13.3)	no cases	no cases	no cases
Brain tumors (age 0–29 years)					
Observed number of cases	195	0	1	0	0
Expected number of cases	195.1	0.4	0.2	0.1	0.2
Standardized incidence ratio (95% confidence interval)	1.0 (0.9–1.2)	no cases	4.4 (0.1-24.6)	no cases	no cases

* Population's proportions for age groups 0–14, 0–19 and 0–29 are equal to the first decimal point.

etc.). With this new method the calculations of ELF MF values generated by all HV PL were performed for the entire territory of Slovenia with the grid of 10 m for average loads of HV PL in the period from 2006 to 2017. The value of ELF MF was higher than 0.1 μT in a little less than 2 million points, which corresponds to an area of about 200 km^2, or one percent of the whole territory of Slovenia. The new method enables relatively fast calculation of the value of ELF MF for arbitrary loads of the power distribution network, as the value of each source for arbitrary load is calculated by scaling the value for nominal load, and at the end the total value is determined by new methodology. The advantage of this approach is also significantly faster adjustment of calculated estimates in the power distribution network, such as a new power line or the reconstruction of an existing power line, as new calculation is required only for a new or modified source. The new methodology was validated on smaller areas by comparing the total values of ELF MF, determined according to the new methodology, with the values obtained with the traditional approach of numerical modelling and with the results of measurements. Both comparisons showed the expected agreement of the results.

Among Slovenian children and adolescents, only 0.5% live in the areas with the mean value of ELF MF 0.1 μT or higher. And only 0.09% of all children were exposed for at least one year in the area of potentially carcinogenic ELF MF density in the vicinity of power lines, which is greater than 0.4 μT. Although the incidence of childhood cancer, which is a rare disease, is gradually increasing in Slovenia, based on our population study, we cannot attribute any case of childhood cancer up to 14 years of age, any leukaemia diagnosed up to 19 years, or any tumour of the central nervous system up to 29 years in the twelve years under study (2005–2016) to the exposure to ELF MF near HV PL.

Finally, although here the new method for estimation of exposures to ELF MF was used for assessment of possible increased cancer risk in children and adolescents, it is also applicable for the broader purpose of exposure assessment, including the planning of proper placement of HV PL and transformer substations into the environment, and of new housing near the existing HV PL.

Acknowledgments

This work was funded by the Slovenian Research Agency (ARRS) and the Slovenian Ministry of Health through the targeted research project "Health risk assessment for exposures of children to lowfrequency electric and magnetic fields

in Slovenia" (grant number V3-1718) and by the Slovenian Research Agency and the Ministry of Education, Science and Sport through the research programme "Slovenian research programme for comprehensive cancer control SLORApro" (grant number P3-0429). The funding sources had no role in study design, the collection, analysis or interpretation of data, the writing of the report, or the decision to submit the article for publication.

References

1. Greenland S, Sheppard AR, Kaune WT, Poole C, Kelsh MA. A pooled analysis of magnetic fields, wire codes, and childhood leukemia. Childhood Leukemia-EMF Study Group. *Epidemiology* 2000; **11:** 624-34. doi: 10.1097/00001648-200011000-00003
2. Ahlbom A, Day N, Feychting M, Roman E, Skinner J, Dockerty J, et al. A pooled analysis of magnetic fields and childhood leukaemia. *Br J Cancer* 2000; **83:** 692-8. doi: 10.1054/bjoc.2000.1376
3. Kheifets L, Ahlbom A, Crespi CM, Draper G, Hagihara J, Lowenthal RM, et al. Pooled analysis of recent studies on magnetic fields and childhood leukaemia. *Br J Cancer* 2010; **103:** 1128-35. doi: 10.1038/sj.bjc.6605838
4. Amoon AT, Swanson J, Magnani C, Johansen C, Kheifets L. Pooled analysis of recent studies of magnetic fields and childhood leukemia. *Environ Res* 2022; **204(Pt A):** 111993. doi: 10.1016/j.envres.2021.111993
5. Bunch KJ, Keegan TJ, Swanson J, Vincent TJ, Murphy MF. Residential distance at birth from overhead high-voltage powerlines: childhood cancer risk in Britain 1962-2008. *Br J Cancer* 2014; **110:** 1402-8. doi: 10.1038/bjc.2014.15
6. Swanson J, Bunch KJ. Reanalysis of risks of childhood leukaemia with distance from overhead power lines in the UK. *J Radiol Prot* 2018; **38:** N30-5. doi: 10.1088/1361-6498/aac89a
7. Zhao G, Lin X, Zhou M, Zhao J. Relationship between exposure to extremely low-frequency electromagnetic fields and breast cancer risk: a meta-analysis. *Eur J Gynaecol Oncol* 2014; **35:** 264-9. PMID: 24984538
8. Kheifets L, Crespi CM, Hooper C, Cockburn M, Amoon AT, Vergara XP. Residential magnetic fields exposure and childhood leukemia: a population-based case-control study in California. *Cancer Causes Control* 2017; **28:** 1117-23. doi: 10.1007/s10552-017-0951-6
9. IARC Working Group on the Evaluation of Carcinogenic Risks to Humans. Nonionizing radiation, part 1: static and extremely low-frequency (ELF) electric and magnetic fields. *IARC Monogr Eval Carcinog Risks Hum* 2002; **80:** 1-395. PMID: 12071196
10. Jin MW, Xu SM, An Q, Wang P. A review of risk factors for childhood leukemia. *Eur Rev Med Pharmacol Sci* 2016; **20:** 3760-4. PMID: 27735044
11. Iglesias ML, Schmidt A, Ghuzlan AA, Lacroix L, Vathaire F, Chevillard S, et al. Radiation exposure and thyroid cancer: a review. *Arch Endocrinol Metab* 2017; **61:** 180-7. doi: 10.1590/2359-3997000000257
12. Miah T, Kamat D. Current understanding of the health effects of electromagnetic fields. *Pediatr Ann* 2017; **46:** e172-4. doi: 10.3928/19382359-20170316-01
13. Serša G. Biological effects of electromagnetic fields (in Slovene). In: Gajšek P, Kotnik T, editors. *Electromagnetic fields - health and the environment: responsible management of the problem of electromagnetic fields (EMP) when placing electric power facilities in environment: scientific monograph*. Ljubljana: Institute for Non-Ionizing Radiation: Projekt FORUM EMS; 2022. p. 38-49. [Internet]. [cited 2021 Oct 8]. Available at: https://inis.si/wp-content/uploads/2022/09/2022_09_05_Monografija_web_pass.pdf.
14. Eržen I. Electromagnetic fields and health risks (in Slovene). In: Gajšek P, Kotnik T, editors. *Electromagnetic fields - health and the environment: responsible management of the problem of electromagnetic fields (EMP) when placing electric power facilities in environment: scientific monograph.* Ljubljana: Institute for Non-Ionizing Radiation: Projekt FORUM EMS; 2022. p. 15-37. [Internet]. [cited 2021 Oct 8]. Available at: https://inis.si/wp-content/uploads/2022/09/2022_09_05_Monografija_web_pass.pdf.
15. European Commission. *Special Eurobarometer 272a: Electromagnetic fields*. [Internet]. [cited 2021 Oct 7]. Available at: https://ec.europa.eu/health/ph_determinants/environment/EMF/ebs272a_en.pdf.
16. Wertheimer N, Leeper E. Electrical wiring configurations and childhood cancer. *Am J Epidemiol* 1979; **109:** 273-84. doi: 10.1093/oxfordjournals.aje.a112681
17. Pedersen C, Brauner EV, Rod NH, Albbieri V, Andersen CE, Ulbak K, et al. Distance to high-voltage power lines and risk of childhood leukemia – an analysis of confounding by and interaction with other potential risk factors. *PLoS One* 2014; **9:** e107096. doi: 10.1371/journal.pone.0107096
18. Wertheimer N, Leeper E. Adult cancer related to electrical wires near the home. *Int J Epidemiol* 1982; **11:** 345-55. doi: 10.1093/ije/11.4.345
19. Savitz DA, Wachtel H, Barnes FA, John EM, Tvrdik JG. Case-control study of childhood cancer and exposure to 60-Hz magnetic fields. *Am J Epidemiol* 1988; **128:** 21-38. doi: 10.1093/oxfordjournals.aje.a114943
20. Severson RK, Stevens RG, Kaune WT, Thomas DB, Heuser L, Davis S, et al. Acute nonlymphocytic leukemia and residential exposure to power frequency magnetic fields. *Am J Epidemiol* 1988; **128:** 10-20. doi: 10.1093/oxfordjournals.aje.a114932
21. London SJ, Thomas DC, Bowman JD, Sobel E, Cheng TC, Peters JM. Exposure to residential electric and magnetic fields and risk of childhood leukemia. *Am J Epidemiol* 1991; **134:** 923-37. doi: 10.1093/oxfordjournals.aje.a116176
22. Rankin RF, Bracken TD, Senior RS, Kavet R, Montgomery JH. Results of a multisite study of U.S. residential magnetic fields. *J Expo Anal Environ Epidemiol* 2002; **12:** 9-20. doi: 10.1038/sj.jea.7500196
23. Feychting M, Ahlbom A. Magnetic fields and cancer in children residing near Swedish high-voltage power lines. *Am J Epidemiol* 1993: **138:** 467-81. doi: 10.1093/oxfordjournals.aje.a116881
24. Petridou E, Hsieh CC, Skalkidis Y, Toupadaki N, Athanassopoulos Y. Suggestion of concomitant changes of electric power consumption and childhood leukemia in Greece. *Scand J Soc Med* 1993; **21:** 281-5. doi: 10.1177/140349489302100408
25. Swanson J. Long-term variations on the exposure of the population of England and Wales to power-frequency magnetic fields. *J Radiol Prot* 1993; **16:** 287-301. doi: 10.1088/0952-4746/16/4/008
26. Tynes T, Haldorsen T. Electromagnetic fields and cancer in children residing near Norwegian high-voltage power lines. *Am J Epidemiol* 1997; **145:** 219-26. doi: 10.1093/oxfordjournals.aje.a009094
27. Sermage-Faure C, Demoury C, Rudant J, Goujon-Bellec S, Guyot-Goubin A, Deschamps F, et al. Childhood leukaemia close to high-voltage power lines – the Geocap study, 2002-2007. *Br J Cancer* 2013; **108:** 1899-906. doi: 10.1038/bjc.2013.128
28. Bessou J, Deschamps F, Figueroa L, Cougnaud D. Methods used to estimate residential exposure to 50 Hz magnetic fields from overhead power lines in an epidemiological study in France. *J Radiol Prot* 2013; **33:** 349-65. doi: 10.1088/0952-4746/33/2/349
29. Vergara XP, Kavet R, Crespi CM, Hooper C, Silva JM, Kheifets L. Estimating magnetic fields of homes near transmission lines in the California Power Line Study. *Environ Res* 2015; **140:** 514-23. doi: 10.1016/j.envres.2015.04.020
30. Varadarajan K. *All nearest neighbours via quadtrees*. Iowa City: The University of Iowa, College of Liberal Arts & Sciences; 2013.
31. Dos Santos Silva I. *Cancer epidemiology: principal and methods*. Lyon: International Agency for Research on Cancer; 1999.
32. Mezei G, Spinelli JJ, Wong P, Borugian M, McBride ML. Assessment of selection bias in the Canadian case-control study of residential magnetic field exposure and childhood leukemia. *Am J Epidemiol* 2008; **167:** 1504-10. doi: 10.1093/aje/kwn086
33. Miravet-Garret L, de Cózar-Macías ÓD, Blázquez-Parra EB, Marín-Granados MD, García-González JB. 3D GIS for surface modelling of magnetic fields generated by overhead power lines and their validation in a complex urban area. *Sci Total Environ* 2021; **796:** 148818. doi: 10.1016/j.scitotenv.2021.148818
34. Zadnik V, Primic Žakelj M, Lokar K, Jarm K, Ivanuš U, Žagar T. Cancer burden in Slovenia with the time trends analysis. *Radiol Oncol* 2017; **51:** 47-55. doi: 10.1515/raon-2017-0008

35. ECIS – European Cancer Information System. *Incidence and mortality estimates 2020*. [Internet]. [cited 2021 Oct 8]. Available at: https://ecis.jrc.ec.europa.eu/

36. Steliarova-Foucher E, Fidler MM, Colombet M, Lacour B, Kaatsch P, Piñeros M, et al. Changing geographical patterns and trends in cancer incidence in children and adolescents in Europe, 1991–2010 (Automated Childhood Cancer Information System): a population-based study. *Lancet Oncol* 2018; **19:** 1159-69. doi: 10.1016/S1470-2045(18)30423-6

37. Schüz J, Erdmann F. Environmental exposure and risk of childhood leukemia: an overview. *Arch Med Re*s 2016; **47:** 607-14. doi: 10.1016/j.arcmed.2016.11.017

38. Patel DM, Jones RR, Booth BJ, Olsson AC, Kromhout H, Straif K, et al. Parental occupational exposure to pesticides, animals and organic dust and risk of childhood leukemia and central nervous system tumors: findings from the International Childhood Cancer Cohort Consortium (I4C). *Int J Cancer* 2020; **146:** 943-52. doi: 10.1002/ijc.32388

39. Greaves M. The 'delayed infection' (aka 'hygiene') hypothesis for childhood leukaemia. Rook GAW, editor. *The Hygiene Hypothesis and Darwinian Medicine* 2009; **17:** 239-55. doi: 10.1007/978-3-7643-8903-1_13

40. Crespi CM, Swanson J, Vergara XP, Kheifets L. Childhood leukemia risk in the California Power Line Study: magnetic fields versus distance from power lines. *Environ Res* 2019; **171:** 530-5. doi: 10.1016/j.envres.2019.01.022

41. Salvan, A, Ranucci A, Lagorio S, Magnani C. Childhood leukemia and 50 Hz magnetic fields: findings from the Italian SETIL case-control study. *Int J Environ Res Public Health* 2015; **12:** 2184-204. doi: 10.3390/ijerph120202184.

42. Zadnik V, Tomšič S. Epidemiology of cancers associated with different types of radiation. [Slovenian]. In: *Sevanja in rak*. XXVII. Seminar »In memoriam of Dr. Dušan Reja«. Ljubljana: Union of Slovenian Cancer Societies, Institute of Oncology Ljubljana, National Institute of Public Health; 2019. p. 98-100.

43. Crespi CM, Vergara XP, Hooper C, Oksuzyan S, Wu S, Cockburn M, et al. Childhood leukaemia and distance from power lines in California: a population-based case-control study. *Br J Cancer* 2016; **115:** 122-8. doi: 10.1038/bjc.2016.142

research article

Comparison of CalliSpheres® microspheres drug-eluting beads and conventional transarterial chemoembolization in hepatocellular carcinoma patients: a randomized controlled trial

Zhongxing Shi[1], Dongqing Wang[1], Tanrong Kang[1], Ru Yi[2], Liming Cui[1], Huijie Jiang[2]

[1] Department of Interventional Radiology, The Second Affiliated Hospital of Harbin Medical University, Harbin, China
[2] Department of Radiology, The Second Affiliated Hospital of Harbin Medical University, Harbin, China

Radiol Oncol 2023; 57(1): 70-79.

Received 3 October 2022
Accepted 8 November 2022

Correspondence to: Huijie Jiang, Ph.D., Department of Radiology, The Second Affiliated Hospital of Harbin Medical University, Harbin, 150001, China. E-mail: jianghuijie@hrbmu.edu.cn

Disclosure: No potential conflicts of interest were disclosed.

Background. This trial aimed to compare the outcomes of drug-eluting beads transarterial chemoembolization (DEB-TACE) with CalliSpheres® microspheres (CSM) and conventional transarterial chemoembolization cTACE in the treatment of patients with unresectable hepatocellular carcinoma (HCC).

Patients and methods. A total of 90 patients were divided into DEB-TACE group (n = 45) and cTACE group (n = 45). The treatment response, overall survival (OS), progression-free survival (PFS), and the safety were compared between the two groups.

Results. The objective response rate (ORR) in the DEB-TACE group was significantly higher than that in cTACE group at 1, 3, and 6 months of follow-up ($P = 0.031$, $P = 0.003$, $P = 0.002$). The complete response (CR) in DEB-TACE group was significantly higher than that in cTACE group at 3 months ($P = 0.036$). Survival analysis revealed that, DEB-TACE group had better survival benefits than cTACE group (median OS: 534 days *vs.* 367 days, $P = 0.027$; median PFS: 352 days *vs.* 278 days $P = 0.004$). The degree of liver function injury was more serious in DEB-TACE group at 1 week, but was similar between the two groups at 1 month. DEB-TACE with CSM caused a high incidence of fever and a severe abdominal pain ($P = 0.031$, $P = 0.037$).

Conclusions. DEB-TACE with CSM showed better treatment response and survival benefits than cTACE group. Although a transient more severe liver damage, high incidence of fever and a severe abdominal pain occurred in the DEB-TACE group, it could be resolved through symptomatic treatment.

Key words: cTACE; CalliSpheres® microspheres; DEB-TACE; hepatocellular carcinoma; tumor response

Introduction

Hepatocellular carcinoma (HCC) is the most common type of primary liver cancer and has been reported to be the sixth most common cancer and the third most frequent cause of cancer-related deaths worldwide, and the leading cause of cancer-related deaths in men in China.[1] HCC occurs in the setting of chronic liver inflammation, which is closely related to chronic viral hepatitis infection (hepatitis B or C) or exposure to toxins, including alcohol or aflatoxin. Despite improvements in the early diagnosis and various treatment methods, most patients with HCC lose the chance of surgical resection, liver transplantation, and radiofrequency ablation.[2,3]

According to Barcelona Clinic Liver Cancer (BCLC) staging system guidelines, transarterial chemoembolization (TACE) is widely applied in HCC patients not suitable for surgical treatment in intermediate and advanced stages.[4] In addition, TACE has been applied as a bridge therapy to liver resection or transplantation in early-stage HCC.[5] The two main protocols for TACE are conventional TACE (cTACE) and drug-eluting beads TACE (DEB-TACE). cTACE uses lipiodol as a chemotherapy drug carrier to embolize targeting arteries, release antitumor medication, and consequent powerful ischemic and cytotoxic effects. However, the rapid decrease of the local antitumor drug concentration and the high systemic toxicity must be investigated.[6] DEB-TACE uses drug-loaded microspheres, which can not only load chemotherapy drugs and release them slowly in local regions but also have less systemic side effects; it also embolizes the tumor supply vessels permanently.[7]

CalliSpheres® microspheres (CSM) are the first DEBs in China and have been applied clinically for a few years. Previous studies on DEB-TACE with CSM have focused on the survival rate, safety, and prognostic factors[8,9], and most were retrospective studies.[10,11] Limited prospective, randomized studies have compared the treatment response of the two methods. A study in 2020 showed that DEB-TACE using CSM loading with arsenic triox is more effective and equally tolerant compared with cTACE in treating unresectable HCC patients. Although the study was prospective, the patients were not randomized and the sample size was not calculated.[12] Thus, the present study aimed to prospectively and randomized evaluate the efficacy and the safety of DEB-TACE with CSM and cTACE in unresectable HCC patients.

Patients and methods

Study design

This was a prospective, randomized, controlled study designed to compare the efficacy and safety of DEB-TACE with CSM and cTACE. All the subjects who participated in this study were randomized in a 1:1 ratio by a computerized system and enrolled by an investigator physician. The results of allocation were placed in a sealed envelope and delivered to the only assistant aware of DEB-TACE/cTACE progress. All the doctors in charge of surgery and data collection were blinded to the trial design and treatment. All participants were informed about the objective and experimental procedure and allowed to withdraw their consent or discontinue participation without restrictions at any time. Then, those who voluntarily participated in the trial signed the written informed consent. All procedures in the trial were in accordance with the World Medical Association's Helsinki Declaration. The study plan was approved by the Ethics Committee of the Second Hospital Affiliated Harbin Medical University (No. KY2020-267) and has been registered at Chictr.org.cn (No. ChiCTR2100044528).

Patients

From March 2020 to March 2021, 115 HCC patients from the Department of Interventional Radiography of the Second Hospital Affiliated Harbin Medical University were recruited in this study through advertisements or physicians. The inclusion criteria were as follows: (1) Patients diagnosed as primary HCC by pathological findings or clinical features and radiographic examinations according to American Association for the Study of the Liver Diseases (AASLD) guidelines; (2) Tumor location and extent not amenable to elective resection or ablation; (3) Patients undergoing treatment for the first time and were willing to accept CSM DEB-TACE or cTACE; (4) Digital substraction sngiography (DSA) showed that the tumor was abundant in blood supply with no hepatic/portal vein invasion; (5) Patients > 18 years old; (6) Patients met Child-Pugh stage A or B and BCLC stage A or B and with an Eastern Cooperative Oncology Group (ECOG) performance status ≤ 1; (7) Life expectancy > 6 months. The exclusion criteria were as follows: (1) Patients with a history of liver transplantation or other malignancies; (2) Patients with coagulation dysfunction or massive ascites; (3) Patients complicated with severe liver or renal dysfunction; (4) Patients with iodine allergy; (5) Patients with cognitive impairment or refusals.

Preparation before the procedure

Each patient had fasted for 6 h and water-deprived for 2 h. The patient was placed in a supine position, and a peripheral intravenous line was established before the procedure. The patient was given inhaled oxygen at 3 L/min with a nasal catheter. Vital signs, including ECG, blood pressure, and oxygen saturation, were monitored. Preoperatively, 3 mg granisetron was injected intravenously over 15 s to prevent nausea and vomiting.

TACE procedure

The groin was prepared in a sterile fashion, and after local anesthesia, percutaneous right common femoral artery was punctured using the modified Seldinger method.

Then, a 5F (Terumo, Tokyo, Japan) /4F (Cordis, USA) RH catheter was introduced through a 5F vascular sheath (Merit Medical, USA), and placed into the celiac trunk under DSA guidance to perform celiac angiography to identify the tumor feeding artery. If the blood vessels in a certain area of the liver are sparse or the tumor is not fully displayed during celiac trunk angiography, look for the extrahepatic tumor blood supply artery, such as superior mesenteric artery, inferior phrenic artery, and right adrenal artery, right inferior intercostal artery, internal mammary artery, etc. After confirming the tumor-feeding artery, a superselective (segmental or subsegmental) approach was used whenever possible using a 2.4 F microcatheter (Merit Medical, USA) for embolization. The tip of the catheter was advanced into the hepatic artery and feeding branch if the size, location, and blood supply were optimal.

The cTACE group was injected an emulsified mixture containing 10 mL lipiodol (Jiangsu Hengrui Medicine Co., Ltd, China) and 40 mg pirarubicin (Shenzhen Wanle Pharmaceutical Co., Ltd, China) into the tumor feeding artery through a microcatheter under fluoroscopic monitoring to avoid reflux of the emulsion. The volume of embolization emulsion was based on the size of the focus. Then according to the blood flow velocity of tumor blood vessels, gelatin sponge particles are appropriately selected to strengthen the embolization until the tumor staining was disappeared.

Patients in the DEB-TACE group received CSM (100-300 μm or 300-500 μm in diameter; Jiangsu Hengrui Medicine Co. Ltd, China) loaded with 40 mg pirarubicin.

TACE upon portal vein visualization achieved "near stasis," with a further pause of 5 minutes to allow redistribution of the embolic agents within the lesion and their distal propulsion by the blood inflow. The second time angiography was conducted to detect the presence of the remaining blushed nodules. The endpoint of the treatment was complete satiation of the tumor vessels with drug and the disappearance of the tumor blush on subsequent angiographic imaging.

Postprocedure management

The puncture wound was bandaged with pressure, and all patients were told to rest in bed in the supine position for at least 6 h post-embolization. The blood supply and temperature of the affected leg should be under intensive focus. The patients were given routine treatment after the operation: (1) Reduced glutathione for liver protection; (2) Granisetron for postoperative nausea and vomiting; (3) Ibuprofen for fever; (4) Non-steroidal anti-inflammatory drugs (Flurbiprofen Axetil) or opioids (morphine) for analgesia; (5) Antibiotics to prevent infection.

Assessment of treatment response

All patients underwent blood test (liver function indexes and alpha-fetoprotein) and imaging examination in the first month after TACE. Patients, who showed tumor progression in the first month after TACE, would receive a second TACE according to the previous grouping. Patients with stables disease were followed with imaging every 3 months.

The treatment response was assessed by two experienced radiologists based on enhanced computed tomography (CT) or magnetic resonance imaging (MRI) according to the modified Response Evaluation Criteria in Solid Tumors (mRECIST) criteria[11] at 1 month, 3 months, 6 months post-treatment: complete response (CR), partial response (PR), stables disease (SD), and progressive disease (PD). In addition, the objective response rate (ORR) was calculated and defined as CR + PR / total × 100%, and the disease control rate (DCR) was calculated and defined as CR + PR + SD / total × 100%.

Although CT response evaluation differentiation between Lipiodol and contrast agent is limited, the tendency to overestimate treatment response was avoided in the cTACE group through comparison of tumor enhancement in the arterial phase and the extent of lipiodol accumulation in the unenhanced phase.

Assessment of overall survival and progression-free survival

The survival status of the two groups was evaluated by overall survival (OS) and progression-free survival (PFS). The OS was defined as the interval between the date of the first TACE treatment and the date of patients'death from any cause or censored at the date of the last follow-up. The PFS was defined as the interval between the start of the first TACE treatment date and the first radiological progression date, patients' death from any cause, or censored at the date of the last follow-up.[12]

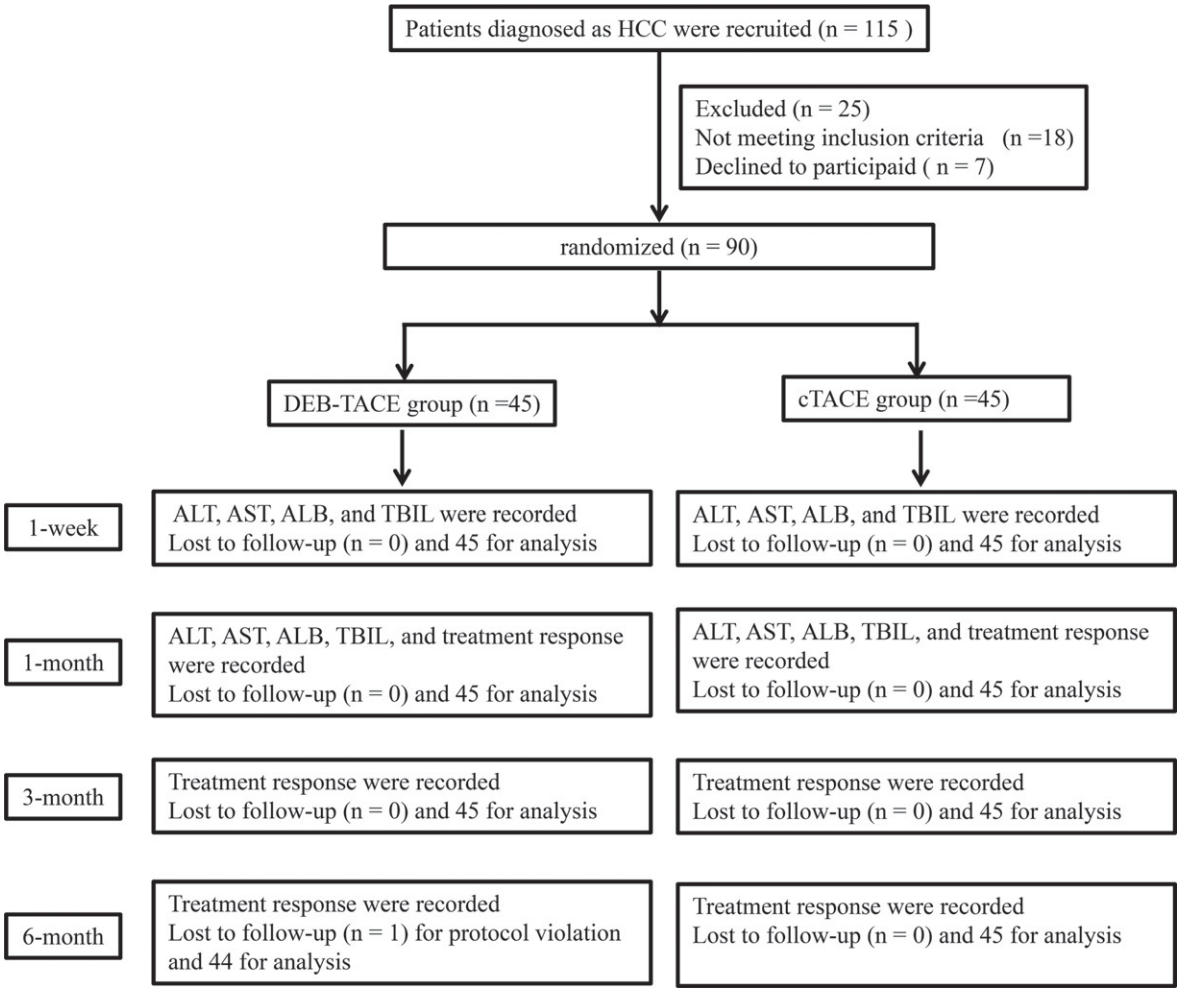

FIGURE 1. Flow diagram of the study.

ALB = albumin; ALT = alanine aminotransferase; AST = aspartate aminotransferase; cTACE = conventional transarterial chemoembolization; DEB-TACE = drug-eluting beads transarterial chemoembolization; HCC = hepatocellular carcinoma; TBIL = total bilirubin

Safety

The safety of the two groups was evaluated by the liver function indexes and post-embolization syndrome. The liver function indexes, including alanine aminotransferase (ALT), aspartate aminotransferase (AST), albumin (ALB), and total bilirubin (TBIL), were assessed before the procedure (baseline), at 1 week, and 1 month post-procedure. The post-embolization symptoms, including fatigue, fever, abdominal distension, abdominal pain, and nausea/emesis, were assessed during the procedure and within 1 month after the procedure. The degree of pain was evaluated by the numeric rating scale (NRS) (0-10), where a score of 0 means no pain and a score of 10 indicates the maximum level of intolerable pain.[11]

Sample size

According to the ORR at 3 months after TACE, as described previously (73.7% in the DEB-TACE group and 42.5% in the cTACE group (P = 0.005))[11], a sample size of at least 39 subjects in each group was required to provide 80% power to detect differences at an α level of 0.05, indicating significance. However, to prevent a 15% attrition rate, we eventually recruited 90 patients with 45 in each group.

Data analysis

GraphPad Prism 8.0.2 software (GraphPad Software Inc., San Diego, CA, USA) was used for statistical analysis and generating graphs. The normally distributed continuous data were presented as the means ± standard deviation, while skewed

TABLE 1. Baseline characteristics of patients

Parameters	DEB-TACE (n = 45)	cTACE (n = 45)	*P* value
Gender (male/female)	40/5	39/6	0.747
Age (years)	58.9 ± 7.1	60.6 ± 6.5	0.229
History of alcohol consumption (n/%)	11 (24.4)	15 (33.3)	0.352
History of viral hepatitis (n/%)	31 (68.9)	27 (60.0)	0.378
Child-Pugh stage (n/%)			
A	33 (73.3)	29 (64.4)	0.326
B	12 (26.7)	16 (35.6)	-
BCLC stage (n/%)			
A	17 (37.8)	14 (31.1)	0.506
B	28 (62.2)	31 (68.9)	-
ECOG performance status (n/%)			
0	17 (37.8)	13 (28.9)	0.371
1	28 (62.2)	32 (71.1)	-
Liver function			
ALT (U/L)	38.0 ± 20.5	35.7 ± 18.7	0.585
AST (U/L)	40.3 ± 16.8	40.1 ± 14.2	0.946
ALB (g/L)	39.9 ± 8.2	40.1 ± 6.2	0.886
TBIL (μmol/L)	19.1 ± 6.1	20.7 ± 7.0	0.246
Tumour location (n/%)			
Unilobar	35 (77.8)	32 (71.1)	0.468
Bilobar	10 (22.2)	13 (28.9)	-
Tumour distribution (n/%)			
Unifocal	36 (80.0)	34 (75.6)	0.612
Multifocal	9 (20.0)	11 (24.4)	
Diameter of the largest tumour (cm)	7.2 ± 2.4	6.8 ± 2.3	0.397

Data were presented as mean ± standard deviation or count (%). Comparisons between two groups were determined by t-test, Wilcoxon rank sum test or Chi-square test. Statistical significance was set at $P < 0.05$.

ALT = alanine aminotransferase; ALB, albumin; AST, aspartate aminotransferase; BCLC = Barcelona Clinic Liver Cancer; cTACE = conventional transarterial chemoembolization; DEB-TACE = drug-eluting beads transarterial chemoembolization; ECOG = Eastern Cooperative Oncology Group; TBIL, total bilirubin

distributed continuous variables were presented as median (25th–75th quantiles) and compared using a t-test. The enumeration data were presented as frequencies and percentages and compared using the chi-squared test. Kaplan–Meier (K–M) method was applied for making the survival curves, and the comparison of OS and PFS between the two groups was estimated by Log-rank test. Statistical significance was set at $P < 0.05$.

Results

Study flow and baseline demographic data

A total of 115 HCC patients were recruited in this trial, 18 did not meet the inclusion criteria, and 7 declined to participate. Finally, 90 patients fulfilled the inclusion criteria and were randomly divided into DEB-TACE or cTACE group (n = 45). The study selection is illustrated in Figure 1. All patients for analysis did not undergo any other treatment previously, including surgery, radiofrequency ablation, TACE, and systematic chemotherapy. At 1 week, 1 month, 3 months, and 6 months all patients in each group were analyzed except 1 patient in the DEB-TACE group died in the 5th month after the procedure.

The mean age of the cohort was 58.9 ± 7.1 years in the DEB-TACE group and 60.6 ± 6.5 years in the cTACE group ($P = 0.229$). In addition, the DEB-TACE group had 40, while the cTACE group consisted of 39 males ($P = 0.747$). The history of alcohol consumption and viral hepatitis, Child–Pugh stage, BCLC stage, ECOG performance status, liver function, tumor location and distribution, and diameter of the largest tumor in the two groups did not differ significantly. The detailed baseline characteristics of patients are listed in Table 1.

Treatment response between the two groups

The treatment response is shown in Table 2. At 1 month after the procedure, the ORR in the DEB-TACE group was significantly higher than that in cTACE group ($P = 0.031$), while there was no significant difference of the CR and DCR between the two groups. At 3 months after the procedure, a significant difference was observed in the treatment response between the two groups. CR, ORR, and DCR in the DEB-TACE group were significantly higher than those in the cTACE group ($P = 0.036$, $P = 0.003$, $P = 0.025$), while PD in the DEB-TACE group was lower than that in the cTACE group ($P = 0.025$). At 6 months after the procedure, CR presented no difference between the two groups, but ORR and DCR were significantly elevated ($P = 0.002$, $P = 0.031$), and PD was significantly reduced in the DEB-TACE group compared to the cTACE group ($P = 0.031$).

Comparison of OS and PFS between the two groups

The final date of survival analysis was March 2022. All patients were followed up until death, or the end of the study and the last follow-up time of the assessment with the median follow-up duration was 365 days (95% CI:150-730 days), which was estimated by reverse Kaplan-Meier method.

Log-rank test revealed that, the median OS of the DEB-TACE group (534 days, 95% CI: 458-634 days) was significantly longer than the cTACE group (367 days, 95% CI: 321-562 days, $P = 0.027$, Figure 2A). The median PFS of the DEB-TACE

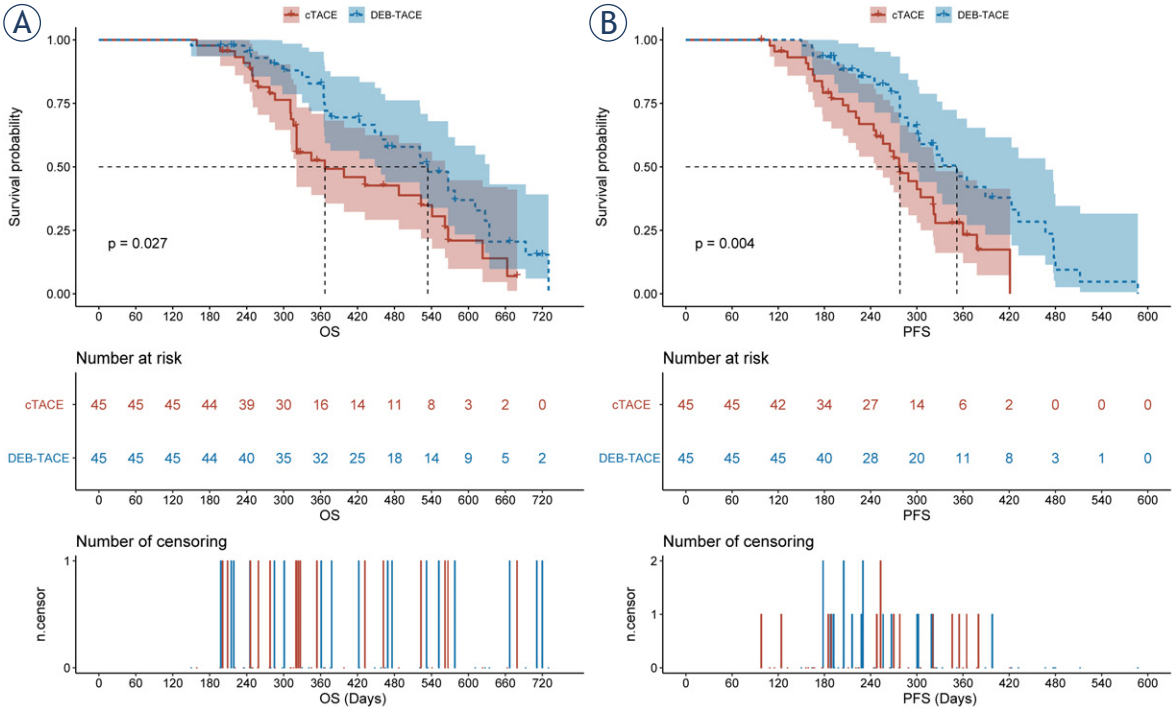

FIGURE 2. The comparison of median overall survival (OS) and progression-free survival (PFS) between the two groups. **(A)** the median OS of the drug-eluting beads transarterial chemoembolization (DEB-TACE) group was significantly longer than the conventional transarterial chemoembolization (cTACE) group (P = 0.027). **(B)** the median PFS of the DEB-TACE group was significantly longer than the cTACE group (P = 0.004).

group (352 days, 95% CI: 301-467 days) was significantly longer than the cTACE group (278 days, 95% CI: 247-324 days, *P* = 0.004, Figure 2B).

Comparison of safety between the two groups

No significant difference was noted in the baseline value of the liver function indexes (AST, ALT, ALB, and TBIL) between the two groups (Figure 3 A–D). At 1 week after the procedure, the AST, ALT, and TBIL indexes were significantly higher in both groups, while the ALB level was lower than the baseline (Table 3). The comparison at 1 week after the procedure between the two groups showed that, the AST, ALT, and TBIL content in the DEB-TACE group was higher than that in cTACE group (Figure 3 A, B, D). However, there was no significant difference of the ALB between the two groups (Figure 3 C). At 1 month after the procedure, all the liver function indexes in the two groups returned to the baseline values (Table 3) and had no difference between the two groups (Figure 3 A–D).

For post-embolization syndrome, the incidence of fatigue, abdominal distension, abdominal pain, and nausea/emesis were similar in the two groups within 1 month after the operation; however, the

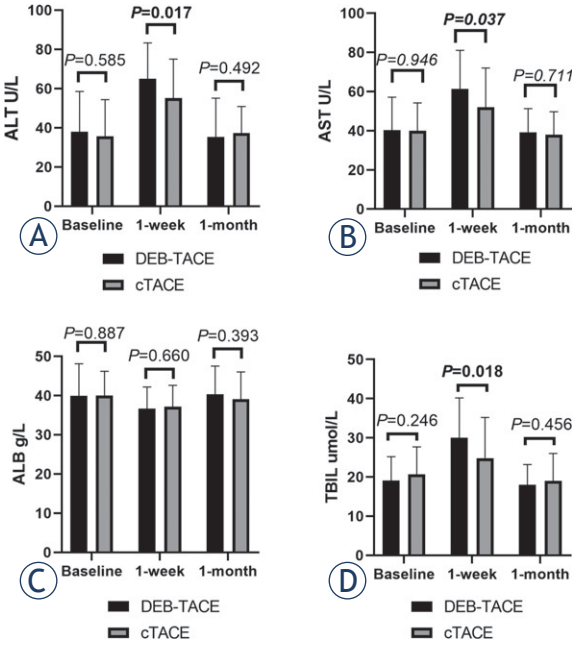

FIGURE 3. Comparison of the liver function between the two groups. The aspartate aminotransferase (AST), alanine aminotransferase (ALT), and total bilirubin (TBIL) levels were higher in the drug-eluting beads transarterial chemoembolization (DEB-TACE) group than in the conventional transarterial chemoembolization (cTACE) group at 1 week (*P* < 0.05) after the operation, and all the liver function indexes had no difference between the 2 groups at 1 month after the operation.

TABLE 2. Comparison of treatment response evaluated at 1-month, 3-month, and 6-month after treatment between the two groups

Parameters	1-month			3-month			6-month		
	DEB-TACE group (n = 45)	cTACE group (n = 45)	*P value*	DEB-TACE group (n = 45)	cTACE group (n = 45)	*P value*	DEB-TACE group (n = 44)	cTACE group (n = 45)	*P value*
CR (%)	8 (17.8)	6 (13.3)	0.561	10 (22.2)	3 (6.7)	**0.036**	7 (15.9)	3 (6.7)	0.168
PR (%)	24 (53.3)	16 (35.6)	0.090	23 (51.1)	16 (35.6)	0.137	23 (52.3)	13 (28.9)	**0.025**
ORR (%)	32 (71.1)	22 (48.9)	**0.031**	33 (73.3)	19 (42.2)	**0.003**	30 (68.2)	16 (35.6)	**0.002**
SD (%)	10 (22.2)	18 (40.0)	0.069	6 (13.3)	11 (24.4)	0.178	10 (22.7)	17 (37.8)	0.123
DCR (%)	42 (93.3)	40 (88.9)	0.459	39 (86.7)	30 (66.7)	**0.025**	40 (90.9)	33 (73.3)	**0.031**
PD (%)	3 (6.7)	5 (11.1)	0.459	6 (13.3)	15 (33.3)	**0.025**	4 (9.1)	12 (26.7)	**0.031**

Data were presented as count (%). Comparison between 2 groups was determined by Chi-square test. Statistical significance was set at P < 0.05, and were shown in boldface.

CR = complete response; cTACE = conventional transarterial chemoembolization; DCR = disease control rate; DEB-TACE = drug-eluting beads transarterial chemoembolization; ORR = objective response rate; PR = partial response; SD = stables disease; PD = progression disease

TABLE 3. Compared with the baseline, the changes of liver function at 1-week and 1-month after procedure in the two groups

Parameters	DEB-TACE (n = 45)					cTACE (n = 45)				
	Baseline	1-week	*P value*	1-month	*P value*	Baseline	1-week	*P value*	1-month	*P value*
ALT (U/L)	38.0 ± 20.5	65.0 ± 18.3	**< 0.001**	35.3 ± 19.8	0.431	35.7 ± 18.7	55.2 ± 19.8	**<0.001**	37.4 ± 13.5	0.558
AST (U/L)	40.3 ± 16.8	61.3 ± 19.7	**< 0.001**	39.1 ± 12.2	0.722	40.1 ± 14.2	52.4 ± 20.0	**0.003**	38.2 ± 11.7	0.534
ALB (g/L)	39.9 ± 8.2	36.7 ± 5.5	**0.004**	40.3 ± 7.21	0.758	40.1 ± 6.2	37.2 ± 5.4	**0.027**	39.1 ± 6.9	0.508
TIBL (umol/L)	19.1 ± 6.1	30.0 ± 10.2	**< 0.001**	18.0 ± 5.2	0.399	20.7 ± 7.0	24.8 ± 10.4	**0.003**	19.0 ± 7.0	0.328

Data were presented as mean ± standard deviation and were determined by t-test or Wilcoxon rank sum test. Statistical significance was set at *P* < 0.05, and were shown in boldface

ALT = alanine aminotransferase; ALB = albumin; AST = aspartate aminotransferase; cTACE = conventional transarterial chemoembolization; DEB-TACE = drug-eluting beads transarterial chemoembolization; TBIL = total bilirubin

incidence of fever was higher in the DEB-TACE group than the cTACE group (*P* = 0.031, Table 4). Notably, the NRS of abdominal pain in the DEB-TACE group (4.4 ± 1.9) was higher than that in cTACE group (3.6 ± 1.6, *P* = 0.037, Table 4). Strikingly, the fever alleviated by drinking excess water and taking ibuprofen, and abdominal pain alleviated by intravenous injection of flurbiprofen axetil or by taking in morphine in 2-3 days. In addition, no serious adverse events, such as liver abscess, acute liver function failure, severe infection, gastrointestinal/intratumoral bleeding, and hepatorenal syndrome, occurred in either group.

Discussion

In the present prospective study, we compared the treatment response, the survival, and the safety of unresectable HCC patients treated with DEB-TACE with CSM and cTACE. The results indicated that DEB-TACE was significantly superior to cTACE in the following aspects: (1) The higher ORR at 1 month, 3 months, and 6 months, and the higher DCR at 3 and 6 months in the DEB-TACE group; (2) The higher CR at 3 months in DEB-TACE group; (3) The lower PD at 3 and 6 months in the DEB-TACE group; (4) The longer OS and PFS in the DEB-TACE group. Although, the liver function indexes (ALT, AST, and TBIL) injury were elevated in the DEB-TACE group at 1 week, but the indexes recovered to the preoperative level at 1 month after treatment in both groups. Moreover, DEB-TACE with CSM increases the incidence of fever and causes severe abdominal pain, which could be controlled by drugs. One patient died 5 months after operation in the DEB-TACE group due to disease progression rather than serious complications of DEB-TACE.

In clinical practice, DEB-TACE and cTACE have become the first-line therapeutic selection for in-

termediate and advanced stage HCC according to the BCLC staging system.[13] Although DEBs have the ability to load chemotherapeutic agents and release them in a controlled mode, the evidence to show that DEB-TACE is superior to cTACE is insufficient. Presently, CSM is the first novel DEB product in China that has been applied clinically only in the last several years. Some studies have compared the tumor response of DEB-TACE with CSM and cTACE for HCC; however, most of them are retrospective studies, and the results were inconsistent. For example, Wu *et al*.[10] indicated that CR, ORR, and DCR rates in the DEB-TACE group were significantly higher than those in the cTACE group at 3 and 6 months. Liang *et al*.[14] showed that compared to cTACE, DEB-TACE with CSM treatment had a higher ORR within 6 months and a higher DCR at 3 and 6 months. Different from the above results, Zhang *et al*.[15] demonstrated that ORR was not different between the two groups, while DCR was significantly higher in the cTACE group than in the DEB-TACE group at 1 month and 3 months. Notably, the articles comparing the efficacy and safety of DEB-TACE with CSM and cTACE are mostly retrospective studies. A recent study adopted prospective design to compare the efficacy and safety of cTACE and DEB-TACE with CSM, and the results were similar to ours. But an uncommon cytotoxic drug (arsenic trioxide) was used in DEB-TACE group, so that the significance of clinical guidance is uncertain.[12]

Herein, we prospectively compared the treatment response within 6 months, OS and PFS of cTACE and DEB-TACE using CSM with pirarubicin (a commonly cytotoxic drug). The results exhibited that DEB-TACE with CSM displayed superior CR (at 3 months), ORR (at 1, 3, and 6 months), and DCR (at 3 and 6 months) over cTACE treatment. The improved treatment responses could be attributed to the fact that CSM has the ability to load chemotherapeutic agents and release them in a controlled pattern, thus maintaining a higher concentration of chemotherapeutic drugs and better efficacy on reducing diameters of the tumor tissues than cTACE.[16,17] In addition, calibrated CSM has shown permanent embolization, which improves the tumor responses in the DEB-TACE treatment with CSM group.[18] This might explain the increased CR and decreased PD in the DEB-TACE group at 3 months in this study. Interestingly, with decreased PD in the DEB-TACE group, HCC patients experienced a reduced frequency of operations and thus economic burden. The higher CR at 3 months in patients receiving DEB-TACE treatment with CSM could be ascribed to the fact that CSM achieves a high concentration of chemotherapeutic agents in 3 months.

TABLE 4. Comparison of post-embolization syndrome

Adverse events	DEB-TACE (n = 45)	cTACE (n = 45)	*P* value
Fatigue (n/%)	5 (11.1)	7 (15.6)	0.535
Fever (n/%)	23 (51.1)	13 (28.9)	**0.031**
Abdominal distension (n/%)	9 (20)	7 (15.6)	0.581
Abdominal pain (n/%) Numeric Rating Scale (NRS)	42 (93.3) 4.4 ± 1.9	43 (95.6) 3.6 ± 1.6	0.645 **0.037**
Nausea/emesis (n/%)	10 (22.2)	12 (26.7)	0.624

Data were presented as mean ± standard deviation or count (%). Comparisons between two groups was determined by t-test, Wilcoxon rank sum test or Chi-square test. Statistical significance was set at $P < 0.05$, and were shown in boldface.

cTACE = conventional transarterial chemoembolization; DEB-TACE = drug-eluting beads transarterial chemoembolization

According to the survey, most of the HCC patients are in intermediate and advanced stages at diagnosis.[19] Hence, short-term efficacy and the safety of the treatment are critical for the HCC patients. A recent multi-center, retrospective registry cohort study[8] showed higher CR and ORR, while the DCR was similar in the DEB-TACE group compared to the cTACE group. A meta-analysis reported that DEB-TACE with CSM displays superior treatment response, which was consistent with our results.[20]

As we know, the most important outcomes in oncology trials are OS and PFS. Accumulating evidence showed that DEB-TACE acquired long-term survival profile (such as OS and PFS) than cTACE in HCC patients.[21,22] The patients in DEB-TACE group showed longer OS and PFS in our study, indicating that the patients underwent DEB-TACE with CSM got more survival benefits compared to patients in cTACE group. While a small amount of literature showed no difference in OS or PFS between DEB-TACE and cTACE groups.[11,23] The difference of survival results may be related to the different types of EDBs, heterogeneity of included patients, and the different types of research. It can be seen that our prospective randomized controlled study is very necessary.

After TACE treatment, liver function injury is one of the major safety concerns in HCC patients. Some studies compared the liver function indexes before and after treatment between DEB-TACE and cTACE and revealed that AST, ALT, and TBIL increased substantially 7 days after TACE and re-

turned to baseline in 1 month.[15,24,25] In this study, the liver function was damaged in both DEB-TACE and cTACE groups at 1 week after the treatment, including the increased ALT, AST, and TBIL and the decreased ALB content. Different from other studies, the current results showed that the ALT, AST, and TBIL in the DEB-TACE group was higher than that in the cTACE group at 1 week. Similar to studies, the indexes recovered to the preoperative level at 1 month after treatment. This phenomenon indicated that DEB-TACE with CSM had more serious damage of liver function compared to cTACE in the short term (about 1 week) and could return to baseline in 1 month. The results also showed that DEB-TACE with CSM and cTACE had parallel effects on the liver function at 1 month, and HCC patients can tolerate both procedures satisfactorily. This observation was consistent with previous studies.[13,25]

Postembolization syndrome is the most common adverse event. Partially in line with these studies[15,24,25], adverse events in the current study included fatigue, abdominal distension, abdominal pain, and nausea/emesis, which were similar between the two groups. However, DEB-TACE with CSM resulted in a high incidence of fever. Although no significant difference was observed in the incidence of abdominal pain between the two groups, the NRS of DEB-TACE group was higher. This might be related to the following effects: (1) The tumors in the DEB-TACE group achieved substantial tumor necrosis and results in severe abdominal pain; (2) Patients in the DEB-TACE group had significant tumor necrosis induced by treatment with CSM, and the incidence of inflammation could be enhanced by substances released from the necrotic tumor tissue. Thus, the patients in the DEB-TACE group experienced severe pain and a high risk of fever. However, the fever was alleviated by ibuprofen, and the pain was alleviated by intravenous injection of flurbiprofen axetil or morphine in 2-3 days in both groups. Also, no serious adverse events, such as liver abscess, acute liver function failure, and severe infection, occurred in either of the groups, which could be attributed to the superselective technique, and the selected patients were controlled in BCLC stages A and B.

This is a randomized controlled trial on the efficacy and safety of DEB-TACE with CSM *vs.* cTACE; hence, confounding factors were minimal, providing accurate evidence to the clinicians. Nevertheless, the current study has some limitations: (1) This is a single-center study with small sample size. However, according to the statistical analysis, 39 patients in each group showed varied ORR between the two groups, with 80% power and a 5% significance level; (2) The tumor responses were followed up for only 6 months, and for survival analysis was not based on the death of all patients. At the last follow-up, 64.4% (29/45) of patients in cTACE group and 60.0% (27/45) of patients in DEB-TACE group died. Therefore, a longer follow-up is necessary in the future study; (3) The amount of pirarubicin administered between DEB-TACE group and cTACE group was not compared, which may have an impact on the results, and further study should compare the dose of the pirarubicin between the two groups.

In conclusion, this study demonstrated that DEB-TACE with CMS had a better tumor response in some aspects (higher CR at 3 months, ORR at 1, 3, and 6 months) than the cTACE group. The liver function injury was more serious in DEB-TACE group at 1 week but returned to the baseline at 1 month in the cTACE group. The increased incidence of fever and severe abdominal pain in the DEB-TACE group could be relieved by symptomatic treatment.

References

1. Chen C, Qiu H, Yao Y, Zhang Z, Ma C, Ma Y, et al. Comprehensive predictive factors for CalliSpheres® microspheres (CSM) drug-eluting bead-transarterial chemoembolization and conventional transarterial chemoembolization on treatment response and survival in hepatocellular carcinoma patients. *Clin Res Hepatol Gastroenterol* 2021; **45:** 101460. doi: 10.1016/j.clinre.2020.05.008
2. Roberts LR, Sirlin CB, Zaiem F, Almasri J, Prokop LJ, Heimbach JK, et al. Imaging for the diagnosis of hepatocellular carcinoma: a systematic review and meta-analysis. *Hepatology* 2018; **67:** 401-21. doi: 10.1002/hep.29487
3. Della Corte C, Triolo M, Iavarone M, Sangiovanni A. Early diagnosis of liver cancer: an appraisal of international recommendations and future perspectives. *Liver Int* 2016; **36:** 166-76. doi: 10.1111/liv.12965
4. Kishore S, Friedman T, Madoff DC. Update on embolization therapies for hepatocellular carcinoma. *Curr Oncol Rep* 2017; **19:** 40. doi: 10.1007/s11912-017-0597-2
5. Park JW, Chen M, Colombo M, Roberts LR, Schwartz M, Chen PJ, et al. Global patterns of hepatocellular carcinoma management from diagnosis to death: the BRIDGE Study. *Liver Int* 2015; **35:** 2155-66. doi: 10.1111/liv.12818
6. de Baere T, Arai Y, Lencioni R, Geschwind JF, Rilling W, Salem R, et al. Treatment of liver tumors with lipiodol TACE: technical recommendations from experts opinion. *Cardiovasc Intervent Radiol* 2016; **39:** 334-43. doi: 10.1007/s00270-015-1208-y
7. Sun J, Zhou G, Xie X, Gu W, Huang J, Zhu D, et al. Efficacy and safety of drug-eluting beads transarterial chemoembolization by CalliSpheres(®) in 275 hepatocellular carcinoma patients: results from the Chinese CalliSpheres(®) Transarterial Chemoembolization in Liver Cancer (CTILC) study. *Oncol Res* 2020; **28:** 75-94. doi: 10.3727/096504019x15662966719585
8. Peng Z, Cao G, Hou Q, Li L, Ying S, Sun J, et al. The comprehensive analysis of efficacy and safety of CalliSpheres(®) drug-eluting beads transarterial chemoembolization in 367 liver cancer patients: a multiple-center, cohort study. *Oncol Res* 2020; **28:** 249-71. doi: 10.3727/096504019x15766663541105
9. Shi Q, Liu J, Li T, Zhou C, Wang Y, Huang S, et al. Comparison of DEB-TACE and cTACE for the initial treatment of unresectable hepatocellular carcinoma beyond up-to-seven criteria: a single-center propensity score matching analysis. *Clin Res Hepatol Gas* 2022; **46:** 101893. doi: 10.1016/j.clinre.2022.101893

10. Wu B, Zhou J, Ling G, Zhu D, Long Q. CalliSpheres drug-eluting beads versus lipiodol transarterial chemoembolization in the treatment of hepatocellular carcinoma: a short-term efficacy and safety study. *World J Surg Oncol* 2018; **16:** 69. doi: 10.1186/s12957-018-1368-8

11. Ma Y, Zhao C, Zhao H, Li H, Chen C, Xiang H, et al. Comparison of treatment efficacy and safety between drug-eluting bead transarterial chemoembolization with CalliSpheres(®) microspheres and conventional transarterial chemoembolization as first-line treatment in hepatocellular carcinoma patients. *Am J Transl Res* 2019; **11:** 7456-70. PMID: 31934293

12. Duan XH, Ju SG, Han XW, Ren JZ, Li FY, Chen PF, et al. Arsenic trioxide-eluting Callispheres beads is more effective and equally tolerant compared with arsenic trioxide/lipiodol emulsion in the transcatheter arterial chemoembolization treatment for unresectable hepatocellular carcinoma patients. *Eur Rev Med Pharmaco* 2020; **24:** 1468-80. doi: 10.26355/eurrev_202002_20206

13. Xiang H, Long L, Yao Y, Fang Z, Zhang Z, Zhang Y. CalliSpheres drug-eluting bead transcatheter arterial chemoembolization presents with better efficacy and equal safety compared to conventional TACE in treating patients with hepatocellular carcinoma. *Technol Cancer Res Treat* 2019; **18:** 1533033819830751. doi: 10.1177/1533033819830751

14. Liang B, Xiang H, Ma C, Xiong B, Ma Y, Zhao C, et al. Comparison of chemoembolization with CalliSpheres(®) microspheres and conventional chemoembolization in the treatment of hepatocellular carcinoma: a multicenter retrospective study. *Cancer Manag Res* 2020; **12:** 941-56. doi: 10.2147/cmar.S187203

15. Zhang L, Sun JH, Ji JS, Zhong BY, Zhou GH, Song JJ, et al. Imaging changes and clinical complications after drug-eluting bead versus conventional transarterial chemoembolization for unresectable hepatocellular carcinoma: Multicenter study. *AJR Am J Roentgenol* 2021; **217:** 933-43. doi: 10.2214/ajr.20.24708

16. Zhang S, Huang C, Li Z, Yang Y, Bao T, Chen H, et al. Comparison of pharmacokinetics and drug release in tissues after transarterial chemoembolization with doxorubicin using diverse lipiodol emulsions and CalliSpheres beads in rabbit livers. *Drug Deliv* 2017; **24:** 1011-7. doi: 10.1080/10717544.2017.1344336

17. Facciorusso A. Drug-eluting beads transarterial chemoembolization for hepatocellular carcinoma: current state of the art. *World J Gastroenterol* 2018; **24:** 161-9. doi: 10.3748/wjg.v24.i2.161

18. Raoul JL, Forner A, Bolondi L, Cheung TT, Kloeckner R, de Baere T. Updated use of TACE for hepatocellular carcinoma treatment: how and when to use it based on clinical evidence. *Cancer Treat Rev* 2019; **72:** 28-36. doi: 10.1016/j.ctrv.2018.11.002

19. Elshaarawy O, Gomaa A, Omar H, Rewisha E, Waked I. Intermediate stage hepatocellular carcinoma: a summary review. *J Hepatocell Carcinoma* 2019; **6:** 105-17. doi: 10.2147/jhc.S168682

20. Liang B, Makamure J, Shu S, Zhang L, Sun T, Zheng C. Treatment response, survival, and safety of transarterial chemoembolization with CalliSpheres(®) microspheres versus conventional transarterial chemoembolization in hepatocellular carcinoma: a meta-analysis. *Front Oncol* 2021; **11:** 576232. doi: 10.3389/fonc.2021.576232

21. Liu YS, Lin CY, Chuang MT, Lin CY, Tsai YS, Wang CK, et al. Five-year outcome of conventional and drug-eluting transcatheter arterial chemoembolization in patients with hepatocellular carcinoma. *BMC Gastroenterol* 2018; **18:** 124. doi: 10.1186/s12876-018-0848-1

22. Song MJ, Chun HJ, Song DS, Kim HY, Yoo SH, Park CH, et al. Comparative study between doxorubicin-eluting beads and conventional transarterial chemoembolization for treatment of hepatocellular carcinoma. *J Hepatol* 2012; **57:** 1244-50. doi: 10.1016/j.jhep.2012.07.017

23. Facciorusso A, Mariani L, Sposito C, Spreafico C, Bongini M, Morosi C, et al. Drug-eluting beads versus conventional chemoembolization for the treatment of unresectable hepatocellular carcinoma. *J Gadtroen Hepatol* 2016; **31:** 645-53. doi: 10.1111/jgh.13147

24. Kloeckner R, Weinmann A, Prinz F, Pinto dos Santos D, Ruckes C, Dueber C, et al. Conventional transarterial chemoembolization versus drug-eluting bead transarterial chemoembolization for the treatment of hepatocellular carcinoma. *BMC Cancer* 2015; **15:** 465. doi: 10.1186/s12885-015-1480-x

25. Ni JY, Xu LF, Wang WD, Sun HL, Chen YT. Conventional transarterial chemoembolization vs microsphere embolization in hepatocellular carcinoma: a meta-analysis. *World J Gastroenterol* 2014; **20:** 17206-17. doi: 10.3748/wjg.v20.i45.17206

research article

Does concurrent gynaecological surgery affect infectious complications rate after mastectomy with implant-based reconstruction?

Nina Pislar[1,2], Barbara Peric[1,2], Uros Ahcan[2,3], Romi Cencelj-Arnez[1,2], Janez Zgajnar[1,2], Andraz Perhavec[1,2]

[1] Department of Surgical Oncology, Institute of Oncology Ljubljana, Ljubljana, Slovenia
[2] Faculty of Medicine, University of Ljubljana, Ljubljana, Slovenia
[3] Department of Plastic Surgery and Burns, University Medical Centre Ljubljana, Ljubljana, Slovenia

Radiol Oncol 2023; 57(1): 80-85.

Received 24 April 2022
Accepted 23 May 2022

Correspondence to: Asst. Prof. Andraz Perhavec, M.D., Ph.D., Department of Surgical Oncology, Institute of Oncology Ljubljana, Zaloška 2, SI-1000 Ljubljana, Slovenia. E-mail: aperhavec@onko-i.si

Disclosure: No potential conflicts of interest were disclosed.

Background. Women who undergo breast cancer surgery often have an indication for gynaecological procedure. The aim of our study was to compare infectious complications rate after mastectomy with implant-based reconstruction in patients with and without concurrent gynaecological procedure.

Patients and methods. We retrospectively reviewed clinical records of 159 consecutively operated patients after mastectomy with implant-based reconstruction. The patients were divided in 2 groups: 102 patients without (Group 1) and 57 with (Group 2) concurrent gynaecological procedure. Infectious complications rates between the groups were compared using χ^2-test. Logistic regression was performed to test for association of different variables with infectious complications.

Results. There were 240 breast reconstructions performed. Median follow-up time was 297 days (10–1061 days). Mean patient age was 47.2 years (95% CI 32.8–65.9); 48.2 years (95% CI 46.1–50.3) in Group 1 and 45.8 years (95% CI 43.2–48.3) in Group 2; p = 0.002). Infectious complications rate was 17.6% (17.6% *vs.* 17.5%, p = 0.987), implant loss occurred in 5.7% (4.9% *vs.* 7.0%, p = 0.58). Obesity (body mass index [BMI] > 30 kg/m^2), age, previous breast conserving treatment (BCT) with radiotherapy (RT) were identified as risk factors for infectious complications in univariate analysis. Obesity (adjusted odds ratio [aOR] 3.319, 95% CI 1.085–10.157, p = 0.036) and BCT with RT (aOR 7.481, 95% CI 2.230–25.101, p = 0.001) were independently associated with infectious complications in multivariate model.

Conclusions. Concurrent gynaecological procedure for patients undergoing mastectomy with implant-based reconstruction did not carry an increased risk for infectious complications.

Key words: breast cancer; infectious complications; implant-based reconstruction; concurrent surgical management; implant loss

Introduction

Combining a clean surgery that involves prosthetic material with a clean-contaminated surgery has always been controversial.[1] Women who undergo mastectomy with implant reconstruction for risk reduction or cancer often have an indication for a gynaecological procedure.[2] In premenopausal women with hormone receptor-positive tumours, ovarian suppression with surgical oophorectomy has been recognised as part of the treatment strategy for more than a century.[3] In high-risk women,

surgical intervention with prophylactic bilateral mastectomy reduces breast cancer risk by up to 95%, while bilateral salpingo-oophorectomy reduces both breast and ovarian cancer risks by around 50% and 80%, respectively.[4,5] It is also associated with improved survival.[6–8]

When immediate implant-based breast reconstruction is planned, skin-sparing mastectomy (SSM) is most commonly performed, but nipple-sparing mastectomy (NSM) can be a safe option in selected cases.[9–11]

Infectious complications in implant-based reconstructions can cause prolonged antibiotic treatment and can result in implant removal.[12,13] This may delay adjuvant treatments for breast cancer and cause scarring that can affect functional as well as aesthetic outcome. Therefore, a low infectious complications rate is important.[14] Infectious complications rate varies between centres and is around 20%.[15]

Due to increased operating time and an intraabdominal procedure, coordinated surgical management of the breast with a concurrent gynaecological procedure could increase the likelihood of infectious complications.[16] On the other hand, combining the procedures adds to patient satisfaction and optimises the time and cost management.[17] The aim of our study was to compare infectious complications rate after mastectomy with implant-based reconstruction in a group of patients with and without concurrent gynaecological procedure.

Patients and methods

Study cohort and data collection

We conducted a retrospective analysis of infectious complications in patients after implant-based reconstruction with or without concurrent gynaecological procedure and followed them until the date of complication, expander-prosthesis exchange surgery, or until last follow-up visit. We retrospectively reviewed records of 159 women (and 240 breast reconstructions) that were consecutively operated at the Institute of Oncology Ljubljana, Slovenia between February 2014 and June 2020 for a new or previously diagnosed breast cancer and/or had an increased risk for developing breast cancer, mainly due to a recognised *BRCA1/2* mutation. Unilateral or bilateral mastectomy was performed, either SSM or NSM, followed by breast reconstruction with either tissue expander or prosthesis. Fifty-seven patients had a laparoscopic gynaecological procedure (salpingectomy, oophorectomy, hysterectomy or a combination) during the same anaesthesia. Postoperative complications were tracked reviewing follow-up visits with surgical oncologist and reconstructive surgeon. We recorded infectious complications requiring the use of oral or parenteral antibiotics, infectious and wound healing complications requiring surgical treatment under general anaesthesia (necrectomy, debridement) and implant loss due to infection.

Treatment protocol

As part of standard treatment protocol at our centre immediate reconstruction is offered after prophylactic or therapeutic mastectomy, either autologous or implant-based. Patients' cases are discussed prior to surgery at a multidisciplinary team meeting between a surgical oncologist, a radiation therapist and a reconstructive surgeon. The patients are operated under general anaesthesia with perioperative antibiotic prophylaxis. Two grams of cephazolin are given for prophylaxis and the antibiotics are continued post-operatively, typically until drains are removed. If a gynaecological procedure is planned, it is performed first, followed by breast surgery. The gynaecological procedure is performed laparoscopically. Mastectomy with or without axillary lymph node surgery is performed by a surgical oncologist, followed by the reconstructive procedure that is performed by a reconstructive surgeon. A tissue implant is inserted in a pocket, which consists of pectoralis major and serratus anterior muscle. Prior to implant insertion, the area is irrigated with antibiotic solution. The drainage stays in place until less than approximately 50 ml discharge daily for two consecutive days. After the drains are removed and the wounds heal, tissue expanders are filled gradually with saline solution in an outpatient setting every two to three weeks.

Statistical analysis

Patients' characteristics were compared between the two groups (with and without gynaecological procedure) with χ^2 test or Fisher's exact test for categorical variables and Student t-test for continuous variables. Data were reported as counts and frequencies for categorical and as median with sample range or mean with 95% confidence interval (CI) for continuous variables. Univariate binary logistic regression was performed to test for association of different variables with infectious complications. Variables with a statistical significance

TABLE 1. Patients characteristics

Variable	All	Group 1	Group 2	p
	N = 159	N = 102 (64.2%)	N = 57 (35.8%)	
Age (years)	47.2 (95% CI 32.8–65,9)	48.2 (95% CI 46.1–50.3)	45.8 (95% CI 43.2–48.3)	**0.002**
BMI (kg/m^2)	24.7 (95% CI 18.9–34,8)	24.4 (95% CI 23.4–25.4)	25.8 (95% CI 24.1–27.4)	0.189
Smoking	37 (23.3%)	22 (21.6%)	15 (26.3%)	0.497
Diabetes mellitus	3 (1.9%)	3 (2.9%)	0	0.191
ASA score				0.622
1	31 (19.5%)	24 (23.5%)	7 (12.3%)	
2	80 (50.3%)	56 (54.9%)	24 (42.1%)	
3	11 (6.9%)	7 (6.9%)	4 (7.0%)	
Unknown	37 (23.3%)	15 (14.7%)	22 (38.6%)	
Previous BCT with RT	29 (18.2%)	8 (7.8%)	21 (36.8%)	**0.001**
NACT	25 (15.7%)	22 (21.6%)	3 (5.3%)	**0.007**
Adjuvant RT	35 (22.0%)	32 (31.4%)	3 (5.3%)	**0.001**
ACT	33 (20.8%)	23 (22.5%)	10 (17.5%)	0.455

Group 1: Patients without gynaecological procedure; Group 2: Patients with gynaecological procedure.

ACT = adjuvant chemotherapy; ASA = American Society of Anaesthesiology; BC = breast cancer; BCT = breast conserving therapy; BMI = body mass index; NACT = neoadjuvant chemotherapy; RT = radiotherapy

of $p < 0.1$ were included in a multivariate binary logistic regression model. Data were analysed using IBM SPSS Statistics software (Statistical package for the Social Sciences Statistical Software, IBM Corporation, Armonk, NY, USA). Statistical significance was set at $p < 0.05$.

The study was reviewed and approved by the Institutional Review Board and Ethics Committee.

Results

In 159 patients, 240 breast reconstructions were performed with 214 tissue expanders and 26 prostheses. All patients were women. Median follow-up time was 297 days (10–1061 days), 321 days (14–712 days) in Group 1 and 273 days (10–1061 days) in Group 2. Expander-prosthesis exchange surgery was mostly performed within a year from initial surgery, median 333.5 days (74 – 712 days).

Fifty-seven patients (35.8%) had a concurrent laparoscopic gynaecological procedure (Group 2). These patients were younger at the time of surgery (Group 1 48.2 years, 95% CI 46.1–50.3 *vs.* Group 2 45.8 years, 95% CI 43.2–48.3, $p = 0.002$) and more likely to have been previously treated with breast conserving therapy (BCT) including radiotherapy (RT) for breast cancer (Group 1 7.8% *vs.* Group 2 36.8%, $p = 0.001$). Patients without combined procedures (Group 1) were more likely treated with neoadjuvant chemotherapy (NACT) (21.6% *vs.* 5.3%, $p = 0.007$) and more likely received adjuvant RT (31.4% *vs.* 5.3%, $p = 0.001$). We present the patients' characteristics in Table 1.

TABLE 2. Surgical site infections after implant reconstruction

	All (%)	Group 1 (%)	Group 2 (%)	p-value
All*	28 (17.6)	18 (17.6)	10 (17.5)	0.987
Surgical intervention needed**	13 (8.2)	8 (7.8)	5 (8.8)	0.84
Implant loss***	9 (5.7)	5 (4.9)	4 (7.0)	0.58

Group 1: Patients without gynaecological procedure; Group 2: Patients with gynaecological procedure.

*all surgical site infectious complications requiring oral or i.v. antibiotic, surgical debridement under general anaesthesia or implant removal surgery**surgical intervention requiring general anaesthesia ***tissue-expander or prosthesis removal due to infection.

Overall infectious complication rate in our cohort of 159 women was 17.6% and did not significantly differ between the groups (17.6% *vs*. 17.5%, p = 0.987). Tissue implants had to be removed due to infection in 5.7% (4.9% *vs.* 7.9%, p = 0.58). We present the comparison between groups in Table 2.

Several covariates were tested for association with overall infectious complications in the entire cohort. Obesity (body mass index [BMI] > 30 kg/m^2), age and previous BCT with RT for breast cancer were identified as risk factors for infectious complications. Concurrent gynaecological procedure, smoking, diabetes, American Society of Anaesthesiology (ASA) score, neo-/adjuvant systemic therapy and adjuvant RT were not significantly associated with infectious complications (Table 3).

Age at the time of surgery, BMI and previous BCT with RT were included in the multivariate model. Obesity (BMI > 30 kg/m^2) and previous BCT with RT were independently associated with infectious complications. Women with a history of BCT and RT for breast cancer had approximately three times higher odds for infectious complications compared to those without previous BCT with RT (adjusted odd ratio [aOR] 3.319, 95% CI 1.085–10.157, p = 0.036). Obese patients (BMI > 30 kg/m^2) had about 7.5-times higher odds for infectious complications compared to women who had a BMI in the normal range between 19 and 25 kg/m^2 (aOR 7.481, 95% CI 2.230–25.101, p = 0.001) (Table3).

TABLE 3. Variables associated with infectious complications

Variable	OR	P	aOR	p
Gynaecological procedure	1.116 (0.486–2.564)	0.796	NA	NA
BMI < 25	1		1	
25–30	3.000 (0.974–9.239)	0.056	2.552 (0.777–8.382)	0.122
> 30	8.100 (2.540–25.826)	**< 0.001**	7.481 (2.230–25.101)	**0.001**
Age > 45	2.707 (1.118–6.552)	**0.027**	1.939 (0.497–3.907)	0.529
Smoking	1.061 (0.413–2.724)	0.903	NA	NA
Diabetes	2.286 (0.200-26.094)	0.506	NA	NA
ASA 1	1			
2	1.821 (0.560-5.921)	0.319	NA	NA
3	0.675 (0.067-6.789)	0.739	NA	NA
Previous BCT with RT	3.802 (1.546-9.354)	**0.004**	3.319 (1.085–10.157)	**0.036**
NACT	0.345 (0.076-1.553)	0.165	NA	NA
ACT	0.995 (0.369-2.687)	0.992	NA	NA
Adj. RT	0.909 (0.338-2.442)	0.849	NA	NA

aOR = adjusted odds ratio; ASA = American Society of Anaesthesiology; ACT = adjuvant chemotherapy; BC = breast cancer; BCT = breast conserving therapy; BMI = body mass index; NACT = neoadjuvant chemotherapy; RT = radiotherapy

Discussion

In presented retrospective single centre series of 159 women, who underwent mastectomy with implant-based reconstruction there was no association between infectious complications rate and concurrent gynaecological procedure.

The results are consistent with other studies. In a group of seventy breast cancer patients that underwent laparoscopic oophorectomy, among which 29 had a concurrent breast surgery, Willshire *et al*. have shown it is safe to carry out the gynaecological procedure in a combined setting. However, only four patients in this cohort had mastectomy with implant-based reconstruction and the focus on postoperative complications was the gynaecological procedure.[2] For 62 high-risk women that opted for breast and ovarian risk-reducing surgery, post-operative complications rate was no different between sequential *vs*. coordinated surgical management. The study included autologous reconstructions.[18] Furthermore, a new approach has been described for performing laparoscopy via a transmammary route to improve aesthetic outcome and avoid abdominal scars.[19]

In a recently published study, the rates of postoperative complications for implant-based reconstructions were comparable between 141 patients with concurrent gynaecological and 29 patients without gynaecological procedure.[20] The complications only represent the perioperative period, but the sample size is comparable to our study.

Overall, infectious complications rate in our cohort was 17.6% and implant loss occurred in 5.7%. In a recent case series of 16 patients with coordinated surgical management, a 37% 30-day postoperative complication rate was observed, but minor complications, such as seroma and excessive drainage were also included.[21] In a subgroup of 19 coordinately managed patients with implant-based reconstruction, implant loss was observed in two women (11%). In larger series, implant loss rates are comparable to our centre.[22]

In our study, patients in the two groups were different for age, history of BCT with RT, NACT and adjuvant RT. Patients that had combined procedures were younger, which is consistent with the fact that gynaecological risk reduction surgery has greater survival gain if performed earlier.[23] A higher proportion of women with a history of BCT in Group 2 is also reasonable, as they would more often have an indication for either endocrine or prophylactic gynaecological procedure.[2]

Obesity, defined as BMI > 30 kg/m^2 is an established risk factor for surgical site infection and our study results are in accordance with this.[12,24] Confidence intervals are relatively large due to low absolute number of obese patients in our study cohort. We can explain the low numbers with the fact that obese patients are more often advised against breast reconstruction at the multidisciplinary team meeting. They often have other comorbidities that can be associated with complications during and after surgery. The association with obesity in our study is statistically significant and displays more than seven times higher odds for infectious complications compared to baseline BMI. Obesity is also a risk factor for implant loss and reduces self-image after reconstructive procedure.[25] Similar is known for age; however, the effect in our cohort was small in univariate and lost in multivariate analysis. This could be because median age was below 50 years and patients in our cohort did not have many comorbidities. Smoking has also been recognised as a risk factor for complications, but in our cohort, no association was observed. The data on smoking was inconsistent due to retrospective data recollection and loose definition of smoking status.

A history of BCT with RT has been associated with an increased complication rate after tissue expander surgery in previous studies and our study shows similar results.[26,27] Postoperative RT is also often recognised as a risk factor for infection and implant loss.[15,28] In a large systematic review, Momoh *et al*. reported no difference in reconstruction failure rates between patients with a history of BCT with RT and postoperative RT.[29] In our cohort, adjuvant RT was not associated with an increased risk for infectious complications. In univariate analysis, it even displayed a protective effect, although not statistically significant, and was therefore not included in the multivariate analysis.

Neither NACT nor adjuvant chemotherapy were associated with infectious complications and the results are consistent with other studies.[30] In a large meta-analysis, NACT was shown to slightly increase implant loss rates, but no delay in starting adjuvant treatment was observed.[31]

The main limitation of our study is retrospective data collection, including quality of data and selection bias. Patients that were at higher risk for complications, were more likely advised against coordinated surgical management in the first place. Sample size was sufficient, but small numbers in subcategories resulted in large confidence intervals. The study was conducted at the only referral centre for breast cancer cases requiring reconstruction in Slovenia. Follow-up is continued in the outpatient setting and patients are seldom lost during follow-up. Other strengths of the study are recent data and a long follow-up time; most patients have been followed until expander-prosthesis exchange surgery.

Concurrent laparoscopic gynaecological procedure for patients undergoing mastectomy with implant-based reconstruction was safe and did not carry an increased risk for postoperative infectious complications. Obesity and previous BCT with RT were independent risk factors for infectious complications.

Acknowledgments

The authors acknowledge the financial support from the Slovenian Research Agency (research core funding No. P3-0352 (C).

References

1. Altemeier W, Burke J, Pruitt B, Sandusky W. *Manual on control of infection in surgical patients.* 2nd edition. Philadelphia: JB Lippincott; 1984.
2. Willsher P, Ali A, Jackson L. Laparoscopic oophorectomy in the management of breast disease. *ANZ J Surg* 2008; **78:** 670-2. doi: 10.1111/j.1445-2197.2008.04614.x
3. McDonald Wade S, Hackney MH, Khatcheressian J, Lyckholm LJ. Ovarian suppression in the management of premenopausal breast cancer: methods and efficacy in adjuvant and metastatic settings. *Oncology* 2008; **75:** 192-202. doi: 10.1159/000163059
4. Fatouros M, Baltoyiannis G, Roukos DH. The predominant role of surgery in the prevention and new trends in the surgical treatment of women with BRCA1/2 mutations. *Ann Surg Oncol* 2008; **15:** 21-33. doi: 10.1245/s10434-007-9612-4
5. Ludwig KK, Neuner J, Butler A, Geurts JL, Kong AL. Risk reduction and survival benefit of prophylactic surgery in BRCA mutation carriers, a systematic review. *Am J Surg* 2016; **212:** 660-9. doi: 10.1016/j.amjsurg.2016.06.010
6. Rebbeck TR, Kauff ND, Domchek SM. Meta-analysis of risk reduction estimates associated with risk-reducing salpingo-oophorectomy in BRCA1 or BRCA2 mutation carriers. *J Natl Cancer Inst* 2009; **101:** 80-7. doi: 10.1093/jnci/djn442
7. Li X, You R, Wang X, Liu C, Xu Z, Zhou J, et al. Effectiveness of prophylactic surgeries in BRCA1 or BRCA2 mutation carriers: a meta-analysis and systematic review. *Clin Cancer Res* 2016; **22:** 3971-81. doi: 10.1158/1078-0432.CCR-15-1465

8. Domchek SM. Association of risk-reducing surgery in BRCA1 or BRCA2 mutation carriers with cancer risk and mortality. *JAMA* 2010; **304:** 967-75. doi: 10.1001/jama.2010.1237

9. Kronowitz SJ, Kuerer HM. Advances and surgical decision-making for breast reconstruction. *Cancer* 2006; **107:** 893-907. doi: 10.1002/cncr.22079

10. Petit JY, Rietjens M, Lohsiriwat V, Rey P, Garusi C, Lorenzi F De, et al. Update on breast reconstruction techniques and indications. *World J Surg* 2012; **36:** 1486-97. doi: 10.1007/s00268-012-1486-3

11. Jakub JW, Peled AW, Gray RJ, Greenup RA, Kiluk JV, Sacchini V, et al. Oncologic safety of prophylactic nipple-sparing mastectomy in a population with BRCA mutations: A multi-institutional study. *JAMA Surg* 2018; **153:** 123-9. doi: 10.1001/jamasurg.2017.3422

12. Reichman DE, Greenberg JA. Reducing surgical site infections: a review. *Rev Obstet Gynecol* 2009; **2:** 212-21. doi: 10.3909/riog0084

13. Peled AW, Stover AC, Foster RD, McGrath MH, Hwang ES. Long-term reconstructive outcomes after expander-implant breast reconstruction with serious infectious or wound-healing complications. *Ann Plast Surg* 2012; **68:** 369-73. doi: 10.1097/SAP.0b013e31823aee67

14. Mioton LM, Jordan SW, Hanwright PJ, Bilimoria KY, Kim JYS. The relationship between preoperative wound classification and postoperative infection: a multi-institutional analysis of 15,289 patients. *Arch Plast Surg* 2013; **40:** 522-9. doi: 10.5999/aps.2013.40.5.522

15. Jagsi R, Jiang J, Momoh AO, Alderman A, Giordano SH, Buchholz TA, et al. Complications after mastectomy and immediate breast reconstruction for breast cancer: a claims-based analysis. *Ann Surg* 2016; **263:** 219-27. doi: 10.1097/SLA.0000000000001177

16. Kryger ZB, Dumanian GA, Howard MA. Safety issues in combined gynecologic and plastic surgical procedures. *Int J Gynecol Obstet* 2007; **99:** 257-63. doi: 10.1016/j.ijgo.2007.05.028

17. Khadim MF, Eastwood P, Price J, Morrison P, Khan K. Multidisciplinary one-stage risk-reducing gynaecological and breast surgery with immediate reconstruction in BRCA-gene carrier women. *Eur J Surg Oncol* 2013; **39:** 1346-50. doi: 10.1016/j.ejso.2013.09.018

18. Chapman JS, Roddy E, Panighetti A, Hwang S, Crawford B, Powell B, et al. Comparing coordinated versus sequential salpingo-oophorectomy for BRCA1 and BRCA2 mutation carriers with breast cancer. *Clin Breast Cancer* 2016; **16:** 494-9. doi: 10.1016/j.clbc.2016.06.016

19. Perabò M, Fink V, Günthner-Biller M, Von Bodungen V, Friese K, Dian D. Prophylactic mastectomy with immediate reconstruction combined with simultaneous laparoscopic salpingo-oophorectomy via a transmammary route: a novel surgical approach to female BRCA-mutation carriers. *Arch Gynecol Obstet* 2014; **289:** 1325-30. doi: 10.1007/s00404-013-3133-0

20. Jayaraman AP, Boyd T, Hampton SN, Haddock NT, Teotia SS. The impact of combined risk-reducing gynecological surgeries on outcomes in DIEP flap and tissue-expander breast reconstruction. *Plast Surg* 2020; **28:** 112-6. doi: 10.1177/2292550320925905

21. D'Abbondanza JA, George R, Kives S, Musgrave MA. Concurrent prophylactic mastectomy, immediate reconstruction, and salpingo-oophorectomy in high-risk patients: a case series. *Plast Surg* 2020; **28:** 243-8. doi: 10.1177/2292550320928551

22. Nahabedian MY, Tsangaris Theodore, Momen B, Manson PN. Infectious complicatious following breast reconstruction with expanders and implants. *Plast Reconstr Surg* 2003; **112:** 467-76. doi: 10.1097/01.PRS.0000070727.02992.54

23. Finch APM, Lubinski J, Møller P, Singer CF, Karlan B, Senter L, et al. Impact of oophorectomy on cancer incidence and mortality in women with a BRCA1 or BRCA2 mutation. *J Clin Oncol* 2014; **32:** 1547-53. doi: 10.1200/JCO.2013.53.2820

24. Elmi M, Azin A, Elnahas A, McCready DR, Cil TD. Concurrent risk-reduction surgery in patients with increased lifetime risk for breast and ovarian cancer: an analysis of the National Surgical Quality Improvement Program (NSQIP) database. *Breast Cancer Res Treat* 2018; **171:** 217-23. doi: 10.1007/s10549-018-4818-7

25. Kern P, Zarth F, Kimmig R, Rezai M. Impact of age, obesity and smoking on patient satisfaction with breast implant surgery - a unicentric analysis of 318 implant reconstructions after mastectomy. *Geburtshilfe Frauenheilkd* 2015; **75:** 597-604. doi: 10.1055/s-0035-1546171

26. Cordeiro PG, Snell L, Heerdt A, McCarthy C. Immediate tissue expander/implast breast reconstruction after salvage mastectomy for cancer recurrence following lumpectomy/irradiation. *Plast Reconstr Surg* 2012; **129:** 341-50. doi: 10.1097/PRS.0b013e318205f203

27. Chetta MD, Aliu O, Zhong L, Sears ED, Waljee JF, Chung KC, et al. Reconstruction of the radiated breast: a national claims-based assessment of postoperative morbidity. *Plast Reconstr Surg* 2017; **139:** 783-92. doi: 10.1097/PRS.0000000000003168

28. Jugenburg M, Disa JJ, Pusic AL, Cordeiro PG. Impact of radiotherapy on breast reconstruction. *Clin Plast Surg* 2007; **34:** 29-37. doi: 10.1016/j.cps.2006.11.013

29. Momoh AO, Ahmed R, Kelley BP, Aliu O, Kidwell KM, Kozlow JH, et al. A systematic review of complications of implant-based breast reconstruction with prereconstruction and postreconstruction radiotherapy. *Ann Surg Oncol* 2014; **21:** 118-24. doi: 10.1245/s10434-013-3284-z

30. Voineskos SH, Frank SG, Cordeiro PG. Breast reconstruction following conservative mastectomies: predictors of complications and outcomes. *Gland Surg* 2015; **4:** 484-96. doi: 10.3978/j.issn.2227-684X.2015.04.13

31. Varghese J, Gohari SS, Rizki H, Faheem I, Langridge B, Kümmel S, et al. A systematic review and meta-analysis on the effect of neoadjuvant chemotherapy on complications following immediate breast reconstruction. *Breast* 2021; **55:** 55-62. doi: 10.1016/j.breast.2020.11.023

research article

The spine and carina as a surrogate for target registration in cone-beam CT imaging verification in locally advanced lung cancer radiotherapy

Jasna But-Hadzic[1,2], Karmen Strljic[1], Valerija Zager Marcius[1,3]

[1] Department of Radiotherapy, Institute of Oncology Ljubljana, Ljubljana, Slovenia
[2] Faculty of Medicine, University of Ljubljana, Ljubljana, Slovenia
[3] Faculty of Health Sciences, University of Ljubljana, Department of Medical Imaging and Radiotherapy, Ljubljana, Slovenia

Radiol Oncol 2023; 57(1): 86-94.

Received 8 May 2022
Accepted 19 October 2022

Correspondence to: Valerija Žager Marciuš, Ph.D., Institute of Oncology Ljubljana, Zaloška 2, SI-100 Ljubljana, Slovenia
E-mail: valerija.zager@zf.uni-lj.si; vzager@onko-i.si

Disclosure: No potential conflicts of interest were disclosed.

Background. The aim of the study was to evaluate the accuracy of volumetric lung image guidance using the spine or carina as a surrogate to target for image registration, as the best approach is not established.

Patients and methods. Cone beam computed tomography images from the 1st, 10th, 15th, and 20th fraction in 40 lung cancer patients treated with radical radiotherapy were retrospectively registered to planning CT, using three approaches. The spine and carina alignment set-up deviations from a reference (tumour/lymph nodes) registration in the lateral (LAT), longitudinal (LONG) and vertical (VRT) directions were analysed and compared. Tumour location and nodal stage influence on registration accuracy were explored.

Results. The spine and carina mean set-up deviation from reference were largest in the LONG, with the best match in the VRT and LAT, respectively. Both strategies were more accurate in central tumours, with the carina being more precise in 50% LAT and 66% LONG mean deviations. For all measurements in all patients a carina *vs*. spine registration comparison showed improved carina accuracy in LAT and LONG. In comparative subgroup analysis the carina was superior compared to spine in LAT and LONG in centrally located tumours, N2 and N3. Both strategies were comparable for peripheral tumours and N0.

Conclusions. Carina registration shows greater accuracy compared to spine in the LAT and LONG directions and is superior in central tumours, N2 and N3. The spine and carina surrogates are equally accurate for peripheral tumours and N0. We propose the carina as a surrogate to target for CBCT image registration in locally advanced lung cancer.

Key words: locally advanced lung cancer; volumetric image verification; tumour registration; carina registration; spine registration; adaptive radiotherapy.

Introduction

Recent advances in systemic and radiotherapy treatment have resulted in improved survival for patients with inoperable locally advanced lung cancer.[1] But still, nearly half of the patients will experience locoregional relapse.[2] The accuracy of different steps in radiotherapy treatment preparation and execution have a strong impact on local control.[3] With the introduction of computed tomography (CT), positron emission computed tomography (PET CT) and four-dimensional (4D) CT simulation, the target delineation accuracy increased.[4] Modern radiation techniques have enabled a more conformal dose delivery, the dose to normal tissue was reduced and the radical treatment of

more advanced N3 disease and/or dose escalation has become possible.[5] Because of the steeper dose gradient and smaller safety margins, the accuracy of treatment delivery became increasingly important. For daily treatment position verification, cone beam CT (CBCT) largely replaced electronic portal imaging because of better soft-tissue visibility. The alignment of the treatment image with the planning CT (pCT) is usually performed by radiation therapists (RTTs), who are not trained in target determination. The fast interpretation of CBCT is also challenging due to the lower quality of CBCT images (no i.v. contrast) and changes with or adjacent to the tumour during treatment.[6] Manual tumour matching is subjected to strong inter-observer variability even among radiation oncologists.[7] The optimal surrogate structure for image matching has not yet been established. Spine alignment is feasible and reproducible, but shows poor correlation with tumour position.[8] Recently, the carina surrogate alignment was explored and showed superior reproducibility compared to spine alignment.[7]

We performed a retrospective study to determine the accuracy of the carina *vs*. spine registration compared to target (primary tumour and lymph nodes) registration as a reference. To avoid interobserver variability, reference registration was performed by individual thoracic radiation oncologist. To consider tumour and normal structure variations during the course of treatment and their possible impact on image registration, the 1st, 10th, 15th, and 20th fraction CBCT were included in the registration analysis.

Materials and methods

Patient selection

We retrospectively included 40 consecutive lung cancer patients treated with on-line cone-beam computer tomography (CBCT) image guided radical radiotherapy from September 2018 to February 2019. All the patients had a visible tumour and/or lymph nodes on CT. They were treated with conventional, or hypofractionated volumetric modulated arc therapy on the Elekta Synergy linear accelerator (Elekta Synergy, Stockholm, Sweden). Clinical and treatment details were retrieved from medical records.

Simulation and planning

The planning CT scan was performed on the Big Bore CT simulator (Philips N.V., Eindhoven, NL), the Somatom Definition AS CT simulator (Siemens, Erlangen, D) and, in 6 patients, on Siemens Biograph mCT 40 (Siemens, Erlangen, D). The patients were immobilised on a Posirest-2 (Civco, Coralville, USA) with the arms abducted above the head (36 patients) or with a long thermoplastic mask (4 patients). The gross tumour volume (GTV) was delineated as the visible tumour and pathologic lymph nodes on free breathing pCT (with i.v. contrast). Additionally, 4D pCT was used for internal target volume (ITV) delineation in 10 tumours. Planning was performed on the Monaco treatment planning system using the Monte Carlo calculation algorithm. Conventional fractionation (1.8–2 Gy daily dose) was used in 37 patients, and hypofractionation in 3 (2.2, 2.2 and 2.75 Gy daily dose). The plan, pCT images and the delineated (target) contours were exported to the Elekta Synergy X-ray Volumetric Imaging (XVI) System.

Imaging

Kilovoltage gantry mounted CBCT systems were used for daily on-line CBCT treatment verification. According to physician instructions, localisation was based on automatic spine or carina matching between CBCT and pCT with additional manual translation correction by RTT. All set-up errors were corrected before treatment delivery.

Study procedure

Retrospective rigid image registration was done in the Elekta XVI System. We used the first treatment verification CBCT image from the 1st, 10th, 15th, and 20th fraction.

The CBCT image was retrospectively registered with pCT based on three different strategies: (a) bony registration on the spine, (b) soft tissue registration on the carina and (c) target (tumour/lymph node) matching on GTV/ITV. For 40 patients, we analysed 160 registration images and recorded 1440 corrections in the x (lateral – LAT), y (longitudinal – LONG) and z (vertical – VRT) directions.

First two retrospective registrations on the spine and carina were performed by RTT and were based on automatic registration using a clip box (Figure 1).

Residual translation errors were corrected manually, if necessary. Next, reference registration on target (tumour/lymph node) matching was performed by an experienced thoracic radiation oncologist. Following automatic bone registration, translational misalignments were manually

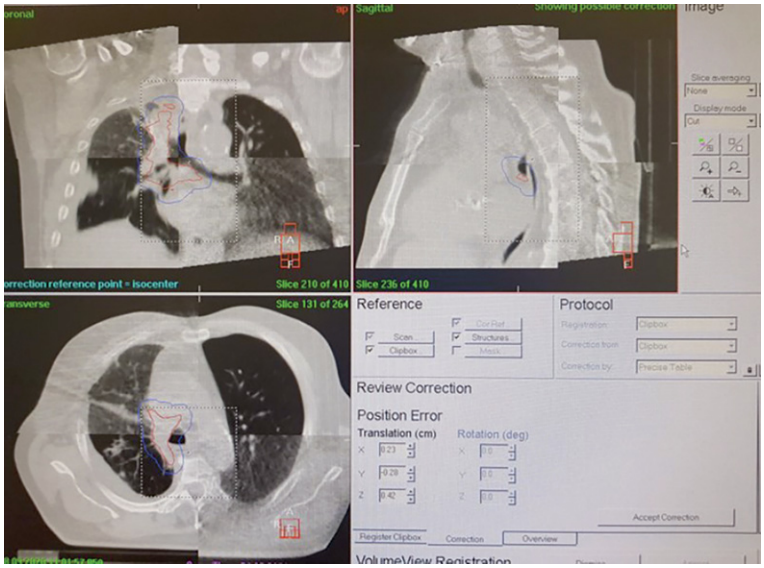

FIGURE 1. Automatic clip box carina registration with manual alignment check. Target contours (gross tumour volume [GTV] inner contour, planning target volume [PTV] outer contour) are imported for target registration.

corrected based on the visual adjustment of the GTV (ITV) contour on the CBCT image, to provide the best match for all known gross disease. If the lymph nodes were not visible, close anatomical surrogates were used. Translation corrections for target matching were recorded and used for the reference position. Spine and carina corrections were compared to the reference position and deviations in LAT, LONG and VRT measurements were analysed.

Statistics

Microsoft Excel 2010 and the Statistical Package for the Social Sciences, version 25.0 (SPSS Inc., Chicago, IL, USA) were used. General data were presented with descriptive statistics. Kolmogorov-Smirnov and Shapiro-Wilk tests rejected normal data distribution. The Nonparametric Mann Whitney U test (MW), Wilcoxon Signed Ranks test and nonparametric Kruskal-Wally's test (KW) were used for the analysis of the set-up deviation. The Wilcoxon Signed Ranks Test for dependent samples was used for comparison (pairwise). The KW and MW were used when we analysed the differences in a certain measurement according in two (MW) or into multiple groups (KW). A p value ≤ 0.05 was considered statistically significant.

Results

Patients, tumour and treatment characteristics

The patients, disease and treatment characteristics are summarised in Table 1. Radiation was the primary treatment of "de novo" lung cancer in 80% of patients. One patient was treated for local progression of epidermal growth factor receptor (EGFR)+ adenocarcinoma and one had postoperative regional recurrence. Five patients received reirradiation for local/regional recurrence. There were three plan adaptations after the 21st or 22nd fraction due to atelectasis (developing, resolution and worsening).

Spine to target registration set-up deviation analysis

The set-up deviation in the LAT, LONG and VRT directions for the spine according to target registration for the 1st, 10th, 15th, and 20th fractions were analysed (Figure 2A). The best registration match was in the VRT direction, with a mean set-up deviation between 1.2 and 1.68 mm. The biggest deviation was detected in the LONG direction (2.03–2.73 mm). Deviation differences from the 1st through 20th fractions were not statistically significant in any direction. There was no time trend detected. Comparison of deviations between directions on the 20th fraction showed a significant set-up difference in deviation between LAT *vs.* LONG ($p = 0.002$) and VRT *vs.* LONG ($p = 0.000$). The mean deviation for all set-up measurements was 1.39 mm in LAT (SD 0.9, range 0–4.0 mm), 2.44 mm in LONG (SD 1.6, range 0.5–8.0 mm) and 1.36 mm in VRT direction (SD 1.04, range 0–4.75 mm).

Carina to target registration set-up deviation analysis

Analysis of the set-up carina registration deviations from the target set-up measurements for the 1st, 10th, 15th, and 20th fractions were also analysed (Figure 2B). The smallest set-up difference was in the LAT direction (from 0.9 to 1.8 mm). The largest discrepancies were detected in the LONG direction (from 1.53 to 2.15). The difference in deviations for different fractions was not significant in any direction. There was no time trend in the deviations. Calculated from all the measurements, the mean deviation for the carina set-up deviations from the reference was 1.03 mm in LAT (SD 0.75,

range 0–3.75mm), 1.78 mm in LONG (SD 1.5, range 0–6.75mm) and 1.33 mm in the VRT direction (SD 1.25, range 0–5.25).

Comparison of spine to target and carina to target set-up deviation differences

The differences in the spine/target and carina/target mean set-up deviations were compared individually for the different fractions and the mean for all measurements in all directions (Table 2). The registration on carina was more accurate according to the reference in all measurements except in the vertical direction on the 1st and 20th fractions. The only significant difference was found on the 10th fraction VRT direction, with the smallest deviation for carina registration.

For all the measurements, registration on the carina was significantly closer to the reference registration in the LAT and LONG direction ($p = 0.003$ and $p = 0.002$, respectively). We found no difference in the set-up deviation in the VRT direction for all measurements.

The impact of tumour location (central/peripheral) and N stage on the spine/target and carina/target registration deviation

Analysis of the spine registration deviations from the reference showed a significantly better registration match for centrally located tumours in LAT on the 1st and 10th fractions, in LONG on the 1st fraction and in VRT on the 10th fraction (Table 3).

The carina/target registration comparison showed significantly smaller differences for central tumours in 50% LAT measurements (10th and 15th fraction), in 2/3 LONG measurements (10th –20th fraction), but not in the VRT direction (Table 4). We found no impact of the node stage on the spine/target registration deviations. When the carina was used for alignment, the differences were significantly smaller for N2 and N3 in the LAT 15th, LAT 20th, LONG 15th and VRT 20th fraction ($p = 0.034$, 0.028, 0.025 and 0.034, respectively) (Supplementary Tables S1–S2). Possible time trend for spine/target LAT deviation difference was detected for central tumours (Table 3).

TABLE 1. Patients, disease, and treatment characteristics

		N = 40
Gender	Female	16 (40 %)
	Male	24 (60 %)
Age (years)	Median (range)	67 (53–81)
Tumour location*	RUL	15 (37.5%)
	RML	3 (7.5%)
	RLL	7 (17.5%)
	LUL	8 (20%)
	LLL	8 (20%)
Central (C)/peripheral (P) tumour location**	C	17 (42.5%)
	P	22 (55%)
Histology	NSCLC	31 (77.5%)
	SCLC	9 (22.5%)
Disease treated	De novo lung cancer	32 (80%)
	Local progression	1 (2.5%)
	Local recurrence reirradiation	2 (5%)
	Regional recurrence	1 (2.5%)
	Locoregional recurrence reirradiation	4 (10%)
Systemic treatment	Concurrent chemotherapy	13 (32.5%)
	Sequential chemotherapy	16 (40%)
	Target therapy	1 (2.5%)
	None	10 (25%)
Tumour (T) stage	T0	1 (2.5%)
	T1	4 (10%)
	T2	14 (35%)
	T3	8 (20%)
	T4	13 (32.5%)
Lymph nodes (N) stage	N0	9 (22.5%)
	N1	1 (2.5%)
	N2	14 (35%)
	N3	16 (40%)
Fractionation	Conventional	37 (92.5%)
	Hypofractionation	3 (7.5%)
Radiation technique	VMAT	40 (100%)

* In one patient, two synchronous tumours were treated (RUL and LUL).
**In one patient, only the lymph nodes were treated (regional recurrence).

LLL = left lower lobe; LUL = left upper lobe; NSCLC = non-small cell cancer; RML = right middle lobe; RLL = right lower lobe; RUL = right upper lobe; SCLC = small cell lung cancer; VMAT = volumetric modulated arc therapy

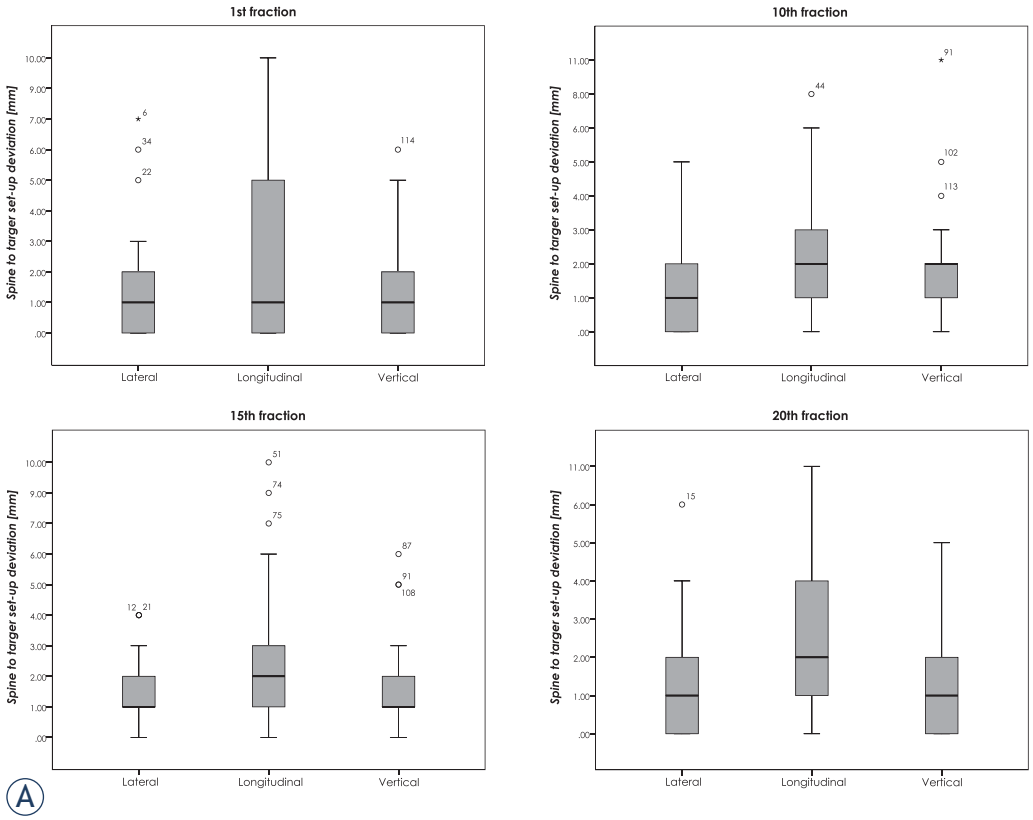

FIGURE 2. Spine to target **(A)** and carina to target **(B)** registration set-up deviation in the lateral (LAT), longitudinal (LONG) and vertical (VRT) directions.

TABLE 2. Mean set-up deviation difference (DD) comparison according to spine/target vs. carina/target registration

Fraction	LAT deviation mean (mm)			p value	LONG deviation mean (mm)			p value	VRT deviation mean (mm)			p value
	Spine/ target	Carina/ target	DD		Spine/ target	Carina/ target	DD		Spine/ target	Carina/ target	DD	
1st	1.28	0.90	0.38	NS	2.65	1.80	0.85	NS	1.20	1.43	-0.23	NS
10th	1.30	1.08	0.22	NS	2.03	1.53	0.50	NS	1.68	1.10	0.58	**0.04**
15th	1.48	1.08	0.4	NS	2.38	1.65	0.73	**0.05**	1.38	1.38	0	NS
20th	1.53	1.05	0.48	NS	2.73	2.15	0.58	NS	1.2	1.43	-0.23	NS
All measurements	1.39	1.03	0.37	**0.003**	2.44	1.78	0.66	**0.002**	1.36	1.33	0.03	NS

DD = deviation difference; LAT = lateral; LONG = longitudinal; NS = non-significant (p>0.05); target = primary tumour and lymph nodes; VRT = vertical

TABLE 3. Spine/target registration deviation according to tumour location

Fraction	LAT mean (mm)		p value	LONG mean (mm)		p value	VERT mean (mm)		p value
	Central	Peripheral		Central	Peripheral		Central	Peripheral	
1st	0.71	1.77	**0.048**	1.18	3.91	**0.002**	1.12	1.32	NS
10th	0.76	1.77	**0.008**	1.53	2.41	NS	1.41	1.86	**0.017**
15th	1.47	1.55	NS	2.59	2.32	NS	1.35	1.45	NS
20th	1.94	1.27	NS	2.29	3.14	NS	1.29	1.09	NS

LAT = lateral; LONG = longitudinal; NS = non significant (p>0.05); target = primary tumour and lymph nodes; VRT = vertical

TABLE 4. Carina/target registration deviation according to tumour location

Fraction	LAT mean (mm)		*p value*	LONG mean (mm)		*p value*	VERT mean (mm)		*p value*
	Central	Peripheral		Central	Peripheral		Central	Peripheral	
1st	0.65	1.14	NS	1.65	2.00	NS	1.06	1.77	NS
10th	0.53	1.55	**0.002**	1.18	1.86	**0.041**	0.82	1.32	NS
15th	0.71	1.41	**0.049**	1.00	2.23	**0.027**	0.88	1.77	NS
20th	1.00	1.14	NS	0.94	3.14	**0.019**	0.88	1.82	NS

LAT = lateral, LONG = longitudinal, NS = non significant (p>0.05); VRT = vertical; target = primary tumour and lymph nodes

The impact of tumour location (central/peripheral) and N stage on the spine/target vs. carina/target deviation differences

The deviation differences analysis between the spine/target and carina/target registration according to tumour location and N stage is shown in Supplementary tables S3–S5. For peripherally located tumours, the carina registration deviation was only smaller compared to the spine set-up deviation in the 1st fraction LONG with a deviation difference of 1.91mm (p = 0.034). In centrally located tumours, the registration on carina was found to be significantly more accurate on the 15th and 20th fractions LAT, (p = 0.012 and 0.048, respectively), the 15th and 20th fractions LONG (p = 0.010 and 0.011, respectively) and for all LAT and LONG measurements (p = 0.003). The deviation differences were 0.76, 0.94, 1.59, 1.35, 0.5 and 0.71mm, respectively. There was no difference in the set-up deviation in the VRT direction regardless of tumour location.

Comparison of the deviation differences according to the N stage showed a better correlation between the carina and target registration for N2 and N3 disease. We found deviation differences

of 0.63mm N2 and 1.17mm N3 in LONG, 0.48mm N3 in LAT for all measurements and 0.94mm N3 10th fraction LONG ($p = 0.013$, 0.015, 0.002 and 0.007, respectively). A small but significant 0.5mm difference in favour of the carina registration was found for N0 in all measurements LAT ($p = 0.034$). Because only 1 patient had the N1 stage, we excluded his measurements from this analysis (Supplementary Table S5).

Discussion

Since the introduction of CBCT into treatment verification, new insights to target position uncertainties have evolved[6], suggesting that image guidance could currently be the weakest link in the radiotherapy procedure.[3,9] Only a few studies have explored the carina as a surrogate in volumetric lung image guidance[7,10,11] and there is a lack of knowledge in this field. Here we present new data on the accuracy of the carina *vs*. spine surrogate compared to the target alignment as a reference in image registration.

A separate analysis of the spine and carina registration set-up differences compared to the reference (target) registration showed the smallest differences in the VRT and LAT directions, with the largest deviation in the LONG direction for both strategies (Fig. 2). The differences were not significantly different in time and no time trend was detected for the cohort, so we evaluated all the measurements together and again showed a good registration match in the VRT and LAT directions, but in LONG direction, the range of misalignment reached above 5 mm in both registration strategies. The greatest area of uncertainty in the LONG direction was also shown in the study by Ottosson *et al*. where they compared the spine and target registration in free-breathing and breath-hold CBCT in locally advanced lung cancer patients. The largest intra- and inter-fractional misalignments were found in the LONG direction, independent of the registration method.[12] Although we found a smaller mean LONG misalignment in the carina *vs*. spine registration (1.78 *vs*. 2.44 mm), uncertainties in image registration should be considered for both strategies, with the enlargement of the PTV in the craniocaudal (CC) direction.

To determine the best registration match compared to the reference, we compared differences in the set-up deviations for the spine and carina alignment. Both strategies were equally accurate in the VRT direction, but the carina was more accurate in the LONG and LAT directions in all measurements. The accuracy of the spine *vs*. carina registration was also tested in a study by a Canadian group, where four independent observers automatically and manually aligned the first fraction CBCT with the pCT in 30 lung cancer patients.[7] They used spine, carina and tumour registration strategies. Automatic spine and carina registrations provided similar tumour coverage, with the tumour inside the ITV in 60% of observations. The same group, in a second study, verified the tumour (T) and lymph node (LN) coverage following spine and carina registration for initial, middle, and final fraction CBCT. Both strategies improved the combined target coverage throughout the treatment course compared to tattoo alignment. Carina better improved the combined coverage and showed significantly superior nodal coverage compared to the spine, without compromising primary tumour coverage.[10] With a significantly better registration match in the LONG and LAT directions, our data supports the suggestion from the Canadian group that the carina may be superior to the spine in the image guidance of locally advanced lung cancer.

The second Canadian study showed similar primary tumour coverage, regardless of the registration strategy.[10] But in our study, the registration accuracy was influenced by tumour location. Both the spine and carina alignment showed smaller set-up differences for centrally located tumours with the difference being more significant in the carina registration LONG (66% fractions) and LAT (50% fractions). For peripheral tumours, we found no difference in the accuracy of spine *vs*. carina alignment, but for centrally located tumours, the carina was more accurate in the LAT and LONG directions. Our data suggests that the carina is a better surrogate for centrally located tumours. Importantly, we also showed that the carina is as accurate as the spine for registration in peripherally located tumours and can be proposed as a registration surrogate regardless of the tumour location.

According to our data, carina matching can also be used regardless of the nodal stage. We found no differences in the spine, but a better match for carina alignment in N2 and N3 disease. In advanced nodal disease, the carina showed superior registration *vs*. the spine in LAT and LONG. The finding is in concordance with the second Canadian study, where carina matching improved the node coverage compared to spine registration.[10] Importantly, we found no set-up difference for N0 disease suggesting that the carina and spine can equally be used as a surrogate in this stage. As there was

only a single case of early nodal disease, we cannot make any conclusions for N1. The reliability of spine matching for LN coverage was investigated in the study by Mohammed *et al*., where an equal geographical target miss was found for spine *vs*. combined target matching, but inferior LN coverage in the case of tumour matching, based on a weekly 4D CBCT registration.[9] Because the same geographical miss was shown for hilar and mediastinal lymph nodes, we can hypothesize that carina matching could safely be used in N1 as well.

Target alignment should be "the ground truth" and have an impact on the therapeutic ratio,[3,12] but is rather difficult to implement clinically. Due to the poor soft tissue contrast on CBCT and tumour changes during the course of treatment, only half of the tumours can clearly be contoured using CBCT.[13] For these reasons, we used contoured-based registration for reference. A similar approach was used for target coverage and geographical miss assessments studies[9,10] and target registration in the study by Ottosson *et al*.[12] Direct tumour registration is also impractical because it is time-consuming and unreliable due to high intra-observer variability.[7] In contrast, the carina is clearly visible on the CBCT and automatic carina alignment shows high reproducibility, superior even to spine alignment.[7] Although the carina shows some respiratory movement, especially in the CC direction, it is still an excellent surrogate for directly adjacent mediastinal lymph nodes. Preliminary data also suggests a good correlation between the carina and GTV motion.[7,11]

We acknowledge the limitations of our study, which was retrospective and relatively small. We also present a heterogeneous group of patients, though they represent real everyday radiotherapists' lung cancer patients. In our study, CBCT image changes were not systematically determined. Because the majority of changes appear in the first five weeks of radiotherapy,[14] we analysed CBCT images from the 1st, 10th, 15th and 20th fractions. Maybe the 25th and 30th fraction CBCT should have been included since we found cases for plan modification in the 6th week of treatment. Nevertheless, we detected no significant set-up differences in time. The rate of plan adaptation was low (7.5%), suggesting the need for a "traffic light" protocol implementation.[3]

In conclusion, carina registration was shown to be feasible, fast, and reproducible. Our data shows that, compared to target registration, carina is equally as accurate as spine registration, with superior accuracy in the LONG and LAT directions. The carina is a better surrogate than the spine for alignment in centrally located tumours, N2 and N3 disease. Although spine alignment can equally be used in N0 and peripheral tumours, for simplicity we propose that the carina should be the primary surrogate for the target in image guidance in locally advanced lung cancer. The next step should be to incorporate carina registration uncertainties into the PTV margin.

Acknowledgement

This research was supported by Slovenian research programme for comprehensive cancer control SLORApro (P3-0429).

Reference

1. Spigel DR, Faivre-Finn C, Gray JE, Vicente D, Planchard D, Paz-Ares LG, et al. Five-year survival outcomes with durvalumab after chemoradiotherapy in unresectable stage III NSCLC: an update from the PACIFIC trial. *J Clin Oncol* 2021; **39:** 8511-11. doi: 10.1200/JCO..39.15_suppl.8511

2. Vrankar M, Stanic K, Jelercic S, Ciric E, Vodusek AL, But-Hadzic J. Clinical outcomes in stage III non-small cell lung cancer patients treated with durvalumab after sequential or concurrent platinum-based chemoradiotherapy - single institute experience. *Radiol Oncol* 2021; **55:** 482-90. doi: 10.2478/raon-2021-0044

3. Tvilum M, Khalil AA, Møller DS, Hoffmann L, Knap MM. Clinical outcome of image-guided adaptive radiotherapy in the treatment of lung cancer patients. *Acta Oncol (Madr)* 2015; **54:** 1430-7. doi: 10.3109/0284186X.2015.1062544

4. Mercieca S, Belderbos JSA, van Herk M. Challenges in the target volume definition of lung cancer radiotherapy. *Transl Lung Cancer Res* 2021; **10:** 1983-98. doi: 10.21037/tlcr-20-627

5. Chan C, Lang S, Rowbottom C, Guckenberger M, Faivre-Finn C. Intensity-modulated radiotherapy for lung cancer: current status and future developments. *J Thorac Oncol* 2014; **9:** 1598-608. doi: 10.1097/JTO.0000000000000346

6. Clarke E, Curtis J, Brada M. Incidence and evolution of imaging changes on cone-beam CT during and after radical radiotherapy for non-small cell lung cancer. *Radiother Oncol* 2019; **132:** 121-6. doi: 10.1016/j.radonc.2018.12.009

7. Higgins J, Bezjak A, Franks K, Le LW, Cho BC, Payne D, et al. Comparison of spine, carina, and tumor as registration landmarks for volumetric image-guided lung radiotherapy. *Int J Radiat Oncol Biol Phys* 2009; **73:** 1404-13. doi: 10.1016/j.ijrobp.2008.06.1926

8. Purdie TG, Bissonnette J-P, Franks K, Bezjak A, Payne D, Sie F, et al. Cone-beam computed tomography for on-line image guidance of lung stereotactic radiotherapy: localization, verification, and intrafraction tumor position. *Int J Radiat Oncol Biol Phys* 2007; **68:** 243-52. doi: 10.1016/j.ijrobp.2006.12.022

9. Mohammed N, Kestin L, Grills I, Shah C, Glide-Hurst C, Yan D, et al. Comparison of IGRT registration strategies for optimal coverage of primary lung tumors and involved nodes based on multiple four-dimensional CT scans obtained throughout the radiotherapy course. *Int J Radiat Oncol Biol Phys* 2012; **82:** 1541-8. doi: 10.1016/j.ijrobp.2011.04.025

10. Lavoie C, Higgins J, Bissonnette J-P, Le LW, Sun A, Brade A, et al. Volumetric image guidance using carina vs spine as registration landmarks for conventionally fractionated lung radiotherapy. *Int J Radiat Oncol Biol Phys* 2012; **84:** 1086-92. doi: 10.1016/j.ijrobp.2012.02.012

11. van der Weide L, van Sörnsen de Koste JR, Lagerwaard FJ, Vincent A, van Triest B, Slotman BJ, et al. Analysis of carina position as surrogate marker for delivering phase-gated radiotherapy. *Int J Radiat Oncol Biol Phys* 2008; **71:** 1111-7. doi: 10.1016/j.ijrobp.2007.11.027

12. Ottosson W, Rahma F, Sjöström D, Behrens CF, Sibolt P. The advantage of deep-inspiration breath-hold and cone-beam CT based soft-tissue registration for locally advanced lung cancer radiotherapy. *Radiother Oncol* 2016; **119:** 432-7. doi: 10.1016/j.radonc.2016.03.012

13. Lim G, Bezjak A, Higgins J, Moseley D, Hope AJ, Sun A, et al. Tumor regression and positional changes in non-small cell lung cancer during radical radiotherapy. *J Thorac Oncol* 2011; **6:** 531-6. doi: 10.1097/JTO.0b013e31820b8a52

14. Elsayad K, Kriz J, Reinartz G, Scobioala S, Ernst I, Haverkamp U, et al. Cone-beam CT-guided radiotherapy in the management of lung cancer: diagnostic and therapeutic value. *Strahlenther Onkol* 2016; **192:** 83-91. doi: 10.1007/s00066-015-0927-y

research article

Effects of gold fiducial marker implantation on tumor control and toxicity in external beam radiotherapy of prostate cancer

Matthias Moll, Magdalena Weiß, Vladimir Stanisav, Alexandru Zaharie, Gregor Goldner

Department of Radiation Oncology, Comprehensive Cancer Center, Medical University of Vienna, Vienna, Austria

Radiol Oncol 2023; 57(1): 95-102.

Received 13 07 2022
Accepted 26 10 2022

Correspondence to: Dr Matthias Moll, M.D., Department of Radiation Oncology, Comprehensive Cancer Center, Medical University of Vienna, Vienna, Austria. E-mail: matthias.moll@meduniwien.ac.at

Disclosure: No potential conflicts of interest were disclosed.

Background. Evidence regarding the effects of fiducials in image-guided radiotherapy (IGRT) for tumor control and acute and late toxicity is sparse.

Patients and methods. Patients with primary low- and intermediate-risk prostate cancer, 40 with and 21 without gold fiducial markers (GFM), and treated between 2010 and 2015 were retrospectively included. The decision for or against GFM implantation took anaesthetic evaluation and patient choice into account. IGRT was performed using electronic portal imaging devices. The prescribed dose was 78 Gy, with 2 Gy per fraction. Biochemical no evidence of disease (bNED) failure was defined using the Phoenix criteria. Acute and late gastrointestinal (GI) and genitourinary toxicity (GU) were assessed using the Radiation Therapy Oncology Group criteria.

Results. Most patients did not receive GFM due to contraindications for anaesthesia or personal choice (60% and 25%). Regarding tumor control, no significant differences were found regarding bNED and overall and disease-specific survival ($p = 0.61$, $p = 0.56$, and $p > 0.9999$, respectively). No significant differences in acute and late GI ($p = 0.16$ and 0.64) and GU toxicity ($p = 0.58$ and 0.80) were observed.

Conclusions. We were unable to detect significant benefits in bNED or in early or late GI and GU side effects after GFM implantation.

Key words: prostate cancer; IGRT; fiducials; tumor control; toxicity

Introduction

Prostate cancer can be treated by external beam radiotherapy (EBRT) brachyradiotherapy or radical prostatectomy; for low-risk disease and highly selected intermediate disease, active surveillance can be offered.[1-5] Important factors in patient decision making are, therefore, the duration of treatment, circumstances of treatment, and treatment-induced side effects. Regarding side effects in EBRT, the use of intensity-modulated radiotherapy (IMRT) has been shown to reduce treatment-associated side effects compared with 3D-conformal radiotherapy.[6,7] Further reduction of side effects is expected using image-guided radiotherapy (IGRT)[8], in which fiducials, ultrasound, MRI, CT scans, or electromagnetic responders are used to locate the prostate before and during radiotherapy.[9] However, to our knowledge, there are as yet no data regarding IGRT in the form of randomized controlled trials, although IGRT is recommended by the NCCN[1], EAU[5], British NICE[10], and German S3[4] guidelines.

With this paper, we explore the role of gold fiducial markers (GFM) used for IGRT in primary prostate cancer treatment. There are only a few studies comparing patients with and without GFM. For example, a retrospective study by Zelefsky *et al.*[11] described an advantage after implanting GFM

in regard to genitourinary (GU) side effects in all patients and biochemical no evidence of disease (bNED) rates in high-risk prostate cancer patients. However, this study compared a group of patients treated with IGRT, but without IMRT with an IMRT-only group, making its results difficult to apply to modern day radiotherapy, in which IMRT is always recommended.[1] The same applies to Sveistrup *et al*.[12], Zapatero *et al*.[13] and Wortel *et al*.[7], which compared patients treated with fiducial-marker IGRT and IMRT with patients treated with 3D conformal radiotherapy.[12] Singh *et al*. compared the use of GFM IGRT with no IGRT *et al*.[14] However, to our knowledge, only one study has compared the use of IGRT with and without GFM[15], and it showed no significant benefits regarding tumor control and toxicity.

In our department, we use cone-beam CT scans and ExacTrac (Brainlab, Munich, Germany), as well as routinely implanted GFM for image guidance. As GFM are implanted with the use of anesthesia, the benefit of the GFM has to be larger than the risks from anesthesia, including, but not limited to, nausea, allergic reactions, intraoperative awareness, or death[16,17], and the risk of the intervention itself, such as infections or injuries to adjacent organs. Local anaesthesia reduces the risks of anaesthesia. Some patients have contraindications against anesthesia or refuse the intervention. A more precise patient positioning due to GFM can be expected to lead to greater treatment precision and hence, possibly, to reduced toxicity and increased tumor control. These assumed benefits can justify its routine application in patients with prostate cancer. Without these advantages, the routine use of GFM would not be justified. Therefore, we wanted to compare a group of patients receiving IGRT with GFM with a group receiving only IGRT to evaluate the potential benefits of GFM regarding tumor control and GI and GU toxicity.

Patients and methods

Design, setting, and participants

Our study protocol was approved by the ethical review board of our university according to local regulations (EK Nr: 1533/2020). We included all patients between 2010 and 2015 with localized primary prostate cancer treated with EBRT by the use of volumetric modulated arc therapy (VMAT) with or without GFM implantation. Patients treated before 2010 were excluded, as routinely prescribed doses were below the currently recommended 75.6 Gy with 1.8 Gy per fraction.[1] Due to the implementation of moderate hypofractionation in our department, patients treated after 2015 were excluded to keep the fractionation uniform among patients. The stage had to be cN0/x and cM0/x, with a risk of lymph node involvement < 15% according to the Roach formula[18], and a clinical T category of 1 or 2.

Interventions

Target volumes were defined using CT and MRI for planning. The prescribed doses were 78 Gy with 2 Gy per fraction. Doses were prescribed to 95% of the planning target volume (PTV) according to International Commission on Radiation Units and Measurements report 83.[19] Safety margins were 7 mm after GFM implantation and 10 mm without. Irradiation was performed with the patient in supine position. All patients received a rectal balloon[20] for prostate immobilization. Cone-beam CT control scans were performed daily for the first week, followed by daily ExacTrac (Brainlab, Munich, Germany) controls for the rest of treatment. The clinical target volume (CTV) included the prostate for low-risk tumors and additionally the base of the seminal vesicles for intermediate-risk tumors.

GFM implantation was recommended to all patients. Reasons for not receiving GFM were contraindications against anesthesia, such as pre-existing pulmonary illness, coronary heart disease, or myocardial infarction, or refusal by the patient. Implantation itself was performed transperineally with ultrasound guidance by the radiation oncologist, under mask narcosis performed by an anaesthesiologist. In each patient, 3 GFM were implanted, one on each side of the prostate and one in the apex. Ciprofloxacin 250 mg 1-0-1 was prescribed as postinterventional prophylaxis for 5 days. If patients received androgen deprivation therapy, it was prescribed by the caretaking urologist.

Outcome measurements

Patient follow-ups were immediately after treatment, 3 months after treatment, 12 months after treatment, and every 12 months from then on. At each follow-up, PSA levels and GI and GU side effects were assessed by the physician. bNED failure was defined using the Phoenix criteria (PSA nadir + 2 ng/mL).[21] Acute and late GI and GU side effects were assessed using the RTOG criteria.[22] Survival data were collected using the local death registry.

Dose-volume histogram (DVH) data were collected using our database. They included the vol-

umes, Dmax/D1, and Dmean of the CTV, PTV, rectum, and bladder, as well as the Dmin of the CTV and the V70 and V60 for the rectum and V70, V50, and V30 for the bladder, as these data were used for plan evaluation.

Statistical analysis

The statistical analysis was performed using GraphPad Prism 9.3.1 (GraphPad Software, San Diego, CA, USA) and SPSS 28.0.1.0 (IBM, Armonk, NY, USA). A p-value of < 0.05 was considered statistically significant. bNED, overall survival, and disease-free survival were compared using the Kaplan-Meier method. Side effects were analyzed by use of the Mann-Whitney U test, the Kruskal-Wallis test, and a Cox regression analysis for the onset of late toxicity grade 2 or higher, as well as bNED and overall survival.

Results

Patient characteristics are displayed in Table 1. We also analyzed the reasons for patients not receiving GFM implantation. Among them, most patients (12, 60%) had medical contraindications for anesthesia, 5 patients (25%) refused GFM implantation, and for 3 patients (15%) who did not receive GFM, the reason was unknown.

bNED rates are displayed in Figure 1. bNED ratios after 5 years for patients with and without GFM implantation were 92% and 100%, respective-

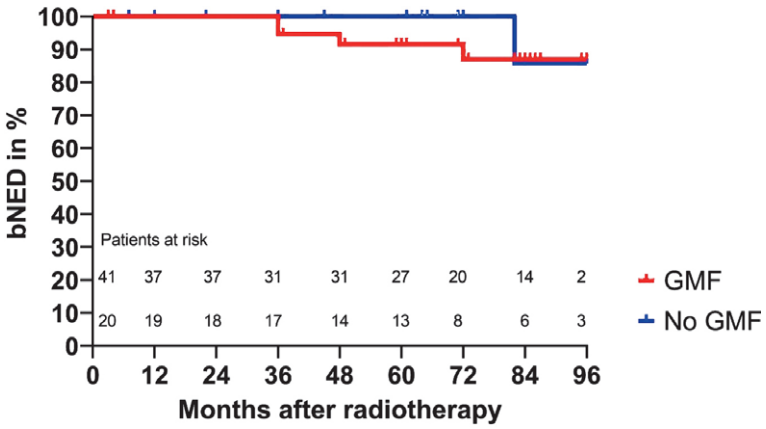

FIGURE 1. Biochemical no evidence of disease (bNED) rates of patients with and without gold fiducial marker (GMF) implantation (p = 0.61).

TABLE 1. Patient characteristics

	GFM	%	No GFM	%
n	41	100%	20	100%
cT category				
1	23	56%	16	80%
2	18	44%	4	20%
iPSA in µg/l, median (IQR)	7 (5.3/8.7)		5.9 (4.4/10.6)	
Gleason score				
6	26	63%	18	90%
7a	12	29%	1	5%
7b	3	7%	1	5%
Risk group				
Low risk	16	39%	10	50%
Intermediate risk	25	61%	10	50%
ADT prescribed	14	34%	3	15%
Median duration of ADT in months (IQR)	9 (3/18)		6 (6/8)	
Median age at RT (IQR)	74 (70/77)		72 (67/72)	
Median follow-up in months (IQR)	72 (49/84)		68 (36/86.5)	

ADT = androgen deprivation therapy; cT = clinical tumor extension; GFM = gold fiducial markers; iPSA = initial prostate-specific antigen; IQR = interquartile range; RT = radiotherapy low risk = PSA < 10 µg/L and Gleason Score 6; intermediate risk = PSA ≥ 10 µg/L or Gleason Score 7a/b

TABLE 2. Maximum acute side effects in patients with and without gold fiducial marker implantation

Grade	Gastrointestinal toxicity		Genitourinary toxicity	
	Gold fiducial markers	No gold fiducial markers	Gold fiducial markers	No gold fiducial markers
0	27%	15%	17%	5%
1	66%	65%	44%	55%
2	7%	20%	39%	40%

No significant differences for acute gastrointestinal and genitourinary side effects were detected (p = 0.15 and p = 0.58, respectively).

TABLE 3. Maximum late side effects in patients with and without gold fiducial marker implantation

Grade	Gastrointestinal toxicity		Genitourinary toxicity	
	Gold fiducial markers	No gold fiducial markers	Gold fiducial markers	No gold fiducial markers
0	59%	50%	37%	35%
1	12%	15%	27%	25%
2	24%	35%	34%	35%
3	5%	0%	2%	5%

No significant differences for late gastrointestinal and genitourinary side effects were detected (p = 0.64 and p = 0.80, respectively).

ly. After 8 years, bNED rates were 87% and 86%, respectively (p = 0.61). We also analyzed disease-specific survival (DSS) and overall survival (OS). Regarding DSS, we did not find a single death due to prostate cancer (p > 0.9999). For OS, survival proportions for patients with and without GFM after 5 years were 93% and 95%, and after 8 years 90% and 95% (p = 0.56).

Maximum acute and late gastrointestinal side effects are displayed in Tables 2 and 3. No significant differences between the two groups were detected. It is noteworthy that at no point was a grade 4 toxicity detected. We also compared late GI and GU toxicity in the two groups after 3, 12, 24, 36, 48, 60, 72, 84, and 96 months, and did not find a significant difference at any point.

For DVH data, we started by comparing the two groups regarding volumes, Dmax/D1, and Dmean of the CTV, PTV, rectum, and bladder, as well as the Dmin of the CTV and the V70 and V60 for the rectum and V70, V50, and V30 for the bladder. Significant differences were found in the PTV (median 124.7 cm^3 with GFM and 157.1 cm^3 without, p = 0.004), the Dmin of the CTV (median 76.0 Gy with GFM and 76.5 Gy without, p = 0.04), the rectal Dmean (median 36.0 Gy with GFM and 39.3 Gy without, p = 0.01), V70 (median 11.4 Gy with GFM and 16.1 Gy without, p < 0.001), and V60 (median 20.0 Gy with GFM and 25.3 Gy without, p < 0.001). An overview of the DVH data is presented in Table 4.

We also performed a univariable, and if more than one variable was significant, a multivariable Cox regression analysis regarding bNED and OS, as displayed in Table 5, as well as the onset of late GI or GU toxicity grade 2 or higher. The results of our Cox regression analysis regarding bNED and OS are displayed in Table 5.

As no patient died of prostate cancer, we did not model a Cox regression for DSS. Analyses including rectal or bladder DVH variables regarding bNED and OS were performed, and none of the variables was significant. Therefore, to improve clarity, we did not add them to Table 5. The results regarding toxicity are displayed in Table 6.

Discussion

As GFM implantation is an invasive procedure, the benefits of implantation have to outweigh the potential risks. There are two categories of risks. The first is the risk due to the implantation itself. Citing our information sheet, these risks are bleeding, injuries of the bladder and urethra, infection including abscess formation, and allergic reactions to the prescribed antibiotic. The second category is risks due to the anaesthesia. Even when only a breathing mask is used to administer anaesthesia, these risks include tissue damage due to patient positioning, allergic reactions, malignant hyperthermia, subsequent confusion, aspiration, and regaining consciousness during anesthesia.[16,17] While these side effects occur rarely in our clinical experience, as well as in the literature[23], they have to be considered in evaluating GFM implantation, aside from its influence on tumor control and side effects.

Several retrospective studies comparing fiducial IGRT with a control group exist. However, most of them compare a 3D conformal group with either an IGRT 3D conformal group[14,24] or an IGRT IMRT group[12], making them hard to apply to today's treatment due to their being outdated or their comparison of two different treatment modalities with inherent differences regarding outcomes. While many international guidelines[1,4,10] suggest the use of IGRT, no study covering this topic is mentioned in the NCCN[1] or NICE[10] guidelines. Napieralska *et al.*[15], to our knowledge the

only other study comparing patients with and without fiducial marker implantation and IMRT, found no significant differences regarding either bNED, with the exception of improved OS in intermediate patients, or late toxicity when comparing fiducial marker guidance and bone structure guidance. A significant difference was found regarding acute GU toxicity. Our results are similar, with no significant differences in acute toxicity. However, the aforementioned study did not include DVH data. Looking at our DVH data, we were unable to translate the differences regarding PTV and rectal variables into differences related to tumor control or toxicity, most likely due to DVH constraints in both groups.

It is quite likely that the most crucial effect regarding potential outcomes in our department is the safety margin reduction by 3 mm in GFM patients, which is absent from the aforementioned studies. The effect of reducing the safety margin by 3 mm can be displayed using math. Assume a spherical form for the prostate, with a radius between 2 and 2.5 cm and safety margins of 7 mm and 10 mm. The radii, including the PTV safety margins, are 2.7 cm and 3 cm, with an initial radius of 2 cm and 3.2 cm, respectively, and 3.5 cm with an initial radius of 2.5 cm. With $4/3*\pi*r^3$ being the formula for the volume of a sphere, reducing the safety margins by 3 mm leads to a decrease in the PTV of 27% for the 2-cm initial radius and 24% for the 2.5-cm initial radius ($2.7^3/3^3$ and $3.2^3/3.5^3$). In our data, the difference in the median volume is 21%, similar to the expected difference. Although this calculation is far from perfect, as the prostate is not a perfect sphere, it allows one to imagine the effect of safety margin variation through the third power of the radius. Zelefsky's conclusion in his IGRT study[11] was that safety margins should be reduced. However, to our knowledge, he has yet to publish any data comparing bNED rates before and after margin reduction.

When comparing our bNED rates with those of groundbreaking studies like those of Peeters *et al.*[25] and Pasalic *et al.*[26], using 78 Gy, and Dearnaley *et al.*[27], using 74 Gy, with bNED rates after 5 years ranging from 64% for Peeters to above 90% for Pasalic, we are leaning toward the top end, with bNED rates after 5 years of 92% and more, while only including patients with low- and intermediate-risk tumors. Regarding late side effects, while there were no significant differences between the two groups, our data, with 29%–35% of maximum GI toxicity at RTOG grade 2 or higher toxicity and approximately 36%–40% of GU toxicity of RTOG grade ≥ 2, are worse than the results presented by Napieralska[15], showing 12% grade ≥ 2 GU side effects and 15%–19% grade ≥ 2 GI side effects, possibly due to differences in side-effect assessment between institutions. Zelefsky reports lower toxicity rates, using CTCAE criteria, complicating a direct comparison.

One weakness of our study is its retrospective nature. On top of that, there is no group of patients with GFM implantation and a safety margin of 10

TABLE 4. Dose-volume histograms for patients with and without gold fiducial markers (GFM)

	GFM	No GFM
PTV prostate cm³ median (IQR)	124.72 (98.68–152.83)	157.12 (128.34–173.66)
PTV Dmax/D1 median (IQR)	81.55 (80.55–82.75)	81.15 (80.46–82.06)
PTV Dmean median (IQR)	78.10 (77.41–78.70)	78.10 (77.00–78.43)
CTV prostate cm³ median (IQR)	44.14 (34.75–64.70)	43.91 (34.40–55.42)
CTV Dmax/D1 median (IQR)	81.24 (80.64–82.57)	81.22 (80.35–81.85)
CTV Dmean median (IQR)	78.58 (77.97–79.47)	78.63 (77.94–79.04)
CTV Dmin median (IQR)	76.00 (75.36–76.32)	76.49 (75.88–77.05)
Rectal volume median (IQR)	113.02 (100.22–134.55)	114.53 (105.57–136.38)
Rectal Dmax median (IQR)	80.06 (78.88–81.98)	80.24 (79.23–81.25)
Rectal Dmean median (IQR)	35.99 (32.94–39.61)	39.30 (37.81–42.99)
Rectal V70 Gy % median (IQR)	11.41 (9.41–13.04)	16.12 (14.55–18.66)
Rectal V70 Gy cm³ median (IQR)	13.21 (11.33–15.93)	18.66 (16.55–21.39)
Rectal V60 Gy % median (IQR)	19.95 (16.39–22.37)	25.25 (23.77–29.26)
Rectal V60 Gy cm³ median (IQR)	23.36 (19.93–25.98)	29.23 (26.74–33.13)
Bladder volume median (IQR)	196.93 (113.66–282.94)	155.76 (127.30–296.44)
Bladder Dmax/D1 median (IQR)	78.78 (77.01–80.53)	79.53 (77.04–80.44)
Bladder Dmean median (IQR)	21.11 (16.92–30.06)	28.10 (18.99–35.20)
Bladder V70 Gy % median (IQR)	7.50 (5.44–11.78)	9.43 (6.06–14.02)
Bladder V70 Gy cm³ median (IQR)	14.14 (10.53–21.16)	19.01 (12.00–22.20)
Bladder V50 Gy % median (IQR)	17.14 (12.00–26,40)	20.81 (13.60–30.86)
Bladder V50 Gy cm³ median (IQR)	34.00 (23.17–42.23)	37.58 (27.16–44.42)
Bladder V30 Gy % median (IQR)	28.24 (21.74–41.73)	41.31 (25.78–51.83)
Bladder V30 Gy cm³ median (IQR)	58.71 (43.43–78.57)	65.38 (48.97–83.61)

CTV = clinical target volume; GFM = gold fiducial marker; IQR = interquartile range; PTV = planning target volume; RT = radiotherapy

TABLE 5. Uni- and multivariable Cox regression of biochemical no evidence of disease (bNED) and overall survival (OS)

bNED	Univariable analysis			Multivariable analysis		
	p-value	exp(HR)	exp(HR) (95% conf.)	p-value	exp(HR)	exp(HR) (95% conf.)
Use of GFM	0.603	1.788	0.200–16.018	-	-	-
Age at RT	0.960	0.996	0.857–1.157	-	-	-
PTV prostate	0.789	1.003	0.980–1.027	-	-	-
PTV Dmax/D1	0.556	1.133	0.747–1.719	-	-	-
PTV Dmean	0.960	0.978	0.410–2.332	-	-	-
CTV prostate	0.006	1.020	1.006–1.035	0.862	0.996	0.947–1.046
CTV Dmax/D1	0.014	0.814	0.690–0.960	0.224	2.583	0.560–11.925
CTV Dmean	0.005	0.858	0.770–0.956	0.298	0.188	0.008–4.393
CTV Dmin	0.005	0.875	0.797–0.960	0.453	2.067	0.310–13.770

OS	Univariable analysis					
	p-value	exp(HR)	exp(HR) (95% conf.)			
Use of GFM	0.564	1.907	0.213–17.063	-	-	-
Age at RT	0.235	1.149	0.913–1.446	-	-	-
PTV Prostate	0.723	1.004	0.984–1.024	-	-	-
PTV Dmax/D1	0.300	0.705	0.364–1.366	-	-	-
PTV Dmean	0.153	0.426	0.132–1.373	-	-	-
CTV Prostate	0.833	1.002	0.980–1.025	-	-	-
CTV Dmax/D1	0.775	0.964	0.747–1.242	-	-	-
CTV Dmean	0.946	0.992	0.791–1.245	-	-	-
CTV Dmin	0.879	1.024	0.758–1.383	-	-	-

bNED = biochemical no evidence of disease; CTV = clinical target volume; GFM = gold fiducial marker; HR = hazard ratio; OS = overall survival; PTV = planning target volume; RT = radiotherapy

mm, complicating the direct comparison of our two groups, as GFM were implanted and the safety margin was reduced to 7 mm together. However, retrospective studies should be used to generate hypotheses, not prove them, and with this study we have generated the hypothesis that the use of GFM for IGRT provides no benefits, but only risks, and should not be performed regularly if other, non-invasive tools for IGRT are in use. Another weakness is the limited sample size.

Regarding strengths, we analyzed a homogeneous patient collective to address this question, with in-depth data including bNED, OS, DSS, and acute and late toxicity, as well as DVH data. Besides, our patient collectives were recruited in parallel, and this reduced any potential bias due to changing treatment modalities over time.

Conclusions

With this study, we have developed the hypothesis that the use of GFM in IGRT does not provide a substantial benefit regarding tumor control or toxicity when other modalities for IGRT are used. To clarify the role of GFM in IGRT, prospective studies based on this hypothesis are needed to possibly reduce the number of unnecessary medical interventions in the treatment of men's most common cancer.

Acknowledgments

Language editing was performed by San Francisco Edit, 1755 Jackson Street, Suite 610, San Francisco, CA 94109, USA.

TABLE 6. Uni- and multivariable Cox regression of the onset of late gastrointestinal or genitourinary toxicity grade 2 or higher

GI	Univariable analysis			Multivariable analysis		
Variable	**p-value**	**exp(HR)**	**exp(HR) (95% conf.)**	**p-value**	**exp(HR)**	**exp(HR) (95% conf.)**
Use of GFM	0.89	0.936	0.368–2.378	-	-	-
Acute GI grade 2	0.09	2.642	0.875–7.981	-	-	-
Age at RT	0.03	1.124	1.010–1.252	0.101	1.092	0.983-1.213
PTV prostate	0.06	0.987	0.974–1.000	-	-	-
PTV Dmax/D1	0.76	1.037	0.824–1.305	-	-	-
PTV Dmean	0.49	1.158	0.767–1.747	-	-	-
CTV prostate	0.03	0.966	0.936–0.996	0.073	0.972	0.942–1.003
CTV Dmax/D1	0.55	1.056	0.884–1.263	-	-	-
CTV Dmean	0.51	1.090	0.843–1.410	-	-	-
CTV Dmin	0.64	1.042	0.877–1.236	-	-	-
Rectal Volume	0.29	1.007	0.994–1.020	-	-	-
Rectal Dmax	0.29	1.125	0.906–1.397	-	-	-
Rectal Dmean	0.25	0.951	0.973–1.036	-	-	-
Rectal V70 Gy %	0.59	0.971	0.875–1.078	-	-	-
Rectal V70 Gy cm^3	0.42	1.040	0.945–1.144	-	-	-
Rectal V60 Gy %	0.42	0.969	0.899–1.046	-	-	-
Rectal V60 Gy cm^3	0.50	1.024	0.955–1.099	-	-	-

GU	Univariable analysis					
Variable	**p-value**	**exp(HR)**	**exp(HR) (95% conf.)**			
Use of GFM	0.93	1.041	0.441–2.459	-	-	-
Acute GU grade 2	0.09	2.042	0.892–4.673	-	-	-
Age at RT	0.50	1.026	0.952–1.106	-	-	-
PTV prostate	0.29	1.006	0.995–1.017	-	-	-
PTV Dmax/D1	0.14	0.808	0.611–1.068	-	-	-
PTV Dmean	0.04	0.573	0.342–0.961	-	-	-
CTV prostate	0.93	0.999	0.989–1.010	-	-	-
CTV Dmax/D1	0.93	1.006	0.895–1.130	-	-	-
CTV Dmean	0.67	1.025	0.916–1.147	-	-	-
CTV Dmin CTV	0.58	1.035	0.918–1.165	-	-	-
Bladder volume	0.72	0.999	0.997–1.002	-	-	-
Bladder Dmax/D1	0.24	0.973	0.696–1.094	-	-	-
Bladder Dmean	0.89	0.997	0.960–1.036	-	-	–
Bladder V70 Gy %	0.49	0.977	0.913–1.045	-	-	-
Bladder V70 Gy cm^3	0.23	0.969	0.921–1.020	-	-	-
Bladder V50 Gy %	0.54	0.988	0.951–1.027	-	-	-
Bladder V50 Gy cm^3	0.29	0.985	0.957–1.013	-	-	-
Bladder V30 Gy %	0.79	0.997	0.974–1.020	-	-	-
Bladder V30 Gy cm^3	0.70	0.997	0.980–1.014	-	-	-

CTV = clinical target volume; GFM = gold fiducial marker; GI = gastrointestinal; GU = genitourinary; PTV = planning target volume; RT = radiotherapy

References

1. Schaeffer EM, Srinivas S, Antonarakis ES, Armstrong AJ, Cheng HH, D'Amico AV, et al. NCCN Guidelines Version 3.2022. Prostate cancer. 2022 [Internet]. [cited 2022 Jul 02]. Available at: https://www.nccn.org/professionals/physician_gls/pdf/prostate.pdf

2. Hamdy FC, Donovan JL, Lane JA, Mason M, Metcalfe C, Holding P, et al. 10-year outcomes after monitoring, surgery, or radiotherapy for localized prostate cancer. *N Engl J Med* 2016; **375:** 1415-24. doi: 10.1056/NEJMoa1606220

3. Kupelian PA, Potters L, Khuntia D, Ciezki JP, Reddy CA, Reuther AM, et al. Radical prostatectomy, external beam radiotherapy <72 Gy, external beam radiotherapy > or =72 Gy, permanent seed implantation, or combined seeds/external beam radiotherapy for stage T1-T2 prostate cancer. *Int J Radiat Oncol Biol Phys* 2004; **58:** 25-33. doi: 10.1016/s0360-3016(03)00784-3

4. Deutsche Gesellschaft für Urologie. [Oncology guideline programme (German Cancer Society, German Cancer Aid, AWMF): S3 guideline on prostate carcinoma, long version 6.0, 2021, AWMF registration number: 043/022OL]. [German]. [cited 2021 Jun 16]. Available at: https://www.leitlinienprogramm-onkologie.de/mwg-internal/de5fs23hu73ds/progress?id=6EduY9K1iK09VZIlf8dOvGrff8piCbbjGVH9Qi0SqOo

5. Mottet N, van den Bergh RCN, Briers E, van den Broeck T, Cuberbatch MG, De Santis M, et al. EAU-EANM-ESTRO-ESUR-SIOG Guidelines on Prostate Cancer-Update. Part 1: screening, diagnosisi, and local treatment with curative intent. *Eur Urol* 2021; **79:** 243-62. doi: 10.1016/j.eururo.2020.09.042

6. Yu T, Zhang Q, Zheng T, Shi H, Liu Y, Feng S, et al. The effectiveness of intensity modulated radiation therapy versus three-dimensional radiation therapy in prostate cancer: a meta-analysis of the literatures. *PLoS One* 2016; **11:** 1-17. doi: 10.1371/journal.pone.0154499

7. Wortel RC, Incrocci L, Pos FJ, Van Der Heide UA, Lebesque JV, Aluwini S, et al. Late side effects after image guided intensity modulated radiation therapy compared to 3d-conformal radiation therapy for prostate cancer: results from 2 prospective cohorts. *Int J Radiat Oncol Biol Phys* 2016; **95:** 680-9. doi: 10.1016/j.ijrobp.2016.01.031

8. Gill S, Thomas J, Fox C, Kron T, Rolfo A, Leahy M, et al. Acute toxicity in prostate cancer patients treated with and without image-guided radiotherapy. *Radiat Oncol* 2011; **6:** 1-7. doi: 10.1186/1748-717X-6-145

9. Dang A, Kupelian PA, Cao M, Agazaryan N, Kishan AU. Image-guided radiotherapy for prostate cancer. *Transl Androl Urol* 2018; **7:** 308-20. doi: 10.21037/tau.2017.12.37

10. NICE guideline [NG131]. Overview. Prostate cancer: diagnosis and management. Guidance NICE. Nice [Internet]. [cited 2021 Aug 18]. Available at: https://www.nice.org.uk/guidance/ng131

11. Zelefsky MJ, Kollmeier M, Cox B, Fidaleo A, Sperling D, Pei X, et al. Improved clinical outcomes with high-dose image guided radiotherapy compared with non-IGRT for the treatment of clinically localized prostate cancer. *Int J Radiat Oncol Biol Phys* 2012; **84:** 125-9. doi: 10.1016/j.ijrobp.2011.11.047

12. Sveistrup J, af Rosenschöld PM, Deasy JO, Oh JH, Pommer T, Petersen PM, et al. Improvement in toxicity in high risk prostate cancer patients treated with image-guided intensity-modulated radiotherapy compared to 3D conformal radiotherapy without daily image guidance. *Radiat Oncol* 2014; **9:** 44. doi: 10.1186/1748-717X-9-44

13. Zapatero A, Roch M, Büchser D, Castro P, Fernández-Banda L, Pozo G, et al. Reduced late urinary toxicity with high-dose intensity-modulated radiotherapy using intra-prostate fiducial markers for localized prostate cancer. *Clin Transl Oncol* 2017; **19:** 1161-7. doi: 10.1007/s12094-017-1655-9

14. Singh J, Greer PB, White MA, Parker J, Patterson J, Tang CI, et al. Treatment-related morbidity in prostate cancer: a comparison of 3-dimensional conformal radiation therapy with and without image guidance using implanted fiducial markers. *Int J Radiat Oncol Biol Phys* 2013; **85:** 1018-23. doi: 10.1016/j.ijrobp.2012.07.2376

15. Napieralska A, Majewski W, Kulik R, Głowacki G, Miszczyk L. A comparison of treatment outcome between fiducial-based and bone-based image guided radiotherapy in prostate cancer patients. *Radiat Oncol* 2018; **13:** 235. doi: 10.1186/s13014-018-1171-2

16. NHS general anaestesia. 2021. [Internet]. [cited 2022 Apr 06]. Available at: https://www.nhs.uk/conditions/general-anaesthesia/

17. Thieme. General anaesthesia and /or regional anaesthesia in adults and adolescents. Thieme Compliance; 2019.

18. Roach M, DeSilvio M, Valicenti R, Grignon D, Asbell SO, Lawton C, et al. Whole-pelvis, "mini-pelvis," or prostate-only external beam radiotherapy after neoadjuvant and concurrent hormonal therapy in patients treated in the Radiation Therapy Oncology Group 9413 trial. *Int J Radiat Oncol Biol Phys* 2006; **66:** 647-53. doi: 10.1016/j.ijrobp.2006.05.074

19. Menzel HG. ICRU Report 83 Prescribing, recording, and reporting photon-beam Intensity-Modulated Radiation Therapy (IMRT). *Journal of the ICRU*. 2010; **15:** 1-2. doi: 10.1093/jicru/ndq001

20. Wachter S, Gerstner N, Dorner D, Goldner G, Colotto A, Wambersie A, et al. The influence of a rectal balloon tube as internal immobilization device on variations of volumes and dose-volume histograms during treatment course of conformal radiotherapy for prostate cancer. *Int J Radiat Oncol Biol Phys* 2002; **52:** 91-100. doi: 10.1016/s0360-3016(01)01821-1

21. Roach M, Hanks G, Thames H, Schellhammer P, Shipley WU, Sokol GH, et al. Defining biochemical failure following radiotherapy with or without hormonal therapy in men with clinically localized prostate cancer: Recommendations of the RTOG-ASTRO Phoenix Consensus Conference. *Int J Radiat Oncol Biol Phys* 2006; **65:** 965-74. doi: 10.1016/j.ijrobp.2006.04.029

22. Cox JD, Stetz J, Pajak TF. Toxicity criteria of the Radiation Therapy Oncology Group (RTOG) and the European Organization for Research and Treatment of Cancer (EORTC). *Int J Radiat Oncol* 1995; **31:** 1341-6. doi: 10.1016/0360-3016(95)00060-C

23. De Cicco L, Bracelli S. Fiducial markers implantation for prostate image-guided radiotherapy: a report on the transperineal approach. *Radiol Medica* 2019; **124:** 132-5. doi: 10.1007/s11547-018-0949-5

24. Valeriani M, Bracci S, Osti MF, Falco T, Agolli L, De Sanctis V, et al. Intermediate-risk prostate cancer patients treated with androgen deprivation therapy and a hypofractionated radiation regimen with or without image guided radiotherapy. *Radiat Oncol* 2013; **8:** 1-8. doi: 10.1186/1748-717X-8-137

25. Peeters STH, Heemsbergen WD, Koper PCM, Van Putten WLJ, Slot A, Dielwart MFH, et al. Dose-response in radiotherapy for localized prostate cancer: results of the Dutch multicenter randomized phase III trial comparing 68 Gy of radiotherapy with 78 Gy. *J Clin Oncol* 2006; **24:** 1990-6. doi: 10.1200/JCO.2005.05.2530

26. Pasalic D, Kuban DA, Allen PK, Tang C, Mesko SM, Grant SR, et al. Dose escalation for prostate adenocarcinoma: a long-term update on the outcomes of a phase 3, single institution randomized clinical trial. *Int J Radiat Oncol Biol Phys* 2019; **104:** 790-7. doi: 10.1016/j.ijrobp.2019.02.045

27. Dearnaley DP, Sydes MR, Graham JD, Aird EG, Bottomley D, Cowan RA, et al. Escalated-dose versus standard-dose conformal radiotherapy in prostate cancer: first results from the MRC RT01 randomised controlled trial. *Lancet Oncol* 2007; **8:** 475-87. doi: 10.1016/S1470-2045(07)70143-2

research article

The five-year KRAS, NRAS and BRAF analysis results and treatment patterns in daily clinical practice in Slovenia in 1st line treatment of metastatic colorectal (mCRC) patients with *RAS* wild-type tumour (wt*RAS*) - a real- life data report 2013–2018

Tanja Mesti[1,2], Martina Rebersek[1,2], Janja Ocvirk[1,2]

[1] Department of Medical Oncology, Institute of Oncology Ljubljana, Ljubljana, Slovenia
[2] Faculty of Medicine, University of Ljubljana, Ljubljana, Slovenia

Radiol Oncol 2023; 57(1): 103-110.

Received 6 September 2022
Accepted 30 September 2022

Correspondence to: Prof. Janja Ocvirk, M.D., Ph.D., Department of Medical Oncology, Institute of Oncology Ljubljana, Zaloska 2, SI-1000 Ljubljana, Slovenia. E-mail: jocvirk@onko-i.si

Disclosure: No potential conflicts of interest were disclosed.

Background. We preformed a Phase IV non-interventional study to assess KRAS, NRAS and BRAF status in metastatic colorectal cancer (mCRC) patients suitable for 1st line treatment and to evaluate the decisions for 1st line treatment considering the treatment goals in the RAS wild type (wt) patients. The aim of our study was also to evaluate the influence of a waiting period for biomarkers analysis on the start of first-line treatment.

Patients and methods. Patients with histologically confirmed mCRC adenocarcinoma suitable for first-line treatment fulfilling all inclusion criteria were included in the study. The KRAS, NRAS and BRAF analysis was performed from tissue samples of primary tumor site or metastatic site. All included patients have given consent to participate in the study by signing the informed consent form.

Results. From April 2013 to March 2018 at the Institute of Oncology Ljubljana 650 patients were included, 637 of them were treated with first- line systemic treatment according to RAS and BRAF status. Remaining 13 patients with mCRC did not receive systemic first-line treatment. The distribution of patients with KRAS mutated and wild-type tumors, was almost equal, 48.8% and 47.9% respectively, 89 % of the patients had wt NRAS tumours and 86.1% had wt BRAF tumours. The most frequently prescribed treatment was bevacizumab-based therapy (53.1%), either in combination with doublet chemotherapy or with mono-chemotherapy. EGFR inhibitors cetuximab and panitumumab were prescribed in wt RAS mCRC patients (30.9%). The waiting period for biomarkers analysis was two weeks.

Conclusions. Our real-world data, single centre 5-year analysis showed that the distribution between wild type and mutated type tumors of the patients with mCRC was approximately the same, as worldwide, so the Slovenian population with mCRC has the same ratio distribution of KRAS, NRAS and BRAF wild and mutated genes. We concluded that a two-week waiting period for biomarkers analysis did not influence the first line treatment decision, so it was in the accordance with the worldwide treatment guidelines based on evidence-based medicine.

Key words: metastatic colorectal cancer; RAS and BRAF biomarkers; systemic treatment

Introduction

Colorectal cancer (CRC) is one of the most common cancers and one of the leading causes of cancer death in the world and also in Slovenia. According to the Cancer Registry of Slovenia 2021, 1349 new patients were diagnosed with CRC in 2018.[1] Approximately 25% of patients present with

metastatic disease at diagnosis, and about 50% of patients with CRC will eventually develop metastases.[2,3] Metastatic disease is still incurable, with 5% five-year overall survival (OS) without treatment. Until 1996 five-fluorouracil (5-FU) was the only approved drug for this disease. Since then, five new agents have been approved in the United States and in Europe for this disease, among them irinotecan, oxaliplatin and the targeted therapies cetuximab, bevacizumab and panitumumab.[2-16] With the current management of metastatic disease, with chemotherapy with oxaliplatin and irinotecan in combination with biologicals, targeting epidermal growth factor mediated growth regulatory pathway and the vascular endothelial growth factor mediated angiogenesis pathway, the progression-free survival (PFS) and OS of these patients can be prolonged. The CRC-related 5-year survival rate approaches 60%.[2,3]

CRC represents a heterogeneous group of diseases. They are promoted by environmental risk factors and various molecular pathways, which influence individual susceptibility to cancer. About 70% of CRCs are sporadic, while 20–30% have a hereditary component, such as Lynch syndrome and familial adenomatous polyposis (FAP).[2,3,15-17] Classification of CRC can be divided in anatomic, genetic and molecular transcriptomic classification. The race, foods, nutrients, carcinogenic agents and increasingly more important the gut microbiome act in a specific manner determined by the primary tumour location to promote carcinogenesis right-sided tumours (RCC) account about to 35% of cases, while left-sided (LCC) and rectal cancer represent about 65% of cases.[17,18] According to genetic classification approximately 85% of CRC, comprises of non-hypermutated, microsatellite stable (MSS) tumours with chromosomal instability with a high frequency of DNA somatic alterations.[17,18]

Several oncogenes play key roles in promoting colorectal cancer.[17-20] Among them firstly in clinical practice of mCRC management, oncogenic mutations of Rat sarcoma virus (RAS) and b-Raf murine sarcoma viral oncogene homolog B (BRAF), which activate the mitogen-activated protein kinase (MAPK) signalling pathway, are the most important.[21-24] Oncogenic RAS mutations have historically been present in approximately 40–50% of CRC patients. According to additional subsequent analysis, the prevalence of RAS mutations in mCRC has been shown to be higher, in 55.9% with mutations in KRAS exon 2 being the most common, they represent 42.6%, followed by KRAS exon 3 in 3.8%, KRAS exon 4 in 6.2%, NRAS exon 2 in 2.9%, NRAS exon3 in 4.2% and NRAS exon4 in 0.3% mutations.[16] NRAS mutant tumours are more frequently in older patients and located on the proximal colon. KRAS and NRAS mutant tumours exhibit similar metastasis patterns. *RAS* mutations are encountered in approximately 50% of the total population worldwide but it also demonstrates geographical variations. Therefore, such a country-by-country determination of the mutation status of the RAS gene in mCRC patients would be meaningful for personalised treatment decision-making.

Selection of patients for anti-epidermal growth factor receptor (EGFR) antibodies based on molecular characteristics of the tumour is very important, because the activity of the anti-EGFR antibodies was confined to wtKRAS tumours (traditionally mutations on codon 12 and 13 of exon 2).[22-26] Than the testing was expanded to the other more rare RAS mutations: codon 61 of exon 3 and codon 117 and 146 of exon 4 of KRAS and exons 2, 3 and 4 of N-Rat sarcoma virus (NRAS), which are also predictive to response to anti-EGFR antibodies.[2] Exon 2 KRAS mutations occur in ~40% of CRC cases, and the other KRAS and NRAS mutations in ~10%–15% of CRC patients. Those mutations influence the response to the combinations of cetuximab or panitumumab alone or with irinotecan- and oxaliplatin-based regimens.[27-42] Treatment with anti-EGFR antibodies may even harm patients with a RAS mutation, especially when combined with oxaliplatin.[4]

BRAF mutations (mt BRAF) are present in about 10–15% of CRCs, with mt BRAFV600E mutations being the most frequent.[15,16] BRAF encodes a serine/threonine protein kinase, a downstream effector of the KRAS protein, and mt BRAF results in constitutive activation of the MAPK signalling pathway. RAS mutations (mt RAS) and mt BRAF mutations are usually mutually exclusive. The most common mutation of the BRAF gene is V600E.[15-18] The same was reported in our previous study carried on Slovenian patients with CRC where the mt BRAF V600E was found in 5.1% of patients.[22,43,44] A mt BRAF is a strong negative prognostic biomarker. The patients with a mt BRAF mCRC have a very poor prognosis. In prognostic analyses, patients with mt BRAF had significantly shorter PFS (7.0 months *vs.* 12.2 months, HR 2.78; $p < 0.001$) and OS (13.4 months *vs*. 37.9 months, HR 5.67; $p < 0.001$) compared with BRAF wild-type (wt BRAF) patients, whilst patients with mt RAS experienced no difference in PFS (11.0 months *vs.*

12.2 months, HR 1.15; p = 0.241); however, OS was significantly shorter compared with wtRAS patients (26.3 months *vs.* 37.9 months, HR 1.44; p = 0.015).[2,3,41,44] Other, non-V600 mt BRAF are a very rare and occur in 2% of metastatic CRC patients, most frequently in younger male patients, with patients, mostly males. Tumours are generally well differentiated tumours, more frequently harbour concurrent mt RAS. Survival of these patients was shown to be improved compared to metastatic CRC patients with V600E mt BRAF or RAS wild-type (wt RAS).[15,16]

As the role of targeted therapy for treatment of advanced or mCRC has become increasingly imported, so currently, determination of tumour gene status for KRAS/NRAS and BRAF mutations, as well as HER2 amplifications and MSI/MMR status, neurotrophic tyrosine receptor kinase (NTRK) fusions are recommended for patients with mCRC. Testing may be carried out for individual genes or as part of an NGS panel.[2,3]

In order to get the real-life data for Slovenian population with mCRC treated at the Oncology Institute of Ljubljana from 30 April 2013 to 5 March 2018 we have performed a Phase IV non-interventional study to assess KRAS, NRAS and BRAF status in mCRC patients suitable for 1st line treatment.

This prospective cohort study was approved by the Institutional Review Board Committee (Approval number: KESOPKR-6 and 03-Z/KESOPKR-6) and was conducted following the ethical standards defned by the Declaration of Helsinki. The study was conducted with the understanding and the consent of the patients. Prior to treatment patients have signed an informed consent for treatment and that their data could be used for scientific purposes.

The aim of this prospective cohort study was to determine in our mCRC patient population the biomarkers status and distribution in the RAS and BRAF genes, and to determine the time from receipt of the histological sample to the determination of the molecular status.

Patients and methods

We performed a prospective, single-arm, single-centre, non-comparative, case-based, observational study from 30 April 2013 to 5 March 2018. The study was comprised of one centre which covers the treatment of all mCRC patients and reflects Slovenian demographic distribution. Originally, all samples for biomarker examination were to be evaluated for KRAS status by the certificated Molecular laboratory at the Institute of Oncology Ljubljana. The data was to be recorded in a collective data base to provide reliability. As from 2013 before initiating treatment with cetuximab, the testing for RAS status included not only KRAS, but also NRAS mutations by an experienced laboratory using validated test methods for detection of KRAS and NRAS. According to this in November 2013 in addition to KRAS we included also NRAS mutations analysis in all patients included in this study. RAS testing had previously been performed for all patients already included.

In this study, 650 mCRC patients treated at the Institute of Oncology Ljubljana were enrolled.

Initially, the planned number of patients for the study was 300. Between April 2013 and February 2014, 300 patients were recruited and underwent KRAS testing. The protocol was then amended in view of full RAS testing becoming standard clinical practice. The protocol was amended again in November 2015, to include an extra 350 above the original plan – a total of 650, and BRAF testing was added to the list of biomarkers analysed. From November 2015 until March 2018, 350 additional patients were recruited, making a total recruitment of 650. Thirteen patients that were included and signed consent to be part of this study, and underwent RAS and BRAF testing, did not present for the first-line systemic treatment afterwards, resulting in complete data for 637 patients.

The basic data about each patient were recorded, as date of birth, gender, performance status Eastern Cooperative Oncology Group (ECOG) performance status and smoking habits. The disease characteristics were also included, including date of diagnosis of the primary tumour, tumour location – colon or rectum, initial stage at the time of diagnosis (according to the TNM (tumour T, nodes N, and metastases M) classification system), the treatment option used for the primary tumour, (radiotherapy or surgery, followed or not by adjuvant chemotherapy, with the duration time treatment and the type of the adjuvant chemotherapy (capecitabine, 5-FU or oxaliplatin). The date of metastatic diagnosis was also included in the analysis, the sites of metastatic spread and the treatment option used, as surgery and systemic treatment, with systemic treatment comprising the treatment goals – curative, potentially curative or palliative, liver and/or lung metastases potentially respectable, depending upon tumour burden. The systemic first line treatment options included vari-

TABLE 1. Patients baseline characteristics

Patients baseline characteristics	Number (%)
Gender	
female	233 (36.6)
male	404 (63.4)
WHO clasiffication:	
0	241 (37.8)
1	300 (47.1)
2	72 (11.3)
Tumor location:	
colon	387 (60.8)
rectum	250 (39.2)
Clinical signs of the primary colorectal cancer present before pathological confirmation	178 (20.9)
Primary metastatic	361 (56.7)
Liver metastases	218 (34.3)

* Some pathohistological reports from external hospital had unclear description, about the TNM status and risk factors

ous combinations of irinotecan, oxaliplatin based therapy, 5-FU, capecitabine, FOLFOXIRI protocol, cetuximab in a weekly or biweekly manner, bevacizumab, panitumumab or other.

The tumour characteristics were assessed regarding with KRAS/RAS and BRAF status. The date of the request for the biomolecular analysis was included, and the date of the analysis receipt.

DNA for molecular analysis was extracted from formalin-fixed, paraffin-embedded tumour tissue of primary tumours or metastases with at least 70% of tumour cells. Molecular testing was performed with RT-PCR KRAS Mutation Analysis Kit (EntroGen, Inc.), RT-PCR NRAS Mutation Analysis Kit (EntroGen, Inc.) and RT-PCR BRAF Mutation Analysis Kit (EntroGen, Inc.), according to manufacturer's instructions. The KRAS and NRAS analyses were assessed on exons 2, 3 and 4, and for BRAF on exon 15.

TABLE 2. Disease characteristics

Disease characteristics	Number (%)
pT4 of primary tumor	186 (29.2)
Affected regional lymph nodes (N):	
N0 (no affected regional lymph nodes)	110 (17.3)
N1 (1 to 3 affected regional lymph nodes)	209 (32.8)
N2 (more than 3 affected regional lymph nodes)	239 (37.5)
Missing data*	62 (11.3)
Vascular invasion	114 (17.9)
Perineural invasion	95 (27.9)
Lymphangiosis	115 (18.1)
Grade of differentiation:	
G1 (well)	19 (3)
G2 (medium)	162 (25.4)
G3 (poorly)	53 (8.3)
G4 (no differentiated)	1 (0.2)
Missing data*	402 (63.2)
Resection of primary tumour	
R0	63 (9.9)
R1	10 (1.6)
R2	16 (2.5)

* Other metastatic locations: brain, ovaries, suprarenal glands, local recurrence, muscular dissemination

Statistical methods

In this study 95% confidence intervals were calculated to indicate the degree of certainty of KRAS, NRAS and BRAF status frequency as being wild type or mutant type.

A sample size of 551-634 patients was necessary for a two-sided 95% confidence interval with a width of 4% anticipating a *BRAF* mutant rate of 5.5% to 6.5%. The planned sample size was increased to 650 patients, to consider non-evaluable biomarker test results and missing data.

Results

In total, 650 patients of the whole mCRC patients treated at Oncology Institute of Ljubljana were enrolled in this prospective clinical study.

Patient's characteristics and treatment

The demographic data about each patient were recorded, such as date of birth, gender, performance status (WHO) and smoking habits. Two thirds of the patients were male and most (84.9%) of the patients initially had a very good (ECOG 0–1) performance status. The main localization of the primary tumour was colon in 60.8% of the patients. All of included patients in this study had pathological confirmation of the carcinoma of the colon or rectum. Almost one third (27.9%) of the patients had clinical signs for CRC, before being pathologically confirmed, including occult bleeding or were asymptomatic and detected in the Slovenian national program for the early detection of the colorectal cancer named SVIT. For more than half (56.7%) of patients the diagnosis was confirmed pathologically, after biopsy was performed at colonoscopy, and for the others after the surgery.

TABLE 3. The most frequent metastatic sites

The most frequent metastatic sites	Number (%)
Total	**637 (100)**
Liver	218 (34.3)
Lungs	70 (11.0)
Lymph nodes	34 (5.3)
Peritoneum	115 (18.1)
Bones	4 (0.6)
Other*	18 (2.8)
Multiple locations	261 (41.0)

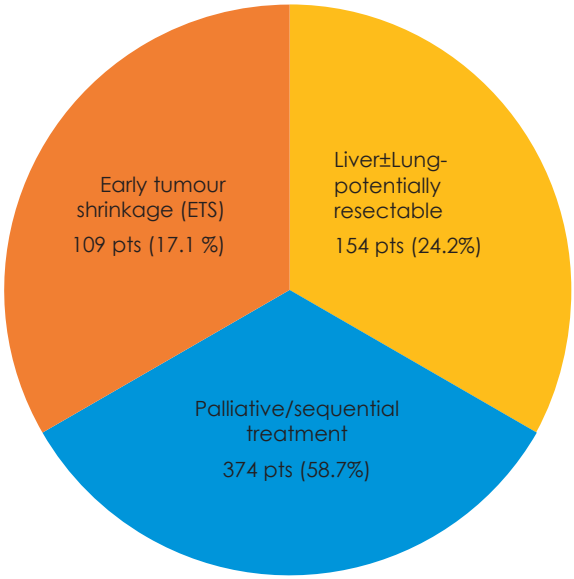

FIGURE 1. Treatment goal options at presentation of the metastatic colorectal cancer (mCRC) patients.

Complete resection (R0) of operated primary tumour was achieved in 9.9%. Most of the included patients were non-smokers (62.6%).

According to the TNM characteristics, initially at the first presentation of the primary CRC, in the external hospitals, 53.7% of patients had T3 tumours, 31.6% of patients had N1 (31,6%) and 34.5% of patients had N2. One third of patients had initially no metastatic disease (33.4%). Mostly, the primary CRC had pathohistological characteristics as follows: grade 2, with one third having vascular invasion, perineural invasion or lymphangiosis. Primary metastatic disease was confirmed in 56.7% of patients. The most common sites of metastases were liver and lung. Some of patients with mCRC in liver and lungs had surgery of the metastasis before the mCRC treatment, 6.8% and 2.0% respectively. In 10% of the mCRC patients R0 resection (70.8% of the total number of resections) was achieved. The metastatic sites were included in the analysis, and the main sites of CRC dissemination were liver (34.2%), lungs (11.0%), lymph nodes (5.3%), peritoneum (5.0%). Sixty-two patients were no previous smokers, and only 9% of patients were smoking at the time of our analysis. Patients' baseline characteristics and are shown in Table 1, disease characteristics are shown in Table 2, the most frequent metastatic site are shown in Table 3, smoking habits of included patients are shown in Table 4.

The treatment goals were in oligometastatic disease as follows: respectable and potentially resectable, or palliative for patients with high burden of the disease. More than a half (58.7%) of the patients were initially candidates for the palliative treatment, and 24.2% were potentially resectable at presentation. Treatment goal options at presentation of the mCRC patients are shown in Figure 1.

More than half (58.7%) of patients were initially candidates for palliative systemic treatment, and 24.2% were potentially resectable at presentation.

Of all 637 mCRC patients had the following possible first line systemic treatment options: chemotherapy - fluoropyrimidine based systemic therapy combined with oxaliplatin and/or irinotecan plus, for subjects with KRAS/RAS wild type tumours, the EGFR inhibitors cetuximab or panitumumab, or the VEGF inhibitor bevacizumab for those with KRAS/RAS mutated tumours. Most

TABLE 4. Treatment regimen decision for the first line treatment of the metastatic colorectal cancer (mCRC)

Systemic therapy options	Number (%)
Fluoropirimidines/Irinotecan/Cetuximab*	73 (11.4)
Fluoropirimidines/Oxaliplatin/Cetuximab*	49 (7.7)
Fluoropirimidines/Irinotecan/Panitumumab*	17 (2.7)
Fluoropirimidines/Oxaliplatin/Panitumumab*	12 (1.9)
EGFR inhibitors other**	46 (7.2)
Fluoropirimidines/Irinotecan/Bevacizumab	126 (19.8)
Fluoropirimidines/Oxaliplatin/Bevacizumab	191 (30.0)
VEGF inhibitor other***	21 (3.3)
Chemotherapy only	102 (16.0)

*EGFR inhibitors for RAS (NRAS and KRAS) wild type only
**EGFR inhibitors monotherapy ± one chemotherapy
***VEGF inhibitor monotherapy ± one chemotherapy

TABLE 5. The RAS/KRAS and BRAF status distribution

The RAS/KRAS and BRAF status distribution	Number (%)
KRAS testing	637 (100)
KRAS mutated	311 (48.8)
KRAS wild type	305 (47.9)
Not possible	21 (3.3)
NRAS testing	637 (100)
NRAS mutated	57 (9.0)
NRAS wild type	567 (89.0)
Not possible	13 (2.0)
BRAF testing	637 (100)
BRAF mutated	84 (13.2)
BRAF wild type	548 (86.1)
Not possible	5 (0.7)

TABLE 6. Methods used for KRAS/RAS and BRAF analysis

Methods used for KRAS/RAS and BRAF analysis	Number (%)
Direct sequencing	223 (35.0)
Pyrosequencing	322 (50.5)
qPCR	92 (14.5)

frequently used was bevacizumab-based therapy (53.1%), either in combination with doublet chemotherapy or with one cytostatic or as monotherapy. EGFR inhibitors cetuximab and panitumumab were used in RAS (KRAS/NRAS) wild type mCRC subjects (30.9%). Data presented in the Table 9. Fifty-one subjects with RAS (KRAS/NRAS) wild type tumours received chemotherapy alone or in combination with Bevacizumab, as first line treatment. The first line treatment decision is made by the oncologist in accordance with NCCN and ESMO guidelines and consider the patient's preferences. Some patients found skin side effects and higher parenteral application frequency important parameters for a possible decrease of their quality of life. Most frequently prescribed treatment protocols are shown in Table 4.

Biomarker status

The assessment of the KRAS/RAS and BRAF status was performed for all 650 patients. The RAS and BRAF status analysis were performed simultaneously, and for the group of subjects from the first Amendment, after the Amendment II was added to the protocol, the NRAS and BRAF data were added to the database. Data of the RAS/KRAS and BRAF status distribution are shown in Table 5. The distribution of patients with KRAS mutated and wild-type tumours, was almost equal, 48.8% and 47.9% respectively. For 3.3% of patients of the assessed population the KRAS status analysis was unsuccessful, due to unrepresentative tumour samples (Table 6). For 2.0% and 0.7% of the subjects the NRAS and BRAF genotyping was not possible due to unrepresentative tumour samples. The KRAS and NRAS analyses were assessed on exons 2, 3 and 4, and for BRAF on exon 15. The most frequent mutation was in KRAS in codon 12 and codon 13, and the same was true for NRAS and for the BRAF V600E mutation. The most frequent mutations, as follows were: pGly12Asp (c35 G>A) 7.8%, pGly 12Val (c35G>T) 6.6%, pGly13Asp (c38 G>A) 4.7% and pGly12Cys (c34 G>T) 2.4%.

The median time for biomarkers status assessment was 14 days.

Mostly direct sequencing was used for KRAS/RAS and BRAF status assessment, but also other methods, as pyrosequencing and qPCR. The Entrogen RT PCR KRAS/RAS and BRAF mutation Kit was used. Methods used for KRAS/RAS and BRAF analysis are shown in Table 6.

Discussion

The aim of the observational mCRC population-based study was to determine the biomarker status in the RAS and BRAF genes, to determine their distribution in the mCRC patient Slovenian population, and to determine the time from receiving the histological sample to the determination of the biomarker status and its impact on the initiation of systemic oncological therapy.

This study was performed in order to achieve a real perspective of the bio-markers status of the patients with metastatic colorectal cancer in comparison with worldwide data. The analysis of KRAS/NRAS and BRAF status was a relatively new approach in the treatment of the patients with metastatic colorectal cancer at the time of conducting of our clinical study, so we also wanted to get real insight of the time frame needed for such analysis and its possible effect on the initiation of the first-line treatment.

The status of mutations in the RAS gene is a molecular predictive factor for response to treatment with EGFR inhibitors inmCRC. Determination of mutational status in KRAS gene has been standard clinical practice since 2008. Additional mutations in the codons of 61 and 146 of KRAS gene, and in codons 12, 13, 61 and 146 of NRAS gene are determined at our Institute of Oncology Ljubljana

since autumn 2013 and are being standard in international clinical practice since 2014. According to the literature data, are about 15%.

In our prospective cohort study KRAS mutations were found in 48.8% of patients, and additionally 9% of NRAS mutations were determined. So approximately 60% of patients had *RAS* mutated mCRC, which is consistent with reports from previous literature.[2,3,22,45] In our retrospective analysis we found 17% of additional mutations in RAS gene, which is a higher percentage than in our prospective cohort study, probably due to characteristics of patient population included.[45]

Also, higher, 13.2% BRAF mutations, were determined in our cohort study. According to the literature, the frequency of this mutation is from 5 to 10%. [2,3,24] According to our previous retrospective analysis, the V600E mutation in the BRAF gene was also present at a similar percentage of patients, in 7.4%.[46] It is assumed that this difference in the percentage of BRAF mutations in clinical studies is due to the characteristics of the patients included in the analysis.

So, according to our study analysis data, the distribution between wild type and mutated type tumours of mCRC patients was approximately the same, as worldwide, so the Slovenian population with mCRC has the same ratio distribution of KRAS, NRAS and BRAF wild and mutated genes.

The two-week time period from the initial presentation of the patient until the biomarker status analysis report did not affect the starting of the systemic treatment or the treatment decision, as usually mCRC patients are given a brief period of time for psychical and physical preparation for the systemic treatment, at which time supportive care – nutritional and symptomatic support, is given.

As for the time spent on biomarkers analysis, we concluded that the two-week period was not influencing the first line treatment decision, because patients started with systemic chemotherapy immediately and after 2 weeks have already received a biologic drug at the 2nd cycle of chemotherapy according to molecular genetic testing, And also in Slovenia we do not have waiting lists and cancer patients, who need treatment are referred to the oncology treatment facility shortly after the diagnosis, so this brief period of time is usual for psychical and physical preparation for the systemic treatment, at which time supportive care – nutritional and symptomatic support, is given.

In conclusion, we have proven that the biomarkers distribution in Slovenian population with mCRC was approximately the same as worldwide, so the decision treatment approach should be in the accordance with the worldwide treatment guidelines based on evidence-based medicine. Secondly, the laboratory for the molecular analysis that we have in the Institute of Oncololgy Ljubljana was performing the needed biomarkers analysis in an acceptable time that didn't affect the treatment decision or delay the needed cancer treatment.

Acknowledgement

The authors acknowledge the financial support from the state budget by the Slovenian Research Agency (ARRS), program No. P3-0321.

References

1. *Cancer in Slovenia 2018*. Ljubljana: Institute of Oncology Ljubljana, Epidemiology and Cancer Registry, Slovenian Cancer Registry; 2021.
2. Schmoll HJ, Van Cutsem E, Stein A, Valentini V, Glimelius B, Haustermans K, et al. ESMO Consensus Guidelines for management of patients with colon and rectal cancer. A personalized approach to clinical decision making. *Ann Oncol* 2012; **23:** 2479-516. doi:10.1093/annonc/mds236
3. van Cutsem E, Cervantes A, Adam R, Sobrero S, J. van Krieken JH, Aderka D, et al ESMO consensus guidelines for the management of patients with metastatic colorectal cancer. *Ann Oncol* 2016; **27:** 1386-422. doi:10.1093/annonc/mdw235
4. National Comprehensive Cancer Network. NCCN Clinical Practice Guidelines in Oncology: Colon Cancer. V.1.2022. [cited 2022 Aug 25]. Avaible at: http://www.nccn.org/profesionals/phisician_gls/PDF/colon.pdf
5. National Comprehensive Cancer Network. NCCN Clinical Practice Guidelines in Oncology: Rectal Cancer. V.1.2022. [cited 2022 Aug 25]. Avaible at: http://www.nccn.org/profesionals/phisician_gls/PDF/colon.pdf
6. Tournigand C, André T, Achille E, Lledo G, Flesh M, Mery-Mignard D, et a. FOLFIRI followed by FOLFOX6 or the reverse sequence in advanced colorectal cancer: a randomized GERCOR study. *J Clin Oncol* 2004; **22:** 229-37. doi: 10.1200/JCO.2004.05.113. Epub 2003 Dec 2. PMID: 14657227
7. Grothey A, Sargent D, Goldberg RM, Schmoll HJ. Survival of patients with advanced colorectal cancer improves with the availability of fluorouracil-leucovorin, irinotecan, and oxaliplatin in the course of treatment. *J Clin Oncol* 2004; **22:** 1209-14. doi: 10.1200/JCO.2004.11.037. PMID: 15051767
8. Hurwitz H, Fehrenbacher L, Novotny W, Cartwright T, Hainsworth J, Heim W, et al. Bevacizumab plus irinotecan, fluorouracil, and leucovorin for metastatic colorectal cancer. *N Engl J Med* 2004; **350:** 2335-42. doi: 10.1056/NEJMoa032691
9. Saltz LB, Clarke S, Díaz-Rubio E, Scheithauer W, Figer A, Wong R, et al. Bevacizumab in combination with oxaliplatin-based chemotherapy as first-line therapy in metastatic colorectal cancer: a randomized phase III study. *J Clin Oncol* 2008; **26:** 2013-9. doi: 10.1200/JCO.2007.14.9930. Erratum in: *J Clin Oncol* 2008; **26:** 3110. Erratum in: *J Clin Oncol* 2009; **27:** 653. PMID: 18421054
10. Van Cutsem E, Köhne CH, Hitre E, Zaluski J, Chang Chien CR, Makhson A, et al. Cetuximab and chemotherapy as initial treatment for metastatic colorectal cancer. *N Engl J Med* 2009; **360:** 1408-17. doi: 10.1056/NEJMoa0805019
11. Bokemeyer C, Bondarenko I, Makhson A, Hartmann JT, Aparicio J, de Braud F, et al. Fluorouracil, leucovorin, and oxaliplatin with and without cetuximab in the first-line treatment of metastatic colorectal cancer. *J Clin Oncol* 2009; **27:** 663-71. doi: 10.1200/JCO.2008.20.8397
12. Bokemeyer C, Bondarenko I, Hartmann JT, de Braud F, Schuch G, Zubel A, et al. Efficacy according to biomarker status of cetuximab plus FOLFOX-4 as first-line treatment for metastatic colorectal cancer: the OPUS study. *Ann Oncol* 2011; **22:** 1535-46. doi: 10.1093/annonc/mdq632

13. Folprecht G, Grothey A, Alberts S, Raab HR, Köhne CH. Neoadjuvant treatment of unresectable colorectal liver metastases: correlation between tumour response and resection rates. *Ann Oncol* 2005; **16:** 1311-9. doi: 10.1093/annonc/mdi246

14. Adam R, Delvart V, Pascal G, Valeanu A, Castaing D, Azoulay D, et al. Rescue surgery for unresectable colorectal liver metastases downstaged by chemotherapy: a model to predict long-term survival. *Ann Surg* 2004; **240:** 644-57; discussion 657-8. doi: 10.1097/01.sla.0000141198.92114.f6

15. Bellio H, Fumet JD, Ghiringhelli F. Targeting BRAF and RAS in colorectal cancer. *Cancers* 2021; **13:** 2201. doi: 10.3390/cancers13092201

16. Gong J, Cho M, Fakih M. RAS and BRAF in metastatic colorectal cancer management. *J Gastrointest Oncol* 2016; **7:** 687-704. doi: 10.21037/jgo.2016.06.12

17. Bos JL, Fearon ER, Hamilton SR, Verlaan-de Vries M, van Boom JH, van der Eb AJ, et al. Prevalence of ras gene mutations in human colorectal cancers. *Nature* 1987; **327:** 293-7. doi: 10.1038/327293a0. PMID: 3587348

18. Vogelstein B, Fearon ER, Hamilton SR, Kern SE, Preisinger AC, Leppert M, et al. Genetic alterations during colorectal-tumor development. *N Engl J Med* 1988; **319:** 525-32. doi: 10.1056/NEJM198809013190901

19. Zhu D, Keohavong P, Finkelstein SD, Swalsky P, Bakker A, Weissfeld J, et al. K-ras gene mutations in normal colorectal tissues from K-ras mutation-positive colorectal cancer patients. *Cancer Res* 1997; **57:** 2485-92. PMID: 9192830

20. Markowitz SD, Bertagnolli MM. Molecular basis of colorectal cancer. *N Engl J Med* 2009; **361:** 2449-60. doi: 10.1056/NEJMra0804588

21. Sebolt-Leopold JS. Advances in the development of cancer therapeutics directed against the RAS-mitogen-activated protein kinase pathway. *Clin Cancer Res* 2008; **14:** 3651-6. doi: 10.1158/1078-0432.CCR-08-0333

22. Ličar A, Cerkovnik P, Novaković S. Distribution of some activating KRAS and BRAF mutations in Slovene patients with colorectal cancer. *Med Oncol* 2011; **28:** 1048-53. doi: 10.1007/s12032-010-9631-z

23. De Roock W, Jonker DJ, De Nicolantonio F, Sartore-Bianchi A, Tu D, Siena S, et al. Association of KRAS p.G13D mutation with outcome in patients with outcome with chemotherapy-refractory metastatic colorectal cancer treated with cetuximab. *JAMA* 2010; **304:** 1812-20. doi: 10.1001/jama.2010.1535

24. De Roock W, Claes B, Bernasconi D, De Schutter J, Biesmans B, Fountzilas G, et al. Effect of KRAS, BRAF, NRAS, and PIK3CA mutations on the efficacy of cetuximab plus chemotherapy in chemotherapy-refractory metastatic colorectal cancer: a retrospective consortium analysis. *Lancet Oncol* 2010; **11:** 753-62. doi: 10.1016/S1470-2045(10)70130-3

25. Artale S, Sartore- Bianchi A, Veronese SM, Gambi V, Sarnataro CS, Gambacorta M, et al. Mutations of KRAS and BRAF in primary and matched metastatic sites of colorectal cancer. *J Clin Oncol* 2008; **26:** 4217-9. doi:10.1200/JCO.2008.18.7266

26. Artale S, Sartore-Bianchi A, Veronese SM, Gambi V, Sarnataro CS, Gambacorta Met al. Mutations of KRAS and BRAF in primary and matched metastatic sites of colorectal cancer. *J Clin Oncol* 2008; **26:** 4217-9. doi: 10.1200/JCO.2008.18.7286

27. Lamprechts D, De Roock W, Prenen H, Schutter JD, Jacobs B, Biesmans B, et al. The role of KRAS, BRAF, NRAS and PIK3CA mutations as a markers of resistence of cetuximab in chemorefractory metastatic colorectal cancer. *J Clin Oncol* 2009; **27:** 9020. doi: 10.1158/1078-0432.CCR-08-2961

28. Tejpar S, De Roock W, Claes B, Fountzilas G. PIKI3CA, BRAF and KRAS mutations and outcome prediction in chemorefractory metastatic colorectal cancer (mCRC) patients treated with EGFR targeting monoclonal antibodies (MoAbs): results of a European Consortium. 8th Annual Meeting of the Japanese-Society-of-Medical-Oncology *Ann Oncol* 2010; **21(Suppl 9):** 6.

29. Loupakis F, Ruzzo A, Cremolini C, Vincenzi B, Salvatore L, Santini D, et al. KRAS codon 61, 146 and BRAF mutations predict resistence to cetuximab + irinotecan in KRAS codon 12 and 13 wild-type metastatic colorectal cancer. *Br J Cancer* 2009; **101:** 715-21. doi: 10.18632/oncotarget.13697

30. Peters M, Douillard JY, Van Cutsem E, Siena S, Zhang K, Williams R et al. Mutant (MT) KRAS codon 12 and 13 alleles in patients (pts) with metastatic colorectal cancer (mCRC): assessment as prognostic and predictive biomarkers of response to panitumumab (pmab*)*. [abstract]. *J Clin Oncol* 2012; **30(Suppl 4):** abstr 383.

31. Tejpar S, Celic I, Schlichting M, Bokemeyer C, Van Cutsem E. Association of KRAS G13D tumor mutations with outcome in patients with metastatic colorectal cancer treated with first-line chemotherapy with or without cetuximab. *J Clin Oncol* 2012; **30:** 3570-7. doi: 10.1200/JCO.2012.42.2592

32. Fujiyoshi K, Yamamoto G, Takahashi A, Arai Y, Yamada M, Kakuta M, et al. High concordance rate of KRAS/BRAF mutations and MSI-H between primary colorectal cancer and corresponding metastases. *Oncol Rep* 2017; **37:** 785-92. doi: 10.3892/or.2016.5323

33. Gaedcke J, Grade M, Jung K, Schirmer M, Jo P, Obermeyer C, et al. KRAS and BRAF mutations in patients with rectal cancer treated with preoperative chemoradiotherapy. *Radiother Oncol* 2010; **94:** 76-81. doi: 10.1016/j.radonc.2009.10.001

34. Pietrantonio F, Cremolini C, Petrelli F, Di Bartolomeo M, Loupakis F, Maggi C, et al. First-line anti-EGFR monoclonal antibodies in panRAS wild-type metastatic colorectal cancer: a systematic review and meta-analysis. *Crit Rev Oncol Hematol* 2015; **96:** 156-66. doi: 10.1016/j.critrevonc.2015.05.016

35. Sorich MJ, Wiese MD, Rowland A, Kichenadasse G, McKinnon RA, Karapetis CS, et al. Extended RAS mutations and anti-EGFR monoclonal antibody survival benefit in metastatic colorectal cancer: a meta-analysis of randomized, controlled trials. *Ann Oncol* 2015; **26:** 13-21. doi: 10.1093/annonc/mdu378

36. Therkildsen C, Bergmann TK, Henrichsen-Schnack T, Ladelund S, Nilbert M. The predictive value of KRAS, NRAS, BRAF, PIK3CA and PTEN for anti-EGFR treatment in metastatic colorectal cancer: a systematic review and meta-analysis. *Acta Oncol* 2014; **53:** 852-64. doi: 10.3109/0284186X.2014.895036

37. Karapetis CS, Khambata-Ford S, Jonker DJ, O'Callaghan CJ, Tu D, Tebbutt NC, et al. K-ras mutations and benefit from cetuximab in advanced colorectal cancer. *N Engl J Med* 2008; **359:** 1757-65. doi: 10.1056/NEJMoa0804385

38. Samowitz WS, Curtin K, Schaffer D, Robertson M, Leppert M, Slattery ML. Relationship of Ki-ras mutations in colon cancers to tumor location, stage, and survival: a population-based study. *Cancer Epidemiol Biomarkers Prev* 2000; **9:** 1193-7. PMID: 11097226

39. Van Cutsem E Köhne CH, La´ng I, Folprecht G, Nowacki MP, Cascinu S, et al. Cetuximab plus irinotecan, fluorouracil, and leucovorin as first-line treatment for metastatic colorectal cancer: updated analysis of overall survival according to tumor KRAS and BRAF mutation status. *J Clin Oncol* 2011; **29:** 2011-9. doi: 10.1200/JCO.2010.33.5091

40. Bokemeyer C, Bondarenko I, Hartmann JT, de Braud F, Schuch G, Zubel A, et al. Efficacy according to biomarker status of cetuximab plus FOLFOX-4 as first-line treatment for metastatic colorectal cancer: the OPUS study. *Ann Oncol* 2011; **22:** 1535-46. doi: 10.1093/annonc/mdq632

41. Douillard JY, Oliner KS, Siena S, Tabernero J, Burkes R, Barugel M, et al. Panitumumab-FOLFOX4 treatment and RAS mutations in colorectal cancer. *N Engl J Med* 2013; **369:** 1023-34. doi: 10.1056/NEJMoa1305275

42. Cremolini C, Loupakis F, Antoniotti C, Lupi C, Sensi E, Lonardi S, et al. FOLFOXIRI plus bevacizumab versus FOLFIRI plus bevacizumab as first-line treatment of patients with metastatic colorectal cancer: updated overall survival and molecular subgroup analyses of the open-label, phase 3 TRIBE study. *Lancet Oncol* 2015; **16:** 1306-15. doi: 10.1016/S1470-2045(15)00122-9.

43. Tol J, Nagtegaal ID, Punt CJA. BRAF mutation in metastatic colorectal cancer. *N Engl J Med* 2009; **361:** 98-9. doi: 10.3978/j.issn.2078-6891.2015.077

44. Samowitz WS, Sweeney C, Herrick J, Albertsen H, Levin TR, Murtaugh MA, et al. Poor survival associatedwith the BRAF V600E mutation in microsatellite-stable colon cancer. *Caner Res* 2005; **65:** 6063-9. doi: 10.1158/0008-5472.CAN-05-0404

45. Rebersek M, Mesti T, Boc M, Ocvirk J. Molecular biomarkers and histological parameters impact on survival and response to first- line systemic therapy of metastatic colorectal cancer patients. *Radiol Oncol* 2019; **53:** 85-95. doi: 10.2478/raon-2019-0013

46. Rebersek M, Boc M, Škerl P, Benedik J, Hlebanja Z, Volk N, et al. Efficacy of First- line systemic treatment in correlation with BRAF V600E and different KRAS mutations colorectal cancer - a single institution retrospective analysis. *Radiol Oncol* 2011; **45:** 285-91. doi: 10.2478/v10019-011-0039-y

research article

Association of *OPRM1*, *MIR23B*, and *MIR107* genetic variability with acute pain, chronic pain and adverse effects after postoperative tramadol and paracetamol treatment in breast cancer

Zala Vidic[1], Katja Goricar[1], Branka Strazisar[2], Nikola Besic[2], Vita Dolzan[1]

[1] Pharmacogenetics Laboratory, Institute of Biochemistry and Molecular Genetics, Faculty of Medicine, University of Ljubljana, Ljubljana, Slovenia
[2] Institute of Oncology, Ljubljana, Slovenia

Radiol Oncol 2023; 57(1): 111-120.

Received 14 September 2022
Accepted 28 September 2022

Correspondence to: Prof. Vita Dolžan, M.D., Ph.D., Pharmacogenetics Laboratory, Institute of Biochemistry and Molecular Genetics, Faculty of Medicine, University of Ljubljana, Vrazov trg 2, 1000 Ljubljana, Slovenia. E-mail: vita.dolzan@mf.uni-lj.si

Disclosure: No potential conflicts of interest were disclosed.

Background. Tramadol is an opioid analgesic often used for pain management after breast cancer surgery. Its analgesic activity is due to the activation of the μ-opioid receptor, encoded by the *OPRM1* gene. This study investigated the association of genetic variability in *OPRM1* and its regulatory miRNA genes with outcomes of tramadol/paracetamol treatment after breast cancer surgery with axillary lymphadenectomy.

Patients and methods. The study included 113 breast cancer patients after breast cancer surgery with axillary lymphadenectomy treated with either 75/650 mg or 37.5/325 mg of tramadol with paracetamol for pain relief within the randomized clinical trial KCT 04/2015-DORETAonko/si at the Institute of Oncology Ljubljana. All patients were genotyped for *OPRM1* rs1799971 and rs677830, *MIR23B* rs1011784, and *MIR107* rs2296616 using competitive allele-specific PCR. The association of genetic factors with acute and chronic pain as well as adverse effects of tramadol treatment was evaluated using logistic regression, Fisher's exact test, and Mann-Whitney test.

Results. The investigated *OPRM1* related polymorphisms were not associated with acute pain assessed with the VAS scale within four weeks after surgery (all $P > 0.05$). Carriers of at least one polymorphic *OPRM1* rs1799971 allele had a higher risk of constipation in the first four weeks after surgery compared to non-carriers (OR = 4.5, 95% CI = 1.6–12.64, P = 0.004). Carriers of at least one polymorphic *OPRM1* rs677830 allele had a higher risk of constipation after third week of tramadol treatment (OR = 3.11, 95% CI = 1.08–8.89, P = 0.035). Furthermore, carriers of two polymorphic *MIR23B* rs1011784 alleles had a higher risk of nausea after 28 days of tramadol treatment (OR = 7.35, 95% CI = 1.27–42.6, P = 0.026), while heterozygotes for *MIR107* rs2296616 allele had a lower risk of nausea after 21 days of tramadol treatment (OR = 0.21, 95% CI = 0.05–0.87, P = 0.031). In carriers of two polymorphic *MIR107* rs2296616 alleles, chronic pain was significantly more common than in carriers of two wild-type alleles (P = 0.004). Carriers of at least one polymorphic *MIR23B* rs1011784 allele experienced more neuropathic pain after adjustment for tramadol dose (OR = 2.85, 95% CI = 1.07–7.59, P = 0.036), while carriers of at least one polymorphic *OPRM1* rs677830 allele experienced less neuropathic pain compared to carriers of two wild-type alleles (OR = 0.38, 95% CI = 0.15–0.99, P = 0.047).

Conclusions. Genetic variability of *OPRM1* and genes coding for miRNAs that could affect *OPRM1* expression may be associated with adverse effects of tramadol/paracetamol treatment as well as with chronic and neuropathic pain after breast cancer surgery with axillary lymphadenectomy.

Key words: breast cancer surgery; miRNA; OPRM1; pain treatment; tramadol

Introduction

Tramadol is a synthetic centrally acting opioid drug that exhibits its analgesic activity by binding to μ-opioid receptor (MOR).[1] It is widely used for the treatment of moderate to severe acute pain after breast cancer surgery with axillary lymphadenectomy.[2] Tramadol is considered a relatively safe opioid drug since it does not cause respiratory depression at therapeutic doses and is less likely to cause addiction compared to many other opioids. However, its analgesic efficiency is lesser compared to morphine.[1-3]

MORs, encoded by the *OPRM1* gene, are members of the Rhodopsin family of G-protein coupled receptors.[4] MORs are expressed in the cerebral cortex, thalamus, periaqueductal gray, nucleus accumbens, and basolateral amygdala, and are therefore responsible for the occurrence of euphoria, dependence, respiratory depression, and activation of the reward system.[5] They are crucial for the analgesic effects of the majority of opioid drugs.[6]

It has been shown that polymorphisms in the *OPRM1* gene can affect the efficacy of analgesic action of several opioid drugs. One of the most studied single nucleotide polymorphisms (SNPs) of the *OPRM1* gene is rs1799971 (c.118A>G; p.Asn40Asp).[4] A study performed in European subjects on long-term treatment for chronic pain with different opioids, including tramadol, reported a higher frequency of adverse effects in wild-type subjects compared to individuals with the AG or GG genotype.[7] A study in Chinese population showed greater analgesic action of tramadol combined with paracetamol (acetaminophen) for the treatment of peripheral neuropathy in wild-type patients compared to carriers of polymorphic G allele.[8] Numerous studies focused on investigating the impact of this SNP on response to morphine treatment in different populations. Many of them confirmed the association between rs1799971 and pain relief or morphine dose requirements.[9-12] Furthermore, a haplotype of seven *OPRM1* SNPs, that included rs1799971 and another non-synonymous SNP, rs677830 (c.1231C>T, p.Gln411Ter) was associated with postoperative morphine response in Caucasians.[12]

OPRM1 gene expression may be regulated by non-coding RNAs such as microRNAs (miRNAs) that bind to target mRNAs molecules and prevent protein translation or promote mRNA degradation.[13,14] It was shown that several miRNAs can affect MOR expression, or lead to opioid dependence or tolerance.[15,16,17] Furthermore, opioids can regulate the expression of several miRNAs.[15]

miRNA-23b was the first identified miRNA molecule that regulates *OPRM1* expression[17], however miRNA-107 was shown to influence *OPRM1* expression as well.[15] Both miR-23b and miR107 were experimentally proven to reduce the expression level of *OPRM1* splice variants in mouse or human neuronal cell lines, human transfected embryonic kidney cell lines, or mouse animal models. The binding of these miRNAs to 3' UTR of *OPRM1* mRNAs prevented them from binding to ribosomes without altering the respective mRNAs levels. Furthermore, these studies also reported that long-term morphine treatment increased miRNAs expression.[15,17,18]

The aim of this study was to evaluate the association of *OPRM1* rs1799971 and rs677830, *MIR23B* 1011784, and *MIR107* rs2296616 polymorphisms with the severity of acute pain and the presence of adverse effects in the first four weeks after breast cancer surgery with axillary lymphadenectomy as well as with chronic and neuropathic pain at one year after surgery.

Patients and methods

Patients

Our study included breast cancer patients that participated in a prospective double-blinded randomized clinical trial at the Institute of Oncology Ljubljana from 2015 to 2018 (Trial KCT 04/2015-DORETAonko/si).[2,19] Written informed consent was obtained from all the patients before the inclusion in the clinical trial. The study was approved by the Institutional Review Board of the Institute of Oncology Ljubljana and by The National Medical Ethics Committee of the Republic of Slovenia (Approval number 32/03/15).

The main inclusion criteria was treatment with tramadol and paracetamol after breast cancer surgery with axillary lymphadenectomy, while exclusion criteria were: concomitant breast reconstruction with a tissue expander or free-flap, hypersensitivity to the drugs used in the study, male gender, pregnancy, high risk of anesthesia according to the criteria of the American Society of Anaesthesiology (ASA over 3), patient's age under 18 and over 70 years, severe liver or kidney disease, regular use of analgesics or antidepressants, history of opioid abuse or presence of psychiatric illness, such as dementia, schizophrenia, or manic depressive illness.

Before the surgery, all patients were examined according to the standard protocol of the Institute of Oncology Ljubljana. Data was collected about the body characteristics, associated diseases or allergies, the presence of pain, the use of other medications, and the anaesthesia risk was assessed according to the criteria of the American Society of Anaesthesiology.[20]

During surgery, patients received standard postoperative local analgesia. On the first postoperative day, all patients received 37.5/325 mg of tramadol with paracetamol every 8 h, 550 mg of naproxen sodium every 12 h, and 10 mg of metoclopramide every 8 h. From the second to the 29th postoperative day inclusive, tramadol and paracetamol dose depended on the group into which a patient was randomized at inclusion in the study. The group with lower analgesia received 37.5/325 mg of tramadol with paracetamol every 8 hours, while the group with higher analgesia received 75/650 mg every 8 hours. The tramadol and paracetamol doses for each patient were unblinded 15 months after the inclusion of the last patient. For four weeks, all patients also received 550 mg of naproxen sodium twice a day and 20 mg of pantoprazole once a day. In the case of severe pain despite taking tramadol/paracetamol and naproxen sodium, patients received 500 mg of metamizole up to 4 g per day.

In the first four weeks after surgery, patients recorded the severity of the acute pain in the area of the breast and shoulder using the standard visual analog scale (VAS) three times a day. Every day, patients recorded the consumption of medications and the frequency of shoulder exercises. Patients also recorded adverse effects and reported the collected data to the healthcare professionals every seven days when they came for the weekly checkups at the outpatients' clinic.

Before surgery, and again at the final follow-up examination at 12 to 15 months after the surgery, the patients filled in the standardized questionnaire of the Institute of Oncology on the presence of chronic pain and the DN4 questionnaire on the presence of neuropathic pain.

Methods

Bioinformatics analysis

First, we searched for potentially functional SNPs in the *OPRM1* gene by performing a literature search in PubMed (https://pubmed.ncbi.nlm.nih.gov/), Scholar (https://scholar.google.com/), and SNPedia (https://www.snpedia.com).[21] Their minor allele frequency (MAF) was obtained from the dbSNP database from The National Center for Biotechnology Information (NCBI) (https://www.ncbi.nlm.nih.gov/snp/) and linkage disequilibrium between polymorphisms was evaluated by the LDlink Tool (https://analysistools.cancer.gov/LDlink/?tab=ldmatrix).[22] We identified four missense or nonsense SNPs in the coding regions of the *OPRM1* gene with potential function in tramadol treatment outcome. Among them, only three met the MAF criteria of at least 5% in Caucasians: rs1799971, rs677830 and rs540825. As *OPRM1* rs540825 and rs677830 were in high linkage disequilibrium ($R^2 = 0.98$), only rs1799971 and rs677830 were included in our study.

Next, we searched PubMed, Scholar, and SNPedia for miRNAs with experimentally proven impact on MOR expression or activity. Moreover, we searched the following online databases that can predict the targets of miRNAs or report known associations between a specific gene and miRNA molecules: miRTarBase (http://mirtarbase.cuhk.edu.cn/php/index.php)[23], miRDB (http://www.mirdb.org)[24], and online tool miRNet (https://www.mirnet.ca)[25], to identify miRNAs that can regulate *OPRM1*. After narrowing down the list of potential miRNAs with impact on MOR function, we identified polymorphisms in genes coding for selected miRNAs with MAF of at least 5% in Caucasians. After the literature search for established roles of these polymorphisms in the expression of *OPRM1* or other genes we have selected two polymorphisms in two miRNA genes for the analysis.

In total, four polymorphisms in three genes were selected for inclusion in our study: *OPRM1* rs1799971 (NP_000905.3: p.Asn40Asp), *OPRM1* rs677830 (NP_001138758.1: p.Gln411Ter), *MIR23B* rs1011784 (NR_029664.1: n.525G>C), and *MIR107* rs2296616 (NR_029524.1: n.-382C>T).

Molecular analysis

DNA samples were isolated from peripheral blood samples using Qiagen FlexiGene Kit (Qiagen, Hilden, Germany) according to the manufacturer's instructions. Genotyping of selected polymorphisms was performed retrospectively using custom made validated competitive allele-specific polymerase chain reaction (KASP) assays following the instructions of the manufacturer (LGC Biosearch Technologies, UK). The analysis was repeated for 10% of samples and the results were concordant.

TABLE 1. Patients' clinical characteristics

		All subjects	Stronger postoperative analgesia with tramadol/ paracetamol	Weaker postoperative analgesia with tramadol/ paracetamol
Sample size		**N = 113**	**N = 55**	**N = 58**
Characteristic		**N (%)**	**N (%)**	**N (%)**
Age (years)	Median (25–75 %)	55 (48–63)	57 (49–64)	53,5 (47.8–61)
Weight (kg)	Median (25–75 %)	72 (63.5–82)	72 (64–82)	72 (63–82.3)
Body Mass Index (kg/m^2)	Median (25–75 %)	27.1 (23.4–31.0)	26.7 (23.0–30.8)	27.6 (23.5–31.2)
Smoking	No	87 (77.7) [1]	41 (75.9) [1]	46 (79.3)
	Yes	25 (22.3)	13 (24.1)	12 (20.7)
ASA score	1	22 (19.6) [1]	10 (18.2)	12 (21.1) [1]
	2	81 (72.3)	39 (70.9)	42 (73.7)
	3	9 (8.0)	6 (10.9)	3 (5.3)
Side of the operation	Left	62 (54.9)	30 (54.5)	32 (55.2)
	Right	50 (44.2)	24 (43.6)	26 (44.8)
	Bilateral	1 (0.9)	1 (1.8)	0 (0.0)
Tumor grade	1	4 (3.6) [1]	1 (1.9) [1]	3 (5.2)
	1–2	3 (2.7)	2 (3.7)	1 (1.7)
	2	39 (34.8)	17 (31.5)	22 (37.9)
	2–3	8 (7.1)	2 (3.7)	6 (10.3)
	3	58 (51.3)	32 (59.3)	26 (44.8)
VAS after 7 days	Median (25–75 %)	2 (1–3) [5]	1.3 (1–2) [3]	2 (1–3) [2]
VAS after 14 days	Median (25–75 %)	1.5 (0–2) [11]	1 (0–2) [9]	2 (1–2) [2]
VAS after 21 days	Median (25–75 %)	1 (0.4–2) [11]	1 (0–2) [9]	1 (1–2) [2]
VAS after 28 days	Median (25–75 %)	1 (0–2) [14]	1 (0–1) [10]	1 (1–2) [4]

ASA = American Society of Anaesthesiology; N = sample size; [n] = number of missing data; VAS = visual analog scale

Genotype frequencies, MAF, and Hardy-Weinberg equilibrium analysis (P_{HWE}) of investigated polymorphisms in all patients enrolled in our study are presented in Table 2.

Statistical analysis

Statistical analysis was performed using IBM SPSS v27.0 (IBM Corporation, Armonk, NY, USA). Continuous data were presented with median and interquartile range, while categorical data were presented with frequencies. For each polymorphism, a standard χ^2-test was used to evaluate whether genotype distribution followed Hardy-Weinberg equilibrium (HWE). Only the dominant genetic model was used in all statistical analyses for *OPRM1* polymorphisms due to the small numbers of carriers of two polymorphic alleles, while both dominant and additive genetic model was used in the analyses for polymorphisms in miRNA genes. The association of genetic factors with adverse effects, chronic and neuropathic pain was evaluated using binary logistic regression to obtain odds ratios (OR) with corresponding 95-% confidence intervals (95% CI). Fisher's exact test was used if there were no subjects within one of the groups. Mann-Whitney test was used to evaluate the association of polymorphisms with the severity of acute pain. All tests were two-sided and the level of statistical significance was set at 0.05.

Results

In total, 113 patients were included in the study, 55 (48.7%) received stronger postoperative analgesia and 58 (51.3%) received weaker postoperative analgesia. Patients' clinical characteristics are shown in Table 1. Among all patients, 14 (12.4%) patients discontinued tramadol treatment due to severe adverse events before the end of four weeks. Adverse

TABLE 2. The investigated polymorphism's characteristics and frequencies

Gene	SNP	Genotype	N (%)	PAF (%)	MAF HapMap CEU expected (%)	P_{HWE}
OPRM1	rs1799971	AA	84 (74.3)	14.2	15.6–16.7	0.570
		AG	26 (23.0)			
		GG	3 (2.7)			
	rs677830	CC	56 (49.6)	27.4	20.7	0.098
		CT	52 (46.0)			
		TT	5 (4.4)			
MIR23B	rs1011784*	CC	63 (56.3) [1]	26.8	23.3	0.153
		CG	38 (33.9)			
		GG	11 (9.8)			
MIR107	rs2296616*	GG	21 (18.6)	57.1	54.2–55.3	0.944
		GA	55 (48.7)			
		AA	37 (32.7)			

ASA = American Society of Anaesthesiology; CEU = Northern Europeans from Utah; HGVS = Human Genome Variation Society; HWE = Hardy-Weinberg equilibrium; N = sample size; PAF = polymorphic allele frequency; SNP = single nucleotide polymorphism; *KASP assays were designed on the reverse strand

events were therefore evaluated in 99 patients. The vast majority of the patients who discontinued tramadol were from the higher dose group (P = 0.004). A total of 101 patients completed the follow-up visit one year after surgery and were included in the analysis of genetic factors associated with the chronic and neuropathic pain.

Within the first four weeks of tramadol/paracetamol treatment, the severity of the self-perceived acute pain assessed with the VAS scale was not associated with the patient's genotypes for any of the investigated polymorphisms in none of the time points (all P > 0.05) (Supplementary Table 1).

Several patients experienced the side effects that could be related to tramadol treatment at least once within the first four weeks: 36 (36.7%) patients experienced nausea, 9 (9.1%) patients experienced vomiting, 35 (35.4%) patients experienced dizziness, and 48 (48.5%) patients experienced constipation.

TABLE 3. The impact of investigated polymorphisms on constipation anytime during the first four weeks of tramadol treatment (N = 99)

SNP	Genotype	Constipation anytime N (%)	OR (95% CI)	P	$OR\ (95\%\ CI)_{adj}$	P_{adj}
OPRM1 rs1799971	AA	30 (40)	Ref.		Ref.	
	AG+GG	18 (75)	4.5 (1.6–12.64)	**0.004**	4.31 (1.52–12.17)	**0.006**
OPRM1 rs677830	CC	24 (48)	Ref.		Ref.	
	CT+TT	24 (49)	1.04 (0.47–2.29)	0.922	0.98 (0.44–2.19)	0.964
MIR23B rs1011784	CC	29 (50)	Ref.		Ref.	
	CG	16 (50)	1 (0.42–2.37)	1.000	0.96 (0.4–2.31)	0.930
	GG	3 (37.5)	0.6 (0.13–2.75)	0.510	0.46 (0.1–2.23)	0.338
	CG+GG	19 (47.5)	0.9 (0.4–2.03)	0.808	0.84 (0.37–1.91)	0.676
MIR107 rs2296616	GG	11 (57.9)	Ref.		Ref.	
	GA	23 (48.9)	0.7 (0.24–2.04)	0.511	0.73 (0.25–2.16)	0.566
	AA	14 (42.4)	0.54 (0.17–1.68)	0.285	0.53 (0.17–1.67)	0.276
	GA+AA	37 (46.3)	0.63 (0.23–1.72)	0.364	0.64 (0.23–1.77)	0.386

adj = adjustment for tramadol dose; N = sample size; OR = odds ratio; SNP = single nucleotide polymorphism; 95% CI = 95% confidence interval

TABLE 4. The impact of investigated miRNA polymorphisms on nausea after 21 and 28 days of tramadol treatment (N = 99)

SNP	Genotype	Nausea 21 days N (%)	OR (95% CI)	P	Nausea 28 days N (%)	OR (95% CI)	P
MIR23B rs1011784	CC	9 (16.4)	Ref.		4 (7.5)	Ref.	
	CG	4 (12.9)	0.76 (0.21–2.7)	0.668	5 (16.1)	2.36 (0.58–9.54)	0.230
	GG	2 (25)	1.7 (0.3–9.83)	0.551	3 (37.5)	7.35 (1.27–42.6)	**0.026**
	CG+GG	6 (15.4)	0.93 (0.3–2.86)	0.898	8 (20.5)	3.16 (0.88–11.39)	0.078
MIR107 rs2296616	GG	6 (31.6)	Ref.		2 (10.5)	Ref.	
	GA	4 (8.9)	0.21 (0.05–0.87)	**0.031**	4 (8.7)	0.81 (0.14–4.84)	0.817
	AA	5 (16.7)	0.43 (0.11–1.69)	0.229	6 (21.4)	2.32 (0.41–12.96)	0.338
	GA+AA	9 (12)	0.30 (0.09–0.97)	**0.045**	10 (13.5)	1.33 (0.27–6.64)	0.730

N = sample size; OR = odds ratio; SNP = single nucleotide polymorphism; 95% CI = 95% confidence interval

Carriers of at least one polymorphic *OPRM1* rs1799971 allele had a higher risk of constipation in the first four weeks compared to carriers of two wild-type alleles (OR = 4.5, 95% CI = 1.6–12.64, P = 0.004). This association remained significant after the adjustment for the tramadol dose (OR = 4.31, 95% CI = 1.52–12.17, P = 0.006). None of the other polymorphisms were associated with the overall risk for constipation during the first month after surgery (Table 3). Data for constipation for each week separately are shown in Supplementary Table 2. Carriers of at least one polymorphic *OPRM1* rs677830 allele had a higher risk of constipation after 21 days of tramadol treatment when compared to carriers of two wild-type alleles (OR = 3.11, 95% CI = 1.08–8.89, P = 0.035).

The risk of nausea after 28 days of tramadol treatment was significantly higher in carriers of two polymorphic *MIR23B* rs1011784 alleles compared to carriers of two wild-type alleles (OR = 7.35, 95% CI = 1.27–42.6, P = 0.026). Heterozygotes for *MIR107* rs2296616 allele had a lower risk of nausea after the third week of tramadol treatment compared to carriers of two wild-type alleles (OR = 0.21, 95% CI = 0.05–0.87, P = 0.031). Similarly, carriers of at least one polymorphic *MIR107* rs2296616 had a lower risk of nausea after the third week of tramadol treatment compared to carriers of two wild-type alleles (OR = 0.30, 95% CI = 0.09–0.97, P = 0.045) (Table 4). None of the investigated polymorphisms were associated with the risk for nausea within the first two weeks after surgery (Supplementary Table 3).

One year after surgery 21 (20.8%) patients experienced chronic pain and 25 (24.8%) experienced neuropathic pain. In carriers of two polymorphic *MIR107* rs2296616 alleles, chronic pain was significantly more common compared to carriers of two wild-type alleles (35.3% compared to 0% of patients, P = 0.004). Carriers of at least one polymorphic *OPRM1* rs677830 allele experienced less neuropathic pain compared to carriers of two wild-type alleles (OR = 0.38, 95% CI = 0.15–0.99, P = 0.047), but the difference was no longer significant after adjustment for tramadol dose (P = 0.060). Carriers of at least one polymorphic *MIR23B* rs1011784 allele experienced more neuropathic pain compared to carriers of two wild-type alleles, but the difference was only significant after adjustment for tramadol dose (OR = 2.85, 95% CI = 1.07–7.59, P = 0.036). The other investigated miRNA polymorphism was not associated with the persistence of chronic or neuropathic pain (Table 5).

Discussion

Our study investigated the association of genetic variability of *OPRM1* and genes coding for miRNAs regulating *OPRM1* expression with acute and long-term pain management as well as adverse effects of tramadol treatment after surgical treatment of breast cancer and axillary lymphadenectomy.

None of the investigated polymorphisms were associated with the intensity of acute pain after the surgery. However, we confirmed the association between some of the investigated polymorphisms and the presence of adverse effects as well as chronic and neuropathic pain. In particular, *OPRM1* rs1799971 polymorphism increased the risk of constipation in the first month of tramadol treatment, while *OPRM1* rs677830 polymorphism

TABLE 5. The impact of investigated polymorphisms on chronic and neuropathic pain (N = 101)

SNP	Genotype	Chronic pain N (%)	OR (95% CI)	P	OR (95% CI)$_{adj}$	P$_{adj}$
OPRM1 rs1799971	AA	15 (20.3)	Ref.		Ref.	
	AG+GG	6 (22.2)	1.12 (0.39–3.28)	0.831	1.2 (0.4–3.57)	0.739
OPRM1 rs677830	CC	14 (27.5)	Ref.		Ref.	
	CT+TT	7 (14)	0.43 (0.16–1.18)	0.101	0.44 (0.16–1.21)	0.112
MIR23B rs1011784	CC	9 (15.3)	Ref.		Ref.	
	CG	10 (32.3)	2.65 (0.94–7.45)	0.065	2.85 (0.99–8.19)	0.052
	GG	2 (20)	1.39 (0.25–7.64)	0.706	1.68 (0.29–9.83)	0.563
	CG+GG	12 (29.3)	2.3 (0.86–6.11)	0.095	2.58 (0.94–7.1)	0.067
MIR107 rs2296616	GG	0 (0)	Ref.		Ref.	
	GA	9 (18.4)	/	0.099*		
	AA	12 (35.3)	/	**0.004***		
	GA+AA	21 (25.3)	/	**0.021***		
SNP	**Genotype**	**Neuropathic pain N (%)**	**OR (95% CI)**	**P**	**OR (95% CI)$_{adj}$**	**P$_{adj}$**
OPRM1 rs1799971	AA	19 (25.7)	Ref.		Ref.	
	AG+GG	6 (22.2)	0.83 (0.29–2.36)	0.722	0.94 (0.32–2.75)	0.915
OPRM1 rs677830	CC	17 (33.3)	Ref.		Ref.	
	CT+TT	8 (16)	0.38 (0.15–0.99)	**0.047**	0.4 (0.15–1.04)	0.060
MIR23B rs1011784	CC	11 (18.6)	Ref.		Ref.	
	CG	12 (38.7)	2.76 (1.04–7.31)	**0.042**	3.25 (1.17–9.02)	**0.023**
	GG	2 (20)	1.09 (0.2–5.87)	0.919	1.59 (0.27–9.24)	0.607
	CG+GG	14 (34.1)	2.26 (0.9–5.68)	0.082	2.85 (1.07–7.59)	**0.036**
MIR107 rs2296616	GG	3 (16.7)	Ref.		Ref.	
	GA	11 (22.4)	1.45 (0.35–5.93)	0.607	1.37 (0.33–5.69)	0.666
	AA	11 (32.4)	2.39 (0.57–10.02)	0.233	2.34 (0.55–9.97)	0.249
	GA+AA	22 (26.5)	1.8 (0.48–6.83)	0.386	1.73 (0.45–6.65)	0.424

adj = adjustment for tramadol dose, N = sample size, OR = odds ratio, SNP = single nucleotide polymorphism, 95% CI = 95% confidence interval; *calculated using Fisher's exact test

increased the risk of constipation in the third week of tramadol treatment. *OPRM1* rs677830 polymorphism also reduced the risk of neuropathic pain one year after the surgery. The presence of *MIR23B* rs1011784 polymorphism increased the risk of nausea in the fourth week of tramadol treatment and increased the risk of neuropathic pain one year after the surgery. Lastly, the presence of *MIR107* rs2296616 polymorphism reduced the risk of nausea in the third week of treatment and increased the risk of chronic pain one year after the surgery.

So far, many studies confirmed the impact of *OPRM1* rs1799971 polymorphism on pain perception, opioid response, the presence of adverse effects, and susceptibility to alcohol or drug dependence, but the majority of studies of *OPRM1* rs1799971 polymorphisms were conducted on Asian population. According to systematic review and metaanalysis, carriers of at least one polymorphic *OPRM1* rs1799971 allele have higher opioid dose requirements to manage postoperative pain.[26] However, after adjustment for different ethnic groups and different opioids, this effect remained significant only for the Asian population and in the group receiving morphine. In the Caucasian population, the association had not been confirmed. The different ethnic origin of patients is, according to the authors of the review, one of the

main reasons for mentioned differences in opioid response among different populations, since MAF for polymorphic *OPRM1* rs1799971 allele in the Caucasian population is lower compared to the Asian population, and thus limiting the recognition of the recessive effect of the polymorphism. Besides, it is possible that other gene variants with an impact on MOR activity, that are in linkage disequilibrium with *OPRM1* rs1799971 polymorphism, are the reason for differences in opioid response.[26] Other authors also state that ethnic origin is an important cause for conflicting research results on the impact of *OPRM1* rs1799971 polymorphism on subjects' response to opioid drugs.[4] According to the 1000Genome project, MAF in the Asian population is between 39 and 42%, while MAF in the European population is 16%.[27] In our group of patients, MAF for *OPRM1* rs1799971 was 14.2%, which coincides with the expected frequency for Europeans. Another study conducted on the Caucasian population, investigating the impact of *OPRM1* and *COMT* polymorphisms on postoperative acute and chronic pain could not confirm the impact of *OPRM1* rs1799971 polymorphism on any of these types of pain[28], which is consistent with the results of our study. The combination of tramadol and paracetamol was more effective for the treatment of neuropathic pain in wild-type homozygotes compared to carriers of *OPRM1* rs1799971 polymorphic allele in a group of the Asian patients with oxaliplatin-induced neuropathy.[8] Furthermore, wild-type homozygotes had lower opioid dose requirements for the treatment of chronic pain compared to carriers of *OPRM1* rs1799971 polymorphic allele in European patients.[29]

Adverse effects, especially nausea and gastrointestinal events, were more common in a group of people with wild-type genotype compared to the carriers of polymorphic *OPRM1* rs1799971 allele.[7,30] A possible reason for this could be a loss of the N-glycosylation site of MOR in the carriers of polymorphic allele[29], since the N-glycosylation site of MOR may be involved in the trafficking into the cell membrane, binding of ligands, and signal transduction.[31] On the other hand, *OPRM1* rs1799971 polymorphism could impact the expression levels of MOR directly and consequently reduce the risk of opioid toxicity.[29] Contrary to expectations, our results showed an increased risk of constipation in the carriers of the polymorphic *OPRM1* rs1799971 allele. Since the expression of MOR is tissue-specific, the impact on constipation cannot be explained by the central action of opioids. Instead, we should investigate the expression patterns and mechanisms of action of MOR on the periphery.

A study of the association between *OPRM1* rs677830 polymorphism and postoperative pain treatment with morphine in the Caucasian population showed no significant influence of polymorphism, although an impact of the haplotype of seven polymorphisms of the *OPRM1* gene, including rs1799971 and rs677830, on morphine requirement has been observed.[12] Due to the presence of a stop codon that leads to reduced expression of MOR caused by *OPRM1* rs677830 polymorphism[32], it was expected that greater severity of acute pain will be reported from the carriers of at least one polymorphic *OPRM1* rs677830 allele. As the greater severity of acute pain is one of the main risk factors for the presence of persistent pain[33], we expected increased risk of chronic or neuropathic pain in carriers of at least one polymorphic allele, yet our results showed no impact on severity of acute pain and even indicated on reduced risk of neuropathic pain in carriers of polymorphic rs677830 allele. A literature search showed no report on the impact of mentioned polymorphism on adverse effects after opioid pain treatment or the presence of chronic or neuropathic pain so far.

A study conducted on the mouse and human neuronal cells showed that long-term morphine treatment cannot influence the transcription of *OPRM1*. On the other hand, it can lead to increased miR-23b levels, which can bind to mRNA for MOR1 and thus prevent the translation of mRNA to the receptor, which causes a drug tolerance.[17,34] Tramadol and morphine have a similar molecular structure, thus there is a possibility that MOR expression may be affected by tramadol in the same way. An altered sequence of miR-23b, caused by *MIR23B* rs1011784 polymorphism, could change its target sequence and therefore prevent binding of miR-23b to mRNA for MOR1. In that case, receptor activity would remain unchanged, but we were unable to confirm these assumptions.

Similar to miR-23b, long-term morphine exposure led to up-regulated miR-107 levels, leading to decreased levels of MOR1A in human neuroblastoma cells and striatum of morphine-tolerant mouse.[15] It would be interesting to evaluate the possible impact of tramadol on miR-107 expression as well. In addition, even though *MIR107* rs2296616 polymorphism does not lead to decreased transcription of DNA to pre-miRNA, it could affect the processing of pre-miR-107 to mature transcript and consequently levels of miR-107.[35] As a result, it

could affect MOR expression, but to confirm this we would have to do the quantification of miR-107 and MOR levels.

Despite the confirmed association between polymorphisms in miRNA genes and tramadol treatment outcome, it is not sure that these miRNA acts through the altered activity of MOR. miR-23b played a crucial role in neuropathic pain relief in a mouse model after spinal cord injury. When a higher level of pain was present, decreased expression level of miR-23b was measured and therefore increased levels of its target gene *NOX4*, coding for NADPH oxidase 4, that contributes to reactive oxygen species formation. After infusion of ectopic miR-23b molecules, an expression level of NOX4 decreased, and the symptoms improved.[36] From the results of the mentioned study, we can conclude that miR-23b can influence the perception of pain through its influence on various genes, not only *OPRM1*.

Additionally, miR-107 paralogue miR-103 that differs in only one nucleotide in 3'-end, therefore regulating overlapping target molecules[15], including mRNA for MOR in mice and humans, was shown to be regulating pain perception in rats and was down-regulated in neuropathic animals. It is responsible for the altered expression level of three subunits of Cav1.2 L-type calcium channels that play a crucial role in the sensation in chronic neuropathic pain.[37] It is reasonable to assume that the miR-107 molecule could have the same effect. If polymorphism in *MIR107* alters the target sequence of a mentioned molecule, it would consequently lead to the same effect as downregulation of the miR-107, therefore increased neuropathic pain. Yet our results only suggested the impact of miR-107 on chronic pain perception.

Our study was one of the few studies inspecting the impact of polymorphisms of the *OPRM1* gene on the tramadol treatment outcome in Caucasians. Nevertheless, it has some limitations such as a relatively small sample size of the patients and that the genotyping analysis was performed retrospectively. Since only a few studies investigated the impact of miRNA on the expression and functionality of MOR, it was a challenge to narrow the selection of miRNA and potentially functional polymorphisms in genes coding for miRNA. Furthermore, we investigated the impact of polymorphisms on pain, which is always liable to subjective assessment, even though we used VAS and other standardized questionnaires to limit this impact. On the other hand, the advantage of our study was an ethnically homogenous group of patients, as well as the unified treatment and follow-up protocol of patients. Overall, it was a longitudinal, prospective, randomized double-blind clinical trial, where neither the healthcare professionals nor the patients knew the dose level of tramadol.

Conclusions

In this study, we observed for the first time to our knowledge, that the presence of *OPRM1* rs677830 polymorphism reduces the risk for the presence of neuropathic pain and increases the risk of constipation in response to tramadol pain treatment. Furthermore, we observed for the first time the association of investigated polymorphisms in miR-23b and miR-107 coding genes with tramadol treatment outcome. The results of our study are expanding the knowledge in the field of personalized medicine that could lead to improved pain management and reduced risk of adverse effects, therefore improving the quality of patient's life.[38]

Acknowledgments

This work was financially supported by the Slovenian Research Agency (ARRS Grants No. P1-0170 and P3-0289).

References

1. Subedi M, Bajaj S, Kumar MS, Yc M. An overview of tramadol and its usage in pain management and future perspective. *Biomed Pharmacother* 2019; **111:** 443-51. doi: 10.1016/j.biopha.2018.12.085
2. Besic N, Smrekar J, Strazisar B. Chronic adverse effects after an axillary lymphadenectomy in breast cancer patients after administering weaker and stronger postoperative analgesia: results of a prospective double-blind randomized study. *Breast Cancer Res Treat* 2020; **182:** 655-63. doi: 10.1007/s10549-020-05713-3
3. World Health Organisation. *Tramadol, update review report*. [Internet]. 2014. p. 1-39. [cited 2022 Aug 14]. Available at: http://www.who.int/medicines/areas/quality_safety/6_1_Update.pdf
4. Crist RC, Berrettini WH. Pharmacogenetics of OPRM1. *Pharmacol Biochem Behav* 2014; **123:** 25-33. doi: 10.1016/j.pbb.2013.10.018
5. Wang S. Historical review: opiate addiction and opioid receptors. *Cell Transplant* 2019; **28:** 233-8. doi: 10.1177/0963689718811060
6. Yoshida K, Nishizawa D, Ide S, Ichinohe T, Fukuda KI, Ikeda K. A pharmacogenetics approach to pain management. *Neuropsychopharmacol Rep* 2018; **38:** 2-8. doi: 10.1002/npr2.12003
7. Muriel J, Margarit C, Barrachina J, Ballester P, Flor A, Morales D, et al. Pharmacogenetics and prediction of adverse events in prescription opioid use disorder patients. *Basic Clin Pharmacol Toxicol* 2019; **124:** 439-48. doi: 10.1111/bcpt.13155
8. Liu YC, Wang WS. Human mu-opioid receptor gene A118G polymorphism predicts the efficacy of tramadol/acetaminophen combination tablets (ultracet) in oxaliplatin-induced painful neuropathy. *Cancer* 2012; **118:** 1718-25. doi: 10.1002/cncr.26430

9. Campa D, Gioia A, Tomei A, Poli P, Barale R. Association of ABCB1/MDR1 and OPRM1 gene polymorphisms with morphine pain relief. *Clin Pharmacol Ther* 2008; **83:** 559-66. doi: 10.1038/sj.clpt.6100385

10. Lötsch J, von Hentig N, Freynhagen R, Griessinger N, Zimmermann M, Doehring A, et al. Cross-sectional analysis of the influence of currently known pharmacogenetic modulators on opioid therapy in outpatient pain centers. *Pharmacogenet Genomics* 2009; **19:** 429-36. doi: 10.1097/fpc.0b013e32832b89da

11. Klepstad P, Rakvåg TT, Kaasa S, Holthe M, Dale O, Borchgrevink PC, et al. The 118 A > G polymorphism in the human mu-opioid receptor gene may increase morphine requirements in patients with pain caused by malignant disease. *Acta Anaesthesiol Scand* 2004; **48:** 1232-9. doi: 10.1111/j.1399-6576.2004.00517.x

12. De Gregori M, Diatchenko L, Ingelmo PM, Napolioni V, Klepstad P, Belfer I, et al. Human genetic variability contributes to postoperative morphine consumption. *J Pain* 2016; **17:** 628-36. doi: 10.1016/j.jpain.2016.02.003

13. Riffo-Campos ÁL, Riquelme I, Brebi-Mieville P. Tools for sequence-based miRNA target prediction: what to choose? *Int J Mol Sci* 2016; **17:** 1987. doi: 10.3390/ijms17121987

14. Xu W, San Lucas A, Wang Z, Liu Y. Identifying microRNA targets in different gene regions. *BMC Bioinformatics* 2014; **15:** S4. doi: 10.1186/1471-2105-15-S7-S4

15. Lu Z, Xu J, Xu M, Pasternak GW, Pan YX. Morphine regulates expression of μ-opioid receptor MOR-1A, an intron-retention carboxyl terminal splice variant of the μ-opioid receptor (OPRM1) gene via miR-103/miR-107. *Mol Pharmacol* 2014; **85:** 368-80. doi: 10.1124/mol.113.089292

16. Zheng H, Law PY, Loh HH. Non-coding RNAs regulating morphine function: with emphasis on the in vivo and in vitro functions of miR-190. *Front Genet* 2012; **3:** 113. doi: 10.3389/fgene.2012.00113

17. Wu Q, Law PY, Wei LN, Loh HH. Post-transcriptional regulation of mouse mu opioid receptor (MOR1) via its 3' untranslated region: a role for microRNA23b. *FASEB J* 2008; **22:** 4085-95. doi: 10.1096/fj.08-108175

18. Rodríguez RE. Morphine and microRNA activity: is there a relation with addiction? *Front Genet* 2012; **3:** 223. doi: 10.3389/fgene.2012.00223

19. Besic N, Smrekar J, Strazisar B. Acute pain and side effects after tramadol in breast cancer patients: results of a prospective double-blind randomized study. *Sci Rep* 2020; **10**: 18766. doi: 10.1038/s41598-020-75961-2

20. Fitz-Henry J. The ASA classification and peri-operative risk. *Ann R Coll Surg Engl* 2011; **93:** 185-7. doi: 10.1308/rcsann.2011.93.3.185a

21. Cariaso M, Lennon G. SNPedia: a wiki supporting personal genome annotation, interpretation and analysis. *Nucleic Acids Res* 2012; **40:** D1308-12. doi: 10.1093/nar/gkr798

22. Machiela MJ, Chanock SJ. LDlink: a web-based application for exploring population-specific haplotype structure and linking correlated alleles of possible functional variants. *Bioinformatics* 2015; **31:** 3555-7. doi: 10.1093/bioinformatics/btv402

23. Huang H-Y, Lin Y-C-D, Li J, Huang K-Y, Shrestha S, Hong H-C, et al. miRTarBase 2020: updates to the experimentally validated microRNA–target interaction database. *Nucleic Acids Research* 2020; **48:** D148-54. doi: 10.1093/nar/gkz896

24. Chen Y, Wang X. miRDB: an online database for prediction of functional microRNA targets. *Nucleic Acids Research* 2020; **48:** D127-31, doi: 10.1093/nar/gkz757

25. Chang L, Zhou G, Soufan O, Xia J. miRNet 2.0: network-based visual analytics for miRNA functional analysis and systems biology. *Nucleic Acids Research* 2020; **48:** W244-51. 10.1093/nar/gkaa467

26. Hwang IC, Park JY, Myung SK, Ahn HY, Fukuda K, Liao Q. OPRM1 A118G gene variant and postoperative opioid requirement: a systematic review and meta-analysis. *Anesthesiology* 2014; **121**: 825-34. doi: 10.1097/ALN.0000000000000405

27. National Library of Medicine (US), National Center for Biotechnology Information. db SNP: rs1799971. [cited 2022 Oct 30]. Available at: https://www.ncbi.nlm.nih.gov/snp/rs1799971

28. Matic M, de Hoogd S, de Wildt SN, Tibboel D, Knibbe CA, van Schaik RH. OPRM1 and COMT polymorphisms: implications on postoperative acute, chronic and experimental pain after cardiac surgery. *Pharmacogenomics* 2020; **21:** 181-93. doi: 10.2217/pgs-2019-0141

29. Muriel J, Margarit C, Planelles B, Serralta MJ, Puga C, Inda MD, et al. OPRM1 influence on and effectiveness of an individualized treatment plan for prescription opioid use disorder patients. *Ann N Y Acad Sci* 2018; **1425:** 82-93. doi: 10.1111/nyas.13735

30. The Pharmacogenomics Knowledge Base (PharmGKB). Variant annotations: rs1799971. [cited 2022 Oct 30]. Avalable at: https://www.pharmgkb.org/variant/PA166156991/variantAnnotation

31. Kroslak T, Laforge KS, Gianotti RJ, Ho A, Nielsen DA, Kreek MJ. The single nucleotide polymorphism A118G alters functional properties of the human mu opioid receptor. *J Neurochem* 2007; **103**: 77-87. doi: 10.1111/j.1471-4159.2007.04738.x

32. National Library of Medicine (US), National Center for Biotechnology Information. db SNP: rs677830. [cited 2022 Oct 30]. Available at: https://www.ncbi.nlm.nih.gov/snp/rs677830

33. Wang L, Guyatt GH, Kennedy SA, Romerosa B, Kwon HY, Kaushal A, et al. Predictors of persistent pain after breast cancer surgery: a systematic review and meta-analysis of observational studies. *CMAJ* 2016; **188:** E352-61. doi: 10.1503/cmaj.151276

34. Wu Q, Zhang L, Law PY, Na Wei LN, Loh HH. Long-term morphine treatment decreases the association of μ-opioid receptor (MOR1) mRNA with polysomes through miRNA23b. *Mol Pharmacol* 2009; **75:** 744-50. doi: 10.1124/mol.108.053462

35. Wang S, Lv C, Jin H, Xu M, Kang M, Chu H, et al. A common genetic variation in the promoter of miR-107 is associated with gastric adenocarcinoma susceptibility and survival. *Mutat Res* 2014; **769:** 35-41. doi: 10.1016/j.mrfmmm.2014.07.002

36. Im YB, Jee MK, Choi JI, Cho HT, Kwon OH, Kang SK. Molecular targeting of NOX4 for neuropathic pain after traumatic injury of the spinal cord. *Cell Death Dis* 2012; **3:** e426. doi: 10.1038/cddis.2012.168

37. Favereaux A, Thoumine O, Bouali-Benazzouz R, Roques V, Papon MA, Salam SA, et al. Bidirectional integrative regulation of Cav1.2 calcium channel by microRNA miR-103: role in pain. *EMBO J* 2011; **3018:** 3830-41. doi: 10.1038/emboj.2011.249

38. Stamer UM, Zhang L, Stüber F. Personalized therapy in pain management: where do we stand? *Pharmacogenomics* 2010; **11:** 843-64. doi: 10.2217/pgs.10.47

research article

Treatment of vulvar cancer recurrences with electrochemotherapy – a detailed analysis of possible causes for unsuccessful treatment

Gregor Vivod[1,2], Tanja Jesenko[2,3], Gorana Gasljevic[4], Nina Kovacevic[1,2,5], Masa Bosnjak[3,6], Gregor Sersa[3,7]; Sebastjan Merlo[1,2,8], Maja Cemazar[3,9]

[1] Department of Gynecological Oncology, Institute of Oncology Ljubljana, Ljubljana, Slovenia
[2] Medical Faculty Ljubljana, University of Ljubljana, Ljubljana, Slovenia
[3] Department of Experimental Oncology, Institute of Oncology Ljubljana, Ljubljana, Slovenia
[4] Department Pathology, Institute of Oncology Ljubljana, Ljubljana, Slovenia
[5] Faculty of Health Care Angela Boškin, Jesenice, Slovenia
[6] Faculty of Pharmacy, University of Ljubljana, Ljubljana, Slovenia
[7] Faculty of Health Sciences, University of Ljubljana, Ljubljana, Slovenia
[8] Medical Faculty, University of Maribor, Maribor, Slovenia
[9] Faculty of Health Sciences, University of Primorska, Izola, Slovenia

Radiol Oncol 2023; 57(1): 121-126.

Received 21 December 2022
Accepted 11 January 2023

Correspondence to: Assist. Prof. Sebastjan Merlo, M.D., Department of Gynecological Oncology, Institute of Oncology Ljubljana, Ljubljana, Slovenia. E-mail: smerlo@onko-i.si and Prof. Maja Čemažar, Ph.D., Department of Experimental Oncology, Institute of Oncology Ljubljana, Ljubljana, Slovenia. E-mail: mcemazar@onko-i.si

Disclosure: No potential conflicts of interest were disclosed.

Background. Electrochemotherapy has good local effectiveness in the treatment of vulvar cancer. Most studies have reported the safety and effectiveness of electrochemotherapy for palliative treatment of gynecological cancers and mostly vulvar squamous cell carcinoma. Some tumors, however, fail to respond to electrochemotherapy. The biological features/determinants for the nonresponsiveness are not determined yet.

Patient and methods. A recurrence of vulvar squamous cell carcinoma was treated by electrochemotherapy using intravenous administration of bleomycin. The treatment was performed by hexagonal electrodes according to standard operating procedures. We analyzed the factors that could determine nonresponsiveness to electrochemotherapy.

Results. Based on the presented case of nonresponsive vulvar recurrence to electrochemotherapy, we hypothesize that the vasculature of the tumors prior to treatment may predict the response to electrochemotherapy. The histological analysis showed minimal presence of blood vessels in the tumor. Thus, low perfusion may reduce drug delivery and lead to a lower response rate because of the minor antitumor effectiveness of vascular disruption. In this case, no immune response in the tumor was elicited by electrochemotherapy.

Conclusions. In this case, of nonresponsive vulvar recurrence treated by electrochemotherapy, we analyzed possible factors that could predict treatment failure. Based on histological analysis, low vascularization of the tumor was observed, which hampered drug delivery and distribution and resulted in no vascular disrupting action of electrochemotherapy. All these factors could contribute to ineffective treatment with electrochemotherapy.

Key words: electrochemotherapy; bleomycin; vulvar cancer; recurrence

Introduction

Vulvar cancer is the fourth most common gynecological cancer, with an incidence of 2.6 per 100,000 women per year.[1] The treatment of vulvar cancer usually involves a combination of surgery and radiotherapy. Systemic treatment is rarely used. Most often, surgery includes radical vulvectomy

and bilateral lymph groin node dissection or sentinel lymph node biopsy.[2] Radiotherapy can be used as adjuvant therapy after initial surgery or as part of primary therapy in locally advanced disease. Most recurrences of vulvar cancer occur locally near the surgical margins or in the contralateral lymph groin region. The therapeutic modalities used depend on the location, the extent of recurrence and previously used radiotherapy or concomitant chemoradiotherapy.[3] The emerging treatment modality for vulvar cancer recurrence is electrochemotherapy.

Literature review of electrochemotherapy

Electrochemotherapy is a local ablative therapy that uses the application of reversible electric pulses to the tumor to permeabilize the cell membrane, hence enabling the entry of cytotoxic drugs into the cells.[4] It is most commonly used for the treatment of superficial tumors such as melanoma, sarcoma, squamous cell carcinoma, basal cell carcinoma, skin metastases from breast cancer and others.[5,6] It can also be utilized for the treatment of deep-seated tumors such as primary hepatocellular carcinoma, colorectal cancer, unresectable colorectal liver metastases or pancreatic carcinoma.[7-12] It is conducted following standard operating procedures, and the method is now used in nearly 180 cancer centers around the world.[6]

Only a small number of papers describing the use of electrochemotherapy for the palliative treatment of gynecological cancers and mostly vulvar squamous cell carcinoma have been presented.[13,14] Safety and local efficacy after electrochemotherapy with bleomycin in locoregional cutaneous recurrences of vulvar carcinomas previously treated with chemotherapy, radiotherapy and surgery or unsuitable for standard treatments have been demonstrated.[15-19] The effectiveness of the clinical cases and studies is presented in Table 1. The success rate of such tumors is 80%, which is lower than the response rate of other skin tumors treated with electrochemotherapy.[13,16,18,20-22]

The biological predictors of unsuccessful treatment have already been reviewed.[5] The clinical predictive factors of the tumor response were identified to be the size of the lesions and previous treatment as well as the tumor type. However, the biology behind this process has still not been explored. Indicated were the intrinsic tumor sensitivity and tumor stroma, where the vascularization of the tumors might be the most important factor, in addition to the involvement of the immune response. The importance of the vasculature and vascular perfusion of tumors has already been shown to have an important role in the responsiveness of tumors to electrochemotherapy due to its role in drug delivery and tumor response due to the vascular disrupting action of electrochemotherapy.[23] However, its importance in the response in clinical cases has not yet been discussed. With the aim of better understanding the pathophysiology of possible causes for unsuccessful treatment with electrochemotherapy in vulvar cancer recurrences, we present a case report of a 75-year-old woman with vulvar cancer recurrence in whom treatment with electrochemotherapy was ineffective and analyzed the possible causes of failure of such a treatment.

A case of unresponsive tumor

A 75-year-old woman was diagnosed with recurrence of vulvar cancer in the clitoral region. At the age of 70, simple vulvectomy of the left labium major and sentinel node biopsy (SNB) were

TABLE 1. Review of studies evaluating electrochemotherapy in vulvar cancer

First author, year published	Included no. of patients	Average age	Histology	Response of vulvar cancer	
				OR	NR
Perrone, 2013[20]	8	84y	8 SCC	6/8 (75%)	2/8 (25%)
Perrone, 2015[21]	25	85y	25 SCC	20/25 (80%)	5/20 (20%)
Pellegrino, 2016[18]	10	68y	9 SCC 1 Paget's	6/10 (60%)	4/10 (40%)
Perrone, 2019[13]	55	79y	57 SCC 3 Paget's 1 melanoma	46/55 (84%)	9/55 (16%)
Corrado, 2020[16]	15	83y	14 SCC 1 CS	12/15 (80%)	3/15 (20%)

CS = carcinosarcoma; No = number; NR = no response; OR = objective response; SCC = squamous cell carcinoma; y = year(s)

performed because of vulvar squamous cell carcinoma. The sentinel inguinal nodes were negative, and the tumor was removed with free surgical margins. Five years after primary treatment, recurrence of vulvar squamous cell carcinoma in the clitoral region was diagnosed on regular follow up (Figure 1A). Inguinal and distal metastases were excluded after clinical assessment and imaging diagnostics. The patient was presented at the Interinstitutional Tumor Board, which decided that electrochemotherapy is a safe and viable treatment approach before eventual surgical treatment. The tumor board comprised medical oncologists, radiotherapists, and gynecological oncologists. The electrochemotherapy protocol was approved by the Institutional Medical Board and Slovenian National Ethical Committee (Number 0120-262/2021/3). Electrochemotherapy with bleomycin was performed according to the standard operating procedure.[6] The patient underwent regional anesthesia. Bleomycin was administered at a dose of 15000 IU/m^2 (Bleomycin medac, Medac GmbH, Germany). Eight minutes after intravenous administration of the drug, electric pulses were applied to the tumor in a way that covered all tumor nodule, including the safety margin of ~ 1 cm. Hexagonal geometry needle electrodes were used, and electric pulses were generated by Cliniporator (IGEA S.P.A., Italy). Altogether, 7 applications of electric pulses were delivered, and their delivery was verified on the screen of the generator (current > 1.5 A). The patient was discharged from the hospital the day after electrochemotherapy with no pain and no symptoms of any disturbance. At regular follow-ups one and two months after electrochemotherapy, we observed no clinical changes in the tumor (Figure 1B). Histologic analysis of repeated biopsy showed the presence of vulvar squamous cell carcinoma. Wide excision of the tumor was performed with free surgical margins. Eighteen months after vulvar cancer recurrence treatment, there were no visible signs of recurrence or progression of the disease.

Histological examination of the first excisional biopsy performed in 2016 showed well-differentiated squamous cell carcinoma arising in the background of differentiated vulvar intraepithelial neoplasm (VIN) (Figure 2A). The absence of high-risk HPV was proven by the negative immunohistochemical reaction to p16. Staining for p16 was negative in the invasive component as well as in precancerous lesions. Additionally, two sentinel lymph nodes were excised and found to be negative. The patient again underwent an excisional

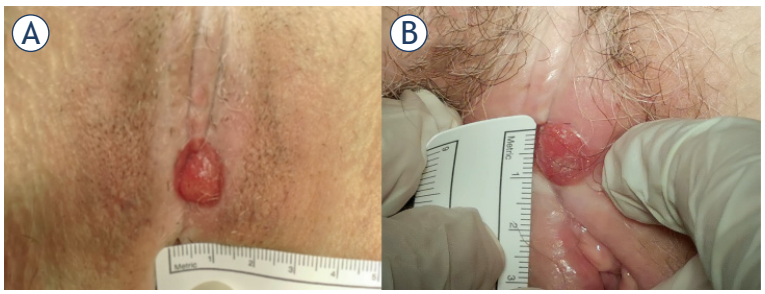

FIGURE 1. (A) Local recurrence of vulvar cancer. **(B)** No response to treatment two months after electrochemotherapy.

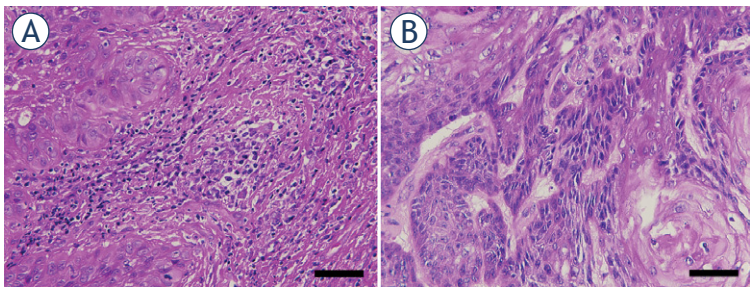

FIGURE 2. Hematoxylin and eosin stained sections of primary **(A)** and post-electrochemotherapy **(B)** biopsy. Scale bar represents 50 µm.

biopsy in 2018 showing differentiated VIN and in 2021 after electrochemotherapy. Histological examination of the post electrochemotherapy biopsy (Figure 2B) showed residual, well to moderately differentiated squamous cell carcinoma, measuring approximately 1.3 cm in the largest diameter, invading 0.4 cm in depth. There was no lymphovascular or perineural invasion present. In the surrounding parenchyma, there were some thrombosed and recanalized blood vessels. Additionally, an immunohistochemical panel consisting of anti CD3, CD20, CD68 PGM1, CD163, and ERG antibodies (markers for T and B lymphocytes, macrophages and blood vessels) was stained on the primary biopsy from 2016 and the post electrochemotherapy biopsy from 2021. Negligible number of cells on the primary as well as post-electrochemotherapy biopsy was stained positive for CD20, therefore we did not include these sections into analysis. For other markers, five different fields of immunohistochemically stained sections were captured with a DP72 CCD camera connected to a BX-51microscope (Olympus,Hamburg,Germany) and analyzed with AxioVision program (Carl Zeiss, Jena, Germany) to determine the number of positive regions per section. These were then averaged and t-test were performed to determine the sta-

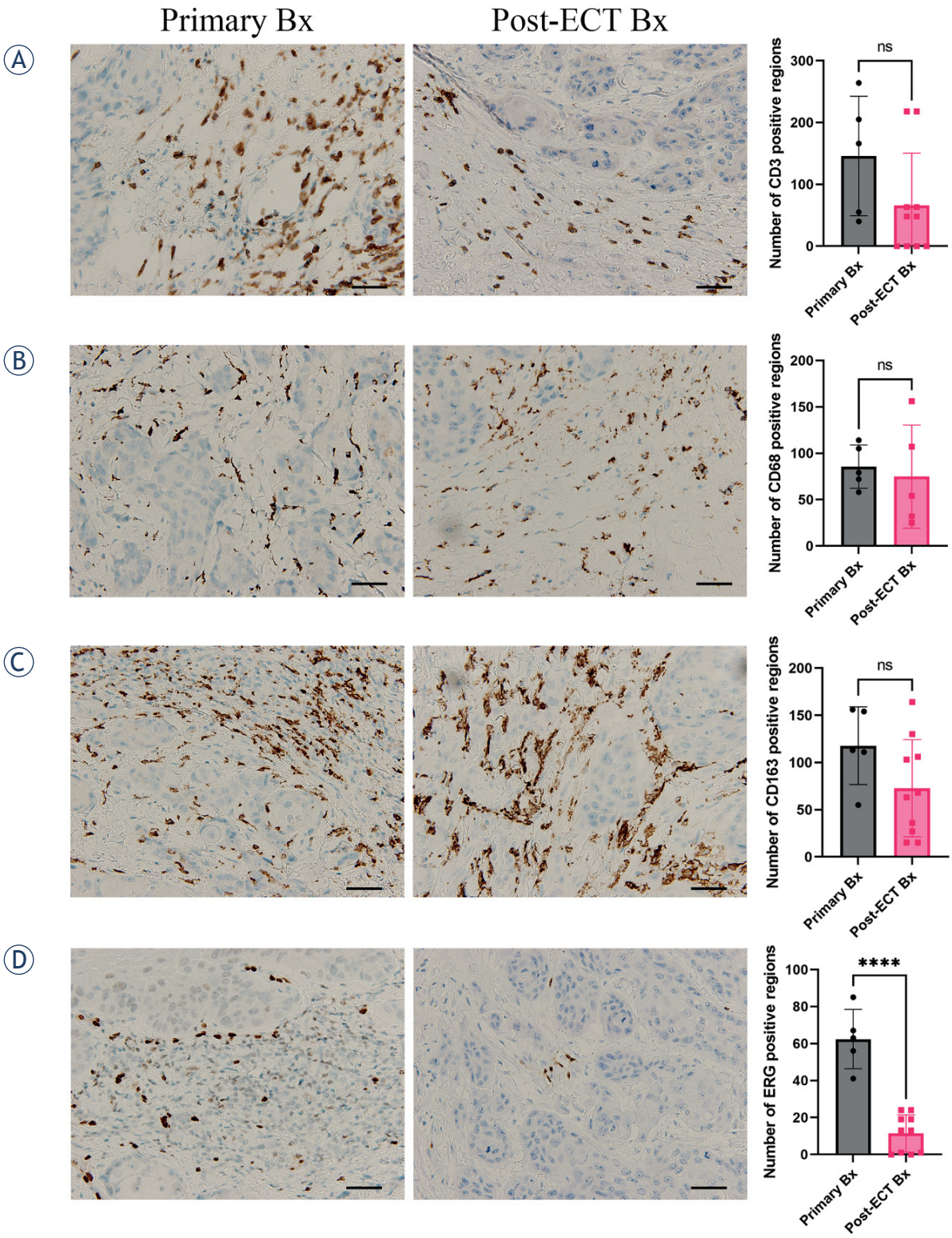

FIGURE 3. Immunohistologically stained sections for lymphocytes CD3 **(A)**, macrophages CD68 PMG1 **(B)** and CD163 **(C)**, and blood vessels ERG **(D)**, from primary biopsy (Primary Bx) and post-electrochemotherapy biopsy (post-ECT Bx) samples. Scale bar represents 50 µm. The number of positively stained regions ± standard error of the mean (SEM) is presented.

tistical significance using GraphPad Prism 9 (La Jolla, CA, USA). Detailed analysis showed significant differences only in the amount of small blood vessels being more numerous in the first pretreatment biopsy in comparison to the posttreatment biopsy (Figure 3). On the other hand, no difference was found in the number of CD3-positive lymphocytes or CD68-positive (pan macrophages marker) or CD163-positive M2 macrophages between the primary biopsy and post electrochemotherapy biopsy.

Discussion

Response to electrochemotherapy is evaluated in accordance with the modified Response Evaluation Criteria in Solid Tumors (RECIST).[24] Complete response for squamous cell carcinoma is observed in 63% of cases, and objective response is observed in 80%.[22] For vulvar cancer, stable disease and progression of disease are observed in 16 to 40% of cases.[14]

There are many clinical factors contributing to predicting the response to treatment with electrochemotherapy. The possibility for unsuccessful treatment increases with tumor size, and a marked drop in response rate occurs after chemotherapy or in previously irradiated tissue compared with nonirradiated tissue.[22]

There are, although, differences in the response rate of different tumor histologies; i.e., melanoma was the most resistant, and basal cell carcinoma was the most sensitive to electrochemotherapy.[22] The underlying biological factors have not yet been fully explored. As indicated in the review[5], stromal factors may play a significant role. Vasculature has already been shown in preclinical studies to play a crucial role in the perfusion of tumors and consequently in drug delivery to tumors.[23] To overcome this obstacle in less perfused tumors, intratumoral drug delivery could be an approach to overcome insufficient drug delivery. The vascular component and its destruction by electrochemotherapy can be a significant factor in the tumor response. The vascular disrupting effect of electrochemotherapy is based on the apoptosis of endothelial cells in small vessels, where the abrogation of the blood flow induces hypoxia in tumors and consequently indirect tumor cell death. The bigger vessels, as demonstrated in a study on electrochemotherapy of normal liver in pigs, are not affected by electrochemotherapy. The histological analysis was performed 2 and 7 days after electrochemotherapy and no thrombosis or other clinically significant damage to large blood vessels and bile ducts in the liver was observed.[25] Another biological factor may contribute to non-responsiveness, tumor cells in low oxygenated parts of tumors are more aggressive and are more resistant to therapy, leading also to higher recurrence rate of the treated tumors.[26,27] Therefore, in less responsive tumors, lower vascularity and slow perfusion could be predictors of a lower response rate. In two clinical studies on electrochemotherapy of liver tumors, one on colorectal liver metastases and the other on hepatocellular carcinoma, the effect of vascularity was evident.[7,8] A clear difference in the response rate of these two tumor types was observed, although the treatment was performed in the same way, even by the same team of experts. Based on the known tumor histology features, colorectal metastases are less perfused tumors than hepatocellular carcinoma. Based on this, it can be deduced that the vascular component is important factor contributing to the response of the tumors. Namely, the vasculature is important for drug delivery and distribution and the vascular disruptive component of electrochemotherapy.

Clinical cases of nonresponsive tumors to electrochemotherapy are lacking. This is the first detailed analyzed case of recurrent vulvar cancer that has not responded to electrochemotherapy. The analysis of the immune component of the tumor stroma showed no significant changes after electrochemotherapy, with lymphocytes present in the margin of the tumor, while macrophages were also distributed in the tumors; however, we can presume that their phenotype was M2, as there were no antitumor effects. In responsive tumors, at least some increase in immune cell infiltration would be expected since electrochemotherapy induces immunogenic cell death.[28,29] On the other hand, the vascularization of the treated lesion was minimal, which may indicate a poor response to electrochemotherapy due to the minimal delivery of bleomycin after intravenous administration to the tumor site, lack of distribution around the tumor and absence of vascular disrupting action of electrochemotherapy.

This case clearly indicates that we have to search for biological determinants of failure of electrochemotherapy. As already suggested, the explanations for the heterogeneity in tumor response may reside in the altered vasculature that occurs with tumor growth and the difference in cell susceptibility or aggressiveness in the hypoxic environment.[5]

In conclusion, we propose to analyze the tumor vasculature with pathohistological biopsy or ultrasound prior to electrochemotherapy. The investigation of tumor vasculature may allow us to predict the treatment response of vulvar cancer with electrochemotherapy, which will help to determine the best individual treatment option and may ultimately improve patient outcomes.

Acknowledgement

The authors acknowledge the financial support from the state budget by the Slovenian Research Agency, program no. P3-0003.

References

1. United States Cancer Statistics (USCS). U.S. Cancer Statistics Data Visualizations Tool. CDC, Centers for Disease Control and prevention. May 24, 2022. [cited 2022 Aug 19]. Available at: https://www.cdc.gov/cancer/uscs/dataviz/index.htm
2. Merlo S. Modern treatment of vulvar cancer. *Radiol Oncol* 2020; **54:** 371-6. doi: 10.2478/raon-2020-0053
3. Salom EM, Penalver M. Recurrent vulvar cancer. *Curr Treat Options Oncol* 2002; **3:** 143-53. doi: 10.1007/s11864-002-0060-x
4. Cemazar M, Sersa G. Recent advances in electrochemotherapy. *Bioelectricity* 2019; **1:** 204-13. doi: 10.1089/bioe.2019.0028
5. Sersa G, Ursic K, Cemazar M, Heller R, Bosnjak M, Campana LG. Biological factors of the tumour response to electrochemotherapy: review of the evidence and a research roadmap. *Eur J Surg Oncol* 2021; **47:** 1836-46. doi: 10.1016/j.ejso.2021.03.229
6. Gehl J, Sersa G, Matthiessen LW, Tobian M, Soden D, Occhini A, et al. Updated standard operating procedures for electrochemotherapy of cutaneous tumours and skin metastases. *Acta Oncol* 2018; **57:** 874-82. doi: 10.1080/0284186X.2018.1454602
7. Djokic M, Cemazar M, Bosnjak M, Dezman R, Badovinac D, Miklavcic D, et al. A prospective phase II study evaluating intraoperative electrochemotherapy of hepatocellular carcinoma. *Cancers* 2020; **12:** E3778. doi: 10.3390/cancers12123778
8. Edhemovic I, Brecelj E, Cemazar M, Boc N, Trotovsek B, Djokic M, et al. Intraoperative electrochemotherapy of colorectal liver metastases: a prospective phase II study. *Eur J Surg Oncol* 2020; **46:** 1628-33. doi: 10.1016/j.ejso.2020.04.037
9. Casadei R, Ricci C, Ingaldi C, Alberici L, Di Marco M, Guido A, et al. Intraoperative electrochemotherapy in locally advanced pancreatic cancer: indications, techniques and results-a single-center experience. *Updat Surg* 2020; **72:** 1089-96. doi: 10.1007/s13304-020-00782-x
10. Spallek H, Bischoff P, Zhou W, de Terlizzi F, Jakob F, Kovàcs A. Percutaneous electrochemotherapy in primary and secondary liver malignancies - local tumor control and impact on overall survival. *Radiol Oncol* 2022; **56:** 102-10. doi: 10.2478/raon-2022-0003
11. Schipilliti FM, Onorato M, Arrivi G, Panebianco M, Lerinò D, Milano A, et al. Electrochemotherapy for solid tumors: literature review and presentation of a novel endoscopic approach. *Radiol Oncol* 2022; **56:** 285-91. doi: 10.2478/raon-2022-0022
12. Bosnjak M, Jesenko T, Markelc B, Cerovsek A, Sersa G, Cemazar M. Sunitinib potentiates the cytotoxic effect of electrochemotherapy in pancreatic carcinoma cells. *Radiol Oncol* 2022; **56:** 164-72. doi: 10.2478/raon-2022-0009
13. Perrone AM, Galuppi A, Pirovano C, Borghese G, Covarelli P, De Terlizi F, et al. Palliative electrochemotherapy in vulvar carcinoma: preliminary results of the ELECHTRA (Electrochemotherapy Vulvar Cancer) multicenter study. *Cancers* 2019; **11:** E657. doi: 10.3390/cancers11050657
14. Tranoulis A, Georgiou D, Founta C, Mehra G, Sayasneh A, Nath R. Use of electrochemotherapy in women with vulvar cancer to improve quality-of-life in the palliative setting: a meta-analysis. *Int J Gynecol Cancer* 2020; **30:** 107-14. doi: 10.1136/ijgc-2019-000868
15. Merlo S, Vivod G, Bebar S, Bosnjak M, Cemazar M, Srsa G, et al. Literature review and our experience with bleomycin-based electrochemotherapy for cutaneous vulvar metastases from endometrial cancer. *Technol Cancer Res Treat* 2021; **20:** 15330338211010134. doi: 10.1177/15330338211010134
16. Corrado G, Cutillo G, Fragomeni SM, Bruno V, Tagliaferri L, Mancini E, et al. Palliative eletrochemotherapy in primary or recurrent vulvar cancer. *Int J Gynecol Cancer* 2020; **30:** 927-31. doi: 10.1136/ijgc-2019-001178
17. Perrone AM, Galuppi A, Borghese G, Corti B, Ferioli M, Della Gatta AN, et al. Electrochemotherapy pre-treatment in primary squamous vulvar cancer. Our preliminary experience. *J Surg Oncol* 2018; **117:** 1813-7. doi: 10.1002/jso.25072
18. Pellegrino A, Damiani GR, Mangioni C, Stripoli D, Loverro G, Cappello A, et al. Outcomes of bleomycin-based electrochemotherapy in patients with repeated loco-regional recurrences of vulvar cancer. *Acta Oncol* 2016; **55:** 619-24. doi: 10.3109/0284186X.2015.1117134
19. Vivod G, Kovacevic N, Čemažar M, et al. Electrochemotherapy as an alternative treatment option to pelvic exenteration for recurrent vulvar cancer of the perineum region. *Technol Cancer Res Treat* 2022; **21:** 15330338221116488. doi: 10.1177/15330338221116489
20. Perrone AM, Galuppi A, Cima S, Pozatti F, Arcelli A, Cortesi A, et al. Electrochemotherapy can be used as palliative treatment in patients with repeated loco-regional recurrence of squamous vulvar cancer: a preliminary study. *Gynecol Oncol* 2013; **130:** 550-3. doi: 10.1016/j.ygyno.2013.06.028
21. Perrone AM, Cima S, Pozzati F, Fraculli R, Cammelli S, Tesei M, et al. Palliative electro-chemotherapy in elderly patients with vulvar cancer: a phase II trial: Electro-chemotherapy in vulvar cancer. *J Surg Oncol* 2015; **112:** 529-32. doi: 10.1002/jso.24036
22. Clover AJP, de Terlizzi F, Bertino G, Curatolo O, Odili J, Campana LG, et al. Electrochemotherapy in the treatment of cutaneous malignancy: Outcomes and subgroup analysis from the cumulative results from the pan-European International Network for Sharing Practice in Electrochemotherapy database for 2482 lesions in 987 patients (2008-2019). *Eur J Cancer* 2020; **138:** 30-40. doi: 10.1016/j.ejca.2020.06.020
23. Groselj A, Kranjc S, Bosnjak M, Krzan M, Kosjek T, Prevc A, et al. Vascularization of the tumours affects the pharmacokinetics of bleomycin and the effectiveness of electrochemotherapy. *Basic Clin Pharmacol Toxicol* 2018; **123:** 247-56. doi: 10.1111/bcpt.13012
24. Eisenhauer EA, Therasse P, Bogaerts J, Schwartz LH, Sergent D, Ford R, et al. New response evaluation criteria in solid tumours: revised RECIST guideline (version 1.1). *Eur J Cancer* 2009; **45:** 228-47. doi: 10.1016/j.ejca.2008.10.026
25. Zmuc J, Gasljevic G, Sersa G, Edhemovic I, Boc N, Seliskar A, et al. Large liver blood vessels and bile ducts are not damaged by electrochemotherapy with bleomycin in pigs. *Sci Rep* 2019; **9:** 1-11. doi: 10.1038/s41598-019-40395-y
26. Wei J, Hu M, Du H. Improving cancer immunotherapy: exploring and targeting metabolism in hypoxia microenvironment. *Front Immunol* 2022; **13:** 845923. doi: 10.3389/fimmu.2022.845923
27. Tannock IF, Gordon Steel G. Cell proliferation, drug distribution and therapeutic effects in relation to the vascular system of solid tumours. *Br J Cancer* 2022 Dec 23. [Ahead of print]. doi: 10.1038/s41416-022-02109-6
28. Calvet CY, Mir LM. The promising alliance of anti-cancer electrochemotherapy with immunotherapy. *Cancer Metastasis Rev* 2016; **35:** 165-77. doi: 10.1007/s10555-016-9615-3
29. Ursic K, Kos S, Kamensek U, Cemazar M, Miceska S, Markelc B, et al. Potentiation of electrochemotherapy effectiveness by immunostimulation with IL-12 gene electrotransfer in mice is dependent on tumor immune status. *J Control Release* 2021; **332:** 623-35. doi: 10.1016/j.jconrel.2021.03.009

research article

CT-guided ^{125}I brachytherapy for hepatocellular carcinoma in high-risk locations after transarterial chemoembolization combined with microwave ablation: a propensity score-matched study

Zixiong Chen[1], Xiaobo Fu[1], Zhenkang Qiu[2], Maoyuan Mu[1], Weiwei Jiang[1], Guisong Wang[1], Zhihui Zhong[1], Han Qi[1], Fei Gao[1]

[1] Department of Minimally Invasive & Interventional Radiology, Sun Yat-sen University Cancer Center and Sun Yat-sen University State Key Laboratory of Oncology in South China, and Collaborative Innovation Center for Cancer Medicine, Guangzhou, Guangdong, China

[2] Interventional Medical Center, Affiliated Hospital of Qingdao University, Qingdao, Shandong, China

Radiol Oncol 2023; 57(1): 127-139.

Received 29 December 2022
Accepted 30 January 2023

Correspondence to: Han Qi, M.D., Ph.D., Department of Minimally Invasive & Interventional Radiology, Sun Yat-sen University Cancer Center and Sun Yat-sen University State Key Laboratory of Oncology in South China, and Collaborative Innovation Center for Cancer Medicine, 651 Dongfeng East Road, Guangzhou 510060, Guangdong Province, China. E-mail: qihan@sysucc.org.cn and Fei Gao, M.D., Ph.D., Department of Minimally Invasive & Interventional Radiology, Sun Yat-sen University Cancer Center and Sun Yat-sen University State Key Laboratory of Oncology in South China, and Collaborative Innovation Center for Cancer Medicine, 651 Dongfeng East Road, Guangzhou 510060, Guangdong Province, China. E-mail: gaof@sysucc.org.cn

Disclosure: No potential conflicts of interest were disclosed.

Zixiong Chen and Xiaobo Fu contributed equally to this work.

Background. This study aimed to evaluate the safety and efficacy of ^{125}I brachytherapy combined with transarterial chemoembolization (TACE) and microwave ablation (MWA) for unresectable hepatocellular carcinoma (HCC) in high-risk locations.

Patients and methods. After 1:2 propensity score matching (PSM), this retrospectively study analyzed 49 patients who underwent TACE +MWA+^{125}I brachytherapy (group A) and 98 patients who only received TACE +MWA (group B). The evaluated outcomes were progression-free survival (PFS), overall survival (OS), and treatment complications. Cox proportional hazards regression analysis survival was used to compare the two groups.

Results. The patients in group A showed a longer PFS than group B (7.9 *vs.* 3.3 months, P = 0.007). No significant differences were observed in median OS between the two groups (P = 0.928). The objective response rate (ORR), disease control rate of tumors in high-risk locations, and the ORR of intrahepatic tumors were 67.3%, 93.9%, and 51.0%, respectively, in group A, and 38.8%, 79.6% and 29.6%, respectively, in group B (P < 0.001, P = 0.025 and P = 0.011, respectively). TACE-MWA-^{125}I (HR = 0.479, P < 0.001) was a significant favorable prognostic factor that affected PFS. The present of portal vein tumor thrombosis was an independent prognostic factor for PFS (HR = 1.625, P = 0.040). The Barcelona clinic liver cancer (BCLC) stage (BCLC C *vs.* B) was an independent factor affecting OS (HR = 1.941, P = 0.038). The incidence of complications was similar between the two groups, except that the incidence of abdominal pain was reduced in the group A (P = 0.007).

Conclusions. TACE-MWA-^{125}I resulted in longer PFS and better tumor control than did TACE-MWA in patients with unresectable hepatocellular carcinoma in high-risk locations.

Key words: hepatocellular carcinoma; high-risk location; transarterial chemoembolization; microwave ablation; ^{125}I brachytherapy

Introduction

Hepatocellular carcinoma (HCC) ranks the third leading cause of cancer-related death worldwide.[1,2] Up to 60% of patients with HCC are diagnosed at the intermediate to the advanced stages and potentially curative treatments are unapplicable.[3,4] Previous studies have demonstrated the benefits of combination therapies in patients with unresectable HCC.[5-8] The combined treatments of transcatheter arterial chemoembolization (TACE) and thermal ablation could induce extensive tumor necrosis and result in a significant survival benefit.[5,9-14] Prior studies of combined therapies have primarily focused on the Barcelona clinic liver cancer (BCLC) 0/A stage patients as a radical treatment.[4] For unresectable HCCs, a meta-analysis demonstrated that microwave ablation (MWA) outperformed radiofrequency ablation (RFA) in large neoplasms.[15]

Tumor location is an important factor for the procedural success of ablative techniques and TACE. For thermal ablation, firstly, tumors close to vital structures may increase the risk of bleeding and injuring of the adjacent organs.[16] Secondly, the blood flow can dissipate the heat away from the ablated lesion due to the heat sink effect.[17] Lesions adjacent to large intrahepatic vessels, hepatic capsules, or extrahepatic organs may lead to insufficient ablation. MWA exhibited better tumor control than RFA for subcapsular HCC within the Milan criteria[18] and the small single periportal HCC.[19] However, most patients with intermediate-advanced HCC require a large ablation volume and more ablation time.[12] For TACE, adjacent to organs, or previous treatment was reported to promote the formation of extrahepatic collateral arteries, leading to incomplete embolization.[20] Overall, the efficacy of combined therapies and complications related to the high-risk locations still need to be carefully considered.

Brachytherapy with iodine-125 (^{125}I) seeds implantation has been accepted as a useful method to achieve local control with low complication rates in prostate cancer, HCC, and some other solid tumors.[21-24] In previous studies, the combination of ^{125}I and RFA, as well as ^{125}I and TACE was reported to be effective for the treatment of HCC in high-risk locations.[25-28] Thus, we have conducted this retrospective study to assess the efficacy, safety, and prognostic factors of computer tomography[3] guided ^{125}I brachytherapy combined with TACE and MWA for HCC in high-risk locations. To reduce the influence of confounding bias, propensity score matching (PSM) was performed to assess survival outcomes.[29]

Patients and methods

Patients

This retrospective study was approved by the institutional review board of Sun Yat-sen University Cancer Center that waived the need for written informed consent. The data of 1577 primary HCC patients who had received TACE plus MWA as first-line therapeutic options between February 2015 to March 2021 at our center were retrospectively identified. A total of 287 patients were identified by the following eligibility criteria: (a) Diagnosed with HCC according to the Guidelines of the European Association for the Study of the Liver or American Association for the Study of Liver Diseases[3,30]; (b) BCLC stage B or C patients who were not eligible for surgical resection or liver transplantation[4]; (c) presenting with HCC in high-risk locations; (d) TACE combined with sequential MWA was performed as the first-line therapy; (e) Patients had not previously undergone liver resection or liver transplantation. Totally 106 patients were excluded based on the following exclusion criteria: (a) HCC complicated with other malignancies; (b) MWA or ^{125}I brachytherapy was not used to treat the tumors in high-risk locations; (c) Incomplete preoperative and postoperative clinical and radiographic data; (d) Child-Pugh class C or D disease and Eastern Cooperative Oncology Group (ECOG) performance status≥2 (Figure 1).

Definition of high-risk locations

Referring to the previous studies[31,32], The high-risk locations were defined as: (1) Type 1: less than 5 mm from the large vessels (the first- or second-grade branches of the portal veins, hepatic veins, and bile ducts); (2) Type 2: less than 5mm from the hepatic capsule or extrahepatic organs (such as heart, thoracic/abdominal wall, diaphragm, gastric, intestinal, and gall bladder). If the tumor was closed to both structures, the nearest one was chosen to define a high-risk location.

TACE MWA treatment protocol

Before TACE-MWA treatment, all patients received a standardized pretreatment evaluation including history, laboratory, and imaging. All TACE and MWA were performed by five interventional

radiologists with experience of more than 5 years. For TACE, a selective 5-F catheter (Yashiro type; Terumo Corporation) was introduced, and hepatic arterial angiography was performed to identify the tumor-feeding arteries. Then the tumor-feeding arteries were super-selective catheterized with a 2.7-F microcatheter (Renegade Hi Flo; Boston Scientific Corporation). The embolization emulsion was a mixture of 50 mg/m^2 of lobaplatin (Hainan Changan International Pharmaceutical Co., Ltd.), 10–40 mg of pirarubicin (Shenzhen Main Luck Pharmaceuticals Inc.) diluted in iodized oil (Lipoid ultra-fluid, Guerbet). MWA was performed within two weeks after TACE. MWA was performed with a commercially available system (ECO-100; ECO Microwave Electronic Institute) under CT guidance. A suitable route for puncture and ablation was designed. According to the size, number and anatomic location of the tumors, physicians chose the number of needles, the power (40–80W), and corresponding time (5–20 min) of ablation as well as the adjustable position of needles to eliminate the residual tumor. All ablations were conducted under intravenous moderate sedation and local anesthesia.

^{125}I seed implantation protocol

After MWA, CT scanning was conducted immediately to assessed the ablation area and residual tumor adjacent to high-risk sites. Then, interstitial needles were inserted into the target zone under CT guidance. The number and distribution of particles were determined by the treatment planning system (TPS) (BT-RSI, Beijing Atom and High Technique Inc.) to achieve a satisfactory dose distribution. After finishing implantation, a repeated CT scan was performed to check for complications and transmitted to TPS for dose verification. A total of 493 ^{125}I seeds (Yunke Pharmaceutical Limited Liability Company) were implanted by three radiologists with at least 5 years' experience in 49 patients with an average of 12.1 ± 15.1 seeds per patient.

Follow-up protocol and study outcomes

In both groups, patients generally underwent contrast-enhanced CT or MRI 4–6 weeks postoperatively to evaluate initial tumor response. Patients were reviewed every 3 months during the first year and every 6 months thereafter. Repeated TACE, MWA, or ^{125}I seeds implantation was performed according to the location and proportion of residual tumor. Intrahepatic tumor response was graded according to the modified Response Evaluation Criteria in Solid Tumors (mRECIST) by two radiologists independently and discrepancies of assessment results was resolved by discussions.[33] Tumor response in the high-risk sites was assessed between baseline and best response according to a modified standard: the product of maximum perpendicular diameters of the tumors in the high-risk sites were calculated and compared to the initial value.[34] The primary study endpoint was progression-free survival (PFS). The secondary endpoints included overall survival (OS), objective response rate [ORR], disease control rate (DCR) and safety. PFS was calculated from the date of the first session of MWA or MWA-^{125}I for the tumor in high-risk site to the date of tumor progression, death, or last follow-up; OS was calculated from the same treatment to the date of death due to any cause or last follow-up. The ORR was defined as the sum of complete and partial response, whereas DCR was defined as ORR plus stable disease rate. The best overall response was categorized as the final response during the treatment. Adverse events were graded according to the Common Terminology Criteria for Adverse Events (Version 5.0).

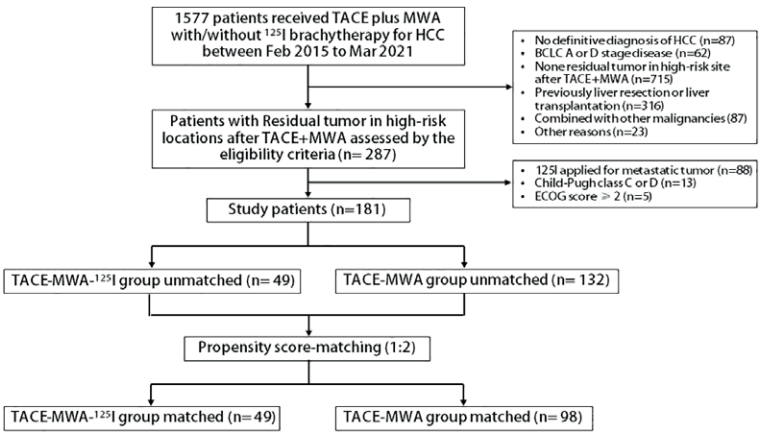

FIGURE 1. Patient flow diagram.

TACE = transarterial chemoembolization; MWA = microwave ablation

Propensity score matching analysis

To decrease the selection bias between the two groups, propensity scores were computed by logistic regression model for each patient using the following covariates: age (y), BCLC stage (B/C), maximum tumor diameter[35], tumor number (1-2/≥3), high-risk site (Type 1/2), portal vein tumor thrombosis (PVTT) (Y/N). A 1:2 propensity score

TABLE 1. Baseline patient characteristics before and after propensity score-matched

Parameter	Total (N = 181)	Total cohort		P value	PSM cohort		P value
		Group A	Group B		Group A	Group B	
		N = 49	N = 132		N = 49	N = 98	
Sex				0.37			0.751
Male	162 (89.5%)	46 (93.9%)	116 (87.9%)		46 (93.9%)	89 (90.8%)	
Female	19 (10.5%)	3 (6.12%)	16 (12.1%)		3 (6.12%)	9 (9.18%)	
Age (y)	56.0 [47.0;64.0]	56.0 [47.0;68.0]	55.5 [48.0;62.0]	0.425	56.0 [47.0;68.0]	55.0 [48.0;62.0]	0.468
BCLC				0.041*			1
B	72 (39.8%)	13 (26.5%)	59 (44.7%)		13 (26.5%)	26 (26.5%)	
C	109 (60.2%)	36 (73.5%)	73 (55.3%)		36 (73.5%)	72 (73.5%)	
Maximum tumor diameter, median (IQR), mm	29.0 [18.0;49.0]	36.0 [22.0;53.0]	26.5 [18.0;46.0]	0.039*	36.0 [22.0;53.0]	31.0 [18.0;57.8]	0.579
Tumor number				0.927			0.66
1-2	60 (33.1%)	17 (34.7%)	43 (32.6%)		17 (34.7%)	29 (29.6%)	
≥ 3	121 (66.9%)	32 (65.3%)	89 (67.4%)		32 (65.3%)	69 (70.4%)	
PVTT				0.202			1
None	108 (59.7%)	25 (51.0%)	83 (62.9%)		25 (51.0%)	49 (50.0%)	
Yes	73 (40.3%)	24 (49.0%)	49 (37.1%)		24 (49.0%)	49 (50.0%)	
Distant metastasis				0.171			0.953
None	109 (60.2%)	25 (51.0%)	84 (63.6%)		25 (51.0%)	52 (53.1%)	
Yes	72 (39.8%)	24 (49.0%)	48 (36.4%)		24 (49.0%)	46 (46.9%)	
High risk location				0.045*			0.76
1	98 (54.2%)	33 (67.3%)	65 (49.2%)		33 (67.3%)	62 (63.3%)	
2	83 (45.8%)	16 (32.7%)	67 (50.8%)		16 (32.7%)	36 (36.7%)	
TACE sessions	2.00 [1.00;3.00]	2.00 [1.00;2.00]	2.00 [1.00;3.00]	0.442	2.00 [1.00;2.00]	1.00 [1.00;3.00]	0.464
MWA sessions	1.00 [0.00;2.00]	1.00 [0.00;2.00]	1.00 [0.00;2.00]	0.162	1.00 [0.00;2.00]	1.00 [0.00;2.00]	0.31
Cause of liver disease:				0.09			0.181
Continued							
HCV/HBV	169 (93.4%)	43 (87.8%)	126 (95.5%)		43 (87.8%)	93 (94.9%)	
Other	12 (6.6%)	6 (12.2%)	6 (4.55%)		6 (12.2%)	5 (5.10%)	
ECOG score				0.189			0.669
0	126 (69.6%)	30 (61.2%)	96 (72.7%)		30 (61.2%)	65 (66.3%)	
1	55 (30.4%)	19 (38.8%)	36 (27.3%)		19 (38.8%)	33 (33.7%)	
Child-pugh score				0.563			0.386
A	82 (45.3%)	46 (93.9%)	36 (27.3%)		46 (93.9%)	86 (87.8%)	
B	99 (54.7%)	3 (6.12%)	96 (72.7%)		3 (6.12%)	12 (12.2%)	
AFP, ng/mL				0.811			0.576
< 400	125 (69.1%)	35 (71.4%)	90 (68.2%)		35 (71.4%)	64 (65.3%)	
≥ 400	56 (30.9%)	14 (28.6%)	42 (31.8%)		14 (28.6%)	34 (34.7%)	
PT (s)	12.2 [11.5;13.1]	12.0 [11.5;12.8]	12.3 [11.6;13.1]	0.167	12.0 [11.5;12.8]	12.2 [11.5;13.1]	0.331
ALB (g/L)	40.35 [36.2;43.9]	40.8 [36.7;44.1]	40.2 [36.0;43.9]	0.329	40.8 [36.7;44.1]	40.3 [36.1;44.1]	0.518
TBIL (mg/dL)	13.55 [10.1;19.32]	12.3 [8.73;18.2]	14.6 [10.4;20.4]	0.167	12.3 [8.73;18.2]	14.6 [10.1;20.2]	0.227

AFP = alpha fetoprotein; ALB = albumin; BCLC = Barcelona Clinic Liver Cancer; ECOG = Eastern Cooperative Oncology Group; IQR = interquartile range; MWA = microwave ablation; PSM = propensity score-matched; PVTT = portal vein tumor thrombosis; PT = prothrombin time; TACE = transcatheter arterial chemoembolization; TBIL = total bilirubin

SI conversion factors: To convert albumin to grams per liter, multiply by 10.0; to convert bilirubin to micromoles per liter, multiply by 17.104; and to convert a-fetoprotein to micrograms per liter, multiply by 1.0.

*p value ≤ 0.05 was considered to indicate statistical significance.

TABLE 2. Intrahepatic and high-risk locations tumor responses in the two groups after propensity score matching (PSM)

Tumor response	Intrahepatic Tumor			Tumor in high-risk locations		
	Group A (n = 49)	Group B (n = 98)	P value	Group A (n = 49)	Group B (n = 98)	P value
Complete response (CR)	4	6		5	9	
Partial response (PR)	21	23		28	29	
Stable disease (SD)	17	41		13	40	
Progressive disease (PD)	7	28		3	20	
Objective response rate (ORR) (%)	51.0%	29.6%	0.011†*	67.3%	38.8%	< 0.001†*
Disease control rate (DCR) (%)	85.7%	71.4%	0.055†	93.9%	79.6%	0.025†*

† Pearson χ2 test was used

* p value ≤ 0.05 was considered to indicate statistical significance.

matching was performed using the nearest-neighbor matching algorithm with an optimal caliper of 0.1 without replacement.

Statistical analysis

Categorical data are reported as counts and percentages, and continuous data are reported as medians or interquartile ranges. The Chi-square test or Fisher's exact test were used to analyze the differences in categorical variables, and the Mann-Whitney test was applied to the continuous variables. PFS and OS curves were constructed by the Kaplan-Meier (KM) method and estimated by the log-rank test. Univariate was used to analyze prognostic factors for PFS and OS using a Cox proportional hazards model. Significant univariate factors were included in the multivariate models. All tests were two-tailed and P values less than 0.05 were considered to indicate a statistically significant difference. All statistical analyses were performed by R statistical package version 3.4.1 (R Foundation for Statistical Computing, Vienna, Austria).

Results

Baseline characteristics

Between February 2015 to March 2021, a total of 181 HCC patients with tumors in high-risk locations were enrolled in this study. Before PSM, there were significant differences between the two groups in the BCLC stage, maximum tumor diameter, and high-risk location. In the TACE-MWA group (group B), 59 (44.7%) and 73 (55.3%) patients were classified as BCLC stage B and C, respectively. The maximum tumor diameter was significantly smaller than that in the TACE +MWA+^{125}I group (group A) (26.5 *vs.* 36.0 mm, P = 0.039). And there were more tumors in type 2 high-risk sites (50.8%) in group B. After PSM, all characteristics were balanced between the two groups. The baseline characteristics of the unweighted and weighted cohorts are outlined in Table 1. During the follow-up, patients in group A required significantly fewer sessions of TACE and MWA than that in group B (0.73 *vs.* 1.27, P = 0.048; 0.88 *vs.* 1.74, P = 0.013, respectively).

Local tumor control

In the PSM cohort, Tumor responses of the intrahepatic tumor and high-risk locations tumor are shown in Table 2. For the tumor in high-risk locations, the ORR and DCR were significantly higher in the group A (67.3% *vs.* 38.8%, P < 0.001; 93.9% *vs.* 79.6%, P = 0.025, respectively). Likewise, the ORR of intrahepatic tumors in the group A was higher than that in the TACE-MWA group (51.0% *vs.* 29.6%, P = 0.011). The DCR in the group A was slightly higher than that in the group B without a statistical difference (85.7% *vs.* 71.4%, P = 0.055)

Progression-free survival and overall survival

In the unweighted cohort, the median PFS time was 7.9 months (95CI%: 10.9–18.5 months) for patients in the group A, and 3.7 months in the group B (95CI%: 7.1–11.4 months) (P = 0.021) (Figure 2A). In the weighted cohort, the median follow-up for the study population was 16.2 months (range, 1.0–80.4 months). At the time of censoring, median

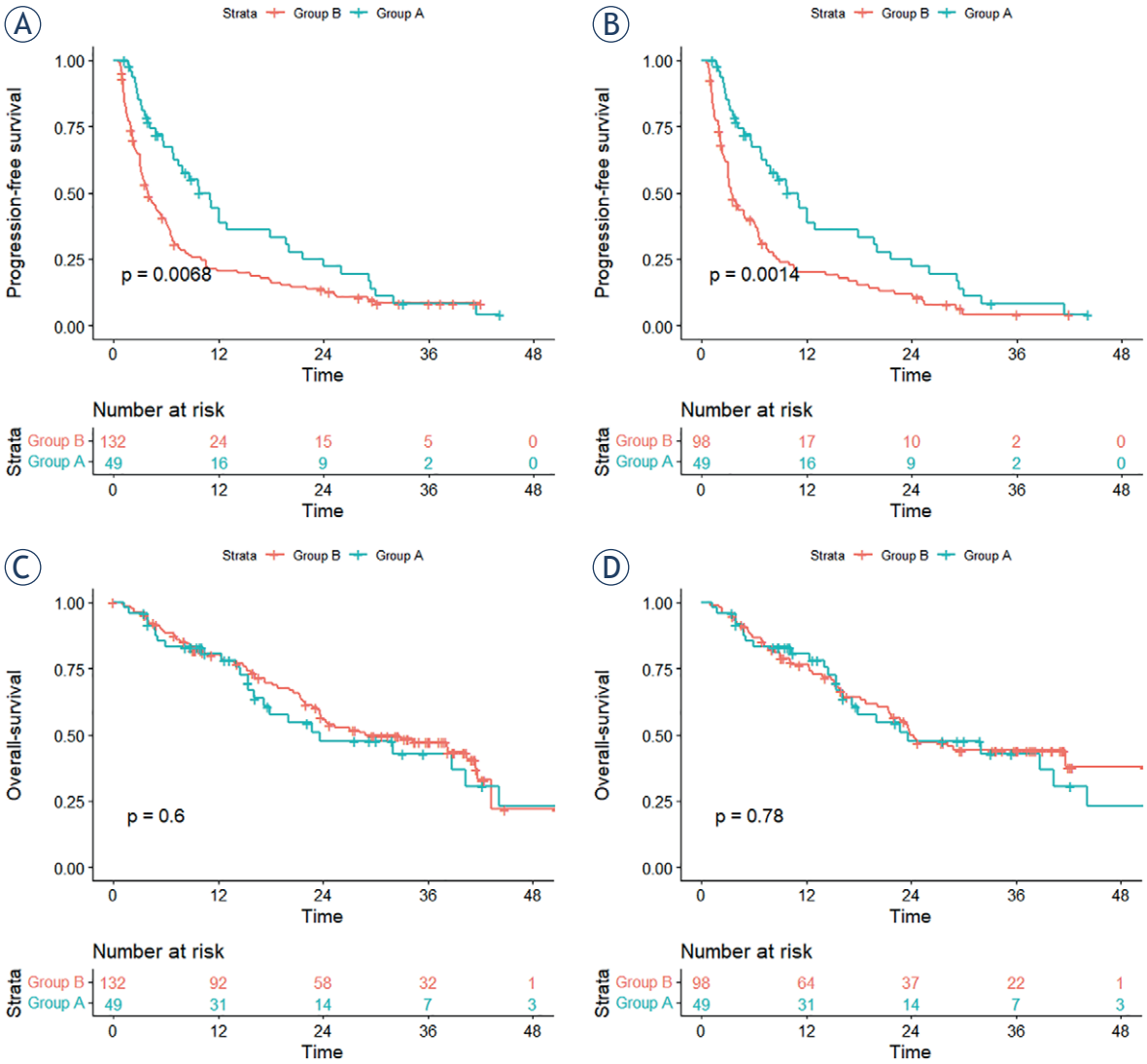

FIGURE 2. Kaplan-Meier curves comparing progression-free survival (PFS) and overall survival overall survival (OS) from different *groups.* **(A)** Cumulative PFS between the unmatched A and B groups. **(B)** Cumulative PFS between the matched A and B groups. **(C)** Cumulative OS between the unmatched A and B groups. **(D)** Cumulative OS between the matched A and B groups.

PFS was 3.3 months (95%CI: 6.1–10.5 months) for patients in the group B, and 7.9 months (95%CI: 10.9–18.5 months) in the group A with significant difference (P = 0.007) (Figure 2B). Univariable analyses revealed that treatment method, maximum tumor diameter, high-risk location, PVTT, and AFP level were significantly correlated with PFS (P < 0.1). Based on these results, the multivariate analysis including all factors of univariate analysis was performed and it identified treatment method and PVTT as independent prognostic factors for PFS (Table 3) (P < 0.05) (Figure 3A).

There was no significant difference in OS between the two groups in both unweighted and weighted cohorts (Figure 2C, 2D). As shown in Supplementary Table 1, univariate analysis results showed that sex, BCLC stage, high-risk location, PVTT, total bilirubin, and Child-pugh class were significant (P < 0.1). Because of assumed collinearity between PVTT and BCLC stage, as well as the total bilirubin and Child-pugh class, PVTT and total bilirubin were deleted from the multivariate model. Results of the multivariate analysis demonstrated that sex and BCLC stage were prognostic

TABLE 3. Multivariate analyses of predictors of progression-free survival after treatment

Risk Factor	Univariate			Multivariate		
	HR	95%CI	P value	HR	95%CI	P value
Sex						
Female	1					
Male	0.755	0.393–1.451	0.399			
Age (y)						
< 60	1					
≥ 60	1.093	0.761–1.569	0.63			
Maximum tumor diameter (mm)	1.006	1.000–1.013	0.071*	1.003	0.996-1.010	0.458
Tumor number						
1-2	1					
≥ 3	1.104	0.915–1.332	0.302			
BCLC stage						
B	1					
C	1.395	0.929–2.095	0.109			
High-risk location						
1	1					
2	0.665	0.456–0.970	0.034**	0.846	0.550-1.302	0.447
PVTT						
None						
Yes	1.615	1.124–2.319	0.010**	1.625	1.015-2.546	0.040**
Distant metastasis						
None						
Yes	1.099	0.772–1.565	0.602			
TACE sessions	1.062	0.964–1.170	0.223			
MWA sessions	1.006	0.914–1.106	0.905			
Treatment						
TACE+MWA	1					
TACE+MWA+ ^{125}I	0.527	0.357–0.778	0.002**	0.479	0.328-0.733	<0.001**
Cause of liver disease						
Other	1					
HBV/HCV	1.36	0.662–2.791	0.402			
ECOG score						
0	1					
1	1.269	0.876–1.837	0.208			
AFP						
≤ 400 ng/mL	1					
Continued						
> 400 ng/mL	1.72	1.164–2.542	0.006**	1.403	0.948-2.129	0.090
Prothrombin time (s)	0.942	0.827–1.073	0.367			
Albumin (g/L)	0.987	0.951–1.024	0.477			
Continued						
Total Bilirubin (μmol/L)	1.001	0.995–1.008	0.649			
Child-pugh class						
A	1					
B	1.216	0.654–2.263	0.536			

AFP = alpha fetoprotein; ALB = albumin; BCLC = Barcelona Clinic Liver Cancer; ECOG = Eastern Cooperative Oncology Group; HR = hazard ratio; MWA = microwave ablation; PVTT = portal vein tumor thrombosis; PT = prothrombin time; TACE = transarterial chemoembolization; TBIL = total bilirubin

*P value ≤ 0.1 in uni,variate were included in multivariate analysis, **P value ≤ 0.05 was considered to indicate statistical significance in multivariate analysis

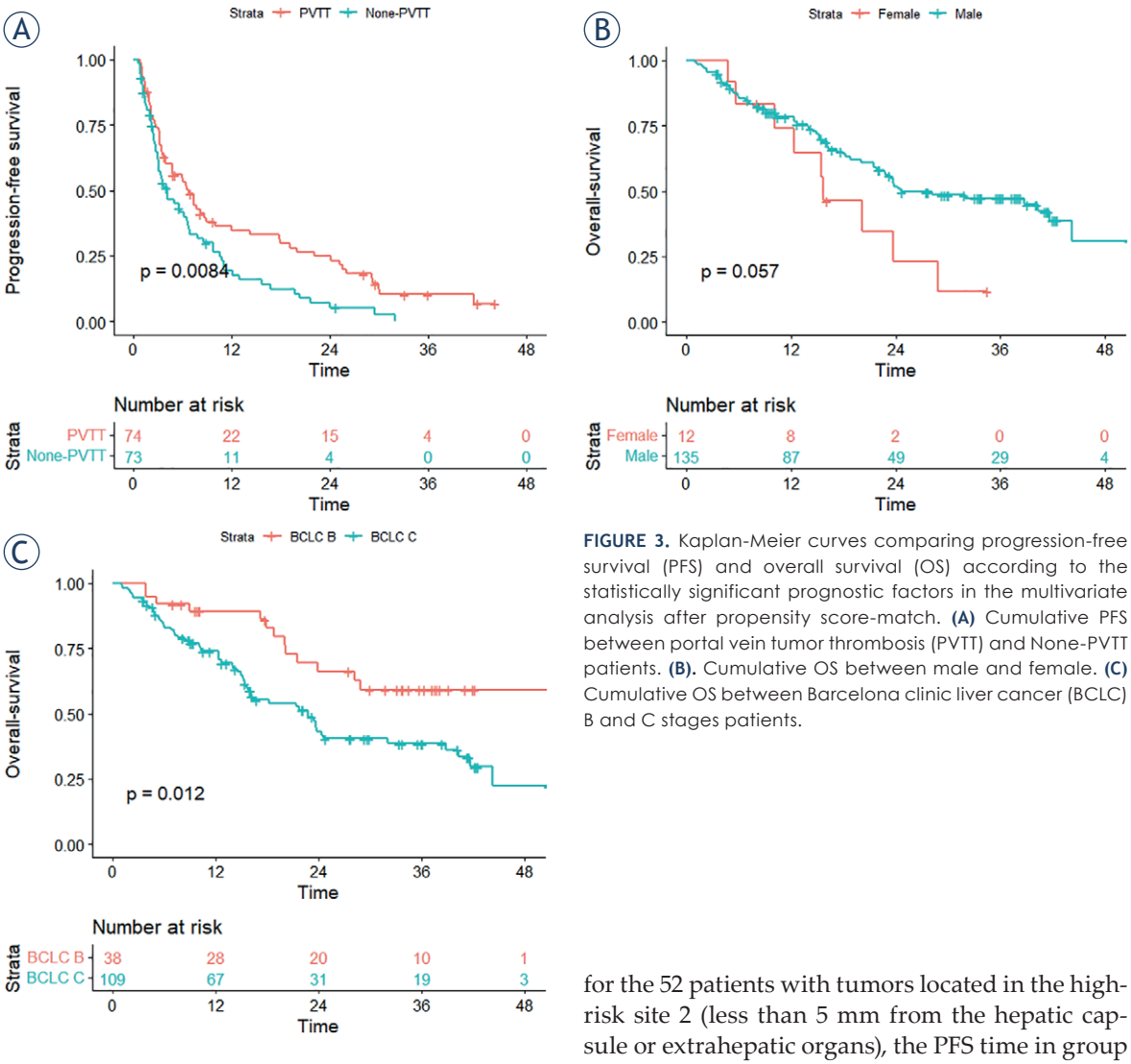

FIGURE 3. Kaplan-Meier curves comparing progression-free survival (PFS) and overall survival (OS) according to the statistically significant prognostic factors in the multivariate analysis after propensity score-match. **(A)** Cumulative PFS between portal vein tumor thrombosis (PVTT) and None-PVTT patients. **(B).** Cumulative OS between male and female. **(C)** Cumulative OS between Barcelona clinic liver cancer (BCLC) B and C stages patients.

factors for OS (P < 0.05). However, no significant difference was detected between male and female groups (P = 0.057). KM analysis showed significant difference between the BCLC B/C groups (P = 0.012) (Figure 3B, 3C).

Subgroup analyses

The patients without PVTT tended to get a better PFS in group B (P < 0.05) (Figure 4A). No significant difference was detected in group A between PVTT and non-PVTT patients (Figure 4B). Moreover, we observed significant differences between the two groups concerning PFS in both PVTT and non-PVTT patients (Figure 4C, 4D). For the 95 patients with tumors located in the high-risk site 1 (less than 5 mm from the large vessels or bile ducts), the mean PFS time was 11.4 months (95%CI: 7.9–14.9 months) in group A and 7.1 months (95%CI: 4.6–9.5 months) in group B (P < 0.01) (Figure 4e). Similarly, for the 52 patients with tumors located in the high-risk site 2 (less than 5 mm from the hepatic capsule or extrahepatic organs), the PFS time in group A was longer than that in group B (20.3 *vs.* 10.1 months, P = 0.02) (Figure 4F).

Complications

Adverse events for both treatment groups were listed in Table 4. During follow-up, there were no treatment-related deaths in either group and all of these patients were relieved after symptomatic treatment. The most common complication after treatment was abdominal pain in both groups and it was more frequent in the group B (P = 0.007). A slightly higher puncture hemorrhage rate was found in the group B (8.2%), without a significant difference (P = 0.274). One patient developed liver abscess after MWA in the group B. No displacement of ^{125}I seeds or radiation-induced liver disease was noted. All of these patients recovered with conservative treatment during the hospital stay.

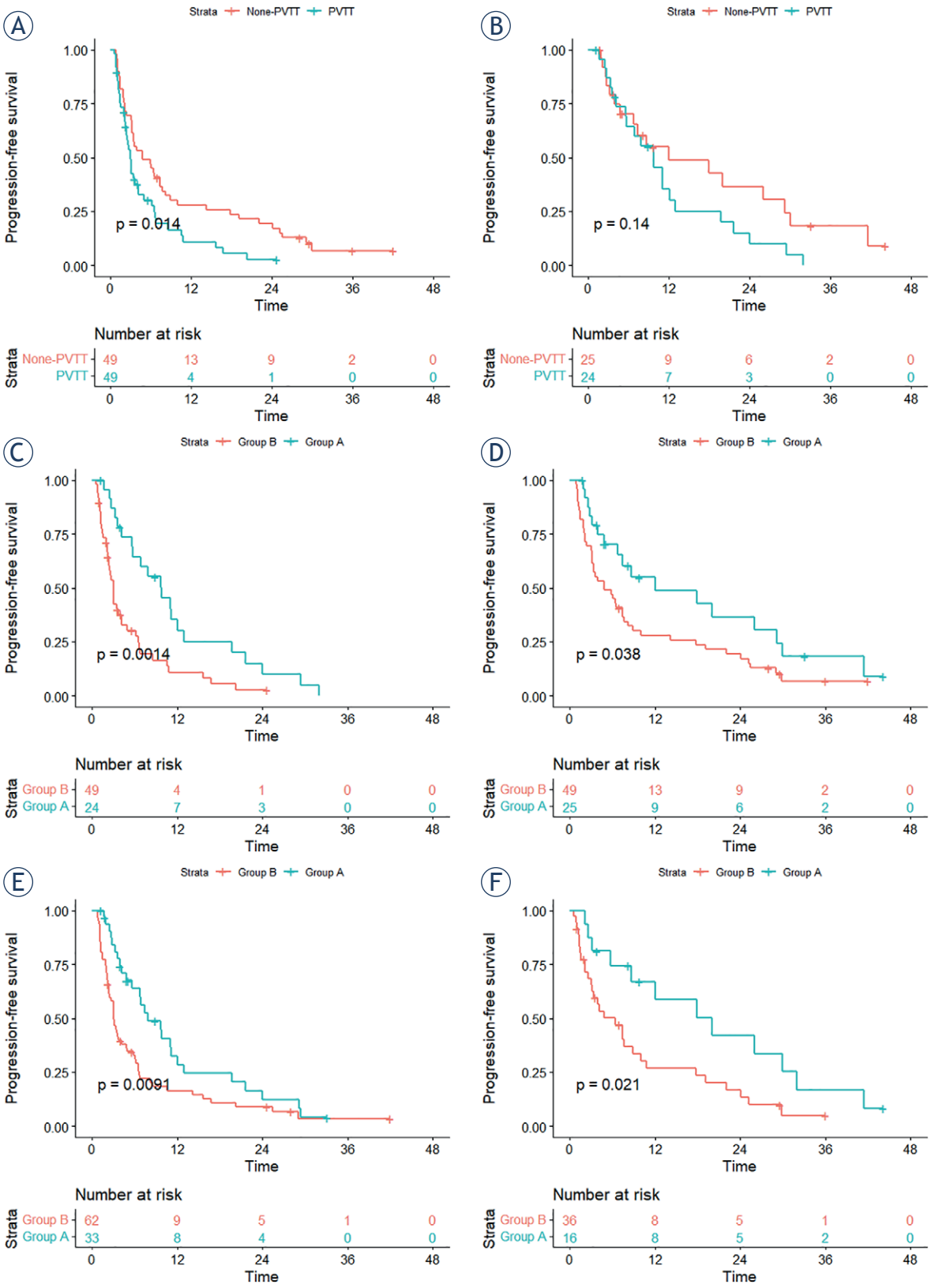

FIGURE 4. Subgroup analyses revealed by Kaplan-Meier curves comparing progression-free survival (PFS). **(A)** Comparison of the PFS between portal vein tumor thrombosis (PVTT) and None-PVTT patients in group B. **(B)** Comparison of the PFS between PVTT and None-PVTT patients in group A. **(C)** Comparison of the PFS between group A and B in patients with PVTT. **(D)** Comparison of the PFS between group A and B in none-PVTT patients. **(E)** Comparison of the PFS between group A and B in high-risk location 1. **(F)** Comparison of the PFS between group A and B in high-risk location 2.

TABLE 4. Complications related to the procedure

Adverse events	Group A (N = 49)	AE Grade			Group B (N = 98)	AE Grade			P value
		1	2	3-4		1	2	3-4	
Fever	3	3	0	0	3	9	10	0	0.608‡
Nausea	5	3	2	0	5	9	11	0	0.852†
Diarrhea	3	2	1	0	3	5	5	0	1‡
Pain required treatment	13	10	3	0	13	39	42	0	0.007†*
Liver abscess	0	0	0	0	0	1	1	0	1‡
Puncture hemorrhage	1	1	0	0	1	5	8	0	0.274‡
Displacement of seeds	0	0	0	0	0	-	-	-	-
RILD	0	0	0	0	0	-	-	-	-

AE = adverse effects; RILD = radiation-induced liver disease
† Pearson χ2 test was used; ‡ Continuity correction was used
*p value ≤ 0.05 was considered to indicate statistical significance.

Discussion

Our study aims to compare the effectiveness and safety outcome of TACE-MWA-^{125}I with that of TACE-MWA in patients with tumors in high-risk locations. As far as we know, this is the first study addressing this topic. A 1:2 PSM was performed to adjust for a variety of covariates and potential confounders between the two groups.

A peri-hepatic-vein location was a risk factor for the regional recurrence and a peri-portal-vein location was a potential high-risk factor for incomplete RFA in small HCCs.[36] Based on that, the results of our study demonstrated that treatment of high-risk sites contributes to the local tumor control and PFS. The initial intrahepatic tumor DCR and ORR of 85.7% and 51.0%, respectively, in the group A, are slightly higher than the published outcomes of Peng *et al.*, who demonstrated that patients with advanced recurrent HCC treated with TACE-RFA combined with sorafenib received DCR and ORR of 84% and 40.6%, respectively.[7] The PFS yielded higher PFS than the previously TACE-MWA outcomes of Zhang *et al.* (median PFS 4.2 months).[37] The results of the group B in our study were slightly lower than the results presented by Zhang *et al.* which may in part be due to the more advanced stage of HCC (BCLC C) patients included in our study. Considering the theoretical advantages of MWA in the controlling of high-risk site tumors, these results indicated the strengths of TACE-MWA-^{125}I in the local tumor control. As a low-dose rate brachytherapy, X-rays and γ-rays emit from the ^{125}I seeds could suppress the proliferation and induce apoptosis in tumor cells.[38,39] Numerous studies have demonstrated the value of brachytherapy in the locoregional therapies.[21-24] Furthermore, the synergy between brachytherapy and TACE-MWA might further increase the therapeutic effect.[40] The tumors neighboring large vessels, hepatic capsule, or extrahepatic organs, may increase the risk of sublethal temperatures and reversible injury due to the heat sink effect or the limited margin of ablation. But the increased vasodilation and vascular permeability due to the hyperthermia would improve the oxygenation in the high-risk tumors. The cytotoxicity of ^{125}I seeds radiation is primarily oxygen dependent, which might explain the synergy and survival advantages.[39]

The previous studies for the high-risk location related to the thermal ablation have mainly focused on the RFA in the small HCCs. The studies by Kang *et al.* suggested that neither perivascular nor subcapsular was a statistically significant risk factor for the OS outcomes.[41,42] Since the ^{125}I seeds implantation was only targeted at high-risk sites and extrahepatic metastasis occurred in 47.6% (n = 70) patients, there was no significant improvement in OS in our study. Interestingly, previous studies indicated that low dose irradiation could lead to an increase in CD8$^+$T cells and promote antitumor immunity.[43,44] These findings suggest that further combination of systemic therapies such as immunotherapy and targeted therapy may yield better survival benefit.

From the Cox proportional hazards regression, we found that the presence of PVTT was an independent prognostic factor for PFS (P = 0.04). In the

subgroup analysis, we were delighted to find that the difference in PFS between the PVTT and non-PVTT patients in the group B was not detected in the group A, and the group A achieved better PFS in both PVTT and non-PVTT patients. ^{125}I seeds implanted around the portal vein might play a role in the treatment of PVTT. Results from previous studies have indicated the effectiveness of ^{125}I seeds implantation for PVTT which might account for the survival advantages.[45,46] Besides, the TACE-MWA-^{125}I therapy achieved superior PFS in both high-risk location 1 and 2 patients, suggesting its potential broad applicability.

In terms of safety, there were no treatment-related deaths. Most adverse events were considered mild or moderate and easily managed. Our results showed that the combination with ^{125}I did not increase the risk of complications, and the incidence of abdominal pain and Puncture hemorrhage was decreased during the follow-up period ($P < 0.01$, $P = 0.274$). This might be due to the ^{125}I seeds implantation providing a sufficiently safe distance from the ablation boundary to the high-risk location, which could reduce the difficulty and risk of ablation. No brachytherapy-related complications such as displacement of seeds and radiation-induced liver disease were detected during follow-up. In addition, as a less invasive treatment, the utility of stereotactic body radiation therapy (SBRT) for the treatment of HCC in high-risk site compensates for the limitations of thermal ablation and the clinical effectiveness of SBRT plus TACE and AMW is worth further investigation.[47]

Nevertheless, there were several limitations in our study. Firstly, the present study was an observational, retrospective, single-center study with inherent limitations. Secondly, the classification of high-risk locations was more meticulous and comprehensive in previous studies.[36,41,42] Considering the complex anatomical structure of inter- to advance-stage HCC included in this study, the classification stratified by peri-hepatic-vein, peri-portal-vein and subcapsular was hard to apply. We can only make a relatively rough classification by referring to the studies by Teratani *et al.* and Lin *et al.*[31,32] Further comparison based on a more comprehensive classification might reveal more valuable information. Third, the gender distribution in this study was unbalanced (Female 12/147), suggesting the impact of sex on OS might be amplified in the multivariate analysis. larger prospective randomized clinical trials are still needed.

Conclusions

TACE-MWA-^{125}I resulted in longer PFS and better tumor control than did TACE-MWA in patients with unresectable hepatocellular carcinoma in high-risk locations.

References

1. Sung H, Ferlay J, Siegel RL, Laversanne M, Soerjomataram I, Jemal A, et al. Global Cancer Statistics 2020: GLOBOCAN estimates of incidence and mortality worldwide for 36 cancers in 185 countries. *CA Cancer J Clin* 2021; **71:** 209-49. doi: 10.3322/caac.21660
2. Hepatocellular carcinoma. *Nat Rev Dis Primers* 2021; **7:** 7. doi: 10.1038/s41572-021-00245-6
3. European Association for the Study of the Liver. Electronic address, European Association for the Study of the L. EASL Clinical Practice Guidelines: management of hepatocellular carcinoma. *J Hepatol* 2018; **69:** 182-236. doi: 10.1016/j.jhep.2018.03.019
4. Reig M, Forner A, Rimola J, Ferrer-Fabrega J, Burrel M, Garcia-Criado A, et al. BCLC strategy for prognosis prediction and treatment recommendation: the 2022 update. *J Hepatol* 2022; **76:** 681-93. doi: 10.1016/j.jhep.2021.11.018
5. Takuma Y, Takabatake H, Morimoto Y, Toshikuni N, Kayahara T, Makino Y, et al. Comparison of combined transcatheter arterial chemoembolization and radiofrequency ablation with surgical resection by using propensity score matching in patients with hepatocellular carcinoma within Milan criteria. *Radiology* 2013; **269:** 927-37. doi: 10.1148/radiol.13130387
6. Li W, Ni CF. Current status of the combination therapy of transarterial chemoembolization and local ablation for hepatocellular carcinoma. *Abdom Radiol* 2019; **44:** 2268-75. doi: 10.1007/s00261-019-01943-2
7. Peng Z, Chen S, Wei M, Lin M, Jiang C, Mei J, et al. Advanced recurrent hepatocellular carcinoma: treatment with sorafenib alone or in combination with transarterial chemoembolization and radiofrequency ablation. *Radiology* 2018; **287:** 705-14. doi: 10.1148/radiol.2018171541
8. Peng ZW, Zhang YJ, Liang HH, Lin XJ, Guo RP, Chen MS. Recurrent hepatocellular carcinoma treated with sequential transcatheter arterial chemoembolization and RF ablation versus RF ablation alone: a prospective randomized trial. *Radiology* 2012; **262:** 689-700. doi: 10.1148/radiol.11110637
9. Seki T, Tamai T, Nakagawa T, Imamura M, Nishimura A, Yamashiki N, et al. Combination therapy with transcatheter arterial chemoembolization and percutaneous microwave coagulation therapy for hepatocellular carcinoma. *Cancer* 2000; **89:** 1245-51. PMID: 11002219
10. Li Z, Jiao D, Han X, Si G, Li Y, Liu J, et al. Transcatheter arterial chemoembolization combined with simultaneous DynaCT-guided microwave ablation in the treatment of small hepatocellular carcinoma. *Cancer Imaging* 2020; **20:** 13. doi: 10.1186/s40644-020-0294-5
11. Zaitoun MMA, Elsayed SB, Zaitoun NA, Soliman RK, Elmokadem AH, Farag AA, et al. Combined therapy with conventional trans-arterial chemoembolization (cTACE) and microwave ablation (MWA) for hepatocellular carcinoma >3-<5 cm. *Int J Hyperthermia* 2021; **38:** 248-56. doi: 10.1080/02656736.2021.1887941
12. Liu C, Liang P, Liu F, Wang Y, Li X, Han Z, et al. MWA combined with TACE as a combined therapy for unresectable large-sized hepotocellular carcinoma. *Int J Hyperthermia* 2011; **27:** 654-62. doi: 10.3109/02656736.2011.605099
13. Shi F, Wu M, Lian SS, Mo ZQ, Gou Q, Xu RD, et al. Radiofrequency ablation following downstaging of hepatocellular carcinoma by using transarterial chemoembolization: Long-term outcomes. *Radiology* 2019; **293:** 707-15. doi: 10.1148/radiol.2019181991
14. Peng ZW, Zhang YJ, Chen MS, Xu L, Liang HH, Lin XJ, et al. Radiofrequency ablation with or without transcatheter arterial chemoembolization in the treatment of hepatocellular carcinoma: a prospective randomized trial. *J Clin Oncol* 2013; **31:** 426-32. doi: 10.1200/JCO.2012.42.9936

15. Facciorusso A, Di Maso M, Muscatiello N. Microwave ablation versus radiofrequency ablation for the treatment of hepatocellular carcinoma: a systematic review and meta-analysis. *Int J Hyperthermia* 2016; **32:** 339-44. doi: 10.3109/02656736.2015.1127434

16. Llovet JM, De Baere T, Kulik L, Haber PK, Greten TF, Meyer T, et al. Locoregional therapies in the era of molecular and immune treatments for hepatocellular carcinoma. *Nat Rev Gastroenterol Hepatol* 2021; **18:** 293-313. doi: 10.1038/s41575-020-00395-0

17. Lu DS, Raman SS, Vodopich DJ, Wang M, Sayre J, Lassman C. Effect of vessel size on creation of hepatic radiofrequency lesions in pigs: assessment of the "heat sink" effect. *AJR Am J Roentgenol* 2002; **178:** 47-51. doi: 10.2214/ajr.178.1.1780047

18. Zheng H, Liu K, Yang Y, Liu B, Zhao X, Chen Y, et al. Microwave ablation versus radiofrequency ablation for subcapsular hepatocellular carcinoma: a propensity score-matched study. *Eur Radiol* 2022. **32:** 4657-66. doi: 10.1007/s00330-022-08537-5

19. An C, Li WZ, Huang ZM, Yu XL, Han YZ, Liu FY, et al. Small single perivascular hepatocellular carcinoma: comparisons of radiofrequency ablation and microwave ablation by using propensity score analysis. *Eur Radiol* 2021; **31:** 4764-73. doi: 10.1007/s00330-020-07571-5

20. Li Q, Ao GK, Duan F, Wang ZJ, Yan JY, Wang MQ. Incidence and therapeutic frequency of extrahepatic collateral arteries in transcatheter arterial chemoembolization of hepatocellular carcinoma: experience from 182 patients with survival time more than 3 years. *Eur J Radiol* 2015; **84:** 2555-63. doi: 10.1016/j.ejrad.2015.10.006

21. Zelefsky MJ, Wallner KE, Ling CC, Raben A, Hollister T, Wolfe T, et al. Comparison of the 5-year outcome and morbidity of three-dimensional conformal radiotherapy versus transperineal permanent iodine-125 implantation for early-stage prostatic cancer. *J Clin Oncol* 1999; **17:** 517-22. doi: 10.1200/jco.1999.17.2.517

22. Chen K, Chen G, Wang H, Li H, Xiao J, Duan X, et al. Increased survival in hepatocellular carcinoma with iodine-125 implantation plus radiofrequency ablation: a prospective randomized controlled trial. *J Hepatol* 2014; **61:** 1304-11. doi: 10.1016/j.jhep.2014.07.026

23. Wang G, Zhang F, Yang B, Xue J, Peng S, Zhong Z, et al. Feasibility and clinical value of CT-guided (125)I brachytherapy for bilateral lung recurrences from colorectal carcinoma. *Radiology* 2016; **278:** 897-905. doi: 10.1148/radiol.2015150641

24. Ruge MI, Simon T, Suchorska B, Lehrke R, Hamisch C, Koerber F, et al. Stereotactic brachytherapy with iodine-125 seeds for the treatment of inoperable low-grade gliomas in children: long-term outcome. *J Clin Oncol* 2011; **29:** 4151-9. doi: 10.1200/JCO.2011.37.3381

25. Ren Y, Dong X, Chen L, Sun T, Alwalid O, Kan X, et al. Combined ultrasound and CT-guided Iodine-125 seeds implantation for treatment of residual hepatocellular carcinoma located at complex sites after transcatheter arterial chemoembolization. *Front Oncol* 2021; **11:** 582544. doi: 10.3389/fonc.2021.582544

26. Lin ZY, Chen J, Deng XF. Treatment of hepatocellular carcinoma adjacent to large blood vessels using 1.5T MRI-guided percutaneous radiofrequency ablation combined with iodine-125 radioactive seed implantation. *Eur J Radiol* 2012; **81:** 3079-83. doi: 10.1016/j.ejrad.2012.05.007

27. Gao FL, Wang Y, Huang XZ, Pan TF, Guo JH. I-125 seeds brachytherapy with transcatheter arterial chemoembolization for subcapsular hepatocellular carcinoma. *BMC Gastroenterol* 2022; **22:** 273. doi: 10.1186/s12876-022-02356-0

28. Wang W, Wang C, Shen J, Ren B, Yin Y, Yang J, et al. Integrated I-125 seed implantation combined with transarterial chemoembolization for treatment of hepatocellular carcinoma with main portal vein tumor thrombus. *Cardiovasc Intervent Radiol* 2021; **44:** 1570-8. doi: 10.1007/s00270-021-02887-1

29. Austin PC. The relative ability of different propensity score methods to balance measured covariates between treated and untreated subjects in observational studies. *Med Decis Making* 2009; **29:** 661-77. doi: 10.1177/0272989x09341755

30. Heimbach JK, Kulik LM, Finn RS, Sirlin CB, Abecassis MM, Roberts LR, et al. AASLD guidelines for the treatment of hepatocellular carcinoma. *Hepatology* 2018; **67:** 358-80. doi: 10.1002/hep.29086

31. Teratani T, Yoshida H, Shiina S, Obi S, Sato S, Tateishi R, et al. Radiofrequency ablation for hepatocellular carcinoma in so-called high-risk locations. *Hepatology* 2006; **43:** 1101-8. doi: 10.1002/hep.21164

32. Lin JW, Lin CC, Chen WT, Lin SM. Combining radiofrequency ablation and ethanol injection may achieve comparable long-term outcomes in larger hepatocellular carcinoma (3.1-4 cm) and in high-risk locations. *Kaohsiung J Med Sci* 2014; **30:** 396-401. doi: 10.1016/j.kjms.2014.04.006

33. Llovet JM, Lencioni R. mRECIST for HCC: Performance and novel refinements. *J Hepatol* 2020; **72:** 288-306. doi: 10.1016/j.jhep.2019.09.026

34. Hong D, Zhou Y, Wan X, Su H, Shao H. Brachytherapy with Iodine-125 seeds for treatment of portal vein-branch tumor thrombus in patients with hepatocellular carcinoma. *BMC Cancer* 2021; **21:** 1020. doi: 10.1186/s12885-021-08680-0

35. Vogel A, Cervantes A, Chau I, Daniele B, Llovet JM, Meyer T, et al. Hepatocellular carcinoma: ESMO Clinical Practice Guidelines for diagnosis, treatment and follow-up. *Ann Oncol* 2018; **29:** iv238-iv55. doi: 10.1093/annonc/mdy308

36. Chen J, Peng K, Hu D, Shen J, Zhou Z, Xu L, et al. Tumor location influences oncologic outcomes of hepatocellular carcinoma patients undergoing radiofrequency ablation. *Cancers* 2018; **10**. 501. doi: 10.3390/cancers10100378

37. Zhang TQ, Huang ZM, Shen JX, Chen GQ, Shen LJ, Ai F, et al. Safety and effectiveness of multi-antenna microwave ablation-oriented combined therapy for large hepatocellular carcinoma. *Therap Adv Gastroenterol* 2019; **12:** 1756284819862966. doi: 10.1177/1756284819862966

38. DeWeese TL, Shipman JM, Dillehay LE, Nelson WG. Sensitivity of human prostatic carcinoma cell lines to low dose rate radiation exposure. *J Urol* 1998; **159:** 591-8. doi: 10.1016/s0022-5347(01)63990-9

39. Koritzinsky M, Wouters BG, Amellem O, Pettersen EO. Cell cycle progression and radiation survival following prolonged hypoxia and re-oxygenation. *Int J Radiat Biol* 2001; **77:** 319-28. doi: 10.1080/09553000010019278

40. Grieco CA, Simon CJ, Mayo-Smith WW, DiPetrillo TA, Ready NE, Dupuy DE. Percutaneous image-guided thermal ablation and radiation therapy: outcomes of combined treatment for 41 patients with inoperable stage I/II non-small-cell lung cancer. *J Vasc Interv Radiol* 2006; **17:** 1117-24. doi: 10.1097/01.Rvi.0000228373.58498.6e

41. Kang TW, Lim HK, Lee MW, Kim YS, Choi D, Rhim H. Perivascular versus nonperivascular small HCC treated with percutaneous RF ablation: retrospective comparison of long-term therapeutic outcomes. *Radiology* 2014; **270:** 888-99. doi: 10.1148/radiol.13130753

42. Kang TW, Lim HK, Lee MW, Kim YS, Rhim H, Lee WJ, et al. Long-term therapeutic outcomes of radiofrequency ablation for subcapsular versus non-subcapsular hepatocellular carcinoma: a propensity score matched study. *Radiology* 2016; **280:** 300-12. doi: 10.1148/radiol.2016151243

43. Formenti SC, Demaria S. Systemic effects of local radiotherapy. *Lancet Oncol* 2009; **10:** 718-26. doi: 10.1016/s1470-2045(09)70082-8

44. De Palma M, Coukos G, Hanahan D. A new twist on radiation oncology: low-dose irradiation elicits immunostimulatory macrophages that unlock barriers to tumor immunotherapy. *Cancer Cell* 2013; **24:** 559-61. doi: 10.1016/j.ccr.2013.10.019

45. Hu HT, Luo JP, Cao GS, Li Z, Jiang M, Guo CY, et al. Hepatocellular carcinoma with portal vein tumor thrombus treated with transarterial chemoembolization and sorafenib vs. (125)Iodine implantation. *Front Oncol* 2021; **11:** 806907. doi: 10.3389/fonc.2021.806907

46. Yang M, Fang Z, Yan Z, Luo J, Liu L, Zhang W, et al. Transarterial chemoembolisation (TACE) combined with endovascular implantation of an iodine-125 seed strand for the treatment of hepatocellular carcinoma with portal vein tumour thrombosis versus TACE alone: a two-arm, randomised clinical trial. *J Cancer Res Clin Oncol* 2014; **140:** 211-9. doi: 10.1007/s00432-013-1568-0

47. Lee J, Shin IS, Yoon WS, Koom WS, Rim CH. Comparisons between radiofrequency ablation and stereotactic body radiotherapy for liver malignancies: meta-analyses and a systematic review. *Radiother Oncol* 2020; **145:** 63-70. doi: 10.1016/j.radonc.2019.12.004

erratum

Similar complication rates for irreversible electroporation and thermal ablation in patients with hepatocellular tumors

Niklas Verloh[1], Isabel Jensch[1], Lukas Lürken[1], Michael Haimerl[1], Marco Dollinger[1], Philipp Renner[2], Philipp Wiggermann[3], Jens Martin Werner[4], Florian Zeman[5], Christian Stroszczynski[1], Lukas Philipp Beyer[1]

[1] Department of Radiology, University Hospital Regensburg, Germany
[2] Department of Surgery, Robert-Bosch-Hospital, Stuttgart, Germany
[3] Department of Radiology, Hospital Braunschweig, Germany
[4] Department of Surgery, University Hospital Regensburg, Regensburg, Germany
[5] Center for Clinical Trials, University Hospital Regensburg, Regensburg, Germany

Radiol Oncol 2019; 53(1): 116-122.

Received 2 November 2018
Accepted 22 January 2019

Correspondence to: Lukas Philipp Beyer, M.D., Department of Radiology, University Hospital Regensburg, 93053 Regensburg, Germany. Phone: +49 941 944 17464; E-mail: lukas@lukasbeyer.com

Disclosure: No potential conflicts of interest were disclosed.

doi: 10.2478/raon-2019-0011

Unfortunately co-author surename is spelled incorrectly (Lukas Lürken), the correct spelling is "Lukas Luerken".

Niklas Verloh[1], Isabel Jensch[1], Lukas Luerken[1], Michael Haimerl[1], Marco Dollinger[1], Philipp Renner[2], Philipp Wiggermann[3], Jens Martin Werner[4], Florian Zeman[5], Christian Stroszczynski[1], Lukas Philipp Beyer[1]

Radiol Oncol 2023; 57(1): 1-11.
doi: 10.2478/raon-2023-0015

Verukozni karcinom ustne votline

Krištofelc N, Zidar N, Strojan P

Izhodišča. Verukozni karcinom je oblika ploščatoceličnega karcinoma s specifičnimi morfološkimi, citokinetičnimi in kliničnimi lastnostmi. Kljub majhni mitotski aktivnosti in počasni rasti se lahko širi v okolna tkiva, vendar ne metastazira v regionalne bezgavke in oddaljene organe. Najpogosteje vznikne v ustni votlini. Predstavljamo etiologijo, klinično sliko, diagnostiko in metode zdravljenja verukoznega karcinoma ustne votline ter izpostavljamo z njim povezane dileme.

Zaključki. Verukozni karcinom ustne votline moramo zaradi manj agresivne narave in boljše napovedi poteka bolezni razlikovati od običajne oblike ploščatoceličnega karcinoma. Za pravilno diagnosticiranje je ključnega pomena tesno sodelovanje med zdravnikom klinikom in patologom. Priporočila o optimalnem načinu zdravljenja temeljijo na opisih posameznih primerov in majhnih retrospektivnih raziskavah ter posledično niso enotna. Načrtovane multicentrične prospektivne raziskave bi lahko omogočile boljšo obravnavo bolnikov z verukoznim karcinomom ustne votline.

Radiol Oncol 2023; 57(1): 12-19.
doi: 10.2478/raon-2023-0013

Molekularno profiliranje redkega timoma z uporabo sekvenciranja naslednje generacije. Metaanaliza

Kostić Perić J, Ćirković A, Srzentić Dražilov S, Samardžić N, Skodrić Trifunović V, Jovanović D, Pavlović S

Izhodišča. Timomi spadajo med redke tumorje, ki vzniknejo iz epitelnega tkiva timusa. Razlikujemo več oblik timoma: A, AB, B1, B2, B3, timični karcinom in timični nevroendokrini timom. V metaanalizni raziskavi smo se osredotočili na timom z uporabo člankov, ki temeljijo na genomskem profiliranju bolezni z metodo sekvenciranja naslednje generacije (NGS).

Materiali in metode. Izvedli smo sistematičen pregled in metaanalizo razširjenosti raziskav, ki so odkrile gene in različice, ki se pojavljajo v manj agresivnih oblikah timičnih epitelijskih tumorjev. Raziskave, objavljene pred 12. decembrom 2022, smo našli v zbirkah podatkov *PubMed*, *Web of Science* in *SCOPUS*. Dva pregledovalca sta preiskala baze podatkov in izbrala članke za končno analizo na podlagi natančno opredeljenih kriterijev za izključitev in vključitev.

Rezultati. V kvalitativno in kvantitativno analizo smo na koncu vključili 12 objav. Trije geni, *GTF2I*, *TP53* in *HRAS*, so se v opazovanih raziskavah pokazali kot pomembne za bolezen. Razmerja obetov (*angl. odds ratio,* OR) za vse tri ekstrahirane gene so bila: *GTF2I* (OR = 1,58; interval zaupanja [*angl. confidence interval,* CI 1,51, 1,66]; p < 0,00001), *TP53* (OR = 1,36; CI [1,12, 1,65]; p < 0,002) in *HRAS* (OR = 1,02; CI [1,00, 1,04]; p < 0,001).

Zaključki. Glede na rezultate, smo videli, da ima gen *GTF2I* pomembno prevalenco v kohorti opazovanih bolnikov s timomom. Prav tako smo pri analizi objavljenih člankov videli, da NGS kaže, da so geni *GTF2I*, *TP53* in *HRAS* najpogosteje mutirani geni v timomu. Ti imajo patogene enonukleotidne različice in insercije/delecije, ki prispevajo k razvoju in napredovanju bolezni. Te različice bi lahko bile dragoceni biološki označevalci in tarčna mesta za zdravila, specifična za timom.

Radiol Oncol 2023; 57(1): 20-34.
doi: 10.2478/raon-2023-0008

Multimodalno računalniškotomografsko slikanje prispeva k izboljšanju diagnostične natančnosti solitarnih pljučnih nodulov. Večinstitucionalna, prospektivna raziskava

Yan G, Li H, Fan X, Deng J, Yan J, Qiao F, Yan G, Liu T, Chen J, Wang L, Yang Y, Li Y, Zhao L, Bhetuwal A, McClure MA, Li N, Peng C

Izhodišča. Solitarni pljučni noduli so klinično ena najpogostejših nenormalnih najdb pri računalniški tomografiji (CT) prsnega koša. Namen večinstitucionalne prospektivne raziskave je bil raziskati vrednost preiskave CT brez kontrasta, CT s kontrastom, perfuzijskega CT-ja in preiskave CT-ja z dvojno energijo, ki jo uporabljamo za razlikovanje benignih in malignih solitarni pljučni nodulov.

Bolniki in metode. Bolnike z 285 solitarnimi pljučnimi noduli smo pregledali s preiskavami: CT bez kontrasta, CT s kotrastom, perfuzijski CT in CT z dvojno energijo. Razlike med benignimi in malignimi noduli smo ocenjevali s posamičnio preiskavo CT ter z različnimi kombinacijami CT-ja brez kontrasta in ostalimi tremi preiskavami. Kombinacije smo ozačili kot metode A, B in C in preiskave kombinirali tudi med seboj (metoda A + B, A + C , B + C in A + B + C). Ugotovitve smo primerjali z analizo karakteristik krivulje sprejemnika (*angl. receiver operating characteristic curve analysis*).

Rezultati. Multimodalno CT slikanje je pokazalo boljše rezultate (občutljivosti od 92,81 % do 97,60 %, specifičnosti od 74,58 % do 88,14 % in natančnost od 86,32 % do 93,68 %) kot tiste pri enomodalnem CT slikanju (občutljivosti od 83,23 % do 85,63 %, specifičnosti 63,56 % do 67,80 % in natančnosti od 75,09 % do 78,25 %, vse $p < 0,05$).

Zaključki. Solitarni pljučni noduli, ovrednoteni z multimodalnim slikanjem CT, prispevajo k izboljšanju diagnostične natančnosti razlikovanja med njihovo benignostjo in malignostjo. CT brez kontrasta pomaga poiskati in oceniti morfološke značilnosti nodulov; CT s kontrastom pomaga oceniti njihovo vaskularnost. Dodatno sta v pomoč pri izboljšanju diagnostične učinkovitosti perfuzijski CT z uporabo parametra prepustne površine in CT z dvojno energijo ter uporabo parametra normalizirane koncentracije joda v venski fazi.

Radiol Oncol 2023; 57(1): 35-41.
doi: 10.2478/raon-2023-0005

Ultrazvočno diagnosticiranje tumorjev perifernih živcev. Skupina primerov

Podnar S

Izhodišča. Tumorji perifernih živcev so redki, a predstavljajo pomemben vzrok okvare perifernih živcev. Namen raziskave je bil predstaviti skupino zaporednih bolnikov s tumorji perifernih živcev, obravnavanih v avtorjevi ultrazvočni praksi.

Bolniki in metode. Retrospektivno smo pregledali elektronske zdravstvene kartoteke bolnikov s tumorji perifernih živcev, ki smo jih izvedli v ultrazvočnem laboratoriju Inštituta za klinično nevrofiziologijo od februarja 2013 do maja 2020. Pri vseh bolnikih smo zbrali podatke o spolu, starosti, kliničnih značilnostih, lokaciji tumorjev perifernih živcev, elektrodiagnostiki in o ultrazvočnih ugotovitvah.

Rezultati. V analiziranem obdobju smo pregledali 2845 pacientov. Med temi smo prepoznal 15 bolnikov (0,5 %) s tumorji perifernih živcev. Štirje izmed njih (3 s potrjeno nevrofibromatozo) so imeli več tumorjev perifernih živcev. Polovica bolnikov (53 %) je imela znake okvare perifernega živca, ostali pa tipno maso ali pa so navajali bolečine. Najpogosteje je bil prizadet ulnarni živec (36 %). Površine preseka tumorjev perifernih živcev so bile od 24 mm^2 do 1250 mm^2 (srednja vrednost 61 mm^2). Na podlagi histološkega izvida smo pri 5 bolnikih in na podlagi ultrazvočnih preiskav pri preostalih bolnikih diagnosticirali švanom, skupaj pri 40 % bolnikov, nevrofibrom pri 27 % in perineuriom pri 27 % bolnikov.

Zaključki. Kot v prejšnjih objavah so se tumorji perifernih živcev kazali z nevrološkimi simptomi, kot tipna masa ali z bolečino. V nasprotju z drugimi žariščnimi nevropatijami so zlasti živci s švanomom, kljub izraziti zadebelitvi, pogosto ohranjali dobro funkcijo. Dodajanje ultrazvoka v klinično prakso nam je omogočilo diagnosticiranje teh redkih lezij perifernih živcev, ki smo jih pred tem praviloma spregledali.

Radiol Oncol 2023; 57(1): 42-50.
doi: 10.2478/raon-2023-0007

Učinki dinamične ojačitve s kontrastnim sredstvom ob slikanju prostate zaradi raka v tranzicijski coni pri poročanju v slikovnem in podatkovnem sistemu diagnostike prostate (PI-RADS), različica 2.1.

Zhang J, Xu L, Zhang G, Zhang X, Bai X, Sun H, Jin Z

Izhodišča. Namen raziskave je bil analizirati učinke dinamične ojačitve s kontrastnim sredstvom v tranzicijski coni prostate pri raku prostate in klinično pomembnem raku prostate v sistemu PI-RADS, različica 2.1.

Bolniki in metode. Diagnostično učinkovitost različnih kombinacij preiskav (T2 poudarjeno slikanje [T2WI] + difuzijsko poudarjeno slikanje [DWI]; T2WI + dinamično ojačano s kontrastnim sredstvom slikanje [DCE]; in T2WI + DWI + DCE) pri raku prostate v tranzicijski coni ter pri klinično pomembnem raku prostate v tranzicijski coni smo primerjali z biopsijo prostate, ki je pomenila referenčni standard. Uporabili smo oceno ≥ 4, ki je predstavljala pozitivni prag.

Rezultati. V raziskavi smo ovrednotili 425 vzorcev. 203 vzorcev je sodilo v skupino rak v tranzicijski coni prostate in 146 vzorcev v skupino klinično pomembni rak prostate v tranzicijski coni. Kombinacija 3 sekvenc je imela podobna področja pod krivuljo pri diagnosticiranju obeh rakov prostate ($P > 0,05$). Senzitivnost T2WI + DCE in T2WI + DWI + DCE (84,7 % in 85,7 % za rak prostate v tranzicijski coni; 88,4 % in 89,7 % za klinično pomemben rak v tranzicijski coni) pri diagnosticiranju obeh vrst rakov je bila značilno večja kot senzitivnost pri T2WI + DWI (79,3 % za rak prostate v tranzicijski coni; 82,9 % za klinično pomemben rak v isti coni). Specifičnost T2WI + DWI (86,5 % za rak v tranzicijski coni; 74,9 % za klinično pomemben rak v tranzicijski coni prostate) je bila značilno večja kot specifičnost pri T2WI + DCE in T2WI + DWI + DCE (68,0 % in 68,5 % za rak v tranzicijski coni; 59.1 % in 59.5 % za klinično pomemben rak v tranzicijski coni.), (vsi $P < 0,05$). Diagnostična učinkovitost T2WI + DCE in T2WI + DWI + DCE ni vsebovala značilnih razlik ($P > 0.05$).

Zaključki. DCE lahko izboljša senzitivnost diagnoze za rak prostate v tranzicijski coni in klinično pomembni rak prostate v tranzicijski coni ter je uporabna pri zaznavi majhnih rakavih lezij.

Radiol Oncol 2023; 57(1): 51-58.
doi: 10.2478/raon-2023-0006

Presaditev otočkov trebušne slinavke v ekstracelularni matriks po ireverzibilni elektroporaciji jeter

Zhang Y, Lv Y, Wang Y, Chang TT, Rubinsky B

Izhodišča. Presaditev otočkov trebušne slinavke z infuzijo skozi portalno veno je postala uveljavljen klinični način zdravljenja bolnikov s sladkorno boleznijo tipa 1. Ker je učinkovitost presaditve majhna, iščejo nove pristope za vsaditev pankreatičnih otočkov. Cilj pričujoče raziskave je bil raziskati možnost, da bi decelularizirani matriks v jetrih, ki smo ga ustvarili z netermično ireverzibilno elektroporacijo (NTIRE), lahko uporabili kot mesto za presaditev pankreatičnih otočkov.

Materiali in metode. Pankreatične otočke ali kontrolne vzorce s fiziološko raztopino smo 16 ur po obdelavi jeter z NTIRE injicirali na ista mesta v jetrih pri 7 podganah. Sedem dni po zdravljenju z NTIRE smo ocenili delovanje otočnih presadkov z zaznavanjem insulina in glukagona v jetrih, kar smo naredili z imunohistokemično preiskavo.

Rezultati. Otočki trebušne slinavke, implantirani v volumen jeter, ki smo ga predhodno obdelali z NTIRE, so se vključili v jetrni parenhim ter proizvajali inzulin in glukagon v 2 od 7 jeter podgan. Možni razlogi za to, da pri preostalih 5/7 podgan nismo zaznali pankreatičnih otočkov, so lahko bila lokalna vnetna reakcija, zavrnitev presadka, majhno število začetnih otočkov ali pa čas implantacije.

Zaključki. Raziskava kaže, da lahko otočke trebušne slinavke vgradimo in da delujejo v prostoru zunajceličnega matriksa, ustvarjenega z NTIRE, čeprav je stopnja uspešnosti nizka. Nadaljnji razvoj na tem področju bi lahko dosegli z boljšim razumevanjem mehanizmov neuspeha in bi tako lahko razvili načine, kako zaobiti ali premagati te mehanizme.

Radiol Oncol 2023; 57(1): 59-69.
doi: 10.2478/raon-2023-0002

Ocena izpostavljenosti nizkofrekvenčnim magnetnim poljem v bližini visokonapetostnih daljnovodov in oceana tveganja za nastanek raka pri slovenskih otrocih in mladostnikih

Žagar T, Valič B, Kotnik T, Korat S, Tomšič S, Zadnik V, Gajšek P

Izhodišča. Posamične predhodne raziskave so pokazale, da bi povprečna dnevna izpostavljenost magnetnim poljem z izjemno nizko frekvenco (MP ENF) vrednosti nad 0,3 ali 0,4 μT lahko potencialno povečala tveganje za otroško levkemijo.

Metode. Da bi omogočili izračune MP ENF okoli visokonapetostnih daljnovodov za celotno Slovenijo, smo razvili novo tri-dimenzionalno metodo za izračun dolgoročnega povprečja MP ENF, ki vključuje natančne podatke o reliefu terena. Iz populacijskega Registra raka smo pridobili podatke o populaciji slovenskih otrok in mladostnikov ter bolnikov z otroškim rakom (0–14 let), levkemijo (0–19 let) ter možganskimi tumorji (0–29 let) za 12-letno obdobje 2005–2016.

Rezultati. V Sloveniji je le 0,5 % otrok in mladostnikov mlajših od 19 let živelo na območju z gostoto MP ENF nad 0,1 μT v bližini visokonapetostnih daljnovodov. Tveganje za raka pri otrocih in mladostnikih, ki so živeli na območjih z višjo MP ENF, se bistveno ni razlikovalo od tveganja njihovih vrstnikov.

Zaključki. Nova metoda omogoča razmeroma hiter izračun vrednosti nizkofrekvenčnih magnetnih polj za poljubne obremenitve elektrodistribucijskega omrežja, saj vrednost posameznega vira za poljubno obremenitev izračunamo s skaliranjem vrednosti za nazivno obremenitev. To omogoča tudi bistveno hitrejše prilagajanje spremembam v elektrodistribucijskem omrežju.

Radiol Oncol 2023; 57(1): 70-79.
doi: 10.2478/raon-2023-0001

Primerjava mikrokroglic CalliSpheres®, ki sproščajo zdravilo, in običajne transarterijske kemoembolizacije pri bolnikih s primarnim rakom jeter. Randomizirana kontrolirana raziskava

Shi Z, Wang D, Kang T, Yi R, Cui L, Jiang H

Izhodišča. Namen raziskave je bil primerjati rezultate transarterijske kemoembolizacije z mikrokroglicami *CalliSpheres®,* ki sproščajo zdravilo (*angl. drug-eluting beads transarterial chemoembolization,* DEB-TACE) in običajne transarterijske kemoembolizacije (*angl. conventional transarterial chemoembolization*, cTACE) pri zdravljenju bolnikov z neoperabilnim hepatocelularnim rakom jeter.

Bolniki in metode. Skupno 90 bolnikov smo razdelili v skupino DEB-TACE (n = 45) in skupino cTACE (n = 45). Obe skupini smo primerjali glede na odgovor na zdravljenje, celokupno preživetje, preživetje brez napredovanja bolezni in varnost zdravljenja.

Rezultati. Objektivni odgovor na zdravljenje v skupini DEB-TACE je bil po 1, 3 in 6 mesecih spremljanja značilno večji kot v skupini cTACE (P = 0,031, P = 0,003, P = 0,002). Prav tako je bil popolni odgovor v skupini DEB-TACE po 3 mesecih pomembno večji kot v skupini cTACE (P = 0,036). Analiza preživetja je pokazala, da so bolniki v skupini DEB-TACE imeli boljše preživetje kot v skupini cTACE (srednja vrednost celokupnega preživetja: 534 proti 367 dni, P = 0,027; srednja vrednost preživetje brez napredovanja bolezni: 352 proti 278 dni, P = 0,004). Stopnja okvare delovanja jeter je bila v skupini DEB-TACE višja v prvem tednu, vendar je bila v obeh skupinah podobna v prvem mesecu. DEB-TACE z mikrokroglicami *CalliSpheres®* je povzročila pogosteje povišane temperature in hude bolečine v trebuhu (P = 0,031, P = 0,037).

Zaključki. Bolniki, ki smo jih zdravili z DEB-TACE z mikrokroglicami *CalliSpheres®* so imeli boljši odgovor na zdravljenje in boljše preživetje kot bolniki v skupini cTACE. Čeprav so se v skupini DEB-TACE pogosteje pojavili prehodne resne poškodbe jeter, povišane telesne temperature in hude bolečine v trebuhu, jih je bilo mogoče obvladati s simptomatskim zdravljenjem.

Radiol Oncol 2023; 57(1): 80-85.
doi: 10.2478/raon-2022-0026

Ali sočasna ginekološka operacija vpliva na stopnjo okužb po mastektomiji in rekonstrukciji z vsadki?

Pišlar N, Perić B, Ahčan U, Cencelj-Arnež R, Žgajnar J, Perhavec A

Izhodišča. Pri bolnicah z rakom dojk, ki potrebujejo operacijo, je pogosto indicirana tudi ginekološka operacija. Namen pričujoče raziskave je bil primerjati stopnjo infekcijskih zapletov po mastektomiji in rekonstrukciji z vsadki pri bolnicah s sočasno ginekološko operacijo in brez nje.

Bolnice in metode. Opravili smo retrospektivno analizo medicinske dokumentacije 159 zaporedno operiranih bolnic, pri katerih smo napravili mastektomijo in rekonstrukcijo z vsadki. Bolnice smo razdelili v dve skupini: 102 bolnici brez (1. skupina) in s sočasno ginekološko operacijo (2. skupina). Primerjali smo stopnjo okužb med skupinama s testom χ^2. Za ugotavljanje povezanosti različnih dejavnikov s stopnjo okužb smo napravili logistično regresijo.

Rezultati. Napravili smo 240 rekonstruktivnih operacij z vsadki. Srednja vrednost časa sledenja bolnicam je bila 297 dni (10–1061 dni). Srednja starost bolnic je bila 47,2 let (95 % interval zaupanja [CI] 32,8–65,9); 48,2 let (95 % CI 46,1–50,3) za 1. skupino in 45,8 let (95 % CI 43,2–48,3) za 2. skupino; p = 0,002). Stopnja okužb je bila 17,6 % (17,6 % proti 17,5 %, p = 0,987), odstranitev vsadka je bila potrebna v 5,7 % (4,9 % proti 7,0 %; p = 0.58). Debelost (indeks telesne mase > 30 kg/m^2), starost in predhodna operacija dojke z obsevanjem so bili dejavniki tveganja za okužbo v univariatni analizi. Debelost (prilagojeno razmerje obetov [aOR] 3,319; 95 % CI 1,085–10,157; p = 0,036) in predhodna operacija dojke z obsevanjem (aOR 7,481; 95 % CI 2,230–25,101; p = 0,001) sta bila neodvisno povezana z okužbami v multivariatnem modelu.

Zaključki. Sočasna ginekološka operacija pri bolnicah po mastektomiji in rekonstrukciji z vsadki ni povečala tveganja za okužbo.

Radiol Oncol 2023; 57(1): 86-94.
doi: 10.2478/raon-2022-0048

Verifikacija lege z računalniško tomografijo s stožčastim snopom ter poravnavo na karino in hrbtenico kot nadomestek poravnave na tarčo pri obsevanju lokalno napredovalega pljučnega raka

But-Hadžić J, Strljič K, Žager Marciuš V

Izhodišča. Namen raziskave je bil oceniti natančnost volumetrične slikovno vodene radioterapije pljučnega raka s poravnavo na hrbtenico ali karino kot nadomestka poravnave na tumor, ker najboljši pristop še ni znan.

Bolniki in metode. Slike računalniške tomografije s stožčastim snopom (*angl. cone beam computed tomography*, CBCT) iz 1., 10., 15. in 20. frakcije obsevanja pri 40 radikalno obsevanih bolnikih s pljučnim rakom smo retrospektivno poravnali s simulatorsko CT sliko in uporabili tri pristope. Analizirali in primerjali smo odstopanja nastavitev poravnave na hrbtenico in karino od referenčne nastavitve na tarčo (na tumor in na bezgavke) v lateralni, longitudinalni in vertikalni smeri. Preverili smo morebitni vpliv lege tumorja in stadija bezgavk na natančnost poravnave.

Rezultati. Povprečno odstopanje nastavitev na hrbtenico in karino od referenčne nastavitve je bilo največje v longitudialni smeri, z najboljšim ujemanjem v vertikalni in lateralni smeri. Obe strategiji poravnave sta bili natančnejši pri centralno ležečih tumorjih, ob tem je bila nastavitev na karino natančnejša v 50 % v lateralni smeri in 66 % v longitudinalni smeri povprečnih odstopanj. Pri vseh meritvah pri vseh bolnikih je primerjava nastavitev na karino in hrbtenico pokazala večjo natančnost karine v lateralni in longitudinalni smeri. V primerjalni analizi podskupin je bila karina v primerjavi s hrbtenico v lateralni in longitudinalni smeri boljša pri centralno ležečih tumorjih, N2 in N3. Obe strategiji sta bili primerljivi pri perifernih tumorjih in N0.

Zaključki. Poravnava CBCT in simulatorskega CT na karino kaže večjo natančnost v primerjavi s hrbtenico v lateralni in longitudialni smeri ter je superiorna pri centralno ležečih tumorjih ter stadiju N2 in N3. Hrbtenica in karina kot nadomestek poravnave na tarčo sta enako natančni za periferno ležeče tumorje in za stadij N0. Predlagamo uporabo karine kot standardnega nadomestka za tarčo pri poravnavi CBCT slikovno vodenega obsevanja pri lokalno napredovalem pljučnem raku.

Radiol Oncol 2023; 57(1): 95-102.
doi: 10.2478/raon-2023-0004

Učinki implantacije zlatih fiducijskih označevalcev na kontrolo tumorja in toksičnost pri teleradioterapiji raka prostate

Moll M, Weiß M, Stanisav V, Zaharie A, Goldner G

Izhodišča. Utemeljitve, ki govorijo o vplivih fiducijskih označevalcev pri slikovno vodeni radioterapiji (*angl. image-guided radiotherapy*, IGRT) na kontrolo tumorja ter akutno in pozno toksičnost so redke.

Bolniki in metode. V retrospektivno raziskavo smo vključili bolnike s primarnim rakom prostate z nizko in srednjo stopnjo tveganja, ki smo jih zdravili med leti 2010 in 2015. 40 bolnikov smo pripravili na obsevanje z in 21 bolnikov brez zlatih fiducijskih označevalcev. Pri odločitvi za ali proti implantaciji označevalcev smo upoštevali anesteziološko oceno in bolnikovo izbiro. IGRT smo izvedli z uporabo elektronskih portalnih slikovnih naprav. Predpisana doza je bila 78 Gy, 2 Gy na frakcijo. Biokemična ponovitev bolezni brez morfološko dokazane bolezni smo opredelili s Phoenixovimi merili. Akutno in pozno gastrointestinalno in genitourinalno toksičnost smo ocenili z merili Onkološke skupine za radioterapijo (*angl. Radiation Therapy Oncology Group*).

Rezultati. Zaradi kontraindikacij za anestezijo ni prejelo fiducijskih označevalcev 60 % bolnikov in zaradi osebne izbire 25 % bolnikov. Ko smo ocenjevali kontrolo tumorja, nismo ugotovili pomembnih razlik glede biokemične ponovitve bolezni ter celokupnega in za bolezen specifičnega preživetja ($p = 0.61$, $p = 0.56$ in $p > 0.9999$). Prav tako nismo ugotovili pomembnih razlik pri ocenjevanju akutnih in poznih gastrointestinalnih ($p = 0,16$ in $0,64$) in genitourinalnih toksičnosti ($p = 0,58$ in $0,80$).

Zaključki. Nismo ugotovili statistično značilne prednosti po implantaciji zlatih fiducijskih označevalcev tako ne pri biokemični ponovitvi bolezni kot ne pri zgodnjih ali poznih gastrointestinalnih in genitourinalnih stranskih učinkih.

Radiol Oncol 2023; 57(1): 103-110.
doi: 10.2478/raon-2023-0014

Petletni rezultati analize KRAS, NRAS in BRAF ter vzorci zdravljenja v vsakdanji klinični praksi v Sloveniji pri zdravljenju prvega reda bolnikov z metastatskim rakom debelega črevesa nemutiranega tipa RAS. Podatki iz vsakodnevne klinične prakse

Mesti T, Reberšek M, Ocvirk J

Izhodišča. Izvedli smo neintervencijsko raziskavo IV. faze za oceno statusa KRAS, NRAS in BRAF pri bolnikih z metastatskim rakom debelega črevesa in danke, ki so bili primerni za sistemsko zdravljenje prvega reda. Analizirali smo odločitve za zdravljenje prvega reda pri bolnikih z nemutiranim tipom RAS.

Bolniki in metode. V raziskavo smo vključili bolnike s histološko potrjenim metastatskim rakom debelega črevesa in danke, ki so bili primerni za sistemsko zdravljenje prvega reda in so izpolnjevali vsa vključitvena merila. Analizo KRAS, NRAS in BRAF smo naredili iz vzorcev tkiva primarnega tumorja ali metastaz. Vsi vključeni bolniki so pisno privolili v sodelovanje v raziskavi.

Rezultati. Od aprila 2013 do marca 2018 smo na Onkološkem inštitutu Ljubljana v raziskavo vključili 650 bolnikov. Med njimi je 637 bolnikov prejelo sistemsko zdravljenjem prvega reda glede na status RAS in BRAF. Porazdelitev bolnikov s tumorsko mutacijo KRAS in brez te mutacije je bila skoraj enaka (48,8 % oziroma 47,9 %), nadalje 89 % bolnikov je imelo nemutirane tumorje NRAS in 86,1 % nemutirane tumorje BRAF. Najpogosteje smo predpisali zdravljenje z bevacizumabom (53,1 %), bodisi v kombinaciji z dvema kemoterapevtikoma ali z enim. Zaviralca EGFR cetuksimab in panitumumab smo predpisali bolnikom, ki so imeli tumorje z nemutiranim RAS (30,9 %).

Zaključki. Petletna analiza naše vsakodnevne klinične prakse v terciarni ustanovi, je pokazala, da je porazdelitev med tumorji nemutiranega in mutiranega tipa pri bolnikih z metastatskim rakom debelega črevesa in danke približno enaka kot v svetu. Slovenska populacija z metastatskim rakom debelega črevesa in danke ima tudi enako razmerje porazdelitve nemutiranih in mutiranih genov KRAS, NRAS in BRAF. Ugotovili smo, da dvotedenska čakalna doba za določitev tumorskih označevalcev ni vplivala na odločitev o načinu zdravljenja prvega reda. Tako so bile odločitve za zdravljenje v skladu s svetovnimi smernicami zdravljenja, ki temeljijo na z dokazi podprti medicini.

Radiol Oncol 2023; 57(1): 111-120.
doi: 10.2478/raon-2023-0003

Vpliv genetske variabilnosti *OPRM1*, *MIR23B* in *MIR107* na akutno in kronično bolečino ter neželene učinke zdravljenja s tramadolom in paracetamolom po operaciji raka dojk

Vidic Z, Goričar K, Stražišar B, Bešić N, Dolžan V

Izhodišča. Tramadol je opioidni analgetik, ki ga pogosto uporabljamo za lajšanje bolečin po operaciji raka dojke. Protibolečinski učinek posreduje preko aktivacije opioidnega receptorja mu, ki ga kodira gen *OPRM1*. V raziskavi smo želeli preveriti povezavo med genetskimi spremembami gena *OPRM1* in genov za njegove regulatorne molekule miRNA ter izidom zdravljenja s tramadolom po operaciji raka dojke z odstranitvijo pazdušnih bezgavk.

Bolnice in metode. Raziskava je vključevala 113 bolnic po operaciji raka dojke z odstranitvijo pazdušnih bezgavk, ki so v randomizirani klinični študiji KCT 04/2015-DORETAonko/si Onkološkega inštituta Ljubljana prejemale 75/650 mg ali 37,5/325 mg tramadola s paracetamoloma za lajšanje pooperativne bolečine. Z genotipizacijo s kompetitivno alelno specifično verižno reakcijo s polimerazo smo pri preiskovankah preverili prisotnost polimorfizmov *OPRM1* rs1799971, *OPRM1* rs677830, *MIR23B* rs1011784 in *MIR107* rs2296616 ter z logistično regresijo, Fisherjevim testom in Mann-Whitneyevim testom preverili povezavo teh genetskih sprememb z akutno in kronično bolečino ter neželenimi učinki zdravljenja s tramadolom.

Rezultati. Pri nobenem izmed preiskovanih polimorfizmov nismo potrdili vpliva na stopnjo akutne bolečine, ocenjene z analogno vizualno skalo (VAS), v prvih štirih tednih po operaciji (P > 0,05). Nosilke vsaj enega polimorfnega alela *OPRM1* rs1799971 so imele v prvih štirih tednih po operaciji večje tveganje za pojav zaprtosti v primerjavi z nosilkami dveh normalnih alelov (razmerje obetov [RO] = 4,5; 95 % interval zaupanja [IZ] = 1,6–12,64; P = 0,004). Nosilke vsaj enega polimorfnega alela *OPRM1* rs677830 so imele po treh tednih zdravljenja s tramadolom večje tveganje za pojav zaprtosti (RO = 3,11; 95 % IZ = 1,08–8,89; P = 0,035). Nosilke dveh polimorfnih alelov *MIR23B* rs1011784 so imele povečano tveganje za pojav slabosti po 28 dneh zdravljenja s tramadolom (RO = 7,35, 95 % IZ = 1,27–42,6, P = 0,026), medtem ko so imeli heterozigoti za *MIR107* rs2296616 nižje tveganje za pojav slabosti po 21 dneh zdravljenja s tramadolom (RO = 0,21, 95 % IZ = 0,05–0,87, P = 0,031). Nosilke dveh polimorfnih alelov *MIR107* rs2296616 so eno leto po operaciji pogosteje navajale kronične bolečine kot nosilke dveh normalnih alelov (P = 0,004). Nosilke vsaj enega polimorfnega alela *MIR23B* rs1011784 so ob prilagoditvi za višino odmerka pogosteje poročale o nevropatski bolečini (RO = 2,85, 95 % IZ = 1,07–7,59, P = 0,036), medtem ko so nosilke vsaj enega polimorfnega alela *OPRM1* rs677830 redkeje poročale o nevropatski bolečini v primerjavi z nosilkami dveh normalnih alelov (RO = 0,38, 95 % IZ = 0,15–0,99, P = 0,047).

Zaključki. Genetske spremembe *OPRM1* in genov, ki kodirajo miRNA s potencialnim vplivom na izražanje *OPRM1*, bi lahko bile povezane tako s pojavom neželenih učinkov zdravljenja s tramadolom/paracetamolom kot tudi prisotnostjo kronične in nevropatske bolečine po operaciji raka dojke z odstranitvijo pazdušnih bezgavk.

Radiol Oncol 2023; 57(1): 121-126.
doi: 10.2478/raon-2023-0010

Zdravljenje ponovitve raka zunanjega spolovila z elektrokemoterapijo. Podrobna analiza možnih vzrokov neučinkovitega zdravljenja

Vivod G, Jesenko T, Gašljević G, Kovačevič N, Bošnjak M, Serša G, Merlo S, Čemažar M

Izhodišča. Zdravljenje z elektrokemoterapijo je lokalno učinkovito pri bolnicah z rakom zunanjega spolovila. Dosedanje raziskave opisujejo varno in učinkovito uporabo elektrokemoterapije pri obravnavi ginekoloških rakov v paliativne namene, večinoma pri ženskah s ploščatoceličnim rakom zunanjega spolovila. V posameznih primerih pa je zdravljenje z elektrokemoterapijo neučinkovito. Biološke lastnosti, ki povzročajo neučinkovitost, še niso opredeljene.

Bolniki in metode. Elektrokemoterapijo z intravenskim apliciranjem bleomicina smo uporabili pri ponovitvi ploščatoceličnega raka v predelu zunanjega spolovila. Zdravljenje smo izvedli po standardnih operativnih postopkih s heksagonalno elektrodo. Zanimalo nas je, katere značilke so določale neučinkovitost elektrokemoterapije.

Rezultati. Na podlagi predstavljenega primera neučinkovitega zdravljenja ponovitve raka zunanjega spolovila z elektrokemoterapijo domnevamo, da lahko analiza ožiljenosti tumorja pred zdravljenjem napove učinkovitost zdravljenja z elektrokemoterapijo. Histološka analiza je pokazala minimalno prisotnost krvnih žil v predelu tumorja. Slabša perfuzija zmanjša količino zdravila v tumorju, kar vodi v zmanjšano učinkovitost elektrokemoterapije. V predstavljenem primeru zdravljenje z elektrokemoterapijo ni povzročilo željenega imunskega odziva v tumorju.

Zaključki. V predstavljenem primeru smo analizirali možne dejavnike, ki bi lahko napovedali neučinkovitost zdravljenja ponovitve raka zunanjega spolovila z elektrokemoterapijo. Na podlagi histološke analize smo ugotovili slabšo ožiljenost tumorja, kar je zmanjšalo vnos in porazdelitev zdravila v tumorju ter povzročilo neučinkovitost elektrokemoterapije.

Radiol Oncol 2023; 57(1): 127-139.
doi: 10.2478/raon-2023-0012

CT-vodena brahiterapija z ^{125}J pri hepatocelularnem raku na mestih z visokim tveganjem, po transkarterijski kemoembolizaciji in v kombinaciji z mikrovalovno ablacijo. Primerjava dveh metod zdravljenja

Chen Z, Fu X, Qiu Z, Mu M, Jiang W, Wang G, Zhong Z, Qi H, Gao F

Izhodišča. Namen raziskave je bil oceniti varnost in učinkovitost brahiterapije z ^{125}J v kombinaciji s transarterialno kemoembolizacijo (*angl. transarterial chemoembolization*, TACE) in mikrovalovno ablacijo (*angl. microwave ablation*, MWA) pri neresektabilnem hepatocelularnem raku na mestih z visokim tveganjem.

Bolniki in metode. Po primerjavi 1 : 2 smo v retrospektivni raziskavi analizirali 49 bolnikov, ki so prejeli TACE + MWA + brahiterapijo z ^{125}J (skupina A) in 98 bolnikov, ki so prejeli samo TACE +MWA (skupina B). Ocenjevali smo preživetje brez napredovanja bolezni, celokupno preživetje in zaplete zdravljenja. Obe skupini smo primerjali s Coxovo regresijsko analizo proporcionalnih tveganj.

Rezultati. Bolniki v skupini A so imeli daljše preživetje brez napredovanja bolezni kot v skupini B (7,9 proti 3,3 meseca, P = 0,007). Med obema skupinama nismo videli pomembnih razlik v srednjem celokupnem preživetju (P = 0,928). Stopnje objektivnega odgovora kontrole bolezni v primerih tumorjev na mestih z visokim tveganjem in stopnje objektivnega odgovora intrahepatičnih tumorjev so bile v skupini A 67,3 %, 93,9 % oziroma 51,0 %, v skupini B pa 38,8 %, 79,6 % in 29,6 % (P < 0,001, P = 0,025 oziroma P = 0,011). Kombinacija TACE-MWA-^{125}J (razmerje obetov [*angl. hazard ratio*, HR] = 0,479, P < 0,001) je bila pomemben in ugoden prognostični dejavnik, ki je vplival na preživetje brez napredovanja bolezni. Tumorska tromboza v portalni veni je bila neodvisen prognostični dejavnik za preživetje brez napredovanja bolezni (HR = 1,625, P = 0,040). Barcelonski stadij jetrnega raka ([*angl. Barcelona clinic liver cancer*, BCLC] C proti B) je bil neodvisen dejavnik, ki je vplival na celokupno preživetje (HR = 1,941, P = 0,038). Incidenca zapletov je bila med obema skupinama podobna, le da je bila incidenca bolečine v trebuhu manjša v skupini A (P = 0,007).

Zaključki. Kombinacija TACE-MWA-^{125}J pri bolnikih z neoperabilnim hepatocelularnim rakom na mestih z visokim tveganjem je omogočila daljše preživetje brez napredovanja bolezni in boljši nadzor tumorja kot TACE-MWA.

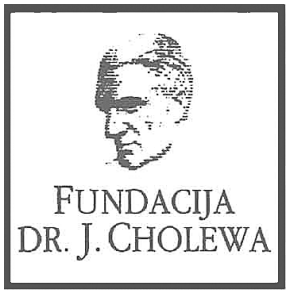

Fundacija "Docent dr. J. Cholewa"
je neprofitno, neinstitucionalno in nestrankarsko
združenje posameznikov, ustanov in organizacij, ki želijo
materialno spodbujati in poglabljati raziskovalno
dejavnost v onkologiji.

Dunajska 106
1000 Ljubljana
IBAN: SI56 0203 3001 7879 431

SKRAJŠAN POVZETEK GLAVNIH ZNAČILNOSTI ZDRAVILA

Za to zdravilo se izvaja dodatno spremljanje varnosti. Tako bodo hitreje na voljo nove informacije o njegovi varnosti. Zdravstvene delavce naprošamo, da poročajo o katerem koli domnevnem neželenem učinku zdravila. Glejte poglavje 4.8, kako poročati o neželenih učinkih.

IME ZDRAVILA: Verzenios 50 mg/100 mg/150 mg filmsko obložene tablete. **KAKOVOSTNA IN KOLIČINSKA SESTAVA:** Ena filmsko obložena tableta vsebuje 50 mg/100 mg/150 mg abemacikliba. Ena filmsko obložena tableta vsebuje 14 mg/28 mg/42 mg laktoze (v obliki monohidrata). **Terapevtske indikacije:** Zgodnji rak dojk: Zdravilo Verzenios je v kombinaciji z endokrinim zdravljenjem indicirano za adjuvantno zdravljenje odraslih bolnikov z na hormonske receptorje (HR – Hormone Receptor) pozitivnim, na receptorje humanega epidermalnega rastnega faktorja 2 (HER2 – Human Epidermal Growth Factor Receptor 2) negativnim zgodnjim rakom dojk s pozitivnimi bezgavkami, pri katerih obstaja veliko tveganje za ponovitev. Pri ženskah v pred- ali perimenopavzi je treba endokrino zdravljenje z zaviralcem aromataze kombinirati z agonistom gonadoliberina (LHRH – Luteinizing Hormone–Releasing Hormone). Napredovali ali metastatski rak dojk: Zdravilo Verzenios je indicirano za zdravljenje žensk z lokalno napredovalim ali metastatskim, na hormonske receptorje (HR – *Hormone Receptor*) pozitivnim in na receptorje humanega epidermalnega rastnega faktorja 2 (HER2 – *Human Epidermal Growth Factor Receptor 2*) negativnim rakom dojk v kombinaciji z zaviralcem aromataze ali s fulvestrantom kot začetnim endokrinim zdravljenjem ali pri ženskah, ki so prejele predhodno endokrino zdravljenje. Pri ženskah v pred- ali perimenopavzi je treba endokrino zdravljenje kombinirati z agonistom LHRH. **Odmerjanje in način uporabe:** Zdravljenje z zdravilom Verzenios mora uvesti in nadzorovati zdravnik, ki ima izkušnje z uporabo zdravil za zdravljenje rakavih bolezni. *Zdravilo Verzenios v kombinaciji z endokrinim zdravljenjem:* Priporočeni odmerek abemacikliba je 150 mg dvakrat na dan, kadar se uporablja v kombinaciji z endokrinim zdravljenjem. *Zgodnji rak dojk:* Zdravilo Verzenios je treba jemati neprekinjeno dve leti, ali do ponovitve bolezni ali pojava nesprejemljive toksičnosti. *Napredovali ali metastatski rak dojk:* Zdravilo Verzenios je treba jemati, dokler ima bolnica od zdravljenja klinično korist ali do pojava nesprejemljive toksičnosti. Če bolnica bruha ali izpusti odmerek zdravila Verzenios, ji je treba naročiti, da naj naslednji odmerek vzame ob predvidenem času; dodatnega odmerka ne sme vzeti. Obvladovanje nekaterih neželenih učinkov lahko zahteva prekinitev in/ali zmanjšanje odmerka. Zdravljenje z abemaciklibom prekinite v primeru povišanja vrednosti AST in/ali ALT >3 x ZMN SKUPAJ s celokupnim bilirubinom > 2,0 x ZMN v odsotnosti holestaze ter pri bolnicah z intersticijsko pljučno boleznijo (ILD)/pnevmonitis stopnje 3 ali 4. Sočasni uporabi močnih zaviralcev CYP3A4 se je treba izogibati. Če se uporabi močnih zaviralcev CYP3A4 ni mogoče izogniti, je treba odmerek abemaciklibа znižati na 100 mg dvakrat na dan. Pri bolnicah, pri katerih je bil odmerek znižan na 100 mg abemaciklibа dvakrat na dan in pri katerih se sočasnemu dajanju močnega zaviralca CYP3A4 ni mogoče izogniti, je treba odmerek abemaciklibа dodatno znižati na 50 mg dvakrat na dan. Pri bolnicah, pri katerih je bil odmerek znižan na 50 mg abemaciklibа dvakrat na dan in pri katerih se sočasnemu dajanju močnega zaviralca CYP3A4 ni mogoče izogniti, je mogoče z odmerkom abemaciklibа nadaljevati ob natančnem spremljanju znakov toksičnosti. Alternativno je mogoče odmerek abemaciklibа znižati na 50 mg enkrat na dan ali prekiniti dajanje abemaciklibа. Če je uporaba zaviralca CYP3A4 prekinjena, je treba odmerek abemaciklibа povečati na odmerek, kakršen je bil pred uvedbo zaviralca CYP3A4 (po 3–5 razpolovnih časih zaviralca CYP3A4). Prilagajanje odmerka glede na starost in pri bolnicah z blago ali zmerno ledvično okvaro ter z blago (Child Pugh A) ali zmerno (Child Pugh B) jetrno okvaro ni potrebno. Pri dajanju abemaciklibа bolnicam s hudo ledvično okvaro sta potrebna previdnost in skrbno spremljanje glede znakov toksičnosti. Način uporabe: Zdravilo Verzenios je namenjeno za peroralno uporabo. Odmerek se lahko vzame s hrano ali brez nje. Zdravilo se ne sme jemati z grenivko ali grenivkinim sokom. Bolnice naj odmerke vzamejo vsak dan ob približno istem času. Tableto je treba zaužiti celo (bolnice je pred zaužitjem ne smejo gristi, drobiti ali deliti). **Kontraindikacije:** Preobčutljivost na učinkovino ali katero koli pomožno snov. **Posebna opozorila in previdnostni ukrepi:** Pri bolnicah, ki so prejemale abemaciklib, so poročali o nevtropeniji, o večji pogostnosti okužb kot pri bolnicah, zdravljenih s placebom in endokrinim zdravljenjem, o povečanih vrednostih ALT in AST. Pri bolnicah, pri katerih se pojavi nevtropenija stopnje 3 ali 4, je priporočljivo prilagoditi odmerek. Do primerov nevtropenične sepse s smrtnim izidom je prišlo pri < 1 % bolnic z metastatskim rakom dojk. Bolnicam je treba naročiti, naj o vsaki epizodi povišane telesne temperature poročajo zdravstvenemu delavcu. Bolnice je treba spremljati za znake in simptome globoke venske tromboze (VTE) in pljučne embolije ter jih zdraviti, kot je medicinsko utemeljeno. Glede na stopnjo VTE bo morda treba spremeniti odmerek abemaciklibа. Glede na povečanje vrednosti ALT ali AST je mogoče potrebna prilagoditev odmerka. Driska je najpogostejši neželeni učinek. Bolnice je treba ob prvem znaku tekočega blata začeti zdraviti z antidiaroiki, kot je loperamid, povečati vnos peroralnih tekočin in obvestiti zdravnika. Sočasni uporabi induktorjev CYP3A4 se je treba izogibati zaradi tveganja za zmanjšano učinkovitost abemaciklibа. Bolnice z redkimi dednimi motnjami, kot so intoleranca za galaktozo, popolno pomanjkanje laktaze ali malapsorpcija glukoze/galaktoze, tega zdravila ne smejo jemati. Bolnice spremljajte glede pljučnih simptomov, ki kažejo na ILD/pnevmonitis, in jih ustrezno zdravite. Glede na stopnjo ILD/pnevmonitisa je morda potrebno prilagajanje odmerka abemaciklibа. **Medsebojno delovanje z drugimi zdravili in druge oblike interakcij.** Abemaciklib se primarno presnavlja s CYP3A4. Sočasna uporaba abemaciklibа in zaviralcev CYP3A4 lahko poveča plazemsko koncentracijo abemaciklibа. Uporabi močnih zaviralcev CYP3A4 sočasno z abemaciklibom se je treba izogibati. Če je močne zaviralce CYP3A4 treba dajati sočasno, je treba odmerek abemaciklibа zmanjšati, nato pa bolnico skrbno spremljati glede toksičnosti. Pri bolnicah, zdravljenih z zmernimi ali šibkimi zaviralci CYP3A4, ni potrebno prilagajanje odmerka, vendar jih je treba skrbno spremljati za znake toksičnosti. Sočasni uporabi močnih induktorjev CYP3A4 (vključno, vendar ne omejeno na: karbamazepin, fenitoin, rifampicin in šentjanževko) se je treba izogibati zaradi tveganja za zmanjšano učinkovitost abemaciklibа. Abemaciklib in njegovi glavni aktivni presnovki zavirajo prenašalce v ledvicah, in sicer kationski organski prenašalec 2 (OCT2) ter prenašalca MATE1. *In vivo* lahko pride do medsebojnega delovanja abemaciklibа in klinično pomembnih substratov teh prenašalcev, kot je dofelitid ali kreatinin. Trenutno ni znano, ali lahko abemaciklib zmanjša učinkovitost sistemskih hormonskih kontraceptivov, zato se ženskam, ki uporabljajo sistemske hormonske kontraceptive, svetuje, da hkrati uporabljajo tudi mehansko metodo. **Neželeni učinki:** Najpogostejši neželeni učinki so driska, okužbe, nevtropenija, levkopenija, anemija, utrujenost, navzea, bruhanje in zmanjšanje apetita. *Zelo pogosti:* okužbe, nevtropenija, levkopenija, anemija, trombocitopenija, limfopenija, zmanjšanje apetita, glavobol, disgevzija, omotica, driska, bruhanje, navzea, stomatitis, alopecija, pruritus, izpuščaj, pireksija, utrujenost, povečana vrednost alanin-aminotransferaze, povečana vrednost aspartat-aminotransferaze. *Pogosti:* povečano solzenje, venska trombembolija, ILD/pnevmonitis, dispepsija, spremembe na nohtih, suha koža, mišična šibkost. *Občasni:* febrilna nevtropenija. **Rok uporabnosti** 3 leta. **Posebna navodila za shranjevanje** Za shranjevanje zdravila niso potrebna posebna navodila. **Imetnik dovoljenja za promet z zdravilom**: Eli Lilly Nederland B.V., Papendorpseweg 83, 3528BJ, Utrecht, Nizozemska. Datum prve odobritve dovoljenja za promet: 27. september 2018 **Datum zadnje revizije besedila**: 1.4.2022 **Režim izdaje:** Rp/Spec - Predpisovanje in izdaja zdravila je le na recept zdravnika specialista ustreznega področja medicine ali od njega pooblaščenega zdravnika.

Reference: 1. Povzetek glavnih značilnosti zdravila Verzenios, zadnja odobrena verzija.

Pomembno: Predpisovanje in izdaja zdravila je le na recept zdravnika specialista ustreznega področja medicine ali od njega pooblaščenega zdravnika. Pred predpisovanjem zdravila Verzenios si preberite zadnji veljavni Povzetek glavnih značilnosti zdravil. Podrobne informacije o zdravilu so objavljene na spletni strani Evropske agencije za zdravila http://www.ema.europa.eu

Eli Lilly farmacevtska družba, d.o.o., Dunajska cesta 167, 1000 Ljubljana, telefon 01 / 580 00 10, faks 01 / 569 17 05

PP-AL-SI-0166, 21.10.2022, Samo za strokovno javnost.

PR/BSI/BEN/2022/017

TANTUM VERDE®

benzidaminijev klorid

Za lajšanje bolečine in oteklin v ustni in žrelu, ki so posledica radiomukozitisa

Bistvene informacije iz Povzetka glavnih značilnosti zdravila

Tantum Verde 1,5 mg/ml oralno pršilo, raztopina
Tantum Verde 3 mg/ml oralno pršilo, raztopina

Sestava: 1,5 mg/ml: 1 ml raztopine vsebuje 1,5 mg benzidaminijevega klorida, kar ustreza 1,34 mg benzidamina. V enem razpršku je 0,17 ml raztopine. En razpršek vsebuje 0,255 mg benzidaminijevega klorida, kar ustreza 0,2278 mg benzidamina. **Sestava 3 mg/ml:** 1 ml raztopine vsebuje 3 mg benzidaminijevega klorida, kar ustreza 2,68 mg benzidamina. V enem razpršku je 0,17 ml raztopine. En razpršek vsebuje 0,51 mg benzidaminijevega klorida, kar ustreza 0,4556 mg benzidamina. **Terapevtske indikacije:** Samozdravljenje: Lajšanje bolečine in oteklin pri vnetju v ustni votlini in žrelu, ki so lahko posledica okužb in stanj po operaciji. Po nasvetu in navodilu zdravnika: Lajšanje bolečine in oteklin v ustni votlini in žrelu, ki so posledica radiomukozitisa. **Odmerjanje in način uporabe:** Uporaba: 2- do 6-krat na dan (vsake 1,5 do 3 ure). Odmerjanje 1,5 mg/ml: Odrasli: 4 do 8 razprškov 2- do 6-krat na dan. Pediatrična populacija: Mladostniki, stari od 12 do 18 let: 4-8 razprškov 2- do 6-krat na dan. Otroci od 6 do 12 let: 4 razprški 2- do 6-krat na dan. Otroci, mlajši od 6 let: 1 razpršek na 4 kg telesne mase; do največ 4 razprške 2- do 6-krat na dan. Odmerjanje 3 mg/ml: Odrasli: 2 do 4 razprški 2- do 6-krat na dan. Pediatrična populacija: Mladostniki, stari od 12 do 18 let: 2 do 4 razprški 2- do 6-krat na dan. Otroci od 6 do 12 let: 2 razprška 2- do 6-krat na dan. Otroci, mlajši od 6 let: 1 razpršek na 8 kg telesne mase; do največ 2 razprška 2- do 6-krat na dan. Starejši bolniki, bolniki z jetrno okvaro in bolniki z ledvično okvaro: niso potrebni posebni previdnostni ukrepi. Trajanje zdravljenja ne sme biti daljše od 7 dni. Način uporabe: Za orofaringealno uporabo. Zdravilo se razprši v usta in žrelo. **Kontraindikacije:** Preobčutljivost na učinkovino ali katero koli pomožno snov. **Posebna opozorila in previdnostni ukrepi:** Pri nekaterih bolnikih lahko resne bolezni povzročijo ustne/žrelne ulceracije. Če se simptomi v treh dneh ne izboljšajo, se mora bolnik posvetovati z zdravnikom ali zobozdravnikom, kot je primerno. Uporaba benzidamina ni priporočljiva za bolnike s preobčutljivostjo na salicilno kislino ali druga nesteroidna protivnetna zdravila. Pri bolnikih, ki imajo ali so imeli bronhialno astmo, lahko pride do bronhospazma. Pri takih bolnikih je potrebna previdnost. To zdravilo vsebuje 13,6 mg alkohola (etanola) v enem razpršku (0,17 ml), kar ustreza manj kot 0,34 ml piva oziroma 0,14 ml vina. Majhna količina alkohola v zdravilu ne bo imela nobenih opaznih učinkov. To zdravilo vsebuje metilparahidroksibenzoat (E218). Lahko povzroči alergijske reakcije (lahko zapoznele). To zdravilo vsebuje manj kot 1 mmol (23 mg) natrija v enem razpršku (0,17 ml), kar v bistvu pomeni 'brez natrija'. Zdravilo vsebuje aromo poprove mete z benzilalkoholom, cinamilalkoholom, citralom, citronelolom, geraniolom, izoevgenolom, linalolom, evgenolom in D-limonen, ki lahko povzročijo alergijske reakcije. Zdravilo z jakostjo 3 mg/ml vsebuje makrogolglicerol hidroksistearat 40. Lahko povzroči želodčne težave in drisko. **Medsebojno delovanje z drugimi zdravili in druge oblike interakcij:** Študij medsebojnega delovanja niso izvedli. **Nosečnost in dojenje:** O uporabi benzidamina pri nosečnicah in doječih ženskah ni zadostnih podatkov. Uporaba zdravila med nosečnostjo in dojenjem ni priporočljiva. **Vpliv na sposobnost vožnje in upravljanja strojev:** Zdravilo v priporočenem odmerku nima vpliva na sposobnost vožnje in upravljanja strojev. **Neželeni učinki:** Neznana pogostnost (ni mogoče oceniti iz razpoložljivih podatkov): anafilaktične reakcije, preobčutljivostne reakcije, odrevenelost, laringospazem, suha usta, navzea in bruhanje, oralna hipestezija, angioedem, fotosenzitivnost, pekoč občutek v ustih. Neposredno po uporabi se lahko pojavi občutek odrevenelosti v ustih in v žrelu. Ta učinek se pojavi zaradi načina delovanja zdravila in po kratkem času izgine. **Način in režim izdaje zdravila:** BRp-Izdaja zdravila je brez recepta v lekarnah in specializiranih prodajalnah. **Imetnik dovoljenja za promet:** Aziende Chimiche Riunite Angelini Francesco – A.C.R.A.F. S.p.A., Viale Amelia 70, 00181 Rim, Italija **Datum zadnje revizije besedila:** 05. 04. 2022

Pred svetovanjem ali izdajo preberite celoten Povzetek glavnih značilnosti zdravila.

Samo za strokovno javnost.

Datum priprave informacije: april 2022

ANGELINI

Odgovoren za trženje: Bonifar d.o.o.

Tagrisso

TAGRISSO® osimertinib

Za adjuvantno zdravljenje po popolni resekciji tumorja pri odraslih bolnikih z EGFRm NSCLC

Končna analiza DFS*

Zdravilo Tagrisso je v adjuvantnem zdravljenju bolnikov v stadijih IB-IIIA NSCLC doseglo mediano preživetje brez ponovitve bolezni 65,8 mesecev (DFS)[1]

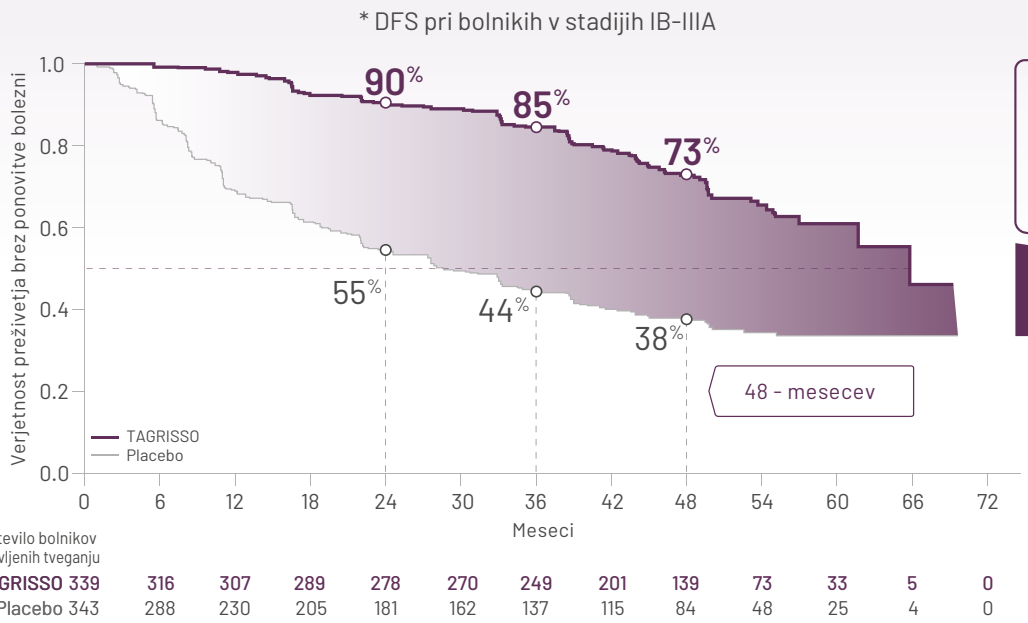

Število bolnikov izpostavljenih tveganju												
TAGRISSO 339	316	307	289	278	270	249	201	139	73	33	5	0
Placebo 343	288	230	205	181	162	137	115	84	48	25	4	0

73%
zmanjšano tveganje za smrt ali ponovitev bolezni

ROg - 0,27
(95% IZ: 0,21, 0,34)

Odstotek bolnikov živih in brez ponovitve bolezni po 48 mesecih

Stadij IB:	Stadij II:	Stadij IIIA:
80% vs 59%	**74%** vs 42%	**65%** vs 14%
ROg=0,41	ROg=0,34	ROg=0,20

* 65,8 mesecev pri bolnikih zdravljenih z zdravilom Tagrisso (95% IZ: 61,7.ND) v primerjavi z 28,1 meseca pri bolnikih zdravljenih s placebom (95% IZ: 22,1–35,0). Zrelost podatkov je bila v času analize 45%.

*Primarni izid učinkovitosti je bilo preživetje brez ponovitve bolezni (DFS - disease-free survival) po oceni raziskovalca v populaciji s stadijem II-IIIA. DFS po oceni raziskovalca v populaciji s stadijem IB-IIIA (celotna populacija) je bil sekundarni izid učinkovitosti.

* DFS... preživetje brez ponovitve bolezni

SKRAJŠAN POVZETEK GLAVNIH ZNAČILNOSTI ZDRAVILA

TAGRISSO 40 mg filmsko obložene tablete / **TAGRISSO 80 mg** filmsko obložene tablete

SESTAVA: Ena filmsko obložena tableta vsebuje 40 ali 80 mg osimertiniba. **INDIKACIJE:** Zdravilo Tagrisso je kot monoterapija indicirano za: adjuvantno zdravljenje po popolni resekciji tumorja pri odraslih bolnikih z nedrobnoceličnim rakom pljuč v stadiju IB-IIIA (NSCLC - non-small cell lung cancer), pri katerem ima tumorski receptor za epidermalni rastni faktor (EGFR - epidermal growth factor receptor) delecije eksona 19 ali substitucije eksona 21 (L858R). • prvo linijo zdravljenja odraslih bolnikov z lokalno napredovalim ali metastatskim nedrobnoceličnim rakom pljuč (NSCLC - "non-small-cell lung cancer"), katerega receptor za epidermalni rastni faktor (EGFR - "epidermal growth factor receptor") ima aktivirajoče mutacije. • zdravljenje odraslih bolnikov z lokalno napredovalim ali metastatskim NSCLC, pozitivnim za mutacijo T790M EGFR. **ODMERJANJE IN NAČIN UPORABE:** Zdravljenje z zdravilom Tagrisso mora uvesti zdravnik, ki ima izkušnje z zdravili za zdravljenje raka. Pri odločanju o uporabi zdravila Tagrisso je treba določiti stanje mutacije EGFR (v vzorcih tumorja pri adjuvantnem zdravljenju in v vzorcih tumorja ali plazme pri lokalno napredovalem ali metastatskem raku) z uporabo validirane testne metode. Odmerjanje: Priporočeni odmerek je 80 mg osimertiniba enkrat na dan. Bolniki na adjuvantnem zdravljenju morajo zdravilo jemati do ponovitve bolezni ali nesprejemljivih toksičnih učinkov. Zdravljenja, daljšega od 3 let, niso preučili. Bolniki z lokalno napredovalim ali metastatskim rakom pljuč morajo zdravilo jemati do napredovanja bolezni ali nesprejemljivih toksičnih učinkov. Če bolnik izpusti odmerek zdravila Tagrisso, ga mora vzeti, razen če je do naslednjega odmerka že manj kot 12 ur. Zdravilo Tagrisso je mogoče vzeti s hrano ali brez nje, vsak dan ob istem času. Prilagoditve odmerka: Glede na varnost in prenašanje pri posameznem bolniku je lahko potrebna prekinitev odmerjanja in/ali zmanjšanje odmerka. V primeru potrebe po zmanjšanju odmerka je treba odmerek zmanjšati na 40 mg enkrat na dan. Smernice za zmanjšanje odmerka v primeru neželenih učinkov/toksičnosti so navedene v preglednici v Povzetku glavnih značilnosti zdravila.To zdravilo je namenjeno za peroralno uporabo. Tableto je treba zaužiti celo z vodo in se je ne sme drobiti, lomiti ali gristi. **KONTRAINDIKACIJE:** Preobčutljivost na učinkovino ali katerokoli pomožno snov. Šentjanževke se ne sme uporabljati skupaj z zdravilom Tagrisso. **OPOZORILA IN PREVIDNOSTNI UKREPI**: Pri odločanju o uporabi zdravila TAGRISSO za adjuvantno zdravljenje bolnikov z NSCLC po popolni resekciji tumorja je pomembno določiti prisotnost mutacije EGFR (delecije eksona 19 (Ex19del) ali substitucije eksona 21 (L858R)). V kliničnem laboratoriju je treba opraviti validirano preiskavo tumorske DNK iz vzorca tkiva, pridobljenega z biopsijo ali kirurškim posegom. Pri odločanju o uporabi zdravila Tagrisso za zdravljenje lokalno napredovalega ali metastatskega NSCLC je pomembno določiti stanje mutacije T790M EGFR. Opraviti je treba validirano preiskavo tumorske DNK, dobljene iz vzorca tkiva, ali tumorske DNK v obtoku (ctDNA – circulating tumor DNA), dobljene iz vzorca plazme. Določitev prisotne mutacije EGFR (aktivirajoče mutacije EGFR pri prvi liniji zdravljenja ali mutacije T790M po napredovanju bolezni med zdravljenjem ali po zdravljenju z zaviralcem tirozin kinaze receptorja za epidermalni rastni faktor) v vzorcu tkiva ali plazme pomeni, da je bolnik primeren za zdravljenje z zdravilom TAGRISSO. A če je uporabljena preiskava za ctDNA iz plazme in je izvid negativen, je priporočljivo opraviti še preiskavo tkivnega vzorca, če je le mogoče. Pri preiskavah vzorcev plazme namreč obstaja možnost lažno negativnih rezultatov. Uporabiti se sme le robustne, zanesljive in občutljive preiskave z dokazano uporabnostjo za določanje stanja mutacije EGFR v tumorski DNK (iz vzorca tkiva ali plazme). O intersticijski bolezni pljuč (IBP) ali neželenih učinkih, podobnih IBP, so poročali pri 3,7 % od 1479 bolnikov, ki so v študijah ADAURA, FLAURA in AURA prejemali zdravilo Tagrisso. Pri zdravljenju lokalno napredovalega ali metastatskega raka so poročali o petih smrtnih primerih. Pri adjuvantnem zdravljenju niso poročali o smrtnih primerih. Pojavnost IBP je bila pri bolnikih japonske etnične pripadnosti 10,49 %, pri bolnikih azijske etnične pripadnosti 1,6 % in pri neazijskih bolnikih 2,5 %. Vse bolnike z akutnim nastankom in/ali nepojasnjenim poslabšanjem pljučnih simptomov (dispneja, kašelj, zvišana telesna temperatura) je treba skrbno pregledati, da bi izključili IBP. V času preiskovanja teh simptomov je treba zdravljenje s tem zdravilom prekiniti. Če je diagnosticirana IBP, je treba ukiniti zdravljenje z zdravilom Tagrisso in uvesti ustrezno zdravljenje, kot je potrebno. Ponovna uvedba zdravila Tagrisso pride v poštev le po skrbnem pretehtanju koristi in tveganj pri posameznem bolniku. Stevens-Johnsonov sindrom (SJS): V povezavi z zdravljenjem z zdravilom TAGRISSO so poročali o redkih primerih SJS. Pred uvedbo zdravljenja je treba bolnike seznaniti z znaki in simptomi SJS. Če se pojavijo znaki ali simptomi, ki nakazujejo SJS, je treba zdravljenje z zdravilom TAGRISSO nemudoma prekiniti ali končati. Podaljšanje intervala QTc: Bolnikom, zdravljenim z zdravilom Tagrisso, se pojavi podaljšanje intervala QTc. Takšno podaljšanje lahko poveča tveganje za ventrikularne tahiaritmije (npr. torsade de pointes) ali nenadno smrt. V študijah ADAURA, FLAURA ali AURA niso poročali o motnjah srčnega ritma. Uporabi osimertiniba se je treba pri bolnikih s prirojenim sindromom dolgega intervala QT izogniti, če je le mogoče. O rednih kontrolah elektrokardiograma (EKG) in elektrolitov je treba razmisliti pri bolnikih s kongestivnim srčnim popuščanjem, elektrolitskimi motnjami in prejemnikih zdravil, za katera je znano, da podaljšajo interval QTc. Prekinite uporabo pri bolnikih, ki se jim interval QTc podaljša preko 500 msec na vsaj 2 ločenih posnetkih EKG, in ga ne uporabljajte, dokler ni interval QTc manj kot 481 msec oziroma do njegove vrnitve na izhodiščno vrednost, če je izhodiščni interval QTc 481 msec ali več. Potem začnite zdravilo Tagrisso znova uporabljati v manjšem odmerku. Trajno ukinite zdravljenje z osimertinibom, če se bolniku pojavi podaljšanje intervala QTc v kombinaciji s čimer koli od naslednjega: torsade de pointes, polimorfna ventrikularna tahikardija, znaki/simptomi resne motnje srčnega ritma. Spremembe v krčljivosti srca: V kliničnih preskušanjih se je zmanjšanje iztisnega deleža levega prekata (LVEF "left ventricular ejection fraction") za ≥ 10 odstotnih točk ali na manj kot 50 % pojavilo pri 3,2 % (40/1233) bolnikov, zdravljenih z zdravilom TAGRISSO, ki so imeli LVEF izmerjen izhodiščno in vsaj še enkrat med obdobjem spremljanja. Pri bolnikih s srčnimi dejavniki tveganja in bolnikih s stanji, ki prizadenejo LVEF, je treba razmisliti o nadziranju delovanja srca, vključno z ocenjevanjem LVEF izhodiščno in med zdravljenjem. Pri bolnikih, ki se jim med zdravljenjem pojavijo pomembni srčni znaki ali simptomi, je treba razmisliti o nadziranju delovanja srca, vključno z ocenjevanjem LVEF. V s placebom nadzorovanem preskušanju adjuvantnega zdravljenja (ADAURA) se je zmanjšanje LVEF za ≥ 10 odstotnih točk ali na manj kot 50 % pojavilo pri 1,6 % (5/312) bolnikov, zdravljenih z zdravilom TAGRISSO, in 1,5 % (5/331) bolnikov, zdravljenih s placebom. Keratitis: O keratitisu so poročali pri 0,7 % bolnikov, zdravljenih z zdravilom Tagrisso v študijah ADAURA, FLAURA in AURA. Bolnike z znaki in simptomi, ki nakazujejo keratitis (na primer vnetje očesa, solzenje, občutljivost na svetlobo, zamegljen vid, bolečine v očesu in/ali pordelost očesa), je treba nemudoma napotiti k specialistu oftalmologu. Aplastična anemija: V povezavi z zdravljenjem z osimertinibom so poročali o redkih primerih aplastične anemije, vključno s smrtnimi primeri. Pred uvedbo zdravljenja je treba bolnike seznaniti z znaki in simptomi aplastične anemije, ki vključujejo, a niso omejeni le na dolgotrajno zvišano telesno temperaturo, podplutbe, krvavitve, bledico, okužbe in utrujenost. Če se pojavijo znaki in simptomi, ki kažejo na aplastično anemijo, je treba razmisliti o natančnem nadziranju bolnika ter o prekinitvi ali prenehanju zdravljenja z osimertinibom. Pri bolnikih s potrjeno aplastično anemijo je treba zdravljenje z osimertinibom ukiniti. Starost in telesna masa: Pri bolnikih starih nad 65 let ali bolnikih z telesno maso pod 50 kg je lahko prisotno povečano tveganje za pojav neželenih učinkov 3. ali višje stopnje. Pri teh bolnikih je priporočeno skrbno spremljanje. **MEDSEBOJNO DELOVANJE Z DRUGIMI ZDRAVILI:** Močni induktorji CYP3A lahko zmanjšajo izpostavljenost osimertinibu. Osimertinib lahko poveča izpostavljenost substratom BCRP in P-glikoproteina (P-gp). Študije in vitro so pokazale, da poteka presnova l. faze osimertiniba pretežno s CYP3A4 in CYP3A5. Podatki iz klinične farmakokinetične študije so pokazali, da ni verjetno, da bi zaviralci CYP3A4 vplivali na izpostavljenost osimertinibu. Dodatnih katalizacijskih encimov niso odkrili. Podatki klinične farmakokinetične študije o sočasni uporabi z rifampicinom kažejo, da se je sočasni uporabi močnih induktorjev CYP3A (npr. fenitoina, rifampicina, karbamazepina) in zdravila Tagrisso priporočljivo izogniti. Izpostavljenost osimertinibu lahko zmanjšajo tudi zmerni induktorji CYP3A4 (npr. bosentan, efavirenz, etravirin, modafinil), zato jih je treba uporabljati previdno oziroma se jim je treba izogniti, če je mogoče. Kliničnih podatkov, ki bi omogočali priporočilo za prilagoditev odmerka zdravila Tagrisso, ni na voljo. Sočasna uporaba šentjanževke je kontraindicirana. Glede na podatke klinične farmakokinetične študije je pri sočasni uporabi zdravila Tagrisso in rosuvastatina ter ostalih zdravil, katerih odstranjevanje je odvisno od BCRP in imajo ozek terapevtski indeks, treba bolnike skrbno spremljati glede znakov spremenjenega prenašanja zaradi večje izpostavljenosti sočasnemu zdravilu med prejemanjem zdravila Tagrisso. Tveganja za manjšo izpostavljenost hormonskim kontraceptivom ni mogoče izključiti. Bolnike, ki sočasno jemljejo zdravila, katerih odstranjevanje je odvisno od P-gp in imajo ozek terapevtski indeks (npr. digoksin, dabigatran, in aliskiren), je treba skrbno spremljati glede znakov spremenjenega prenašanja zaradi večje izpostavljenosti sočasnemu zdravilu v času prejemanja zdravila Tagrisso. **NEŽELENI UČINKI:** Podatki iz treh randomiziranih študij III. faze (ADAURA – adjuvantno zdravljenje, FLAURA – prva linija in AURA3 – le druga linija) in iz dveh študij z eno samo skupino (AURAex in AURA2 – druga linija ali več) in eni študiji I. faze (AURA1 – prva linija ali več) povzemajo izpostavljenost zdravilu Tagrisso pri 1479 bolnikih z nedrobnoceličnim rakom pljuč in pozitivno mutacijo EGFR. Večina neželenih učinkov je bila glede na resnost 1. ali 2. stopnje. Najpogostejši neželeni učinki zdravila so bili driska (47 %), izpuščaj (45 %), paronihija (33 %), suha koža (32 %) in stomatitis (24 %). V vseh študijah skupaj je bilo neželenih učinkov 3. stopnje 10 % in 4. stopnje 0,1 %. Med bolniki, ki so prejemali zdravilo Tagrisso 80 mg enkrat na dan, so zaradi neželenih učinkov odmerek zmanjšali 3,4 % bolnikom. Ukinitev uporabe zdravila zaradi neželenih učinkov je bilo 4,8 %. Zelo pogosti neželeni učinki: zmanjšan apetit, driska, stomatitis, izpuščaj, suha koža, paronihija, srbenje ter zmanjšano število levkocitov, limfocitov trombocitov in nevtrofilcev. Pogosti neželeni učinki: epistaksa, intersticijska bolezen pljuč, alopecija, urtikarija, sindrom palmarno-plantarne eritrodizestezije, zvišanje ravni kreatinina v krvi, zvišanje ravni kreatin fosfokinaze v krvi, zmanjšan iztisni delež levega prekata.
VRSTA IN VSEBINA OVOJNINE: Al/Al perforirani pretisni omoti za enkratni odmerek. Škatle z 28 x 1 tableto (4 pretisni omoti). **NAČIN IZDAJANJA ZDRAVILA:** samo na recept **DATUM REVIZIJE BESEDILA:** 6.10.2022 (SI-2632)
IMETNIK DOVOLJENJA ZA PROMET: AstraZeneca AB, S-151 85, Sodertalje, Švedska

Zdravilo Tagrisso v Sloveniji še ni razvrščeno na listo zdravil za adjuvantno zdravljenje po popolni resekciji tumorja pri odraslih bolnikih z nedrobnoceličnim rakom pljuč v stadiju IB-IIIA (NSCLC - non-small cell lung cancer), pri katerem ima tumorski receptor za epidermalni rastni faktor (EGFR - epidermal growth factor receptor) delecije eksona 19 ali substitucije eksona 21 (L858R).
Pred predpisovanjem, prosimo, preberite celoten povzetek glavnih značilnosti zdravila.
Dodatne informacije so na voljo pri družbi AstraZeneca UK Limited, Podružnica v Sloveniji, Verovškova 55, Ljubljana, telefon +386 1 51 35 600.

AstraZeneca

Reference: *1. Tsuboi M, Wu YL, Grohe C, et al. Osimertinib as adjuvant therapy in patients with resected EGFRm stage IB-IIIA NSCLC: updated results from ADAURA. Presented at: ESMO Congress 2022; September 9-13, 2022; Paris, France.*

Samo za strokovno javnost. Informacija pripravljena novembra 2022.

SI-24172

SEDAJ ODOBRENO PO VSAJ ENI PREDHODNI TERAPIJI NA PODLAGI ANTI-HER2[1]

ENHERTU®
trastuzumab derukstekan

NEPRIMERLJIVO PREŽIVETJE*
POSTAVLJA NOVE STANDARDE ZDRAVLJENJA RAZSEJANEGA HER2+ RAKA DOJK[2]

Zdravilo ENHERTU se uporablja v monoterapiji in je v raziskavi DESTINY-Breast03 dokazalo neprimerljivo podaljšanje PFS v primerjavi s trenutnim standardom zdravljenja (T-DM1). Poročali so o primerih intersticijske pljučne bolezni (ILD) in pnevmonitisa. Za diagnozo je ključno prepoznavanje simptomov, zato je bolnike treba spremljati in pričeti z zdravljenjem ob prvih znakih ILD.[1,2]

SKRAJŠAN POVZETEK GLAVNIH ZNAČILNOSTI ZDRAVILA

▼Za to zdravilo se izvaja dodatno spremljanje varnosti. Tako bodo hitreje na voljo nove informacije o njegovi varnosti. Zdravstvene delavce naprošamo, da poročajo o katerem koli domnevnem neželenem učinku zdravila.

ENHERTU 100 mg prašek za koncentrat za raztopino za infundiranje

SESTAVA: Ena viala praška za koncentrat za raztopino za infundiranje vsebuje 100 mg trastuzumab derukstekana. Po rekonstituciji ena viala s 5 ml raztopine vsebuje 20 mg/ml trastuzumab derukstekana. Trastuzumab derukstekan je konjugat protitelesa in zdravila, ki vsebuje humanizirano monoklonsko protitelo IgG1 proti HER2 z istim zaporedjem aminokislin, kot ga ima trastuzumab. Proizvajajo ga sesalske celice (ovarij kitajskega hrčka) in je prek razcepljivega veznika na tetrapeptidni bazi kovalentno vezan na DXd, ki je derivat eksatekana in zaviralec topoizomeraze I. Na vsako molekulo protitelesa je vezanih približno 8 molekul derukstekana. *Pomožne snovi:* L-histidin, L-histidinijev klorid monohidrat, saharoza, polisorbat 80. **TERAPEVTSKE INDIKACIJE:** ***Rak dojk:*** *HER2-pozitiven rak dojk:* Zdravilo Enhertu kot monoterapija je indicirano za zdravljenje odraslih bolnikov z neresektabilnim ali metastatskim HER2-pozitivnim rakom dojk, ki so pred tem že prejeli eno ali več shem zdravljenja na podlagi anti-HER2. *Rak dojk z nizkim statusom HER2:* Zdravilo Enhertu kot monoterapija je indicirano za zdravljenje odraslih bolnikov z neresektabilnim ali metastatskim rakom dojk z nizkim statusom HER2, ki so pred tem že prejeli kemoterapijo v prisotnosti metastaz ali pa se je pri njih bolezen ponovila med adjuvantno kemoterapijo ali znotraj 6 mesecev po njenem zaključku. ***Rak želodca:*** Zdravilo Enhertu v obliki monoterapije je indicirano za zdravljenje odraslih bolnikov z napredovalim HER2-pozitivnim adenokarcinomom želodca ali gastroezofagealnega prehoda, ki so pred tem že prejeli shemo na podlagi trastuzumaba. **ODMERJANJE IN NAČIN UPORABE:** Zdravilo Enhertu mora predpisati zdravnik in njegovo dajanje nadzorovati zdravstveni delavec, ki sta izkušena v uporabi zdravil proti raku. Za preprečitev napak, povezanih z zdravili, je pomembno, da preverite nalepke na vialah in se prepričate, da je zdravilo, ki se pripravlja in daje, res zdravilo Enhertu (trastuzumab derukstekan), in ne trastuzumab ali trastuzumab emtanzin. Zdravilo Enhertu se ne sme zamenjati s trastuzumabom ali trastuzumab emtanzinom. Bolniki, ki se zdravijo s trastuzumab derukstekanom zaradi *HER2-pozitivnega raka dojk, raka želodca ali gastroezofagealnega prehoda*, morajo imeti dokumentiran HER2-pozitiven status tumorja, ki je opredeljen kot ocena 3 + na podlagi imunohistokemije (IHC) ali razmerje ≥ 2,0 na podlagi *in situ* hibridizacije (ISH) ali fluorescenčne *in situ* hibridizacije (FISH), ocenjeno z *in vitro* diagnostičnim (IVD) medicinskim pripomočkom z oznako CE. Bolniki, ki se zdravijo s trastuzumab derukstekanom zaradi *raka dojk z nizkim statusom HER2*, morajo imeti dokumentiran nizek status HER2 tumorja, ki je opredeljen kot ocena IHC 1+ ali IHC 2+/ISH-, ocenjeno z IVD z oznako CE. Če IVD z oznako CE ni na voljo, je treba status HER2 oceniti z drugim potrjenim testom Odmerjanje: *Rak dojk:* Priporočeni odmerek zdravila Enhertu je 5,4 mg/kg, ki se daje z intravensko infuzijo enkrat vsake 3 tedne (21-dnevni cikel) do napredovanja bolezni ali nesprejemljive toksičnosti. *Rak želodca:* Priporočeni odmerek zdravila Enhertu je 6,4 mg/kg, ki se daje z intravensko infuzijo enkrat vsake 3 tedne (21-dnevni cikel) do napredovanja bolezni ali nesprejemljive toksičnosti. Začetni odmerek je treba dati z 90-minutno intravensko infuzijo. Če bolnik prejšnjo infuzijo dobro prenaša, se lahko naslednji odmerki zdravila Enhertu dajejo kot 30-minutne infuzije. Hitrost infundiranja zdravila Enhertu je treba zmanjšati ali infundiranje prekiniti, če se pri bolniku razvijejo simptomi, povezani z infuzijo. V primeru hudih reakcij na infuzijo je treba zdravilo Enhertu trajno ukiniti. Premedikacija: Zdravilo Enhertu je emetogeno, kar vključuje zapoznelo navzeo in/ali bruhanje. Pred vsakim odmerkom zdravila Enhertu je treba bolnike premedicirati s kombiniranim režimom dveh ali treh zdravil (npr. deksametazon z antagonistom receptorjev 5-HT3 in/ali antagonistom receptorjev NK1 ter drugimi zdravili, kot je indicirano) za preprečevanje navzee in bruhanja zaradi kemoterapije. Prilagajanje odmerka: Obvladovanje neželenih učinkov lahko zajema začasno prekinitev uporabe, zmanjšanje odmerka ali ukinitev zdravljenja z zdravilom Enhertu, skladno s smernicami, podanimi v povzetku glavnih značilnosti zdravila (preglednici 1 in 2). Po zmanjšanju odmerka zdravila Enhertu se odmerek ne sme več ponovno povečati. Načrt zmanjševanja odmerka: Priporočeni začetni odmerek je 5,4 mg/kg pri raku dojk oz. 6,4 mg/kg pri raku želodca; prvo zmanjšanje odmerka (4,4 mg/kg oz. 5,4 mg/kg), drugo zmanjšanje odmerka (3,2 mg/kg oz. 4,4 mg/kg), pri potrebi po nadaljnjem zmanjšanju odmerka ukinite zdravljenje. *Prosimo, glejte celoten povzetek glavnih značilnosti zdravila Enhertu za prilagajanje odmerka zaradi neželenih učinkov: intersticijska pljučna bolezen (IPB)/pnevmonitis* (asimptomatska IPB/asimptomatski pnevmonitis (stopnja 1), simptomatska IPB/simptomatski pnevmonitis (stopnja 2 ali višja)), *nevtropenija* (stopnja 3 (manj kot 1,0-0,5 × 10^9/l), stopnja 4 (manj kot 0,5 × 10^9/l)), *febrilna nevtropenija* (absolutno število nevtrofilcev manj kot 1,0 × 10^9/l in telesna temperatura, višja od 38,3 °C, ali telesna temperatura 38 °C ali višja, ki vztraja več kot eno uro), *zmanjšan iztisni delež levega prekata* (LVEF) (LVEF več kot 45 % in absolutno zmanjšanje glede na izhodiščno vrednost za 10 % do 20 %; LVEF 40 % do 45 %; LVEF manj kot 40 % ali absolutno zmanjšanje glede na izhodiščno vrednost za več kot 20 %; simptomatično kongestivno srčno popuščanje). Zakasnjen ali izpuščen odmerek: Če se načrtovani odmerek zakasni ali izpusti, ga je treba dati takoj, ko je mogoče, brez čakanja na naslednji načrtovani cikel. Časovni načrt dajanja je treba prilagoditi, da se ohrani 3-tedenski razmik med odmerki. Infuzijo je treba dati s hitrostjo in odmerkom, ki ga je bolnik prenašal pri zadnji infuziji. Posebne populacije: *Starejši:* Pri bolnikih, starih 65 let ali starejših, prilagajanje odmerka zdravila Enhertu ni potrebno. Podatki pri bolnikih, starih ≥ 75 let, so omejeni. *Okvara ledvic:* Prilagajanje odmerka pri bolnikih z blago (očistek kreatinina [CLcr] ≥ 60 in < 90 ml/min) ali zmerno (CLcr ≥ 30 in < 60 ml/min) okvaro ledvic ni potrebno. Morebitne potrebe po prilagajanju odmerka pri bolnikih s hudo okvaro ledvic ali končno ledvično odpovedjo ni mogoče opredeliti, ker je bila huda okvara ledvic v kliničnih študijah izključitveni kriterij. Pri bolnikih z zmerno okvaro ledvic so opazili višjo pogostnost IPB stopnje 1 in 2/pnevmonitisa, ki sta vodila do zvečanja števila prekinitev zdravljenja. Pri bolnikih z zmerno okvaro ledvic v izhodišču, ki so prejemali zdravilo Enhertu 6,4 mg/kg, so ugotovili večjo pogostnost resnih neželenih učinkov kot pri tistih z normalnim delovanjem ledvic. Bolnike z zmerno ali hudo okvaro ledvic je treba natančno spremljati glede neželenih učinkov, vključno z IPB/pnevmonitisom. *Okvara jeter:* Pri bolnikih, ki imajo celokupni bilirubin ≤ 1,5-kratnik zgornje meje normalnih vrednosti (ZMN), ne glede na vrednost aspartat transaminaze (AST), odmerka ni treba prilagajati. Morebitne potrebe po prilagajanju odmerka pri bolnikih, ki imajo celokupni bilirubin > 1,5-kratnik ZMN, ne glede na vrednost AST, ni mogoče opredeliti zaradi pomanjkanja podatkov. Zato je treba te bolnike natančno spremljati. Način uporabe: Zdravilo Enhertu je za intravensko uporabo. Zdravstveni delavec ga mora rekonstituirati in razredčiti. Treba ga je dati z intravenskim infundiranjem. Zdravilo Enhertu se ne sme dati kot hitro intravensko injekcijo ali bolus. **KONTRAINDIKACIJE:** Preobčutljivost na učinkovino ali katero koli pomožno snov. **POSEBNA OPOZORILA IN PREVIDNOSTNI UKREPI:** Intersticijska pljučna bolezen/pnevmonitis: Pri zdravilu Enhertu so poročali o primerih intersticijske pljučne bolezni (IPB) in/ali pnevmonitisa. Nekateri primeri so bili smrtni. Bolnikom je treba naročiti, naj takoj poročajo o kašlju, dispneji, zvišani telesni temperaturi in/ali katerih koli novih dihalnih simptomih ali poslabšanju obstoječih. Bolnike je treba spremljati glede znakov in simptomov IPB/pnevmonitisa. Dokaze za IPB/pnevmonitis je treba takoj proučiti. Bolnike s sumom na IPB/pnevmonitis je treba oceniti z radiografskimi posnetki, najbolje z računalniško tomografijo (CT). Treba je razmisliti o posvetu s pulmologom. Nevtropenija: V kliničnih študijah z zdravilom Enhertu so poročali o primerih nevtropenije, vključno s primeri febrilne nevtropenije s smrtnim izidom. Pred uvedbo zdravila Enhertu in pred vsakim odmerkom ter vsakič, ko je klinično indicirano, je treba preveriti celotno krvno sliko. Morda bo treba začasno prekiniti dajanje zdravila Enhertu ali zmanjšati odmerek, odvisno od tega, kako huda je nevtropenija. Zmanjšanje iztisnega deleža levega prekata: Pri zdravljenjih anti-HER2 so poročali o zmanjšanem iztisnem deležu levega prekata (LVEF). Pred uvedbo zdravljenja z zdravilom Enhertu in v rednih intervalih med njim (v skladu s kliničnimi indikacijami) je treba izvesti standardne preiskave delovanja srca (ehokardiografija ali slikanje MUGA) za oceno LVEF. Zmanjšanje LVEF je treba obvladovati s prekinitvami zdravljenja. Zdravljenje z zdravilom Enhertu je treba trajno ukiniti, če se potrdi LVEF manj kot 40 % ali absolutno zmanjšanje glede na izhodiščno vrednost za več kot 20 %. Zdravilo Enhertu je treba trajno ukiniti pri bolnikih s simptomatskim kongestivnim srčnim popuščanjem. Embrio-fetalna toksičnost: Zdravilo Enhertu lahko ima škodljiv vpliv na plod, če se da nosečnici. Pri ženskah v rodni dobi je treba pred uvedbo zdravljenja z zdravilom Enhertu preveriti status nosečnosti. Bolnice je treba seznaniti z možnimi tveganji za plod. Ženskam v rodni dobi je treba svetovati, da uporabljajo učinkovito kontracepcijo med zdravljenjem in še vsaj 7 mesecev po zadnjem odmerku zdravila Enhertu. Moškim bolnikom s partnerkami v rodni dobi je treba svetovati, da uporabljajo učinkovito kontracepcijo med zdravljenjem z zdravilom Enhertu in še vsaj 4 mesece po zadnjem odmerku zdravila Enhertu. Bolniki z zmerno ali hudo okvaro jeter: Zdravilo Enhertu je treba pri bolnikih z zmerno in hudo okvaro jeter dajati previdno. **MEDSEBOJNO DELOVANJE Z DRUGIMI ZDRAVILI IN DRUGE OBLIKE INTERAKCIJ:** Pri sočasnem dajanju trastuzumab derukstekana z zdravili, ki so zaviralci CYP3A ali OATP1B ali prenašalcev P-gp, odmerka ni treba prilagajati. **PLODNOST, NOSEČNOST IN DOJENJE:** Nosečnost: Dajanje zdravila Enhertu nosečnicam se ne priporoča. Bolnice je treba seznaniti z možnimi tveganji za plod, preden zanosijo. Ženske, ki zanosijo, se morajo takoj obrniti na zdravnika. Če ženska zanosi med zdravljenjem z zdravilom Enhertu ali v obdobju 7 mesecev po zadnjem odmerku zdravila Enhertu, se priporoča natančno spremljanje. Dojenje: Ni znano, ali se trastuzumab derukstekan izloča v materino mleko. Humani IgG se izloča v materino mleko in potencial za absorpcijo in resne neželene učinke na dojenčka ni znan. Zato ženske ne smejo dojiti med zdravljenjem z zdravilom Enhertu in še 7 mesecev po zadnjem odmerku. Odločiti se je treba med prenehanjem dojenja in prenehanjem zdravljenja z zdravilom Enhertu, pri čemer je treba pretehtati prednosti dojenja za otroka in prednosti zdravljenja za mater. Plodnost: Namenskih študij plodnosti s trastuzumab derukstekanom niso izvedli. Ni znano, ali so trastuzumab derukstekan ali njegovi presnovki prisotni v semenski tekočini. Pred začetkom zdravljenja je treba moškim bolnikom svetovati, da se posvetujejo o možnosti shranjevanja semena. Moški bolniki v celotnem obdobju zdravljenja in še najmanj 4 mesece po zadnjem odmerku zdravila Enhertu ne smejo zamrzniti ali darovati semena. **NEŽELENI UČINKI:** *Zdravilo Enhertu 5,4 mg/kg:* Združeno varnostno populacijo so ocenili pri bolnikih, ki so v kliničnih študijah dobili vsaj en odmerek 5,4 mg/kg zdravila Enhertu (N = 944) zaradi različnih vrst tumorjev. Mediani čas trajanja zdravljenja v tej združeni populaciji je bil 39,6 meseca (razpon: 0,2-37,9 meseca). *Zelo pogosti:* okužba zgornjih dihal, anemija, nevtropenija, trombocitopenija, levkopenija, zmanjšan apetit, hipokaliemija, glavobol, omotica, intersticijska pljučna bolezen, kašelj, dispneja, epistaksa, navzea, bruhanje, driska, zaprtje, bolečina v trebuhu, stomatitis, dispepsija, zvišane transaminaze, alopecija, izpuščaj, mišično-skeletna bolečina, utrujenost, pireksija, zmanjšanje telesne mase, zmanjšan iztisni delež. *Pogosti:* pljučnica, limfopenija, febrilna nevtropenija, dehidracija, disgevzija, zamegljen vid, abdominalna distenzija, flatulenca, gastritis, pruritus, hiperpigmentacija kože, perifermni edem, zvišana alkalna fosfataza v krvi, zvišan bilirubin v krvi, zvišan kreatinin v krvi, reakcije povezane z infuzijo. *Zdravilo Enhertu 6,4 mg/kg:* Združeno varnostno populacijo so ocenili za bolnike, ki so v kliničnih študijah dobili vsaj en odmerek 6,4 mg/kg zdravila Enhertu (N = 619) zaradi različnih vrst tumorjev. Mediani čas trajanja zdravljenja v tej združeni populaciji je bil 5,6 meseca (razpon: 0,7-41,0 meseca). *Zelo pogosti:* okužba zgornjih dihal, pljučnica, anemija, nevtropenija, trombocitopenija, levkopenija, limfopenija, zmanjšan apetit, hipokaliemija, glavobol, disgevzija, intersticijska pljučna bolezen, kašelj, navzea, bruhanje, driska, zaprtje, bolečina v trebuhu, stomatitis, zvišane transaminaze, alopecija, mišično-skeletna bolečina, utrujenost, pireksija, perifermni edem, zmanjšanje telesne mase, zmanjšan iztisni delež. *Pogosti:* febrilna nevtropenija, dehidracija, omotica, zameglјen vid, dispneja, epistaksa, dispepsija, izpuščaj, pruritus, hiperpigmentacija kože, zvišana alkalna fosfataza v krvi, zvišan bilirubin v krvi, zvišan kreatinin v krvi, reakcije povezane z infuzijo. **IMETNIK DOVOLJENJA ZA PROMET Z ZDRAVILOM:** Daiichi Sankyo Europe GmbH, Zielstattstrasse 48, 81379 München, Nemčija **DATUM ZADNJE REVIZIJE BESEDILA:** 23. 1. 2023 (SI-2799) **REŽIM PREDPISOVANJA IN IZDAJE:** H **Prosimo, da pred predpisovanjem preberete celoten povzetek glavnih značilnosti zdravila.** Dodatne informacije so na voljo pri podjetju AstraZeneca UK Limited, Podružnica v Sloveniji, Verovškova 55, 1000 Ljubljana, telefon: 01/51 35 600.

* zmanjšanje tveganja za napredovanje bolezni ali smrti (PFS)

** tveganje za napredovanje bolezni ob zdravljenju z zdravilom ENHERTU v primerjavi s T-DM1 (HR: 0,28; 95 % IZ: 0,22-0,37; p<0,000001, ključni opazovani dogodek raziskave: PFS glede na BICR;)[1,2]

***po oceni raziskovalca je mediani PFS znašal **25,1 mesecev** pri bolnikih, ki so prejemali ENHERTU, v primerjavi s **7,2 mesecev** pri bolnikih zdravljenih s T-DM1 (HR: 0,26; 95 % IZ: 0,20, 0,35; sekundarni opazovani dogodek;)[2]

PFS - preživetje brez napredovanja bolezni, **mPFS** - mediano preživetje brez napredovanja bolezni, **T-DM1** - trastuzumab emtanzin, **BICR** - ocena slepega neodvisnega centralnega pregleda, **IZ** - interval zaupanja, **HR** - razmerje ogroženosti

Literatura: 1. Povzetek glavnih značilnosti zdravila ENHERTU, 23. 1. 2023 **2.** Cortes J et al; Trastuzumab Deruxtecan versus Trastuzumab Emtansine for Breast Cancer; NEJM 2022;386(12):1143-1154

Zdravilo Enhertu v Sloveniji še ni razvrščeno na listo zdravil.

Daiichi-Sankyo | AstraZeneca

Datum priprave materiala: februar 2023. Samo za strokovno javnost. SI-2807

5 NA NOVO razvrščenih indikacij:[1]

KEYTRUDA®
(pembrolizumab, MSD)

- **MELANOM,** adjuvantno zdravljenje melanoma v stadiju IIB/IIC[2]
- **RAK LEDVIČNIH CELIC,** adjuvantno zdravljenje po nefrektomiji[2]
- **KOLOREKTALNI RAK,** z MSI-H ali dMMR, metastatski, samostojno zdravljenje v 1L[2]
- **TROJNO NEGATIVNI RAK DOJK:**
  – v kombinaciji s kemoterapijo za neoadjuvantno, v nadaljevanju samostojno adjuvantno zdravljenje lokalno napredovalega TNRD ali TNRD v zgodnjem stadiju z visokim tveganjem za ponovitev bolezni[2]
  – v kombinaciji s kemoterapijo za zdravljenje lokalno ponovljenega neoperabilnega ali metastatskega TNRD z PD-L1 CPS ≥ 10[2]

Okrajšave: MSI-H - visoka mikrosatelitska nestabilnost; dMMR - pomankljivo popravljanje neujemanja pri podvojevanju DNA; 1L - prva linija zdravljenja; TNRD - trojno negativni rak dojk

Referenci: 1. www.zzzs.si; https://www.zzzs.si/zzzs-api/e-gradiva/vsa-gradiva/?vrsta=BR3A2Q326 (22.12.2022) 2. KEYTRUDA SPC

Ime zdravila: KEYTRUDA 25 mg/ml koncentrat za raztopino za infundiranje vsebuje pembrolizumab. Terapevtske indikacije: Zdravilo KEYTRUDA je kot samostojno zdravljenje indicirano za zdravljenje: odraslih in mladostnikov, starih 12 let ali več, z napredovalim (neoperabilnim ali metastatskim) melanomom; za adjuvantno zdravljenje odraslih in mladostnikov, starih 12 let ali več, z melanomom v stadiju IIB, IIC ali III, in sicer po popolni kirurški odstranitvi; metastatskega nedrobnoceličnega pljučnega raka (NSCLC) v prvi liniji zdravljenja pri odraslih, ki imajo tumorje z ≥ 50 % izraženostjo PD-L1 (TPS) in brez pozitivnih tumorskih mutacij EGFR ali ALK; lokalno napredovalega ali metastatskega NSCLC pri odraslih, ki imajo tumorje z ≥ 1 % izraženostjo PD-L1 (TPS) in so bili predhodno zdravljeni z vsaj eno shemo kemoterapije, bolniki s pozitivnimi tumorskimi mutacijami EGFR ali ALK so pred prejemom zdravila KEYTRUDA morali prejeti tudi tarčno zdravljenje; odraslih in pediatričnih bolnikov, starih 3 leta ali več, s ponovljenim ali neodzivnim klasičnim Hodgkinovim limfomom (cHL), pri katerih avtologna presaditev matičnih celic (ASCT) ni bila uspešna, ali po najmanj dveh predhodnih zdravljenjih kadar ASCT ne pride v poštev kot možnost zdravljenja; lokalno napredovalega ali metastatskega urotelijskega raka pri odraslih, predhodno zdravljenih s kemoterapijo, ki je vključevala platino; lokalno napredovalega ali metastatskega urotelijskega raka pri odraslih, ki niso primerni za zdravljenje s kemoterapijo, ki vsebuje cisplatin in imajo tumorje z izraženostjo PD-L1 ≥ 10, ocenjeno s kombinirano pozitivno oceno (CPS); ponovljenega ali metastatskega ploščatoceličnega raka glave in vratu (HNSCC) pri odraslih, ki imajo tumorje z ≥ 50 % izraženostjo PD-L1 (TPS), in pri katerih je bolezen napredovala med zdravljenjem ali po zdravljenju s kemoterapijo, ki je vključevala platino; za adjuvantno zdravljenje odraslih z rakom ledvičnih celic s povišanim tveganjem za ponovitev bolezni po nefrektomiji, ali po nefrektomiji in kirurški odstranitvi metastatskih lezij, za zdravljenje odraslih z MSI-H (microsatellite instability-high) ali dMMR (mismatch repair deficient) kolorektalnim rakom v naslednjih terapevtskih okoliščinah: prva linija zdravljenja metastatskega kolorektalnega raka; zdravljenje neoperabilnega ali metastatskega kolorektalnega raka po predhodnem kombiniranem zdravljenju, ki je temeljilo na fluoropirimidinu; in za zdravljenje MSI-H ali dMMR tumorjev pri odraslih z: napredovalim ali ponovljenim rakom endometrija, pri katerih je bolezen napredovala med ali po predhodnem zdravljenju, ki je vključevalo platino, v katerih koli terapevtskih okoliščinah, in ki niso kandidati za kurativno operacijo ali obsevanje; neoperabilnim ali metastatskim rakom želodca, tankega črevesa ali žolčnika in žolčnih vodov, pri katerih je bolezen napredovala med ali po vsaj enem predhodnem zdravljenju. Zdravilo KEYTRUDA je kot samostojno zdravljenje ali v kombinaciji s kemoterapijo s platino in 5-fluorouracilom (5-FU) indicirano za prvo linijo zdravljenja metastatskega ali neoperabilnega ponovljenega ploščatoceličnega raka glave in vratu pri odraslih, ki imajo tumorje z izraženostjo PD-L1 s CPS ≥ 1. Zdravilo KEYTRUDA je v kombinaciji s pemetreksedom in kemoterapijo na osnovi platine indicirano za prvo linijo zdravljenja metastatskega neploščatoceličnega NSCLC pri odraslih, pri katerih tumorji nimajo pozitivnih mutacij EGFR ali ALK; v kombinaciji s karboplatinom in bodisi paklitakselom bodisi nab-paklitakselom je indicirano za prvo linijo zdravljenja metastatskega ploščatoceličnega NSCLC pri odraslih; v kombinaciji z aksitinibom ali v kombinaciji z lenvatinibom je indicirano za prvo linijo zdravljenja napredovalega raka ledvičnih celic (RCC) pri odraslih; v kombinaciji s kemoterapijo s platino in fluoropirimidinom je indicirano za prvo linijo zdravljenja lokalno napredovalega neoperabilnega ali metastatskega raka požiralnika ali HER-2 negativnega adenokarcinoma gastroezofagealnega prehoda pri odraslih, ki imajo tumorje z izraženostjo PD-L1 s CPS ≥ 10; v kombinaciji s kemoterapijo za neoadjuvantno zdravljenje, in v nadaljevanju kot samostojno adjuvantno zdravljenje po kirurškem posegu, je indicirano za zdravljenje odraslih z lokalno napredovalim trojno negativnim rakom dojk ali trojno negativnim rakom dojk v zgodnjem stadiju z visokim tveganjem za ponovitev bolezni; v kombinaciji s kemoterapijo je indicirano za zdravljenje lokalno ponovljenega neoperabilnega ali metastatskega trojno negativnega raka dojk pri odraslih, ki imajo tumorje z izraženostjo PD-L1 s CPS ≥ 10 in predhodno niso prejeli kemoterapije za metastatsko bolezen; v kombinaciji z lenvatinibom je indicirano za zdravljenje napredovalega ali ponovljenega raka endometrija (EC) pri odraslih z napredovalo boleznijo med ali po predhodnem zdravljenju s kemoterapijo, ki je vključevala platino, v katerih koli terapevtskih okoliščinah, in ki niso kandidati za kurativno operacijo ali obsevanje; v kombinaciji s kemoterapijo, z bevacizumabom ali brez njega, je indicirano za zdravljenje persistentnega, ponovljenega ali metastatskega raka materničnega vratu pri odraslih bolnicah, ki imajo tumorje z izraženostjo PD-L1 s CPS ≥ 1. **Odmerjanje in način uporabe:** Testiranje PD-L1: Če je navedeno v indikaciji, je treba izbiro bolnika za zdravljenje z zdravilom KEYTRUDA na podlagi izraženosti PD-L1 tumorja potrditi z validirano preiskavo. Testiranje MSI/MMR: Če je navedeno v indikaciji, je treba izbiro bolnika za zdravljenje z zdravilom KEYTRUDA na podlagi MSI-H/dMMR statusa tumorja potrditi z validirano preiskavo. Odmerjanje: Priporočeni odmerek zdravila KEYTRUDA pri odraslih je bodisi 200 mg na 3 tedne ali 400 mg na 6 tednov, apliciran z intravensko infuzijo v 30 minutah. Priporočeni odmerek zdravila KEYTRUDA za samostojno zdravljenje pri pediatričnih bolnikih s cHL, starih 3 leta ali več, ali bolnikih z melanomom, starih 12 let ali več, je 2 mg/kg telesne mase (do največ 200 mg) na 3 tedne, apliciran z intravensko infuzijo v 30 minutah. Za uporabo v kombinaciji glejte povzetke glavnih značilnosti zdravil sočasno uporabljenih zdravil. Če se uporablja kot del kombiniranega zdravljenja skupaj z intravensko kemoterapijo, je treba zdravilo KEYTRUDA aplicirati prvo. Bolnike je treba zdraviti do napredovanja bolezni ali nesprejemljivih toksičnih učinkov (in do maksimalnega trajanja zdravljenja, če je le to določeno za indikacijo). Pri adjuvantnem zdravljenju melanoma ali RCC je treba zdravilo uporabljati do ponovitve bolezni, pojava nesprejemljivih toksičnih učinkov oziroma mora zdravljenje trajati do enega leta. Za neoadjuvantno in adjuvantno zdravljenje TNBC morajo bolniki neoadjuvantno prejeti zdravilo KEYTRUDA v kombinaciji s kemoterapijo, in sicer 8 odmerkov po 200 mg na 3 tedne ali 4 odmerke po 400 mg na 6 tednov, ali do napredovanja bolezni, ki izključuje definitivni kirurški poseg, ali do pojava nesprejemljivih toksičnih učinkov, čemur sledi adjuvantno zdravljenje z zdravilom KEYTRUDA kot samostojnim zdravljenjem, in sicer 9 odmerkov po 200 mg na 3 tedne ali 5 odmerkov po 400 mg na 6 tednov ali do ponovitve bolezni ali pojava nesprejemljivih toksičnih učinkov. Bolniki, pri katerih pride do napredovanja bolezni, ki izključuje definitivni kirurški poseg, ali do nesprejemljivih toksičnih učinkov povezanih z zdravilom KEYTRUDA kot neoadjuvantnim zdravljenjem v kombinaciji s kemoterapijo, ne smejo prejeti zdravila KEYTRUDA kot samostojnega zdravljenja za adjuvantno zdravljenje. Če je aksitinib uporabljen v kombinaciji s pembrolizumabom, se lahko razmisli o povečanju odmerka aksitiniba nad začetnih 5 mg v presledkih šest tednov ali več. V primeru uporabe v kombinaciji z lenvatinibom je treba zdravljenje z enim ali obema zdraviloma prekiniti, kot je primerno. Uporabo lenvatiniba je treba zadržati, odmerek zmanjšati ali prenehati z uporabo, v skladu z navodili v povzetku glavnih značilnosti zdravila za lenvatinib, in sicer za kombinacijo s pembrolizumabom. Pri bolnikih starih ≥ 65 let, bolnikih z blago do zmerno okvaro ledvic, bolnikih z blago ali zmerno okvaro jeter prilagoditev odmerka ni potrebna. Odložitev odmerka ali ukinitev zdravljenja: Zmanjšanje odmerka zdravila KEYTRUDA ni priporočljivo. Za obvladovanje neželenih učinkov je treba uporabo zdravila KEYTRUDA zadržati ali ukiniti, prosimo, glejte celoten Povzetek glavnih značilnosti zdravila. **Kontraindikacije:** Preobčutljivost na učinkovino ali katero koli pomožno snov. **Povzetek posebnih opozoril, previdnostnih ukrepov, interakcij in neželenih učinkov:** Imunsko pogojeni neželeni učinki (pnevmonitis, kolitis, hepatitis, nefritis, endokrinopatije, neželeni učinki na kožo in drugi): Pri bolnikih, ki so prejemali pembrolizumab, so se pojavili imunsko pogojeni neželeni učinki, vključno s hudimi in smrtnimi primeri. Večina imunsko pogojenih neželenih učinkov, ki so se pojavili med zdravljenjem s pembrolizumabom, je bila reverzibilnih in so jih obvladali s prekinitvami uporabe pembrolizumaba, uporabo kortikosteroidov in/ali podporno oskrbo. Pojavijo se lahko tudi po zadnjem odmerku pembrolizumaba in hkrati prizadanejo več organskih sistemov. V primeru suma na imunsko pogojene neželene učinke je treba poskrbeti za ustrezno oceno za potrditev etiologije oziroma izključitev drugih vzrokov. Glede na izrazitost neželenega učinka je treba zadržati uporabo pembrolizumaba in uporabiti kortikosteroide – za natančna navodila, prosimo, glejte Povzetek glavnih značilnosti zdravila Keytruda. Zdravljenje s pembrolizumabom lahko poveča tveganje za zavrnitev pri prejemnikih presadkov čvrstih organov. Pri bolnikih, ki so prejemali pembrolizumab, so poročali o hudih z infuzijo povezanih reakcijah, vključno s preobčutljivostjo in anafilaksijo. Pembrolizumab se iz obtoka odstrani s katabolizmom, zato presnovnih medsebojnih delovanj zdravil ni pričakovati. Uporabi sistemskih kortikosteroidov ali imunosupresivov pred uvedbo pembrolizumaba se je treba izogibati, ker lahko vplivajo na farmakodinamično aktivnost in učinkovitost pembrolizumaba. Vendar pa je kortikosteroide ali druge imunosupresive mogoče uporabiti za zdravljenje imunsko pogojenih neželenih učinkov. Kortikosteroide je mogoče uporabiti tudi kot premedikacijo, če je pembrolizumab uporabljen v kombinaciji s kemoterapijo, kot antiemetično profilakso in/ali za ublažitev neželenih učinkov, povezanih s kemoterapijo. Ženske v rodni dobi morajo med zdravljenjem s pembrolizumabom in vsaj še 4 mesece po zadnjem odmerku pembrolizumaba uporabljati učinkovito kontracepcijo, med nosečnostjo in dojenjem se ga ne sme uporabljati. Varnost pembrolizumaba pri samostojnem zdravljenju so v kliničnih študijah ocenili pri 7.631 bolnikih, ki so imeli različne vrste raka, s štirimi odmerki (2 mg/kg telesne mase na 3 tedne, 200 mg na 3 tedne in 10 mg/kg telesne mase na 2 ali 3 tedne). V tej populaciji bolnikov je mediani čas opazovanja znašal 8,5 meseca (v razponu od 1 dneva do 39 mesecev), najpogostejši neželeni učinki zdravljenja s pembrolizumabom pa so bili utrujenost (31 %), diareja (22 %) in navzea (20 %). Večina poročanih neželenih učinkov pri samostojnem zdravljenju je bila po izrazitosti 1. ali 2. stopnje. Najresnejši neželeni učinki so bili imunsko pogojeni neželeni učinki in hude z infuzijo povezane reakcije. Pojavnost imunsko pogojenih neželenih učinkov pri uporabi pembrolizumaba samega za adjuvantno zdravljenje (n = 1.480) je znašala 36,1 % za vse stopnje in 8,9 % od 3. do 5. stopnje, pri metastatski bolezni (n = 5.375) pa 24,2 % za vse stopnje in 6,4 % od 3. do 5. stopnje. Pri adjuvantnem zdravljenju niso zaznali nobenih novih imunsko pogojenih neželenih učinkov. Varnost pembrolizumaba pri kombiniranem zdravljenju s kemoterapijo so ocenili pri 3.123 bolnikih z različnimi vrstami raka, ki so v kliničnih študijah prejemali pembrolizumab v odmerkih 200 mg, 2 mg/kg telesne mase ali 10 mg/kg telesne mase na vsake 3 tedne. V tej populaciji bolnikov so bili najpogostejši neželeni učinki naslednji: anemija (55 %), navzea (54 %), utrujenost (38 %), nevtropenija (36 %), zaprtost (35 %), alopecija (35 %), diareja (34 %), bruhanje (28 %) in zmanjšanje apetita (27 %). Pojavnost neželenih učinkov 3. do 5. stopnje je pri bolnikih z NSCLC pri kombiniranem zdravljenju s pembrolizumabom znašala 67 % in pri zdravljenju samo s kemoterapijo 66 %, pri bolnikih s HNSCC pri kombiniranem zdravljenju s pembrolizumabom 85 % in pri zdravljenju s kemoterapijo v kombinaciji s cetuksimabom 84 %, pri bolnikih z rakom požiralnika pri kombiniranem zdravljenju s pembrolizumabom 86 % in pri zdravljenju samo s kemoterapijo 83 %, pri bolnikih s TNBC pri kombiniranem zdravljenju s pembrolizumabom 80 % in pri zdravljenju samo s kemoterapijo 77 % in pri bolnicah z rakom materničnega vratu pri kombiniranem zdravljenju s pembrolizumabom 82 % in pri zdravljenju samo s kemoterapijo 75 %. Varnost pembrolizumaba v kombinaciji z aksitinibom ali lenvatinibom pri napredovalem RCC in v kombinaciji z lenvatinibom pri napredovalem EC so ocenili pri skupno 1.456 bolnikih z napredovalim RCC ali napredovalim EC, ki so v kliničnih študijah prejemali 200 mg pembrolizumaba na 3 tedne skupaj s 5 mg aksitiniba dvakrat na dan ali z 20 mg lenvatiniba enkrat na dan, kot je bilo ustrezno. V teh populacijah bolnikov so bili najpogostejši neželeni učinki diareja (58 %), hipertenzija (54 %), hipotiroidizem (46 %), utrujenost (41 %), zmanjšan apetit (40 %), navzea (40 %), artralgija (30 %), bruhanje (28 %), zmanjšanje telesne mase (28 %), disfonija (28 %), bolečine v trebuhu (28 %), proteinurija (27 %), sindrom palmarno-plantarne eritrodizestezije (26 %), izpuščaj (26 %), stomatitis (25 %), zaprtost (25 %), mišično-skeletna bolečina (23 %), glavobol (23 %) in kašelj (21 %). Neželenih učinkov od 3. do 5. stopnje je bilo pri bolnikih z RCC med uporabo pembrolizumaba v kombinaciji z aksitinibom ali lenvatinibom 80 % in med uporabo sunitiniba samega 71 %. Pri bolnicah z EC je bilo neželenih učinkov od 3. do 5. stopnje med uporabo pembrolizumaba v kombinaciji z lenvatinibom 89 % in med uporabo kemoterapije same 73 %. Za celoten seznam neželenih učinkov, prosimo, glejte celoten Povzetek glavnih značilnosti zdravila. Za dodatne informacije o varnosti v primeru uporabe pembrolizumaba v kombinaciji glejte povzetke glavnih značilnosti zdravila za posamezne komponente kombiniranega zdravljenja. **Način in režim izdaje zdravila:** H – Predpisovanje in izdaja zdravila je le na recept, zdravilo se uporablja samo v bolnišnicah. **Imetnik dovoljenja za promet z zdravilom:** Merck Sharp & Dohme B.V. , Waarderweg 39, 2031 BN Haarlem, Nizozemska.

MSD
Merck Sharp & Dohme inovativna zdravila d.o.o.,
Ameriška ulica 2, 1000 Ljubljana, tel: +386 1/ 520 42 01, fax: +386 1/ 520 43 50;
Pripravljeno v Sloveniji, 01/2023; SI-KEY-00501 EXP: 01/2025

Samo za strokovno javnost.

H - Predpisovanje in izdaja zdravila je le na recept, zdravilo pa se uporablja samo v bolnišnicah. Pred predpisovanjem, prosimo, preberite celoten Povzetek glavnih značilnosti zdravila Keytruda, ki je na voljo pri naših strokovnih sodelavcih ali na lokalnem sedežu družbe.

CILJ JE OZDRAVITEV.

Za adjuvantno zdravljenje po radikalni resekciji in kemoterapiji na osnovi platine za odrasle bolnike z NDRP in velikim tveganjem za ponovitev, katerih tumorji izražajo PD-L1 na ≥ 50 % tumorskih celic (TC) in nimajo EGFR mutiranega ali ALK pozitivnega NDRP.

NDRP = nedrobnocelični rak pljuč

TECENTRIQ®
atezolizumab

ZDRAVILO TECENTRIQ JE INDICIRANO ZA ZDRAVLJENJE RAZLIČNIH VRST RAKA:

- NEDROBNOCELIČNI RAK PLJUČ
- DROBNOCELIČNI RAK PLJUČ
- TROJNO NEGATIVNI RAK DOJK
- UROTELIJSKI KARCINOM
- HEPATOCELULARNI KARCINOM

Vir: 1. Povzetek glavnih značilnosti zdravila Tecentriq je dosegljiv na povezavi: https://www.ema.europa.eu/en/documents/product-information/tecentriq-epar-product-information_sl.pdf

Skrajšan povzetek glavnih značilnosti zdravila Tecentriq

Ime zdravila: Tecentriq 840 mg/1200 mg koncentrat za raztopino za infundiranje. **Kakovostna in količinska sestava:** 840 mg: ena 14-ml viala s koncentratom vsebuje 840 mg atezolizumaba.1200 mg: ena 20-ml viala s koncentratom vsebuje 1200 mg atezolizumaba. Po redčenju je končna koncentracija razredčene raztopine med 3,2 mg/ml in 16,8 mg/ml. Atezolizumab je humanizirano monoklonsko protitelo IgG1 z inženirsko obdelano domeno Fc, ki je pridobljeno iz celic jajčnika kitajskega hrčka s tehnologijo rekombinantne DNA in deluje na ligand za programirano celično smrt 1 (PD-L1). **Terapevtske indikacije:** Urotelijski karcinom (UC): Zdravilo Tecentriq je kot monoterapija indicirano za zdravljenje odraslih bolnikov z lokalno napredovalim ali razsejanim UC, ki: so bili predhodno zdravljeni s kemoterapijo na osnovi platine ali niso primerni za zdravljenje s cisplatinom in katerih tumorji izražajo PD-L1 v ≥ 5 %. Zgodnji stadij nedrobnoceličnega raka pljuč (NDRP): Zdravilo Tecentriq je kot monoterapija indicirano za adjuvantno zdravljenje po popolni resekciji in kemoterapiji na osnovi platine za odrasle bolnike z NDRP in velikim tveganjem za ponovitev, katerih tumorji izražajo PD-L1 na ≥ 50 % tumorskih celic (TC) in nimajo EGFR mutiranega ali ALK pozitivnega NDRP. Razsejani NDRP: Zdravilo Tecentriq je v kombinaciji z bevacizumabom, paklitakselom in karboplatinom indicirano v prvi liniji zdravljenja odraslih bolnikov z razsejanim neploščatoceličnim NDRP. Pri bolnikih z EGFR mutiranim ali ALK pozitivnim NDRP je zdravilo Tecentriq v kombinaciji z bevacizumabom, paklitakselom in karboplatinom indicirano le, ko so izčrpana ustrezna tarčna zdravljenja. Zdravilo Tecentriq je v kombinaciji z nab-paklitakselom in karboplatinom indicirano kot prva linija zdravljenja odraslih bolnikov z razsejanim neploščatoceličnim NDRP, ki ni EGFR mutiran ali ALK pozitiven. Zdravilo Tecentriq je kot monoterapija indicirano v prvi liniji zdravljenja odraslih bolnikov z razsejanim NDRP, pri katerih je PD-L1 izražen na ≥ 50 % TC ali ≥ 10 % imunskih celic (IC), ki infiltrirajo tumor, ter nimajo EGFR mutiranega ali ALK pozitivnega NDRP. Zdravilo Tecentriq je kot monoterapija indicirano za zdravljenje odraslih bolnikov z lokalno napredovalim ali razsejanim NDRP, ki so bili predhodno zdravljeni s kemoterapijo. Bolniki z EGFR mutiranim ali ALK pozitivnim NDRP morajo pred uvedbo zdravila Tecentriq prejeti tudi tarčna zdravljenja. Drobnocelični rak pljuč (DRP): Zdravilo Tecentriq je v kombinaciji s karboplatinom in etopozidom indicirano kot prva linija zdravljenja odraslih bolnikov z razsejanim DRP. Trojno negativni rak dojk (TNRD): Zdravilo Tecentriq je v kombinaciji z nab-paklitakselom indicirano za zdravljenje odraslih bolnikov z inoperabilnim lokalno napredovalim ali razsejanim TNRD, katerih tumorji izražajo PD-L1 v ≥ 1 % in predhodno še niso prejemali kemoterapije zaradi razsejane bolezni. Hepatocelularni karcinom (HCC): Zdravilo Tecentriq je v kombinaciji z bevacizumabom indicirano za zdravljenje odraslih bolnikov z napredovalim ali neresektabilnim HCC, ki predhodno še niso prejemali sistemskega zdravljenja. **Odmerjanje in način uporabe:** Zdravilo Tecentriq morajo uvesti in nadzorovati zdravniki z izkušnjami pri zdravljenju raka. Odmerjanje: priporočeni odmerek zdravila Tecentriq je 840 mg, danega intravensko na dva tedna, ali 1200 mg, danega intravensko na tri tedne, ali 1680 mg, danega intravensko na štiri tedne, kot je navedeno v celotnem Povzetku glavnih značilnosti zdravila Tecentriq. Kadar zdravilo Tecentriq dajete v kombinaciji, glejte tudi celotne informacije za predpisovanje zdravil, ki se uporabljajo v kombinaciji. *Prilagoditev odmerka med zdravljenjem:* odmerkov zdravila Tecentriq ni priporočljivo zmanjševati. *Zapoznitev odmerka ali prenehanje uporabe* glede na neželeni učinek je opisano v SmPC. Način uporabe: zdravilo Tecentriq je namenjeno za intravensko uporabo. Infuzij se ne sme dajati kot hiter intravenski odmerek ali bolus. Začetni odmerek zdravila Tecentriq je treba dati v 60 minutah. Če bolnik prvo infuzijo dobro prenese, je mogoče vse nadaljnje infuzije dati v 30 minutah. **Kontraindikacije:** Preobčutljivost na atezolizumab ali katero koli pomožno snov. **Posebna opozorila in previdnostni ukrepi:** Sledljivost: Za izboljšanje sledljivosti bioloških zdravil je treba lastniško ime in številko serije uporabljenega zdravila jasno zabeležiti v bolnikovi dokumentaciji. Imunsko pogojeni neželeni učinki: Večina imunsko pogojenih neželenih učinkov, ki so se pojavili med zdravljenjem z atezolizumabom, je bila po prekinitvi atezolizumaba in uvedbi kortikosteroidov in/ali podpornega zdravljenja reverzibilna. Opazili so imunsko pogojene neželene učinke, ki vplivajo na več kot en organski sistem. Imunsko pogojeni neželeni učinki, povezani z atezolizumabom, se lahko pojavijo po zadnjem odmerku atezolizumaba. Pri sumu na imunsko pogojene neželene učinke je treba opraviti temeljito oceno za potrditev etiologije oziroma izključitev drugih vzrokov. Glede na izrazitost neželenega učinka je treba uporabo atezolizumaba odložiti in uvesti kortikosteroide. Atezolizumab je treba trajno prenehati uporabljati pri vseh imunsko pogojenih neželenih učinkih 3. stopnje, ki se ponovijo, in pri vseh imunsko pogojenih neželenih učinkih 4. stopnje, z izjemo endokrinopatij, ki jih je mogoče nadzorovati z nadomestnimi hormoni. Bolnike je treba spremljati glede znakov in simptomov pnevmonitisa ter izključiti druge možne vzroke, razen imunsko pogojenega pnevmonitisa. Bolnike je treba spremljati glede znakov in simptomov hepatitisa. Vrednosti AST, ALT in bilirubina je treba spremljati pred začetkom zdravljenja z atezolizumabom, redno med zdravljenjem in kot je potrebno glede na klinično oceno. Bolnike je treba spremljati glede znakov in simptomov kolitisa in endokrinopatij, meningitisa ali encefalitisa. V primeru meningitisa ali encefalitisa je treba zdravljenje z atezolizumabom trajno ukiniti ne glede na njuno stopnjo. Bolnike je treba spremljati glede znakov in simptomov motorične in senzorične nevropatije. V primeru miastenijskega sindroma/miastenije gravis ali Guillain-Barréjevega sindroma je treba zdravljenje z atezolizumabom trajno prekiniti ne glede na njihovo stopnjo. Bolnike je treba nadzorovati glede znakov in simptomov, ki kažejo na akutni pankreatitis. Bolnike je treba nadzorovati glede znakov in simptomov, ki kažejo na miokarditis. Imunsko pogojeni nefritis: Bolnike je treba nadzorovati glede sprememb v delovanju ledvic. Bolnike je treba nadzorovati glede znakov in simptomov, ki kažejo na miozitis. Z infundiranjem povezane reakcije: pri zdravljenju z atezolizumabom so opažali z infundiranjem povezane reakcije. Pri bolnikih, ki imajo z infundiranjem povezane reakcije 1. ali 2. stopnje, je treba hitrost infundiranja zmanjšati ali zdravljenje prekiniti. Pri bolnikih, ki imajo z infundiranjem povezane reakcije 3. ali 4. stopnje, je treba zdravljenje z atezolizumabom trajno ukiniti. Bolniki, ki imajo z infundiranjem povezane reakcije 1. ali 2. stopnje, lahko še naprej prejemajo atezolizumab pod natančnim nadzorom; v poštev pride premedikacija z antipiretikom in antihistaminikom. Pri bolnikih, ki so prejemali atezolizumab, so poročali o imunsko pogojenih hudih kožnih neželenih učinkih, vključno s primeri Stevens-Johnsonovega sindroma (SJS) in toksične epidermalne nekrolize (TEN). Bolnike je treba spremljati glede sumov na hude kožne neželene učinke in izključiti druge vzroke. V primeru suma na hude kožne neželene učinke je treba bolnike napotiti k specialistu po nadaljnjo diagnozo in zdravljenje. Uporabo atezolizumaba je treba odložiti pri bolnikih s sumom na SJS ali TEN. Pri potrjenem SJS ali TEN je treba trajno prenehati z uporabo atezolizumaba. Kartica za bolnika: Zdravnik, ki predpiše zdravilo, se mora z bolnikom pogovoriti o tveganjih zdravljenja z zdravilom Tecentriq. Bolniku je treba dati kartico za bolnika in mu naročiti, naj jo ima vedno pri sebi. **Medsebojno delovanje z drugimi zdravili in druge oblike interakcij:** Formalnih farmakokinetičnih študij medsebojnega delovanja z atezolizumabom niso izvedli. Ker se atezolizumab odstrani iz obtoka s katabolizmom, ni pričakovati presnovnih medsebojnih delovanj med zdravili. Uporabi sistemskih kortikosteroidov ali imunosupresivov se je pred uvedbo atezolizumaba treba izogibati, ker lahko vplivajo na farmakodinamično aktivnost in učinkovitost atezolizumaba. Vendar pa se sistemske kortikosteroide ali druge imunosupresive lahko uporabi po začetku zdravljenja z atezolizumabom za zdravljenje imunsko pogojenih neželenih učinkov. **Neželeni učinki:** Informacije o varnosti atezolizumaba v monoterapiji: najpogostejši neželeni učinki (> 10 %) so bili utrujenost, zmanjšan apetit, navzea, izpuščaj, zvišana telesna temperatura, kašelj, diareja, dispneja, artralgija, astenija, bolečina v hrbtu, bruhanje, okužba sečil in glavobol. Varnost atezolizumaba v kombinaciji z drugimi učinkovinami: najpogostejši neželeni učinki (≥ 20 %) so bili anemija, nevtropenija, navzea, utrujenost, alopecija, izpuščaj, diareja, trombocitopenija, zaprtost, zmanjšan apetit in periferna nevropatija. Poročanje o domnevnih neželenih učinkih: Poročanje o domnevnih neželenih učinkih zdravila po izdaji dovoljenja za promet je pomembno. Omogoča namreč stalno spremljanje razmerja med koristmi in tveganji zdravila. Od zdravstvenih delavcev se zahteva, da poročajo o katerem koli domnevnem neželenem učinku zdravila na: Javna agencija Republike Slovenije za zdravila in medicinske pripomočke, Sektor za farmakovigilanco, Nacionalni center za farmakovigilanco, Slovenčeva ulica 22, SI-1000 Ljubljana, Tel: +386 (0)8 2000 500, Faks: +386 (0)8 2000 510, e-pošta: h-farmakovigilanca@jazmp.si, spletna stran: www.jazmp.si. Za zagotavljanje sledljivosti zdravila je pomembno, da pri izpolnjevanju obrazca o domnevnih neželenih učinkih zdravila navedete številko serije biološkega zdravila. **Režim izdaje zdravila:** H. **Imetnik dovoljenja za promet:** Roche Registration GmbH, Emil-Barell-Strasse 1, 79639 Grenzach-Wyhlen, Nemčija. **Verzija: 3.0/22**

M-SI-00000783(v1.0) Datum priprave informacije: februar 2023

DODATNE INFORMACIJE SO NA VOLJO PRI: Roche farmacevtska družba d.o.o., Stegne 13G, 1000 Ljubljana

Samo za strokovno javnost.

Zdravilo Lonsurf je indicirano v monoterapiji za zdravljenje odraslih bolnikov z metastatskim kolorektalnim rakom (KRR), ki so bili predhodno že zdravljeni ali niso primerni za zdravljenja, ki so na voljo. Ta vključujejo kemoterapijo na osnovi fluoropirimidina, oksaliplatina in irinotekana, zdravljenje z zaviralci žilnega endotelijskega rastnega dejavnika (VEGF – Vascular Endothelial Growth Factor) in zaviralci receptorjev za epidermalni rastni dejavnik (EGFR – Epidermal Growth Factor Receptor).[1]

Zdravilo Lonsurf je indicirano v monoterapiji za zdravljenje odraslih bolnikov z metastatskim rakom želodca vključno z adenokarcinomom gastro-ezofagealnega prehoda, ki so bili predhodno že zdravljeni z najmanj dvema sistemskima režimoma zdravljenja za napredovalo bolezen.[1]

VEČ ČASA

za več trenutkov, ki štejejo

Podaljša celokupno preživetje
v 3. liniji zdravljenja bolnikov z mCRC in mGC[2,3]

Literatura: 1. Povzetek glavnih značilnosti zdravila Lonsurf, december 2020.
2. Mayer R et al. N Engl J Med. 2015;372:1909-19. 3. Shitara K et al.
Lancet Oncol. 2018;19:1437-1448.
Družba Servier ima licenco družbe Taiho za zdravilo Lonsurf®.
Pri globalnem razvoju zdravila sodelujeta obe družbi
in ga tržita na svojih določenih področjih.

Lonsurf®
trifluridin/tipiracil

Skrajšan povzetek glavnih značilnosti zdravila: Lonsurf 15 mg/6,14 mg filmsko obložene tablete in Lonsurf 20 mg/8,19 mg filmsko obložene tablete
SESTAVA*: Lonsurf 15 mg/6,14 mg: Ena filmsko obložena tableta vsebuje 15 mg trifluridina in 6,14 mg tipiracila (v obliki klorida). **Lonsurf 20 mg/8,19 mg**: Ena filmsko obložena tableta vsebuje 20 mg trifluridina in 8,19 mg tipiracila (v obliki klorida). **TERAPEVTSKE INDIKACIJE*:** Kolorektalni rak - v monoterapiji za zdravljenje odraslih bolnikov z metastatskim kolorektalnim rakom, ki so bili predhodno že zdravljeni ali niso primerni za zdravljenja, ki so na voljo. Ta vključujejo kemoterapijo na osnovi fluoropirimidina, oksaliplatina in irinotekana, zdravljenje z zaviralci žilnega endotelijskega rastnega dejavnika (VEGF - Vascular Endothelial Growth Factor) in zaviralci receptorjev za epidermalni rastni dejavnik (EGFR - Epidermal Growth Factor Receptor). Rak želodca - v monoterapiji za zdravljenje odraslih bolnikov z metastatskim rakom želodca vključno z adenokarcinomom gastro-ezofagealnega prehoda, ki so bili predhodno že zdravljeni z najmanj dvema sistemskima režimoma zdravljenja za napredovalo bolezen. **ODMERJANJE IN NAČIN UPORABE*:** Priporočeni začetni odmerek zdravila Lonsurf pri odraslih je 35 mg/m^2/odmerek peroralno dvakrat dnevno na 1. do 5. dan in 8. do 12. dan vsakega 28-dnevnega cikla zdravljenja, najpozneje 1 uro po zaključku jutranjega in večernega obroka (20 mg/m^2/odmerek dvakrat dnevno pri bolnikih s hudo ledvično okvaro). Odmerek, izračunan glede na telesno površino, ne sme preseči 80 mg/odmerek. Možne prilagoditve odmerka glede na varnost in prenašanje zdravila: dovoljena so zmanjšanja odmerka na najmanjši odmerek 20 mg/m^2 dvakrat dnevno (oz. 15 mg/m^2 dvakrat dnevno pri bolnikih s hudo ledvično okvaro). Potem ko je bil odmerek zmanjšan, povečanje ni dovoljeno. **KONTRAINDIKACIJE*:** Preobčutljivost na učinkovini ali katero koli pomožno snov. **OPOZORILA IN PREVIDNOSTNI UKREPI*:** Supresija kostnega mozga: Pred uvedbo zdravljenja in po potrebi za spremljanje toksičnosti zdravila, najmanj pred vsakim ciklom zdravljenja, je treba pregledati celotno krvno sliko. Zdravljenja ne smete začeti, če je absolutno število nevtrofilcev < 1,5 x 10^9/l, če je število trombocitov < 75 x 10^9/l ali če se je pri bolniku zaradi predhodnih zdravljenj pojavila klinično pomembna nehematološka toksičnost 3. ali 4. stopnje, ki še traja. Bolnike je treba skrbno spremljati zaradi morebitnih okužb, uvesti je treba ustrezne ukrepe, kot je klinično indicirano. Toksičnost za prebavila: Potrebna je uporaba antiemetikov, antidiarikov ter drugih ukrepov, kot je klinično indicirano. Če je potrebno, prilagodite odmerke. Ledvična okvara: Uporaba zdravila ni priporočljiva pri bolnikih s končno stopnjo ledvične okvare. Bolnike z ledvično okvaro je potrebno med zdravljenjem skrbno spremljati; bolnike z zmerno ali hudo ledvično okvaro je treba zaradi hematološke toksičnosti bolj pogosto spremljati. Jetrna okvara: Uporaba zdravila Lonsurf pri bolnikih z obstoječo zmerno ali hudo jetrno okvaro ni priporočljiva. Proteinurija: Pred začetkom zdravljenja in med njim je priporočljivo spremljanje proteinurije z urinskimi testnimi lističi. Pomožne snovi: Zdravilo vsebuje laktozo. **INTERAKCIJE*:** Previdnost: Zdravila, ki medsebojno delujejo z nukleozidnimi prenašalci CNT1, ENT1 in ENT2, zaviralci OCT2 ali MATE1, substrati humane timidin-kinaze (npr. zidovudin), hormonski kontraceptivi. **PLODNOST*. NOSEČNOST IN DOJENJE*:** Ni priporočljivo. **KONTRACEPCIJA*:** Ženske in moški morajo uporabljati zelo učinkovite metode kontracepcije med zdravljenjem in do 6 mesecev po zaključku zdravljenja. **VPLIV NA SPOSOBNOST VOŽNJE IN UPRAVLJANJA STROJEV*:** Med zdravljenjem se lahko pojavijo utrujenost, omotica ali splošno slabo počutje. **NEŽELENI UČINKI*:** *Zelo pogosti:* nevtropenija, levkopenija, anemija, trombocitopenija, zmanjšan apetit, diareja, navzea, bruhanje, utrujenost. *Pogosti:* okužba spodnjih dihal, febrilna nevtropenija, limfopenija, hipoalbuminemija, disgevzija, periferna nevropatija, dispneja, bolečina v trebuhu, zaprtje, stomatitis, bolezni ustne votline, hiperbilirubinemija, sindrom palmarne plantarne eritrodisestezije, izpuščaj, alopecija, pruritus, suha koža, proteinurija, pireksija, edem, vnetje sluznice, splošno slabo počutje, zvišanje jetrnih encimov, zvišanje alkalne fosfataze v krvi, zmanjšanje telesne mase. *Občasni:* septični šok, infekcijski enteritis, pljučnica, okužba žolčevoda, gripa, okužba sečil, gingivitis, herpes zoster, tinea pedis, okužba s kandido, bakterijska okužba, okužba, nevtropenična sepsa, okužba zgornjih dihal, konjunktivitis, bolečina zaradi raka, pancitopenija, granulocitopenija, monocitopenija, eritropenija, levkocitoza, monocitoza, dehidracija, hiperglikemija, hiperkaliemija, hipokaliemija, hipofosfatemija, hipernatriemija, hiponatriemija, hipokalciemija, protin, anksioznost, nespečnost, nevrotoksičnost, disestezija, hiperestezija, hipoestezija, sinkopa, parestezija, pekoč občutek, letargija, omotica, glavobol, zmanjšana ostrina vida, zamegljen vid, diplopija, kataraka, suho oko, vrtoglavica, neugodje v ušesu, angina pektoris, aritmija, palpitacije, embolija, hipertenzija, hipotenzija, vročinski oblivi, pljučna embolija, plevralni izliv, izcedek iz nosu, disfonija, orofaringealna bolečina, epistaksa, kašelj, hemoragični enterokolitis, krvavitev v prebavilih, akutni pankreatitis, ascites, ileus, subileus, kolitis, gastritis, refluksni gastritis, ezofagitis, moteno praznjenje želodca, abdominalna distenzija, analno vnetje, razjede v ustih, dispepsija, gastroezofagealna refluksna bolezen, proktalgija, bukalni polip, krvavitev dlesni, glositis, parodontalna bolezen, bolezen zob, siljenje na bruhanje, flatulenca, slab zadah, hepatotoksičnost, razširitev žolčnih vodov, luščenje kože, urtikarija, preobčutljivostne reakcije na svetlobo, eritem, akne, hiperhidroza, žulj, bolezni nohtov, otekanje sklepov, artralgija, bolečina v kosteh, mialgija, mišično-skeletna bolečina, mišična oslabelost, mišični krči, bolečina v okončinah, ledvična odpoved, neinfektivni cistitis, motnje mikcije, hematurija, levkociturija, motnje menstruacije, poslabšanje splošnega zdravstvenega stanja, bolečina, občutek spremembe telesne temperature, kseroza, nelagodje, zvišanje kreatinina v krvi, podaljšanje intervala QT na elektrokardiogramu, povečanje mednarodnega umerjenega razmerja (INR), podaljšanje aktiviranega parcialnega tromboplastinskega časa (aPTČ), zvišanje sečnine v krvi, zvišanje laktatne dehidrogenaze v krvi, znižanje celokupnih proteinov, zvišanje C-reaktivnega proteina, zmanjšan hematokrit. *Post-marketinške izkušnje:* intersticijska bolezen pljuč. **PREVELIKO ODMERJANJE*:** Neželeni učinki, o katerih so poročali v povezavi s prevelikim odmerjanjem, so bili v skladu z uveljavljenim varnostnim profilom. Glavni pričakovani zaplet prevelikega odmerjanja je supresija kostnega mozga. **FARMAKODINAMIČNE LASTNOSTI*:** *Farmakoterapevtska skupina:* zdravila z delovanjem na novotvorbe, antimetaboliti, oznaka ATC: L01BC59. Zdravilo Lonsurf sestavljata antineoplastični timidinski nukleozidni analog, trifluridin, in zaviralec timidin-fosforilaze (TPaze), tipiracilijev klorid. Po privzemu v rakave celice timidin-kinaza fosforilira trifluridin. Ta se v celicah nato presnovi v substrat deoksiribonukleinske kisline (DNA), ki se vgradi neposredno v DNA ter tako preprečuje celično proliferacijo. TPaza hitro razgradi trifluridin in njegova presnova po peroralni uporabi je hitra zaradi učinka prvega prehoda, zato je v zdravilo vključen zaviralec TPaze, tipiracilijev klorid. **PAKIRANJE*:** 20 filmsko obloženih tablet. **NAČIN PREDPISOVANJA IN IZDAJE ZDRAVILA:** Rp/Spec. **Imetnik dovoljenja za promet:** Les Laboratoires Servier, 50, rue Carnot, 92284 Suresnes cedex, Francija. Številka dovoljenja za promet z zdravilom: EU/1/16/1096/001 (Lonsurf 15 mg/6,14 mg), EU/1/16/1096/004 (Lonsurf 20 mg/8,19 mg). **Datum zadnje revizije besedila: december 2020. *Pred predpisovanjem preberite celoten povzetek glavnih značilnosti zdravila. Celoten povzetek glavnih značilnosti zdravila in podrobnejše informacije so na voljo pri: Servier Pharma d.o.o., Podmilščakova ulica 24, 1000 Ljubljana, tel: 01 563 48 11, www.servier.si.**

LON AD1 C1 2022-23. Samo za strokovno javnost.
Datum priprave informacije: oktober 2022.

SERVIER
moved by you

Instructions for authors

The editorial policy

Radiology and Oncology is a multidisciplinary journal devoted to the publishing original and high-quality scientific papers and review articles, pertinent to oncologic imaging, interventional radiology, nuclear medicine, radiotherapy, clinical and experimental oncology, radiobiology, medical physics, and radiation protection. Papers on more general aspects of interest to the radiologists and oncologists are also published (no case reports).

The Editorial Board requires that the paper has not been published or submitted for publication elsewhere; the authors are responsible for all statements in their papers. Accepted cannot be published elsewhere without the written permission of the editors.

Submission of the manuscript

The manuscript written in English should be submitted to the journal via online submission system Editorial Manager available for this journal at: **www.radioloncol.com**.

In case of problems, please contact Sašo Trupej at **saso.trupej@computing.si** or the Editor of this journal at **gsersa@onko-i.si**

All articles are subjected to the editorial review and when the articles are appropriated they are reviewed by independent referees. In the cover letter, which must accompany the article, the authors are requested to suggest 3-4 researchers, competent to review their manuscript. However, please note that this will be treated only as a suggestion; the final selection of reviewers is exclusively the Editor's decision. The authors' names are revealed to the referees, but not vice versa.

Manuscripts which do not comply with the technical requirements stated herein will be returned to the authors for the correction before peer-review. The editorial board reserves the right to ask authors to make appropriate changes of the contents as well as grammatical and stylistic corrections when necessary. Page charges will be charged for manuscripts exceeding the recommended length, as well as additional editorial work and requests for printed reprints.

Articles are published printed and on-line as the open access: (**https://content.sciendo.com/raon**).

All articles are subject to 1200 EUR + VAT publication fee. Exceptionally, waiver of payment may be negotiated with editorial office, at the time of article submission.

Manuscripts submitted under multiple authorship are reviewed on the assumption that all listed authors concur in the submission and are responsible for its content; they must have agreed to its publication and have given the corresponding author the authority to act on their behalf in all matters pertaining to publication. The corresponding author is responsible for informing the coauthors of the manuscript status throughout the submission, review, and production process.

Preparation of manuscripts

Radiology and Oncology will consider manuscripts prepared according to the Uniform Requirements for Manuscripts Submitted to Biomedical Journals by International Committee of Medical Journal Editors (www.icmje.org). The manuscript should be written in grammatically and stylistically correct language. Abbreviations should be avoided. If their use is necessary, they should be explained at the first time mentioned. The technical data should conform to the SI system. The manuscript, excluding the references, tables, figures and figure legends, must not exceed 5000 words, and the number of figures and tables is limited to 8. Organize the text so that it includes: Introduction, Materials and methods, Results and Discussion. Exceptionally, the results and discussion can be combined in a single section. Start each section on a new page, and number each page consecutively with Arabic numerals. For ease of review, manuscripts should be submitted as a single column, double-spaced text.

The Title page should include a concise and informative title, followed by the full name(s) of the author(s); the institutional affiliation of each author; the name and address of the corresponding author (including telephone, fax and E-mail), and an abbreviated title (not exceeding 60 characters). This should be followed by the abstract page, summarizing in less than 250 words the reasons for the study, experimental approach, the major findings (with specific data if possible), and the principal conclusions, and providing 3-6 key words for indexing purposes. Structured abstracts are required. Slovene authors are requested to provide title and the abstract in Slovene language in a separate file. The text of the research article should then proceed as follows:

Introduction should summarize the rationale for the study or observation, citing only the essential references and stating the aim of the study.

Materials and methods should provide enough information to enable experiments to be repeated. New methods should be described in details.

Results should be presented clearly and concisely without repeating the data in the figures and tables. Emphasis should be on clear and precise presentation of results and their significance in relation to the aim of the investigation.

Discussion should explain the results rather than simply repeating them and interpret their significance and draw conclusions. It should discuss the results of the study in the light of previously published work.

Charts, Illustrations, Images and Tables

Charts, Illustrations, Images and Tables must be numbered and referred to in the text, with the appropriate location indicated. Charts, Illustrations and Images, provided electronically, should be of appropriate quality for good reproduction. Illustrations and charts must be vector image, created in CMYK color space, preferred font "Century Gothic", and saved as .AI, .EPS or .PDF format. Color charts, illustrations and Images are encouraged, and are published without additional charge. Image size must be 2.000 pixels on the longer side and saved as .JPG (maximum quality) format. In Images, mask the identities of the patients. Tables should be typed double-spaced, with a descriptive title and, if appropriate, units of numerical measurements included in the column heading. The files with the figures and tables can be uploaded as separate files.

References

References must be numbered in the order in which they appear in the text and their corresponding numbers quoted in the text. Authors are responsible for the accuracy of their references. References to the Abstracts and Letters to the Editor must be identified as such. Citation of papers in preparation or submitted for publication, unpublished observations, and personal communications should not be included in the reference list. If essential, such material may be incorporated in the appropriate place in the text. References follow the style of Index Medicus, DOI number (if exists) should be included.

All authors should be listed when their number does not exceed six; when there are seven or more authors, the first six listed are followed by "et al.". The following are some examples of references from articles, books and book chapters:

Dent RAG, Cole P. In vitro maturation of monocytes in squamous carcinoma of the lung. *Br J Cancer* 1981; **43:** 486-95. doi: 10.1038/bjc.1981.71

Chapman S, Nakielny R. *A guide to radiological procedures*. London: Bailliere Tindall; 1986.

Evans R, Alexander P. Mechanisms of extracellular killing of nucleated mammalian cells by macrophages. In: Nelson DS, editor. *Immunobiology of macrophage.* New York: Academic Press; 1976. p. 45-74.

Authorization for the use of human subjects or experimental animals

When reporting experiments on human subjects, authors should state whether the procedures followed the Helsinki Declaration. Patients have the right to privacy; therefore, the identifying information (patient's names, hospital unit numbers) should not be published unless it is essential. In such cases the patient's informed consent for publication is needed, and should appear as an appropriate statement in the article. Institutional approval and Clinical Trial registration number is required. Retrospective clinical studies must be approved by the accredited Institutional Review Board/Committee for Medical Ethics or other equivalent body. These statements should appear in the Materials and methods section.

The research using animal subjects should be conducted according to the EU Directive 2010/63/EU and following the Guidelines for the welfare and use of animals in cancer research (Br J Cancer 2010; 102: 1555 – 77). Authors must state the committee approving the experiments, and must confirm that all experiments were performed in accordance with relevant regulations.

These statements should appear in the Materials and methods section (or for contributions without this section, within the main text or in the captions of relevant figures or tables).

Transfer of copyright agreement

For the publication of accepted articles, authors are required to send the License to Publish to the publisher on the address of the editorial office. A properly completed License to Publish, signed by the Corresponding Author on behalf of all the authors, must be provided for each submitted manuscript.

Conflict of interest

When the manuscript is submitted for publication, the authors are expected to disclose any relationship that might pose real, apparent or potential conflict of interest with respect to the results reported in that manuscript. Potential conflicts of interest include not only financial relationships but also other, non-financial relationships. In the Acknowledgement section the source of funding support should be mentioned. The Editors will make effort to ensure that conflicts of interest will not compromise the evaluation process of the submitted manuscripts; potential editors and reviewers will exempt themselves from review process when such conflict of interest exists. The statement of disclosure must be in the Cover letter accompanying the manuscript or submitted on the form available on **www.icmje.org/coi_disclosure.pdf**

Page proofs

Page proofs will be sent by E-mail to the corresponding author. It is their responsibility to check the proofs carefully and return a list of essential corrections to the editorial office within three days of receipt. Only grammatical corrections are acceptable at that time.

Open access

Papers are published electronically as open access on **https://content.sciendo.com/raon**, also papers accepted for publication as E-ahead of print.

LORVIQUA®
LORLATINIB

Pri bolnikih z metastazami v CŽS ali brez njih

SOOČITE

ALK+ mNSCLC Z ZDRAVILOM LORVIQUA

Zdravilo **LORVIQUA** v monoterapiji je indicirano za zdravljenje odraslih bolnikov z napredovalim nedrobnoceličnim rakom pljuč (NSCLC), ki je ALK pozitiven, in se predhodno niso zdravili z zaviralcem ALK.[1]

Zdravilo **LORVIQUA** v monoterapiji je indicirano za zdravljenje odraslih bolnikov z napredovalim NSCLC, ki je ALK-pozitiven, pri katerih je bolezen napredovala po:

- zdravljenju z alektinibom ali ceritinibom kot prvim ALK zaviralcem tirozin kinaze (TKI); ali
- zdravljenju s krizotinibom in vsaj še 1 drugim ALK TKI.[1]

BISTVENI PODATKI IZ POVZETKA GLAVNIH ZNAČILNOSTI ZDRAVILA

Lorviqua 25 mg, 100 mg filmsko obložene tablete
▼Za to zdravilo se izvaja dodatno spremljanje varnosti. Tako bodo hitreje na voljo nove informacije o njegovi varnosti. Zdravstvene delavce naprošamo, da poročajo o kateremkoli domnevnem neželenem učinku zdravila. Glejte poglavje 4.8 povzetka glavnih značilnosti zdravila, kako poročati o neželenih učinkih. **Sestava in oblika zdravila:** Ena filmsko obložena tableta vsebuje 25 mg ali 100 mg lorlatiniba in 1,58 mg oz. 4,20 mg laktoze monohidrata. **Indikacije:** Zdravljenje odraslih bolnikov z napredovalim nedrobnoceličnim rakom pljuč (NSCLC – *Non-Small Cell Lung Cancer*), ki je ALK (anaplastična limfomska kinaza) pozitiven in se predhodno niso zdravili z zaviralcem ALK, ter pri bolnikih, pri katerih je bolezen napredovala po: zdravljenju z alektinibom ali ceritinibom kot prvim ALK zaviralcem tirozin kinaze (TKI – *Tyrosine Kinase Inhibitor*) ali zdravljenju s krizotinibom in vsaj še 1 drugim ALK TKI. **Odmerjanje in način uporabe:** Zdravljenje mora uvesti in nadzorovati zdravnik, ki ima izkušnje z uporabo zdravil za zdravljenje rakavih bolezni. Odkrivanje ALK-pozitivnega NSCLC je potrebno pri izbiri bolnikov, saj so to edini bolniki, pri katerih so dokazali korist. Priporočeni odmerek je 100 mg peroralno enkrat na dan. Zdravljenje je treba nadaljevati do napredovanja bolezni ali nesprejemljive toksičnosti. Če bolnik izpusti odmerek, ga mora vzeti takoj, ko se spomni, razen če do naslednjega odmerka manjka manj kot 4 ure. Bolniki ne smejo vzeti 2 odmerkov hkrati, da bi nadomestili izpuščeni odmerek. Prilagajanje odmerkov: Ravni zmanjšanja odmerka: *prvo zmanjšanje odmerka*: 75 mg peroralno enkrat na dan; *drugo zmanjšanje odmerka*: 50 mg peroralno enkrat na dan. Zdravljenje je treba trajno prekiniti, če bolnik ne prenaša odmerka 50 mg peroralno enkrat na dan. Za prilagajanje odmerkov zaradi neželenih učinkov glejte preglednico 1 v SmPC-ju. Posebne populacije: *Starejši bolniki (≥ 65 let)*: Zaradi omejenih podatkov priporočil o odmerjanju ni mogoče dati. *Okvara ledvic*: Prilagajanje odmerkov pri bolnikih z normalnim delovanjem in blago ali zmerno okvaro [absolutna ocena hitrosti glomerulne filtracije (eGFR – estimated Glomerular Filtration Rate): ≥ 30 ml/min] ni potrebno. Pri bolnikih s hudo okvaro ledvic (absolutna vrednost eGFR < 30 ml/min) je priporočljiv zmanjšan odmerek lorlatiniba, npr. začetni odmerek 75 mg peroralno enkrat na dan. Podatkov pri bolnikih na ledvični dializi ni na voljo. *Okvara jeter*: Pri bolnikih z blago okvaro ni potrebno prilagajanje odmerkov. Podatkov o uporabi pri zmerni ali hudi okvari ni, zato uporaba ni priporočljiva. *Pediatrična populacija*: Varnost in učinkovitost pri otrocih in mladostnikih, starih < 18 let, nista bili dokazani. Način uporabe: Peroralna uporaba, vsak dan ob približno istem času, s hrano ali brez nje. Tablete je treba pogoltniti cele. **Kontraindikacije:** Preobčutljivost na učinkovino ali katerokoli pomožno snov. Uporaba močnih induktorjev CYP3A4/5. **Posebna opozorila in previdnostni ukrepi:** Hiperlipidemija: Uporaba je povezana z zvečanji vrednosti holesterola in trigliceridov v serumu – morda bo treba uvesti ali povečati odmerek zdravil za zniževanje ravni lipidov. Učinki na osrednje živčevje: Opazili so učinke na osrednje živčevje, vključno s psihotičnimi učinki in spremembami v kognitivni funkciji, razpoloženju, duševnem stanju ali govoru – morda bo treba prilagoditi odmerek ali prekiniti zdravljenje. Atrioventrikularni blok: Pri bolnikih, ki so prejemali lorlatinib, so poročali o podaljšanju intervala PR in AV-bloku. Potrebno je spremljanje EKG in morda bo treba prilagoditi odmerek. Zmanjšanje iztisnega deleža levega prekata: Pri bolnikih, ki so prejemali lorlatinib in pri katerih so opravili izhodiščno in še vsaj eno nadaljnjo oceno iztisnega deleža levega prekata (LVEF – *Left Ventricular Ejection Fraction*), so poročali o zmanjšanju LVEF. Če imajo bolniki dejavnike tveganja za srce ali stanja, ki vplivajo na LVEF, ali se jim med zdravljenjem pojavijo pomembni srčni znaki/simptomi, je treba razmisliti o spremljanju srca, vključno z oceno LVEF. Zvečanje vrednosti lipaze in amilaze: Pri bolnikih, ki so prejemali lorlatinib, se je pojavilo zvečanje vrednosti lipaze in/ali amilaze. Zaradi sočasne hipertrigliceridemije in/ali morebitnega intrinzičnega mehanizma je treba upoštevati tveganje za pankreatitis. Bolnike je treba spremljati glede zvečanja vrednosti lipaze in amilaze. Intersticijska bolezen pljuč (ILD – *Interstitial Lung Disease*)/pnevmonitis: Pri uporabi lorlatiniba so se pojavili hudi ali življenjsko ogrožajoči pljučni neželeni učinki, skladni z ILD/pnevmonitisom. Vse bolnike, pri katerih pride do poslabšanja respiratornih simptomov, ki kažejo na ILD/pnevmonitis, je treba takoj pregledati glede ILD/pnevmonitisa. Hipertenzija: Pri bolnikih, ki so prejemali loratinib, so poročali o hipertenziji. Pred uvedbo lorlatiniba mora biti krvni tlak pod nadzorom. Med zdravljenjem je treba krvni tlak preveriti po 2 tednih in nato najmanj enkrat na mesec ter glede na stopnjo resnosti zdravljenje prekiniti in nato nadaljevati z zmanjšanim odmerkom ali trajno prekiniti. Hiperglikemija: Pri bolnikih, ki so prejemali loratinib, se je pojavila hiperglikemija. Pred uvedbo je treba oceniti koncentracijo glukoze v serumu na tešče in jo nato redno spremljati v skladu z nacionalnimi smernicami ter glede na stopnjo resnosti zdravljenje prekiniti in nato nadaljevati z zmanjšanim odmerkom ali trajno prekiniti. Laktoza: Vsebuje laktozo. Bolniki z redko dedno intoleranco za galaktozo, odsotnostjo encima laktaze ali malabsorpcijo glukoze/galaktoze ne smejo jemati tega zdravila. **Medsebojno delovanje z drugimi zdravili in druge oblike interakcij:** Učinek zdravil na lorlatinib: *Induktorji CYP3A4/5:* Sočasna uporaba močnih induktorjev CYP3A4/5 (npr. rifampicin, karbamazepin, enzalutamid, mitotan, fenitoin in šentjanževka) je kontraindicirana. *Zaviralci CYP3A4/5:* Sočasni uporabi močnih zaviralcev CYP3A4/5 (npr. boceprevir, kobicistat, itrakonazol, ketokonazol, posakonazol, troleandomicin, vorikonazol, ritonavir, paritaprevir v kombinaciji z ritonavirom in ombitasvirom in/ali dasabuvirom ter ritonavir v kombinaciji z elvitegravirom, indinavirom, lopinavirom ali tipranavirom in grenivka ali grenivkin sok), se je treba izogibati, saj lahko pride do zvečanja koncentracij lorlatiniba v plazmi (če je sočasna uporaba nujna, je priporočljivo zmanjšati odmerek lorlatiniba). Učinek lorlatiniba na druga zdravila: *Substrati CYP3A4/5:* Izogibati se je treba sočasnemu dajanju lorlatiniba in substratov CYP3A4/5 z ozkimi terapevtskimi indeksi (npr. alfentanil, ciklosporin, dihidroergotamin, ergotamin, fentanil, hormonski kontraceptivi, pimozid, kinidin, sirolimus in takrolimus), saj lahko lorlatinib zmanjša koncentracije teh zdravil. *Substrati P-glikoproteina:* Substrate P-gp, ki imajo ozke terapevtske indekse (npr. digoksin, dabigatraneteksilat), je treba v kombinaciji z lorlatinibom uporabljati previdno, saj obstaja verjetnost, da se koncentracija teh substratov v plazmi zmanjša. *Študije in vitro s prenašalci zdravil, ki niso P-gp:* Lorlatinib je treba v kombinaciji s substrati BCRP, OATP1B1, OATP1B3, OCT1, MATE1 in OAT3 uporabljati previdno, saj klinično pomembnih sprememb v plazemski izpostavljenosti teh substratov ni mogoče izključiti. **Plodnost, nosečnost in dojenje:** Ženskam v rodni dobi je treba svetovati, naj se med zdravljenjem z lorlatinibom izogibajo zanositvi in naj med zdravljenjem uporabljajo visoko učinkovito nehormonsko metodo kontracepcije, saj lahko lorlatinib povzroči, da hormonski kontraceptivi postanejo neučinkoviti. Učinkovito kontracepcijo je treba uporabljati še vsaj 35 dni po zaključku zdravljenja. Med zdravljenjem in še vsaj 14 tednov po zadnjem odmerku morajo bolniki, ki imajo partnerice v rodni dobi, uporabljati učinkovito kontracepcijo. Nosečnost: Študije na živalih so pokazale embriofetalno toksičnost, zato uporaba med nosečnostjo ali pri ženskah v rodni dobi, ki ne uporabljajo kontracepcije, ni priporočljiva. Dojenje: Med zdravljenjem in še 7 dni po zadnjem odmerku je treba prenehati z dojenjem. Plodnost: Zdravljenje lahko ogrozi plodnost pri moških. **Vpliv na sposobnost vožnje in upravljanja strojev:** Ima zmeren vpliv na sposobnost vožnje in upravljanja strojev. Potrebna je previdnost, saj se pri bolnikih lahko pojavijo učinki na osrednje živčevje. **Neželeni učinki:** Zelo pogosti: anemija, hiperholesterolemija, hipertrigliceridemija, učinki na razpoloženje, učinki na kognitivne funkcije, periferna nevropatija, glavobol, motnja vida, hipertenzija, diareja, navzea, zaprtje, izpuščaj, artralgija, mialgija, edem, utrujenost, zvečanje telesne mase, zvečanje vrednosti lipaze, zvečanje vrednosti amilaze. **Način in režim izdaje:** Rp/Spec - Predpisovanje in izdaja zdravila je le na recept zdravnika specialista ustreznega področja medicine ali od njega pooblaščenega zdravnika. **Imetnik dovoljenja za promet:** Pfizer Europe MA EEIG, Boulevard de la Plaine 17, 1050 Bruxelles, Belgija. **Datum zadnje revizije besedila:** 04.04.2022

Pred predpisovanjem se seznanite s celotnim povzetkom glavnih značilnosti zdravila.

Literatura: 1. Povzetek glavnih značilnosti zdravila Lorviqua, 4.4.2022.

ALK = anaplastična limfomska kinaza, **CŽS** = centralni živčni sistem, **mNSCLC** = (Metastatic Non-Small Cell Lung Cancer) metastatski nedrobnocelični rak pljuč, **NSCLC** = (Non-Small Cell Lung Cancer) nedrobnocelični rak pljuč, **TKI** = (Tyrosine Kinase Inhibitor) zaviralec tirozin kinaze.

Pfizer Luxembourg SARL, GRAND DUCHY OF LUXEMBOURG, 51, Avenue J.F. Kennedy, L – 1855,
Pfizer, podružnica Ljubljana, Letališka cesta 29a, 1000 Ljubljana

PP-LOR-SVN-0005
Datum priprave: april 2022.
Samo za strokovno javnost.

Radiology and Oncology | Ljubljana | Slovenia | https://sciendo.com/journal/RAON

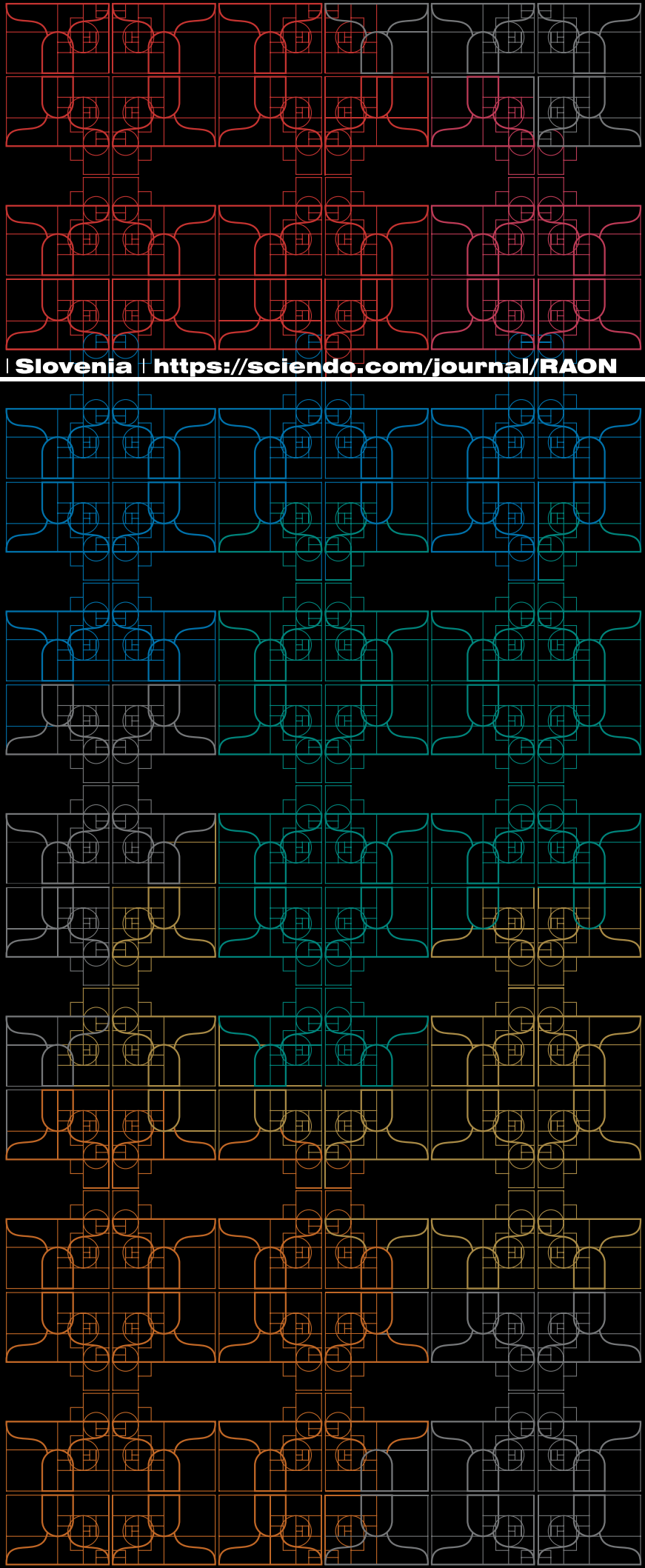

ISSN 1318 - 2099